Development of a Biological Electrochemical System for Decentralised Wastewater Treatment and Energy Production in Remote and Under-Served Regions

Author: Thomas Fudge

College of Engineering, Design and Physical Sciences

Thesis submitted in partial fulfillment of the requirements for the degree of Doctor of Philosophy in Sustainable Engineering

Department of Mechanical and Aerospace Engineering

September 2020

Table of Contents

Declaration of Authorship

I declare that the research within this thesis is the original work of the author. The research has not been previously submitted as part of the requirement for an award or higher degree in this or any other university. The research work was conducted by the author except where specified, or where acknowledgments are made and by references.

I do not authorise Brunel University to reproduce this thesis by any means or to share the work with other institutions or individuals for the purpose of scholarly research or for any other purpose apart from the requirement to assess the research.

Name: Thomas Fudge

Signed:

Date: 05/10/2020

Abstract

Wastewater treatment is one of many global challenges that we face, where currently 80% of wastewater discharges into our environment go untreated. The most widely used approach is a centralised model using sewage networks to collect the waste, often treating it linearly. The linear approach does not explore the value in the waste that can be extracted. The research explored opportunities to transition towards a circular economy where we extract the value from within the wastewater; to develop a new sustainable approach for decentralised wastewater treatment for remote and underserved regions that lack wastewater infrastructure. The research undertaken was to explore the ability of Biological Electrochemical Systems (BES) to transform our approach to wastewater treatment. BES can recover valuable resources such as energy in the form of electricity, hydrogen and methane as well as nutrients. The project explored the various BES technologies to understand which system will likely provide the initial route to commercialisation.

Academic research on BES is spread mainly across Microbial Fuel Cells (MFCs) and Microbial Electrolysis Cells (MECs) with both technologies showing potential to revolutionise wastewater treatment. However, both MFCs and MECs face challenges with commercial deployment to meet the needs of underserved communities, from the complexity of design to cost. The research aimed to assess whether a less researched route of Electro-Methanogenesis is technologically and economically feasible. Electro-Methanogenic Reactors (EMR) can accelerate the performance of Anaerobic Digestion (AD); a widely commercially available technology. EMR provides multiple opportunities to improve our current approach to wastewater management and provide a compact decentralised treatment. The United Nations Sustainable Development Goals (SDG) have identified multiple challenges that could be tackled by EMR; including clean water and sanitation (SDG6), affordable and clean energy (SDG7) and sustainable cities and communities (SDG11).

The research explored the scaleup of EMR from lab scale (2.3 L) to pilot (1300 L) , assessing both the technical challenges but also the economic viability. The lab experiments highlighted challenges, including, designing a continuous flow system and regulating pH through the organic loading rate. During batch testing, the EMR systems operating on brewery spent grain demonstrated a high substrate efficiency of 99.2 ± 15.3%, identifying that the system is effectively converting the breakdown of the organics into methane. The batch test results identified that EMR could provide better pH regulation and organic removal compared to AD systems. EMR was able to breakdown the Volatile Fatty Acids (VFA) once the pH had dropped below 5, which in the case of AD systems inhibited the microbial community. EMR is still susceptible to having a high Volatile Solids (VS) concentration as an increase in the concentration from 14.6 g/L to 21.1 g/L did not recover as quickly; with the EMR taking initially 7 days to increase the pH above 6 whilst the increased VS meant the pH reached 4.92 after 28 days.

Scaling up the lab research to pilot scale proved to be a challenge with unforeseen operational barriers affecting performance. The pilot identified that defining the EMR operational parameters are crucial to ensure commercial applications where the technology will be deployed in less controlled environments. The results showed that EMR would likely require further post-treatment to reduce the COD and pathogens within the effluent. A Technological Economic Analysis (TEA) is used to compare the current solutions that are widely used in Kenya, including pit latrines, septic tanks and

anaerobic digestions systems with EMR. The TEA was based on lab results and assumptions on future increases in EMR performance. Including COD removal increases through improved reactor design and updated costs obtained from manufacturers. The TEA identified that EMR had a lower lifetime cost compared to fixed dome AD systems, which are commonly used in Kenya.

BES still have a long way to go before becoming widely commercially viable. EMR offers a route to commercialisation that could provide decentralised wastewater treatment. The research identifies the barriers and next steps to reach the goal of moving EMR towards implementation.

Outcomes

During the research, there have been multiple successful outcomes leading to the creation of new knowledge and dissemination of the work.

Contribution to new knowledge

1. Submitted Research Articles *"Microbial Electrolysis Cells for Decentralised Wastewater Treatment: The Next Steps"* Water Science & Engineering
2. European Pending Patent: Wastewater treatment systems and methods (20156264.2 – 1101)

Successful Grant Applications

1. United Nations World Food Program (WFP)– Sprint technology funding accelerator program – "Supporting food systems and nutrition through the use of electro-methanogenic reactors (EMR) that turn waste into energy". The grant was to demonstrate EMR at scale, further information in Chapter 9 – Pilot Scale Electro-Methanogenic Reactor.
2. Innovate UK Energy Catalyst round 6 – Lead Applicant "Decentralised Electro-Methanogenic Wastewater Treatment (DEMWT)". The project is leading on from the WFP grant to demonstrate decentralised EMR systems within the humanitarian context. The project is building a micro wastewater treatment and bioenergy generation system in WFP's compound at Dadaab refugee camp. The plant will treat human waste so that it can be safely used to irrigate the gardens around the compound. The pilot will assess the water effluent quality to understand the suitability of using treated waste for irrigation within agriculture. Reusing the water will enable the recovery and reuse of the nutrients within wastewater. The recovery of nutrients can create an organic fertiliser. The organic waste from the kitchen will be treated in two 1.5m^3 anaerobic digesters, with one having electrodes inserted so that it operates as an EMR system. The biogas produced will be used for cooking, reducing the need for coal and propane that are used within the compound. Providing new knowledge in circular approaches to wastewater and waste management at a decentralised scale and within the humanitarian context.
3. Innovate UK Energy Catalyst round 6 - Collaborator "Bitesize Energy Access (BEE)". BEE is trialling the distribution of bitesise energy packages through the supply of surplus electrical energy from Solar Household Systems (SHS) through battery distribution, enhancement of biogas production, direct supply to commercial (e.g. irrigation pump or grain milling). The PhD research is feeding into the enhancement of biogas production. Where electrode modules will be retrofitted into a household biogas tube/bag system in Tanzania. The system will be powered by excess solar energy providing new insights into the performance of intermittent power supply on EMR. The research will also analyse the economics of microscale biogas distribution between households.

Dissemination

1. 3 Minute Thesis - Brunel University (Presentation)

2. 3 Minute Thesis - UK Final (Presentation) “Distributed Sanitation for Developing Communities with Energy and Nutrient Recovery” https://www.youtube.com/watch?v=a3ckm5a343k&t=2s
3. Falling Walls Conference – Huddersfield University (Presentation)
4. Falling Walls Conference – Berlin, Germany (Presentation) “Breaking the wall of sanitation.”
5. Silibersalz Conference – Halle, Germany (Presentation) “Decentralised wastewater treatment systems.”
6. Brunel Conference (Poster)
7. Three Days of Fat Conference – (Presentation & Panellist) “Rethinking Fatbergs”
8. The Science Museum - Fame Lab (Presentation)
    a. “The power of poo.”
    b. “Fatbergs to cocaine, modern challenges for wastewater treatment.”
9. World Bank Water Week – Washington DC, USA (Poster & Presentation) “A new pathway for wastewater treatment.”
10. Ocean Exchange – Florida, USA (Presentation) “Rethinking wastewater.”
11. The Sanitation Economy – Pune, India (Presentation) “Accelerating wastewater treatment.”
12. The Conversation (Article) “To fight the fatbergs, we have to rethink how we treat sewage waste.” https://theconversation.com/to-fight-the-fatbergs-we-have-to-rethink-how-we-treat-sewage-waste-84714

Outreach

1. Royal Institute of Engineering Master Class- I developed an interactive workshop for children aged 10 - 13 engaging them in science, water, and our environment. I carried out multiple workshops across the country, including the Beamish Museum in Durham.

2. Volunteer Placement Supervisor - I took it upon myself to volunteer and ran a Nuffield summer placement for 6 A level students over the summer break. During the placement, I set the students a challenge to design and solution to provide basic services for Bidi-Bidi Refugee camp in Uganda. During the placement, the students developed key skills in analysis, sustainability, design thinking and presentation skills.

3. Mentorship Program - I mentored 3 French university students for three months as part of their international exchange professional development program.

4. Teaching assistant on the Brunel Ready Program - The program enables students to develop an interdisciplinary skillset through a project about providing new solutions for Zambian refugee camps.

Awards

1. Taylor & Francis - 3 Minute Thesis UK Winner 2017
2. Falling Walls – Huddersfield University Winner 2017
3. Climate Launchpad Competition UK – Winner 2017
4. Climate Launchpad Competition European finalist 2017
5. UK Energy Innovation Awards – Winner of Best University Technology 2017

6. NACUE – 2018
7. Santander – Entrepreneur of the Year 2018
8. Chartered Institute of Water and Environmental Management – Young Environmentalist of the Year 2019

Acknowledgements

I would like to thank the following people who have helped me undertake this research:
My supervisor Dr. Zahir Dehouche., for his enthusiasm and active support of for the project and it's future progression. Dr Abdul Chaudry for his support and patience, particularly for the encouragement to pursue a PhD.

The Engineering and Physical Sciences Research Council (EPSRC) for the funding and support to pursue this research.

For their contributions to data collection:

Isabella Bulmer

Kyle Bowman

William Gambier

Llyr Williams

George Fudge

The team at WASE that provided support and encouragement to continue the research and providing the facilities to carry out the research. My friends and family that have provided me with continual support and encouragement and to my late Grandad who always said how proud he was that I was pursuing a PhD and I would one day be the first Dr in the family.

List of Figures

List of Tables

Nomenclature

A_c	Administration Costs	£
A_u	Compartment up-flow area	m^2
V_{app}	Applied Voltage	Volts
CD	Current Density	$Amps/m^2$
CE	Coloumbic Efficiency	%
σ	Conductivity	mS/cm (milli Siemens) or S/m
CH_4	Methane	
C_o	The concentration of the oxidised products	
C_R	The concentration of the reduced products	
ΔCOD	Change in COD over period	mg/L
$C_{W:L}$	Compartment width to length ratio	m:m
d	Distance between the electrodes	m
DO	Dissolved Oxygen	mg/L
ηE	Electrical Energy Efficiency	%
E_{anode}	Anode potential	anode potential
E°	The standard potential at pH 0	V
$E^{\ominus}_{cell}$	Standard cell potential	V
E_{cell}	Cell potential at the temperature of interest	V
$E_{KA,EC}$	Rate-limiting electrode cell potential at which current density is half of the maximum current density	V
E_{ps}	Applied Voltage of the power supply	V
ΔE_{EET}	Average energy loss in conductive EET of the third electron-transfer step	V
F	Faraday's Constant	96,485 C/mol e-
f_e^o	Fraction of electrons used for catabolism	
$\Delta H_{WW/COD}$	Internal Energy of Substrate	kJ/gCOD
H_p	Heating Power Requirements	kWh
ΔH_{CH_4}	Standard Heating value of Methane	MJ/mol
i	Discount Rate	%
I^2R_{ex}	Losses caused by external resistor	V

I_c	Installation Cost	£
j	Current density	A/m^2
K_{bio}	the biofilm conductivity	S/m
$K_{sd,app}$	Apparent half-saturation concentration of electron donor	g COD/m3
$L_f/2$	Biofilm Midpoint	m
OCP	Open Circuit Potential	V
OCV	Open Cell Voltage	V
OLR	Organic Loading Rate	kgCOD/day
M_c	Manufacturing Cost	£
MK_c	Marketing Cost	£
n	Number of years	years
NaH_2PO_4	Sodium hydrogen phosphate	
Na_2HPO_4	Disodium hydrogen phosphate	
N_{CE}	Theoretical moles of methane in the current produced	mol
N_{CH_4}	Moles of methane	mol
η_{E+S}	Total Energy Efficiency	%
N_s	Theoretical moles of Methane in the substrate removed	mol
PR	Rated biogas power output	kW
PW_E	Electrode Power Cost	£
PW_H	Heating Power Cost	£
PW_P	Pumping Power Cost	£
L	Labour Cost	£
LCOE	Levelised Cost of Energy	£/kWh
LCOWT	Levelised Cost of Wastewater Treated	$£/m^3$
L_f	Biofilm thickness	m
Q	Flow Rate	m^3/d
q	specific rate of electron donor utilisation	mmol-ED mg-VS
Q_r	Reaction quotient of the cell reaction	
R	The molar gas constant	8.314 J/mol/K
r_L	Reactor Length	m

r_W	Reactor Width	m
$R_{U:D}$	Upflow to downflow area ratio	m^2:m^2
S_d	donor substrate	g COD/m^3
SE	Substrate Efficiency	%
STP	Standard Temperature and Pressure	Hg
SVI	Sludge Volume Index	mL/g
T	Temperature	K
Δt	Data points over time	
TDS	Total Dissolved Solids	mg/L
TSS	Total Suspended Solids	mg/L
U_c	Utility Costs	£
V	Stoichiometric coefficients	
V_{up}	Up-flow Velocity	m/hr
	Turbidity	NTU (Nephelometric Turbidity Units)
$\Delta V_{\Omega wastewater}$	Ohmic loss in wastewater	Ohms
V_d	Design flow velocity	m/h
VR	Volume flow rate input of the wastewater to be treated	m^3/h
VS	Volatile Solids	g/L
V_p	Peak up-flow Velocity	m/h
V_{up}	Up-flow Velocity	m/hr
W_{E+S}	Electrical and Substrate Energy Input	kWh
W_{in}	Electrical Energy Input	kWh
W_{out}	Energy Recovered in Methane	kWh
X_f	Biofilm density of active exoelectrogens	g VS/m^3
Z	Number of electrons transferred in the cell reaction or half-reaction	No. electrons

Abbreviations

AC	Activated Carbon
AD	Anaerobic Digestion
AS	Activated Sludge
V_{app}	Applied Voltage
BES	Bio-Electrochemical Systems
CAPEX	Capital Expenditure
CAP	Chloramphenicol
CE	Coloumbic Efficiency
COD	Chemical Oxygen Demand
CRF	Capital Recovery Factor
DO	Dissolved Oxygen
DIET	Direct Interspecies Electron Transfer
EAB	Electrochemically Active Bacteria
EAM	Electrochemically Active Microorganisms
EET	Extracellular Electron Transfer
EMR	Electro-Methanogenic Reactor
FC	Fuel Cells
G+	Gram-negative Bacteria
G-	Gram-positive Bacteria
HDI	Human Development Index
HER	Hydrogen Evolution Reaction
HRT	Hydraulic Retention Time
IBC	Intermediate Bulk Containers
LCC	Life Cycle Cost
LCA	life Cycle Assessment
MBR	Membrane Bioreactor
MEC	Microbial Electrolysis Cells
MFC	Microbial Fuel Cells
MTBF	Mean Time Between Failure
NF+G	Nickel Foam + Graphene
NEMA	National Environment Management Authority of Kenya
OCP	Open Circuit Potential

OCV	Open Cell Voltage
OLR	Organic Loading Rate
ORR	Oxygen Reduction Reaction
OPEX	Operation Expenditure
PEM	Polymeric Proton Exchange Membranes
R	Reactor
ROI	Return on Investment
RPD	Residual Biogas Potential
SA	Surface Area
SDG	Sustainable Development Goals
SS	Stainless Steel
SVI	Sludge Volume Index
TBL	Triple Bottom Line
TDS	Total Dissolved Solids
TEA	Technological Economic Analysis
TRL	Technology Readiness Level
TSS	Total Suspended Solids
TS	Total Solids
UASB	Up-flow Anaerobic Sludge Blanket
VFA	Volatile Fatty Acids
VS	Volatile Solids
WHO	World Health Organisation
WFP	United Nations World Food Program
WW	Wastewater
WWT	Wastewater Treatment
WWTP	Wastewater Treatment Plant

1 Chapter 1 - Introduction

The chapter outlines the research thesis, the importance of the research at this present time and the motivations for carrying out the research. The chapter will cover a background of the research area, while the aims and objectives of the study will be outlined, to highlight the new scientific contribution to the field.

The research proposes an alternative approach to wastewater treatment, centred on the circular economy and decentralisation. The circular approach is proposing the use of Biological Electrochemical Systems (BES) to treat wastewater and to recover the chemical energy.

1.1 The Global Outlook

An assessment of the long-term global threats by the World Economic Forum found ten risks that could shape the world as a result of their impact Figure 1-1. The top three include biodiversity loss, climate change and a future water crisis as being the most significant threats that need addressing (World Economic Forum, 2020). Water is intricately linked with most sectors (UN-Water, 2014) and if issues to do with water are not addressed, there could be a significant impact on society. Water demand is estimated to rise by 55% from 2000 to 2050 (Leflaive et al., 2012). The increasing demand will multiply the burden on ageing infrastructure, which is not able to cope with our needs as 80% of wastewater is discharged untreated (WWAP, 2017). Even with this growing threat, water management is not integrated into development planning within a majority of countries, leading to inadequate monitoring of wastewater, sanitation and drinking water. Lack of action and planning for future wastewater infrastructure could cause severe economic implications with $45 trillion of assets at risk from the result of water stresses by 2050 (Wojciechowska-Shibuya, 2015).

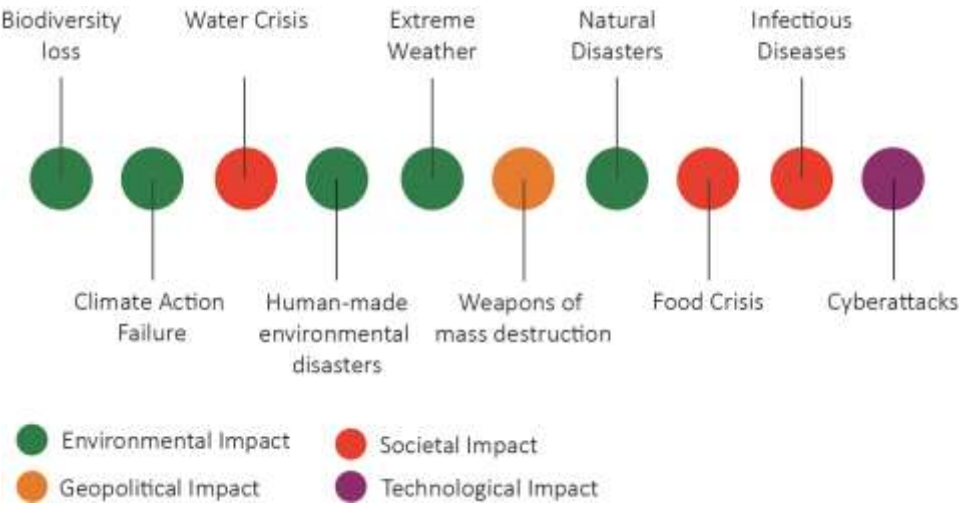

Figure 1-1: Global Long-Term Risk Outlook adapted from (World Economic Forum, 2020)

Alongside the threats of climate change and a water crisis, inadequate sanitation is a global issue affecting over half of the population (WHO, 2016). Often affecting communities in rural areas where 9 out of 10 people open defecate (Chakraborty et al., 2014). In some countries, only 6% of the population has safely managed sanitation, resulting in 1.8 billion people using drinking water contaminated with faecal matter (The World Bank, 2020). To eradicate open defection by 2025 The United Nations Children's Fund (UNICEF) and the World Health Organisation (WHO) set up the Joint Mentoring Partnership. To achieve the goal of being open defecation free in less than 5 years, radical changes to our current approaches need to be implemented.

Tied to the efforts of tackling open defecation, there need to be solutions to treat the waste. Table 1-1 shows the clear distinction between a country's economic growth and the level of untreated wastewater. Future aspirations to half the level of untreated wastewater leave an immense challenge that will require multiple solutions and approaches. Two new ISO standards were recently published to aid in the development of new decentralised wastewater treatment systems for onsite sanitation. The ISO 30500:2008 aim is to standardise non-sewered sanitation systems with prefabricated integrated treatment units. The second, which is still under revision, is the ISO/FDIS 31800 aimed at faecal sludge treatment units that are energy independent, prefabricated, community-scale, resource recovery systems. The ISO/FDIS 31800 highlights the need for circular wastewater treatment systems that do not require external energy supply which in many areas is not accessible.

Table 1-1: Untreated wastewater compared to countries economic growth and security of regions adapted from (WWAP, 2017)

Countries	*Untreated wastewater (2015)*	*Aspiration 2030*
Low Income	92%	46%
Lower - Middle Income	72%	36%
Upper Middle Income	62%	31%
High Income	30%	15%
Average	64%	32%

BES not only treat wastewater but can also recover energy enabling the solution to target other challenges around energy access. Globally 940 million people lack access to electricity, and 3 billion people do not have access to clean cooking facilities (World Bank Group, 2020a). Energy access issues predominantly affect Sub-Saharan Africa and developing Asia (SE4ALL, 2011). Improving energy access and services has a positive effect on the Human Development Index (HDI). Providing sustainable energy access can remove the need for fuels that lead to indoor air pollution such as charcoal and kerosene. The transition to sustainable energy can provide economic savings and healthier living environments, that contribute to the HDI increasing by 38% (Craine et al., 2014).

To highlight the importance of tackling the global threats that threaten society, the UN set up the 17 Sustainable Development Goals (SDGs). Both clean water and sanitation (SDG6) and affordable clean energy (SDG7) are included along with industry, innovation and infrastructure (SDG9) and sustainable cities and communities (SDG11). Since the release of the SDGs, the issues have been brought to the

attention of the world. The attention is increasing the interest to invest and develop new renewable energy and wastewater treatment infrastructure. The UN Secretary General, and their advisory board highlights the need for research institutions to carry out further developments in renewable energy, wastewater pollution, treatment and recycling technologies and solutions (SE4ALL, 2011; Wojciechowska-Shibuya, 2015).

1.2 Conventional Wastewater Treatment

Conventional wastewater treatment systems connect to extensive sewerage networks, using 'end of pipe' technologies to treat the waste in a linear approach. Conventional secondary wastewater treatment has both high energy requirements and Capital Expenditure (CAPEX) (Hernández-Sancho et al., 2015). In the UK the water industry accounts for 2-4% of the country's energy demand, with the most energy-intensive aspect of the process being the aeration beds used for activated sludge (Heidrich et al., 2014).

Thus, the conventional centralised system has been unsuccessful at making a significant impact in underserved low-income countries (Werner et al., 2009). Especially when countries like the USA have inadequate funding for maintenance of their wastewater infrastructure (Anand and Apul, 2014)

The cost is only one of the disadvantages in centralised sewer networks and conventional treatment, where other issues listed below are also present: (Starkl et al., 2015; Werner et al., 2009)

- Unsatisfactory purification or uncontrolled discharge
- Pollution of water
- Environmental damage
- High water consumption
- High investment, energy, maintenance and operating costs
- Nutrient loss
- Health and hygiene

Centralised sewerage networks also require water to transport waste from its source to treatment facilities. Using sewer networks require water to transport the waste to a central location. The approach can pollute water and also dilute waste streams making centralised approaches less sustainable (Starkl et al., 2015; Werner et al., 2009). In many cases, centralised systems produce drinking quality of water for industrial applications, irrigation and flushing,
wasting resources and energy (Anand and Apul, 2014). Even with these disadvantages, there is a bias by political organisations towards centralised networks.

There is a severe lack of finance and planning for wastewater infrastructure compared to other sectors, with water continually being an undervalued resource (Wojciechowska-Shibuya, 2015). A vast amount of countries have insufficient finances to meet their targets to implement wastewater

infrastructure (World Health Organization, 2014). Investing in wastewater and sanitation has significant societal and economic benefits with a 3-34 USD return on investment for every dollar invested (UNESCO, 2016). A third of water utilities are unable to cover their costs (Danilenko et al., 2014). Therefore the UN wants to focus on the underperforming municipal water and sanitation facilities (Wojciechowska-Shibuya, 2015).

Table 1-2 shows a comparison of centralised and decentralised wastewater treatment processes. The data has been adapted from Sun et al., removing costs of supplementary equipment and CAPEX of pipe networks to compare the technologies directly. An analysis of the full lifetime cost of wastewater treatment systems, including sewage pipelines, demonstrated that decentralised WWTP had 9% higher costs. The higher costs were associated with having black and grey water pipelines that used vacuum instead of gravity flow. In some cases, having a decentralised treatment with combined flows may be more appealing and would reduce the pipeline CAPEX. The table shows that Activated Sludge (AS) has a higher CAPEX and significantly higher OPEX compared to Upflow Anaerobic Sludge Blanket (UASB). Membrane Bioreactors (MBRs) were significantly higher in both CAPEX and OPEX. The research highlights the potential benefits of moving away from centralised WWTP, which offers significant environmental benefits and an increase in infrastructure resilience.

Table 1-2: Review of WWTP designs comparing centralised and decentralised options, based on a population of 30,000 adapted from (Sun et al., 2020)

Technology	*COD Reduction (%)*	*TSS Reduction (%)*	*Energy Balance (kWh/m3)*	*CAPEX (£/(per person))*	*OPEX (£/(per person/year))*	*Treatment to Pipeline costs ratio*	*Direct GHG emission (kg/m3)*
AS - Centralised	99.1	-	-0.592	330	645	41:59	0.062
MBR - Centralised	99.6	-	-1.59	415	729	41:59	0.025
UASB - Decentralised	78 (95 including trickling filter)	93	-0.142	312	192	33:67	0.004

Despite the bias for centralised systems, distributed and non-networked technologies offer an attractive option (Starkl et al., 2015). There is an emerging opportunity to develop new wastewater treatment technologies that are adaptable to the changing environment, with a lower economic and environmental cost. Transitioning from seeing wastewater as a problem of waste, to one where we see it as a resource which can be reused, could have significant economic and environmental benefits. New solutions that can adapt and fit into conventional systems to improve efficiencies or allow decentralised treatment could provide solutions to our current unsustainable wastewater management.

1.3 A pathway to a Circular Model

A transition to a closed-loop model, which recovers resources (energy, nutrients and water), is required (Werner, et al., 2009, (Beck et al., 2010; Guest et al., 2009). The high volumes of water and energy required for centralised sewage treatment systems reduce the chances of them being a sustainable option for the future (Anand and Apul, 2014; Schouten and Mathenge, 2010; Sun et al., 2020).

Future urban infrastructure needs re-engineering so that it benefits the environment and counteracts the human interventions in the natural cycle. Sustainable water management needs to encompass environmental, economic and social assessments (Guest et al., 2009); these three elements comprise the triple bottom line (TBL). Elkington's (1994) TBL ensures that organisations do not solely concentrate on the economic value they add, but also the environmental and social value they create or destroy. The TBL approach gives a holistic view of the organisation or proposed solution so that improvements make the idea sustainable and should be used as a platform for future developmental research.

Wastewater Treatment Plants (WWTPs) need to go beyond treating water to become sustainable. WWTPs need to reduce their reliance on non-renewable resources through energy efficiency improvements and remove waste generation through resource recycling (Mo and Zhang, 2013). There is a consensus that new technologies and designs should integrate water, nutrient and energy recovery (Guest et al., 2009). Resource recovery will lead to new uses of human waste (WHO, 2014), that create net positive systems (Beck et al., 2010). Circular economy approaches which focus on resource recovery can alleviate the financial costs that are typically associated with wastewater treatment and sanitation.

For the wastewater sector to adapt its linear approach to treatment, we need to understand its interaction with other vital sectors that support society. Figure 1-2 depicts the Water-Energy-Food nexus, which illustrates the interconnections between these three areas. Energy and food production requires water for cooling and irrigation. Energy is used to treat water, and we can transport water through the embedded water within crops. The nexus illustrates that we cannot view the three most vital pillars of our society as separate entities; they have significant impacts and interconnections between them.

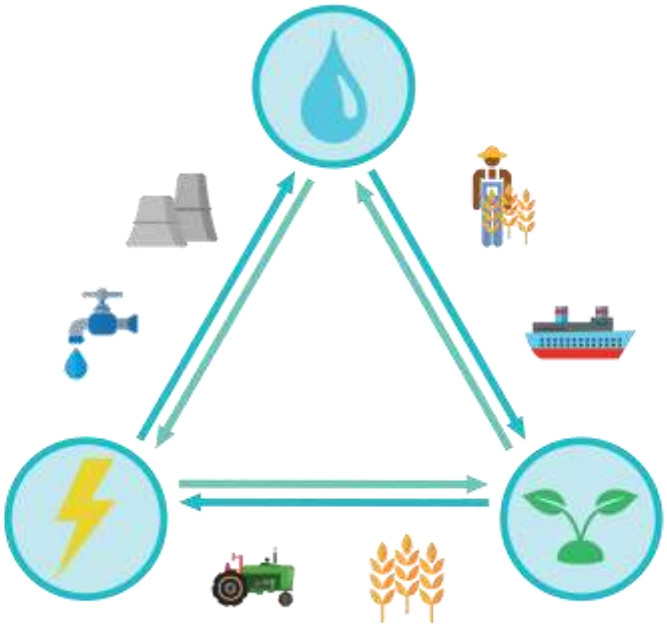

Figure 1-2: Water-Energy-Food Nexus

Within a circular economy, wastewater can sit at the centre of the nexus providing energy, water and nutrients, producing resources for the three pillars that are essential for society. Wastewater contains excessive amounts of Nitrogen, Potassium and Phosphate, which if not removed, cause environmental issues like eutrophication (Lovins, 2016). However, the nutrients in wastewater have a commercial value. Recovering them to produce organic fertilisers can be profitable and necessary in the future, as we are currently facing global phosphorus shortages (Cordell et al., 2011). Energy generation from wastewater is not a novel concept. It is estimated that the inherent chemical energy of wastewater from organic materials is ≈ 9.3 times greater than the energy needed for conventional wastewater treatment (Kim et al., 2018).

As mentioned, centralised systems present a high cost and they are not suitable for every situation. Centralised solutions in India, for example, are being overwhelmed with increasing demand and decentralised WWTPs can offer a solution to the immediate access needs (Schellenberg et al., 2020). Decentralised solutions have proved successful using both conventional treatment methods alongside new innovations. However, one of the main challenges is that WWTPs cannot take a one system fits all approach and need to be designed for the specific users and the local conditions, encompassing the triple bottom line (Kaundinya et al., 2009; Werner et al., 2009).

One approach for energy recovery used within WWTPs is through biogas production using Anaerobic Digestion (AD) of sludge. To recover electrical energy requires additional Combined Heat and Power (CHP) systems which typically require a large volume of biogas. The large volume of gas required restricts their implementation in small wastewater systems (Mo and Zhang, 2013). As a result, AD systems are typically implemented in communities with more than 40,000 people (Garrido-Baserba et al., 2018). New small CHP systems (Yanmar) or low-cost generators (Oaktek) could open the door to smaller WWTP to generate electricity from biogas.

AD generates biogas via the digestion of acetate to form methane and CO_2 (Van Eerten-Jansen et al., 2012a). However, the process is relatively slow and produces high volumes of CO_2 within the biogas, reducing the energy density. The high CO_2 content makes the biogas challenging to store as it requires large amounts of space or requires extensive chemical treatment, including cryogenic separation, to remove CO_2 (Awe et al., 2017). The large space requirements or the post biogas treatment significantly increase CAPEX.

There are emerging technologies which allow energy recovery. BES offers an attractive alternative for energy recovery from wastewater. BES can recover energy at a faster rate directly into electricity within Microbial Fuel Cells (MFC), hydrogen within Microbial Electrolysis Cells (MEC) or methane in Electro-Methanogenic Reactors (EMR). The promise of BES has driven a significant amount of research interest in recent years. The majority of research has focused on lab systems which offer the opportunity to develop an understanding of the complex interactions of the biological and electrochemical processes within a controlled environment.

BES have been used as alternative methods for sustainable wastewater management, including onsite sanitation in Ghana and larger scale wastewater treatment. A pit latrine was constructed with a three-chamber MFC and composting chamber for solid waste for onsite sanitation. Urine flowed into a separate nitrification chamber and liquid from the solid waste was fed into the MFCs anodic chamber, the effluent from both flowed into the cathodic chamber for oxidation. The system successfully demonstrated energy generation, although it faced low power production due to ohmic losses resulting from simplified design and high cost due to import fees and the experimental nature (Castro et al., 2014). Other researchers have explored combing BES with constructed wetlands to create an optimised system with high performance and lower footprint. Of the options outlined in the research, the constructed wetland MFC is indicated as the most novel option to provide nutrient and solid removal whilst extracting energy. The cathode is located below the plants in the root bed (aerobic zone), water flows upwards through the anode, which is below in the anaerobic zone (Ramírez-Vargas et al., 2018).

Going forward, in order to accelerate the implementation of BES, we need to scaleup the research focus into pilot systems. Figure 1-3 shows the logarithmic scale of 77 MFC and MEC research articles. The graph illustrates the distribution of research for different sized reactors, which shows that the main focus of research has been on systems below 10L. However, we are now seeing a shift with an increase in research into systems larger than 10L.

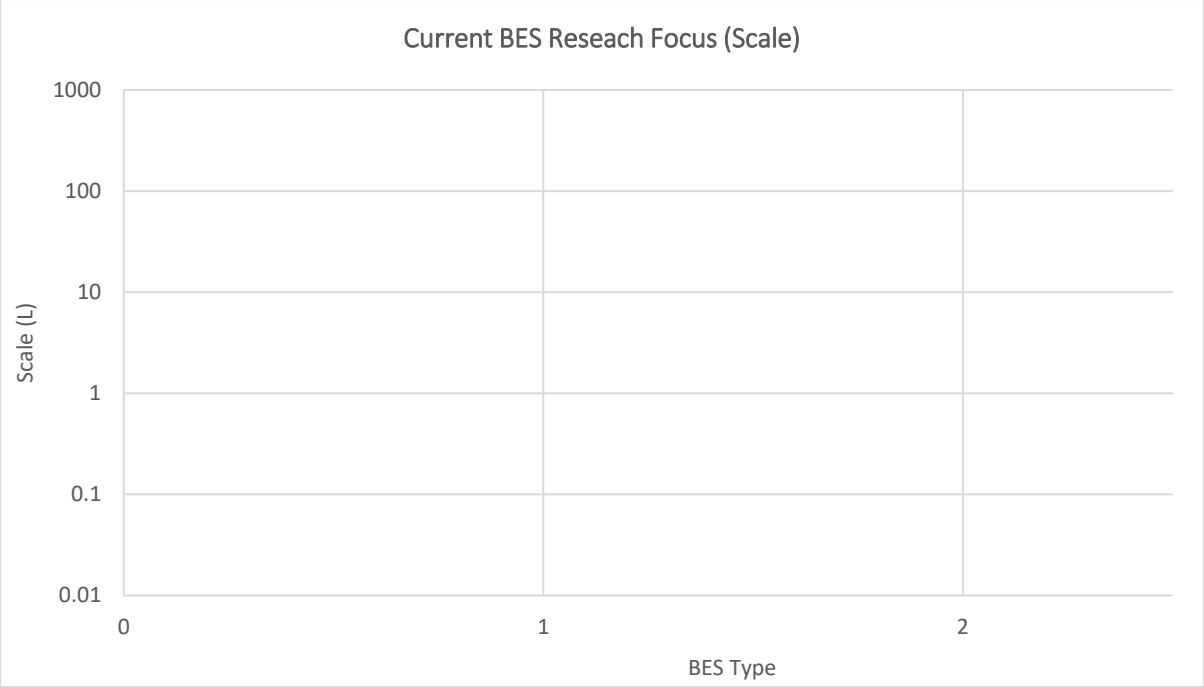

Figure 1-3: Articles reviewed within the research on MFCs and MECs reactor size distribution, the darker the shadows indicate a higher concentration of research articles.

1.4 Summary

There is a need to revise the current implementation of wastewater treatment systems to meet the global needs of today. Centralised systems have historically proven pivotal to the development of the urban societies which have implemented them, but now a new circular approach is required. The research aims to build a case that the future is one where we unlock the potential of wastewater to become a resource that can deliver energy, water and food to global societies.

The thesis will focus on the application of BES systems to recover energy from wastewater and sludge to create a circular solution for either decentralised or centralised waste management.

2 Chapter 2 - Overview of Previous Works

2.1 Biological Electrochemical Systems

Bio-electrochemical systems (BES) are comprised of an anode and cathode, whereby the reaction of at least one electrode involves an electrochemical reaction which uses microorganisms as a catalyst (Escapa et al., 2016a). The microorganisms create an electrically active biofilm on the electrode surface. They convert chemical energy present in organic substances into electrical and extractable chemical energy as well as other valuable chemicals (Pant et al., 2012).

BES can convert the chemical energy within a variety of waste streams creating a circular approach to wastewater treatment, allowing the recovery of valuable resources within the wastewater. The technology combines a variety of interdisciplinary areas of research, including electrochemistry, microbiology and engineering. The field opens up an opportunity to explore the relatively unknown area of microbial electrochemistry. BES have a wide range of applications, but they all contain an anode where a biofilm is grown. The microorganisms within the anode biofilm oxidise the biodegradable substrates releasing electrons which create an electrical current (Wang and Ren, 2013).

There are a variety of different designs of BES that have different applications and outputs. Microbial Fuel Cells (MFC) capture the current produced within the cell to generate electrical energy (Scott, 2016). Microbial Electrolysis Cells (MEC) have an additional current applied to the electrodes, which enables the production of hydrogen and other value-added chemicals at the cathode (Cotterill et al., 2016) as well as dichlorination (Aulenta et al., 2008). Research in BES has been consistently growing due to the potential impact the field could have on a variety of sectors. The main BES focus of research is currently between MFCs and MECs.

2.1.1 Performance Parameters

One of the central parameters in assessing the wastewater quality before it can be discharged is the amount of organics it contains. The concentration of organic material present in wastewater is measured using the Chemical Oxygen Demand (COD). When the COD drops below 200 mg/L the performance of BES drops due to lower current densities that lower energy recovery (X. Zhang et al., 2015). The reason BES lower in performance at low COD levels is due to the microorganisms requiring a carbon-based feedstock for fuel. The current EU discharge standards for COD are 125 mg/L. Therefore using BES in isolation may not be suitable as they will likely require tertiary treatment to polish the water to meet discharge standards. Combining BES with other treatment processes can enable consistent energy recovery and ensure the effluent reaches acceptable discharge levels (X. Zhang et al., 2015).

BES have a difference in electrode potential between the cathode and the anode, if the $E_{cathode} > E_{anode}$ the system is an MFC, which will generate electricity. Alternately, if the $E_{anode} > E_{cathode}$ external power is required, which makes the system a MEC (Bajracharya et al., 2016).

The microorganisms in BES operate anaerobically, similarly to AD systems. AD, typically like temperatures within the mesophilic (30-39^{o}C) and thermophilic (48-60^{o}C) range (Streitwieser, 2017). As a result, BES could be affected by temperature fluctuations which could reduce their efficiency. The temperature will also affect the energy within the system according to the first law of thermodynamics.

However, it's been shown that the microbes present in BES may be less temperature-sensitive than AD systems. Different species of microorganisms are dominant in the biofilm of BES, which are active in temperatures from 4^{o}C to 35^{o}C (Saratale et al., 2017).

BES can be used to treat a variety of waste streams from complex to simple substrates. The relationship between substrate and system performance is complex with reactors showing a diverse difference in microbial communities, coulombic efficiency and COD removal. Research suggests that reactors fed simple substrates such as acetate are not able to predict the performance of complex substrate reactors fed wastewater (Heidrich et al., 2017). The temperature coefficient (Q_{10}) for wastewater fed reactors was found to range from 1.1 to 1.6 (Ahn and Logan, 2010). Values of 1 indicate thermal independence whilst those greater than one and up to three show thermal dependence. Due to seasonal changes in temperature, the ability to sustain a consistent performance is critical. In the future, there may be novel ways to sustain higher temperatures for small-scale remote systems. Since bacteria, metabolic activity generates heat as a byproduct, and in research the temperature of the effluent was found to be higher than the influent (Heidrich et al., 2013a).

2.1.2 Biofilm Development

Biocatalysts used in BES offer a sustainable catalyst that can regenerate and adapt to the environmental conditions (Premier et al., 2016). All organisms depend on the combination of electron donors and acceptors through an oxidation and reduction process to support their energy requirements. The majority of organisms can only use soluble electron donors and acceptors. In some cases, insoluble and solid-state electron donors can be used. Using insoluble electron donors and acceptors requires extracellular electron transfer, which is a mechanism that allows the microbes to transport electrons from the donor within the cell to an acceptor outside of the cell (Philips et al., 2016). The group of microbes are called exoelectrogens, which are electrochemically active microorganisms. Exoelectrogens can transfer electrons extracellularly to iron and other metal oxides, carbon electrodes and other microbes (Logan and Regan, 2006). The solution conditions affect the development of the biofilm. If they are favourable to the electrochemically active biofilm, it can significantly increase system performance. However, this presents the risk that the environmental conditions can decrease microbial activity, leading to low performance and the destruction of the biofilm (Premier et al., 2016).

Electrochemically active microbes are found in various waste streams, including wastewater, sludge and sediments (Logan and Regan, 2006). Heidrich et al., hypothesises that a diverse range of microbes within the system may be critical to the performance (2017). Biodiversity increases the system stability during fluctuations of the system conditions (Babanova et al., 2017). It is difficult to measure and analyse all the complex interactions that take place within the biofilm due to the relationships between different microbial species. Mixed bio-cultures interact in a symbiotic nature for Extracellular

Electron Transfer (EET) to the anode (Read et al., 2010) and they also allow broader substrate utilisation (Babanova et al., 2017; Du et al., 2007). The composition of the microbes within the biofilm can alter vastly under the same conditions. Different microbial communities affect performance in different ways. Biofilms with lower exoelectrogenic microorganisms showed an increase in hydrogen production (Heidrich et al., 2014). The interactions of microbial community and system performance are relatively unknown and complex. There is an increasing need to understand the EET mechanisms used by different microbes to get a better understanding of why microbial composition affects performance.

Gram-Negative Bacteria (G-) have a thin peptidoglycan layer with an outer plasma membrane while Gram-Positive Bacteria (G+) have a thick peptidoglycan cell wall with teichoic acids. Most research has shown that G- species (i.e *Shewanella* and *Geobacter*) can transfer electrons without a mediator whereas G+ are commonly unable to, occasionally at a much lower performance than G- (Read et al., 2010). *Pseudomonas* (G-) produce phenazine-based metabolites, and G+ species can utilise these metabolites for EET and increase power production (Logan and Regan, 2006; Pham et al., 2008).

In early experiments of MFCs extraneous mediators were used to aid electron transfer from the microbes to the anode for species which cannot achieve EET directly. Mediators allow the transfer of electrons by shuttling between the anode and the microbe. In some cases, microorganisms can produce their own mediators like *Pseudomonas aeruginosa.* Anodophiles can directly transfer electrons to the anode, but EET is enhanced with the addition of mediators (Du et al., 2007). Other metal-reducing microbes can use the anode as an electron acceptor like *Shewanella, Rhodoferax* and *Geobacter* (Bond and Lovley, 2003a; Du et al., 2007; Philips et al., 2016). The same principle applies to the cathode for electrophilic microbes that can accept electrons from solid-state electron donors (Philips et al., 2016). *Shewanella* and *Geobacter* species produce conductive nanowires that contact the anode surface so they can directly transfer electrons without being on the anode surface. *Geobacter sulfurreducens* have long thin filament nanowires and *Shewanella oneidensis* MR-1 have bundles of nanowires that have multiple filaments. *Shewanella oneidensis* MR-1 rapidly produce these nanowires during the colonisation to touch the anode surface and other microbes (Logan and Regan, 2006).

Not all microbes within the systems are beneficial to performance. Exoelectrogens are also in competition with fermentative and methanogenic microorganisms. Both of which can diverge electron transfer from the anode to other electron acceptors like carbon, nitrate and oxygen (Premier et al., 2016), reducing the Coloumbic Efficiency (CE) of the system (Logan and Regan, 2006). Exposing the anode to air can reduce the methanogens that are anaerobes; however, it may also affect exoelectrogenic microorganisms like *Geobacter spp*. that are anaerobes (Call and Logan, 2008a).

Most lab BES systems are operated at mesophilic temperatures, as microbes are more active at this temperature range. However, most industrial wastewater is usually at lower temperatures. Acclimatising microbes at low temperatures allow them to adapt to the conditions, whereas systems inoculated at mesophilic temperatures tend to fail if the temperature is reduced dramatically (Heidrich et al., 2014). In low-temperature systems, the inoculation source could create mixed cultures that thrive better within the conditions, and artic soils that have extensive microbial communities can be used (Heidrich et al., 2017). Although research into the biofilm composition of a

pilot MEC found that the microorganisms present were almost identical despite the temperature fluctuations, (Heidrich et al., 2013a).

Alongside soils previously mentioned microorganisms could be found in multiple natural environments for BES including seawater (Hidalgo et al., 2015), bogs (Siegert et al., 2014a), rice paddy soils (Holmes et al., 2017; Li et al., 2020). *Geobacter* species directly supply electrons to *Methanothrix* species in rice paddy fields to support the reduction of CO_2 into CH_4 (Holmes et al., 2017). *Geobacter* species are widely known as one of the main microorganisms populating the anode in BES and are responsible for Direct Interspecies Electron Transfer (DIET). DIET is the free flow of electrons between cells through syntrophic metabolism without the need of shuttling electrons between reduced molecules such as hydrogen. The research demonstrated that they work with other microorganisms to support electron transfer allowing the generation of other chemicals, in this case, methane, which would make rice paddy soils a suitable inoculum for EMR systems.

DIET is relatively unknown, and it is thought that the pilli on species such as the *Geobacter sulfurreducens* were responsible for supplying the electrons to the anode. However, recent research into *Geobacter* species repressed the pili genes but not the extracellular cytochromes. The study found that the Gmet_2896 cytochrome of *Geobacter metallireducens* is a significant part of DIET, and conductive pili are not necessary for DIET to occur in cocultures of *Geobacter* (X. Liu et al., 2018)

The soil properties including pH, amorphous Fe and electrical conductivity (EC) have been found to affect MECs and the microbial community (Li et al., 2020). Soils with high EC were found to reduce overpotentials in MEC biocathodes. The higher EC soils also had a higher concentration of electrotrophs which can receive electrons from the cathode in MECs and are crucial for bioremediation. The dominant electrotrophic species found on the enriched MEC cathodes were Firmicutes bacterial phylm and with this *Bacillus* genes. Soils with pH of 5.2-6.7 had higher electrotrophic species and soils with amphorous Fe of 16.22g/Kg of dry soil may support the microbial community within the soils (Li et al., 2020). The research supports the argument that bacteria found in the environment are well suited as an inoculum source in MFC, MEC and EMR systems. More research into soil properties may allow quick identification of possible inoculum sources.

2.1.3 Applications of BES for Wastewater treatment

Alongside energy and nutrient recovery, BES can have been shown to have other benefits. Antibiotics and pharmaceuticals are another factor that needs considering in wastewater treatment. The field has gained interest due to antibiotic contaminants considered as an emerging contaminant and raises serious public health issues due to antimicrobial resistance (Baker et al., 2018). There have been multiple studies exploring the ability of BES to remove antibiotics from wastewater. BES are a promising solution for antibiotic removal due to the microbial metabolism coupled with the electrochemical redox reactions (Yan et al., 2019).

Removal antibiotics is an alternative treatment solution and will likely require different operational and physical parameters such as electrode material. However, there is limited research into different electrode materials with only one study exploring different foam metal cathodes to break down

Chloramphenicol (CAP). The study found that copper foam was more effective than carbon rod and nickel foam, removing 100% of 32mg/L of CAP at a Vapp of 0.5 V in just 12 hours (Wu et al., 2017). Temperature and pH also affect CAP removal, and optimal conditions were found to be a pH of 7.12 at a temperature of 31.48^{o}C, removing 96.53% of CAP in three days with a concentration of 106.37mg/L (Zhang et al., 2017). Antibiotic resistance genes are diverse, and further research into the interaction with BES is required (Yan et al., 2019)

Metal contamination is another health hazard, as they are non-biodegradable and can accumulate in natural resources. Bio-electrochemical systems show promise for recovering and removing metal from wastewater streams (Nancharaiah et al., 2015). BES can remove heavy metals through biosorption, bio-electrochemical reduction, bioaccumulation and biomineralisation (Nancharaiah et al., 2015). The bio-electrochemical pathway requires a carbon source at the anode to complete the electron transfer sequence and reduce heavy metals (Jugnia et al., 2019). Both MFCs and MECs can remove heavy metals. MFCs have been shown to remove chromium (Wang et al., 2008), cobalt (Huang et al., 2013a), copper (Tao et al., 2011), mercury (Wang et al., 2011) and silver (Yun-Hai et al., 2013) to name a few. While MECs have been shown to remove cadmium (Choi et al., 2014), cobalt (L. Jiang et al., 2014), nickel (Qin et al., 2012), chromium (Huang et al., 2010), zinc, iron, aluminium and lead (Jugnia et al., 2019).

GAC is also regularly used as an absorption material for various gases and pollutants in wastewater. As a result, GAC electrodes show promise as they can also support biofilm growth for both biotic anode and cathodes. MECs using GAC electrodes have been shown to remove up to 99% of Cu, Zn, Pb, Al & Fe at a HRT of 4-6 days from wastewater collected at a firing range. The MEC removed the metals through bio-electrochemical pathways and sulphur, reducing bacteria (Jugnia et al., 2019). The study used a peat moss layer to provide a slowly degrading carbon source that required replacing for the anodic biofilm and the sulphur reducing bacteria in both the MEC and GAC control. Integrating a modified GAC electrode for heavy metal removal as a tertiary treatment for both sludge and wastewater could increase the attractiveness of BES to demonstrate both energy recovery and complex pollutant removal. Wastewater from food and drinks industries and urban communities will contain a carbon source readily available for the microorganisms within the system, simplifying the reactor design.

Alongside pharmaceuticals and heavy metals, synthetic chemicals in wastewater present risk to human health and environmental degradation. Often synthetic chemicals are found in industrial, agricultural and household wastewaters such as endocrine-disrupting compounds, detergents, plasticisers, surfactants, food additives, dyes, disinfectants, pesticides and insecticides (Chakraborty et al., 2020). The majority of research into BES to remove these emerging pollutants has focused on textile wastewater to remove dyes (Cui et al., 2020; Liang et al., 2018). Research shows that combining BES to treated mixed dye waste can increase performance. A MEC (Granular Graphite electrodes at a Vapp of 0.5) followed by an Aerobic Biofilm reactor and denitrification reactor were optimised to treat azo dye, anthraquinone dye, and triarylmethane dye, whilst the denitrification stage was vital in decolourisation and further reducing COD (Cui et al., 2020). 4-Chlorophenol is derived from pesticides and other chlorinated compounds, MFCs have been shown breakdown 4-Chlorophenol at a rate of 0.58 ± 0.036 mg/L/h from concentrations of 25mg/L (Huang et al., 2013b). The system demonstrated co-metabolically mineralisation, whilst the current generation from the

MFC accelerated the degradation via phenol production, which was further degraded. Going froward BES do show promise of synthetic chemical removal through oxidation and mineralisation and is another promising benefit of these emerging technologies.

2.2 Microbial Fuel Cells

Fuel cells have sparked much interest due to their ability to produce carbon-neutral energy and are viewed as a vital part in a clean energy future. The majority of research, however, has mainly focused on hydrogen fuel cells (HFC). HFCs use hydrogen as a feedstock to produce electricity. HFCs require expensive materials making them economically unsuitable for many applications. MFCs were first explored by Potter (1911), although it was not until the 1980s that research in the field gained momentum when it was discovered that current density and power output could be increased with electron mediators (Du et al., 2007). Although the power density of MFCs is considerably lower than chemical fuel cells due to the chemical energy present in substrates suitable for MFCs. MFCs must also sustain the microbial population, requiring water and inorganic nutrients which increase internal resistance (Kim et al., 2007). The development of MFCs are still in their infancy and need to overcome a variety of challenges before they become commercially viable. The challenges include; inoculating with efficient microbial communities, optimisation of EET, architecture (membranes and chamber design), integration of MFCs into the wastewater treatment process and economical system scale-up (Keshavarz et al., 2019).

In a basic MFC shown in Figure 2-1, both the anode and cathode are submerged in aqueous solutions separated by a membrane. Microorganisms form a biofilm on the anode which oxidise the organic matter within the wastewater acting as an electron donor. During the oxidation, the microbes produce electrons and protons. An electrical current is produced due to the microbes on the biofilm transferring the electrons to the anode. The electrons go through a circuit to the cathode (electron acceptor) which is at a higher electrochemical potential. Within the cathode chamber, both the protons and electrons are consumed during a reduction reaction of oxygen to water (K Scott, 2016). Ions are transferred through three mechanisms (K. Scott, 2016):

1. Convection - Ion transfer through the mechanical motion of the electrolyte
2. Electric Migration – Ion transfer through an electric potential gradient
3. Diffusion – Ion transfer though a potential chemical gradient

MFCs have advanced in architecture design implementing air cathodes which remove the need for oxygen flowing through the cathode chamber (Fan et al., 2007; Shaoan Cheng et al., 2006; X. Zhang et al., 2015). MFCs offer high particulate COD reduction >89% for a variety of waste streams at varying temperatures (Ahn and Logan, 2010). Although at a certain level of COD, the energy recovery drops below a useful limit, making other treatments more suitable (Zhang et al., 2015).

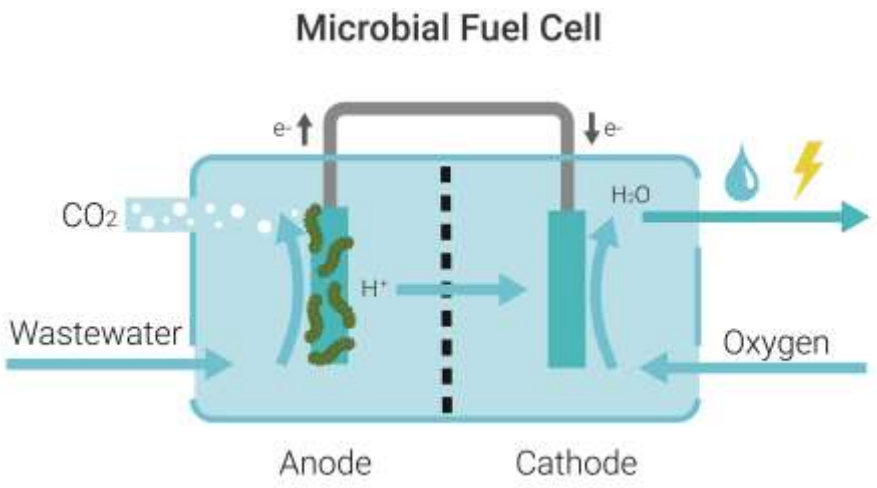

Figure 2-1: Microbial Fuel Cell diagram showing the biofilm on the anode breaking down the organic compounds within the substrate producing carbon dioxide and H+, which migrates to the cathode and is oxidised to form water.

2.2.1 Reactions in MFCs

Within the MFC anodic oxidation and cathodic reduction reactions take place, the potential difference between these reactions within the MFC regulates the power output. The oxidation and reduction reactions that take place depend on the feedstock, where almost all biodegradable organic substances can be used for the oxidation (Bajracharya et al., 2016). Equation 2-1 to Equation 2-4 show the oxidation reactions, and Equation 2-5 to Equation 2-13 show the reduction reactions that take place during the treatment of wastewater within an MFC (Gude, 2016). The Standard electrode potential (E0) is shown and compared to the Standard Hydrogen Electrode (SHE). SHE is used as a reference for half-cell reactions and has a standard electrode potential of zero.

Oxidation Reactions (Anode)

Equation 2-1	*Glucose:* $C_6H_{12}O_6 + 12H_2O \rightarrow 6HCO_3^- + 30H^+ + 24e^-$	E° *= -0.429 V vs. SHE*
Equation 2-2	*Glycerol:* $C_3H_8O_3 + 6H_2O \rightarrow 3HCO_3^- + 17H^+ + 14e^-$	E° *= - 0.289 V vs. SHE*
Equation 2-3	*Malate:* $C_4H_5O_5^- + 7H_20 \rightarrow 4H_2CO_3 + 11H^+ + 12e^-$	E° *= -0.289 V vs. SHE*
Equation 2-4	*Sulphur:* $HS^- \rightarrow S^0 + H^+ + 2e^-$	E° *= -0.230 V vs. SHE*

Reduction Reactions (Cathode)

Equation 2-5	$O_2 + 4H^+ + 4e^- \rightarrow 2H_2O$	E° *= + 1.230 V vs. SHE*
Equation 2-6	$O_2 + 2H^+ + 2e^- \rightarrow H_2O_2$	E° *= + 0.684 V vs. SHE*

Equation 2-7	$NO_3^- + 2H^+ + 2e^- \rightarrow NO2^- + H_2O$	*E° = + 0.433 V vs. SHE*
Equation 2-8	$NO_2^- + 2H^+ + e^- \rightarrow NO + H2O$	*E° = + 0.350 V vs. SHE*
Equation 2-9	$NO + H^+ + e^- \rightarrow 1/2N_2O + 1/2H_2O$	*E° = + 1.175 V vs. SHE*
Equation 2-10	$1/N_2O + H + e^{-+} \rightarrow 1/2N_2 + 1/2H_2O$	*E° = + 1.355 V vs. SHE*
Equation 2-11	$2NO_3^- + 12H^+ + 10e^- \rightarrow N2^+ 6H_2O$	*E° = + 0.734 V vs. SHE*
Equation 2-12	$Fe^{3+} + H^+ + e^- \rightarrow Fe^{2+} + 1/2H_2O$	*E° = + 0.773 V vs. SHE*
Equation 2-13	$MnO_2 + 4H^+ + 3e^- \rightarrow Mn^{2+}\ 2H2O$	*E° = + 0.602 V vs. SHE*

Wastewater COD Removal

Wastewater is a complex substrate with a combination of suspended solids with readily and slowly degradable COD components. Zhang et al., found that the first 4 hours of treating domestic wastewater with an MFC showed a high current production that dropped in the following 4 to 24 hours. The results were similar for both filtered wastewater which contained only Soluble COD (sCOD) and raw wastewater which had a total COD. The COD removal was similar when the cells were under current production and open-circuit conditions. The study found that the HRT for wastewater should not be longer than 8 hours (Zhang et al., 2015).

2.2.2 Measuring Performance in MFCs

Electrochemical methods are used to measure the performance of MFCs. Compared to chemical fuel cells, the additional microbial community and the biological influences make measuring performance difficult in comparison. Using one or two reference electrodes as well as the anode and cathode can help explain the variety of different limiting factors in the system; including exoelectrogens activity, EET, overpotential losses, impedances and cathode efficiency (Premier et al., 2016). Using just the anode and cathode (2 electrode system) gives an overview, whereas the addition of reference electrode which has a well known electrode potential means the anode and cathode characteristics can be controlled (Premier et al., 2016).

2.2.3 Rate limiting Factors in MFCs

Multiple limiting factors need considering when designing MFCs and their possible applications.

A low organic concentration within the wastewater can limit the performance of the anode biofilm. Whilst the wastewater conductivity can affect the ion transfer from the anode to the cathode. Increasing the concentration of organics increases the available chemical energy. As concentrations

increase the power density also increases up to a peak (1 g/L acetate), at this point increases in concentration levels plateau and show no further power increase (Cheng and Logan, 2011a). The peak energy output could be a result of the anode size and biofilm density, which could limit the redox reactions within the cell. Concentration levels affect the anode potential by increasing its negativity as concentrations go up, which will increase the power density (Cheng and Logan, 2011a).

The composition within the feedstock also determines the availability of energy that the microbes can harness. Exoelectrogens have shown good performance for energy recovery when Volatile Fatty Acids (VFA) are in high concentrations. In particular acetate, a short-chain fatty acid, has been tested extensively within MFCs due to its easy digestibility by micro-organisms. Research has explored that potential pre-treatment of substrates may increase the conversion of complex substrates to VFAs and increase the solubilisation of COD (Premier et al., 2016). The conductivity of wastewater is another limiting factor in inhibiting system performance. Wastewater conductivity is typically 1.7 μS/cm, which impedes the potential power output of the system, where 107% power increase was observed when conductivity was increased to 7.8 μS/cm (Cheng and Logan, 2011a), making some substrates more suitable than others.

The temperature could be seen as a limiting factor in MFCs because most bacterial systems operate at mesophilic and even thermophilic temperature ranges to increase efficiency. MFCs operated under mesophilic conditions (30 ± 1˚C) where shown to have higher COD degradation for both total COD and particulate COD, and higher nitrogen removal rates (Ahn and Logan, 2010). However, BES has operated in temperatures as low as 4℃. The inoculation period is key as microorganisms need to form a biofilm at the desired operating temperatures (Heidrich et al., 2013a). Using inoculums containing microorganisms found in conditions that are similar to the operational temperature is important; for example, arctic soils have exoelectrogens present that has adapted to cold conditions and could be used within BES (Heidrich et al., 2017).

2.2.4 Architecture

The architecture of the cell can play a significant role in the performance of the MFC. The research into the system architecture can include material cost reduction, increased stability to reduce bio-inhibition and scalability. Changing the cell design/architecture can reduce the ohmic resistance and increase performance through electrode spacing, increase mixing for mass transfer and activation losses are dependent on material properties (Premier et al., 2016). The first MFCs used a two-chamber design with a membrane between them to stop oxygen diffusion into the anode chamber, which is under anaerobic conditions. Typically, Polymeric Proton Exchange Membranes (PEM) are used to allow H^+ ions to transfer to the cathode chamber. Two-chamber systems require oxygen to be pumped into the aqueous cathode chamber, which combines with the H^+ ions to form water acting as the proton collector (Du et al., 2007).

A significant issue with a membrane is the hindrance of proton transfer from the anode to the cathode. The membrane results in an accumulation of protons in the anode chamber and negatively charged ions in the cathode chamber, resulting in a pH difference between the chambers (Gude,

2016). Rozendal et al., looked into the cation transfer through a Nafion 117 membrane which is commonly used in MFCs. The study found that the number of cations (K^+, Na^+, $NH4^+$, Mg^{2+}, Ca^{2+}) that transferred from the anode chamber to the cathode chamber equalled the electrons transferred through the external circuit (Rozendal et al., 2006a). Cation transport is due to an electrodialysis process, resulting in very low proton transfer in the MFC, and the cation transfer is maintaining the system electroneutrality (Kim et al., 2007). During operation of the MFC, the membrane can become soiled, and a build-up of a biofilm and salt precipitation will reduce its performance. Membranes with larger pore sizes are less affected by this and are a more promising option for long term use (S. Zhang et al., 2015). Proton mass transfer is the main constraint in an MFC, where proton diffusion is slow in an aqueous phase. Electrolytes with a higher salt concentration speed up the process in a membrane-less system but hinder proton transfer through a membrane as previously mentioned (Kim et al., 2007).

The dual-chamber MFC has an intricate design with additional components making them more challenging to scale, more expensive and more likely to fail. Single chamber systems can reduce the architecture complexity by removing the membrane and aeration, reducing the system cost (Du et al., 2007). Most research assessing commercial systems has explored single chamber air cathode systems because they do not require aeration like aqueous cathode systems (Premier et al., 2016). Proton Exchange Membranes (PEMs) can be directly applied to the cathode. However, the membrane increases internal resistance within the cell and therefore by removing the PEM altogether, the maximum power density will increase. However, with the PEM removed the coulombic efficiency deceases due to oxygen diffusion into the anode chamber (Liu and Logan, 2004). Reducing oxygen within the anaerobic anodic chamber increases the overall coulombic efficiency as the oxygen can lead to aerobic oxidation of the substrate. Adding diffusion layers to the air cathode can reduce oxygen diffusion and can stop water loss due to leakage (Cheng et al., 2006).

A variety of parameters, including pH and temperature, can affect the equilibrium potential (*Ee*) of an electrode at open-circuit conditions. These can be calculated using the Nernst Equation (Equation 2-15)

Equation 2-14

$$E_e = E° + 2.303 \frac{RT}{nF} log \frac{C_O}{C_R}$$

E˚ = the standard potential at pH 0, R is the molar gas constant (8.314 J/mol/K), T is the temperature (K), n is the number of electrons transferred, F is the Faraday's constant (96,485 C/mol), C_O and C_R are the concentration of the oxidised and reduced products at the electrode surface (Bajracharya et al., 2016).

Electrode Spacing

The electrode spacing plays a significant role in the MFC performance. Increasing the distance between the anode and cathode increases the internal resistance within the system. However, the performance is dependent on whether the system is in batch or flow mode, and the direction of flow. During batch mode the system showed to have a decrease in performance with a 1 cm spacing, this is

due to the increase in the Open Circuit Potential (OCP) of the anode, whereas the OCP and Open Cell Voltage (OCV) of a system in continuous flow were constant. The effect of the OCV on power is shown in Equation 2-16 (Shaoan Cheng et al., 2006).

$$P = \frac{OCV^2 R_{ex}}{A(R_{int}+R_{ex})^2} \qquad \textit{Equation 2-15}$$

A is the surface area of the electrode (projected surface area). The change of the OCP within the batch system is due to the increased dissolved oxygen (DO) within the system leaching from the air cathode. With the increased distance between the cathode and anode in this scenario, the performance increases (Shaoan Cheng et al., 2006). The oxygen competes with the microorganisms within the MFC, oxidising the organic compounds within the system and affecting the growth of the anaerobic microorganisms. When the flow was directed through the anode at a 1cm electrode spacing, the power density of the system increased, and there was no dissolved oxygen found near the anode (Shaoan Cheng et al., 2006). Having the substrate flow directed through the anode to the cathode could increase the chances of the anode clogging if the substrate has a suspended solids content, and where carbon cloth anodes may not be suitable. In this case mixing within the chamber can help remove these issues.

Anode

Different materials have been explored for the anode material; typically, they are carbon or graphite-based cloth, paper, granules, fibre and brushes. Increasing the surface area of the anode can increase the biofilm area, which can lead to increased cell performance (Dumitru and Scott, 2016). Initially, mediators were used within MFCs, as most bacteria are unable to release electrons to the anode (Ieropoulos et al., 2005). Synthetic redox mediators (neutral red, methylene blue, thinonine, meldola's blue and 2-hydroxy-1 ,4-naphthoquinone) were used first (Park and Zeikus, 2000; Roller et al., 1984; Tayhas et al., 1994). However, these are not sustainable, going forward due to their toxicity. Natural mediator properties of sulphate/sulphide were then explored (Habermann and Pommer, 1991) before mediator-less MFCs were introduced when it was found that *Geobacter sulfurreducens* and *anodophile* species form a layer on the anode allowing it to transfer electrons directly to the anode (Bond and Lovley, 2003b). Synthetic mediators were found to have the lowest performance compared to natural mediators and mediator-less MFCs and also present other risks due to their toxicity. The sulphate/sulphide mediators showed potential as they are naturally present in wastewater, which will replenish the system. As they are naturally occurring they can also boost performance within mediator-less MFCs. Besides the mediator-less MFCs showed the most promise as they do not require any inputs solely relying on the microbial EET (Ieropoulos et al., 2005).

Pre-treating the anode with ammonia gas and heat treatment increases the biofilm adhesion to the anode. The increased adhesion is due to the increased charge on the anode, which reduces the inoculation period by 50%. The treatment increases the electron transfer from the biofilm to the anode, which results in a higher power density. The process requires high-temperature ammonia and helium gas treatment (Cheng & Logan, 2007). The process was deemed to be too complicated for the minimal performance increase and is no longer used by the researchers. However, it does show that

surface treatments offer an exciting pathway to increase the performance of low-cost anodes. New approaches to designing electrodes can include; (i) larger specific surface area of nitrogen/metal-doped carbon structures, (ii) nitrogen-doped, 3D porous carbon with metal nanoparticles, (iii) binary/ternary metal composition on a large surface area of carbon structures, (v) incorporating of metal nanoparticles into the porous structures (Palanisamy et al., 2019). Surface treatments could show promise, however researchers should consider the by-products to ensure they will not have an environmental impact.

Cathode

A variety of chemical redox reactions can take place at the cathode in MFC, although Oxygen Reduction Reaction (ORR) offer the best cathode reaction for MFCs due to its positive redox potential and the abundance of oxygen; although ORR is limited due to the low oxygen solubility in electrolytes (Bajracharya et al., 2016). Alternative redox couples to ORR have been explored, which offer greater mass transfer efficiencies such as ferri/ferrocyanide (Bajracharya et al., 2016; Oh et al., 2004). However, these chemicals are not sustainable due to their toxicity (Rabaey et al., 2005). A method to tackle the low oxygen solubility is to implement air cathodes into MFCs, where this issue is removed (Oh et al., 2004).

Platinum (Pt) catalysts have been used in fuel cells, but they are susceptible to lower performance or 'poisoning' in the presence of Cl^-, HSO_4^-, HPO_4^{2-} and HS^-, which are present in some of the waste streams used in MFCs, and could be part of the reason why non-Pt catalysts have similar performance (Zhao et al., 2009). Much research has focused on developing alternative ORR catalysts to Pt due to the considerable cost (Premier et al., 2016), which can hinder commercialisation as it is not justifiable given the low power output. A variety of catalysts have been tested including cobalt and iron and co-naphthalocyanine which have shown comparable results to Pt, but activated carbon seems to be the most promising alternative (Premier et al., 2016). The ability to use low-cost catalysts is one of the advantages in MFCs making them more economically viable. The high cost is a barrier when introducing new technology and has hampered the widespread introduction of hydrogen fuel cells, which are slowly decreasing in price. Although a Pt catalyst is recommended if the coulombic efficiency of the system is high due to the increased performance and energy output; justifying the higher cost (Trapero et al., 2017).

Introducing diffusion layers onto the cathode increases the performance, due to the decrease in water flooding of the catalyst. Diffusion layers have two purposes, to reduce oxygen permeability into the system and reduce water loss through the air cathode. Reducing oxygen into the system stops aerobic oxidation of the substrate, which competes with the oxidation reactions at the anode. This is less of an issue if there is a short HRT or if the power density is high as there is less time for aerobic oxidation and minimal power losses will occur (Cheng et al., 2006). Two methods have proved to be the most successful; a PTFE and carbon diffusion layer (Cheng et al., 2006), and a PVDF diffusion layer (Yang et al., 2014). Using four-layer PTFE and carbon diffusion layers increased the maximum power density by 42% (766 mW/m^2) thought to be due to a three-phase interface for oxygen reduction. The coulombic efficiency also increased by 200%. At two layers, oxygen permeability was reduced, but at

four, no water loss was measured (Cheng et al., 2006). The MFC durability and performance is affected by the diffusion layer porosity as high percentage porosity can have an initial higher power production (70% porosity - 1214 ± 2 mW/m^2) this decreases over time (1 year 40% decrease to 734 ± 2 mW/m^2) as a biofilm builds up reducing the catalysts SA. A 30% porosity diffusion layer only had a 22% reduction over the year from 1014 ± 2 mW/m^2 to 789 ± 63 mW/m^2. The biofilm can be cleaned increasing the partial initial performance of 12% (70%) and 11% (30%) in power production, with fresh cathodes the performance increased to the original, highlighting the cathode and not the anode degradation (Zhang et al., 2011).

2.2.5 Challenges for Scale Up

Typically AD generates 1 kWh for every 1 kg of COD, which equates to a power density of 400 W/m^3, whereas MFCs could theoretically generate four times this value (Pham et al., 2006). Setting a power density of 400 W/m^3 would demonstrate that MFCs can compete with AD in terms of energy recovery. Currently, the electricity produced by MFCs is minimal, especially when compared to chemical fuel cells. Increasing the size does not increase the energy output, so scaling is envisaged to be multiple MFCs connected in a parallel and series combination (Ieropoulos et al., 2013; Jiang et al., 2011; Premier et al., 2016). Another method to achieve commercial power output is to use small liquid volumes and electrode spacing (Cheng and Logan, 2011a). Other considerations should be considered when scaling up MFCs for industrial use as this will impact the design of the system. Deciding the required outputs such as high power output of low COD levels need to be confirmed as this will affect the system.

The cathode specific SA is the most critical factor for scaling up MFCs to achieve high power densities (Cheng and Logan, 2011a), but the cathode size will not increase COD removal as it is solely responsible for the ORR and not the redox reactions which are responsible for COD removal and take place at the anode (Premier et al., 2016). Changing the electrode has different effects due to the different oxidation or reduction reactions taking place. Doubling the cathode SA was shown to increase power by 50% more than doubling the anode SA (Cheng and Logan, 2011a), which could be due to oxidation of ions be a rate-limiting factor. Developing low-cost systems is one of the barriers and reducing the cost of electrodes and membrane will reduce scaleup challenges (Palanisamy et al., 2019)

2.3 Microbial Electrolysis Cells

Two research groups discovered that MFCs with an additional voltage were able to produce hydrogen, these technologies where called MECs (Liu et al., 2005a; Rozendal et al., 2006b). MECs operate in a similar way to MFCs using an anaerobic anode chamber with exoelectrogenic microbes. The microbes are grown on the anode to collect electrons from the oxidation of organic matter, producing an electrical current. The electrons are transferred to the cathode via a circuit and the protons (H^+ ions) transfer to the cathode side, which, unlike MFCs, is anaerobic to prevent the H^+ ions

reducing to water. The applied voltage increases the electrode potentials allowing the formation of hydrogen on the cathode from the H^+ ions (Cotterill et al., 2016). One of the main advantages of MECs compared to water electrolysis is that the oxidation of organic compounds requires lower redox potentials. Water electrolysis requires -1.229 V at 25oC at pH 0, however modern-day electrolysers require a cell voltage of 1.8 – 2.2 V (Subramani et al., 2016), compared to MEC which can operate between 0.6 – 1.2 V.

Hydrogen production from electrolysis usually requires high energy input to force the chemical reactions required. The combination of the energy input and the energy produced by the biofilm reduces the electrical input required compared to water electrolysis and higher at higher efficiencies than fermentation (Cotterill et al., 2016). MECs offer an attractive option for wastewater treatment with simultaneous hydrogen production.

There are multiple key components to consider when analysing MECs for wastewater treatment and energy production; strength of feedstock, anode and cathode materials, system architecture, outputs, cost, water consumption and footprint. These will affect the system performance and the economic viability of commercialising the technology (Rabaey, 2009).

2.3.1 Mechanism of Microbial Electrolysis Cells for Wastewater Treatment

MECs use a bio-catalytic process to produce hydrogen. The biofilm on the anode will break down organic compounds such as acetate into CO_2, H^+ ions and electrons shown in Figure 2-2. The applied voltage directs the flow of electrons and increases the electrode potentials. At the anode, Electrochemically Active Microbes (EAM) grow to form a biofilm which uses electrical energy to oxidise organic matter to CO_2, as shown in Equation 2-17 (Kadier et al., 2016a). The additional current applied to the cathode, allows the production of hydrogen from the H^+ ions, as shown in Equation 2-18 & Equation 2-19 (Cotterill et al., 2016). The current can be from varying sources included from the energy generated if it is converted into electricity. Figure 2-2 shows the underlying architecture of a MECs, with an anodic and cathodic chamber with a membrane to separate the two chambers. The membrane forms multiple functions, increasing hydrogen purity, reducing microbial crossover and hydrogen evolution to methane (Kadier et al., 2016a). The anodic chamber is fed wastewater, and the cathodic chamber will typically contain a catholyte to reduce resistance and increase current densities, especially if it is also recirculated (Kim et al., 2017).

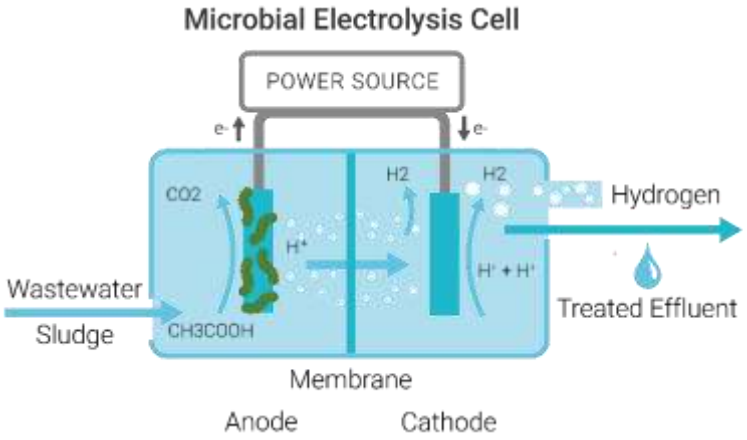

Figure 2-2: Schematic of a dual-chamber Microbial Electrolysis Cell for treating wastewater to produce hydrogen, with a membrane separated anode and cathode chamber connected via an external power source.

Anodic Reactions

Equation 2-16 *Anode:* $C_2H_4O_2 + 2H_2O \rightarrow 2CO_2 + 8H^+ + 8e^-$

Cathodic Reactions

Equation 2-17 *Acidic Conditions:* $2H^+ + 2e^- \rightarrow H_2$

Equation 2-18 *Alkaline Conditions:* $2H_2O + 2e^- \rightarrow H_2 + 2OH^-$

Bioelectrochemistry is used to treat wastewater and produce methane via a process called electromethanogenesis. MECs can be used for methane production, using a biocathode with a methanogenic biofilm to generate methane from the H_2 and CO_2. These types of cells are called Electro-Methanogenic Reactors (EMR). Inside the EMRs the anode and cathode are connected to a power source, under anaerobic conditions the same as MECs. Within the EMRs, the cell architecture can be simplified by removing the membranes because methane evolution is preferred over hydrogen, as shown in Figure 2-3.

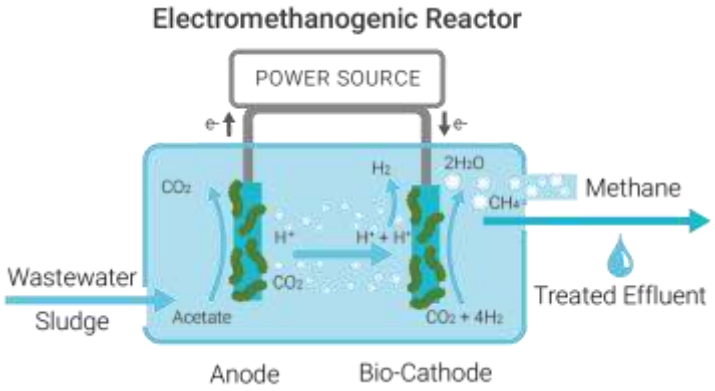

Figure 2-3: Schematic of an anaerobic Electro-Methanogenic Reactor for treating wastewater to produce methane showing the wastewater influent and effluent and an anode and cathode connected to a power source.

Unlike MECs, methane production takes place at the cathode. There are several different pathways to methane production through direct or indirect electron transfer (Kadier et al., 2016a), as shown in Figure 2-4.

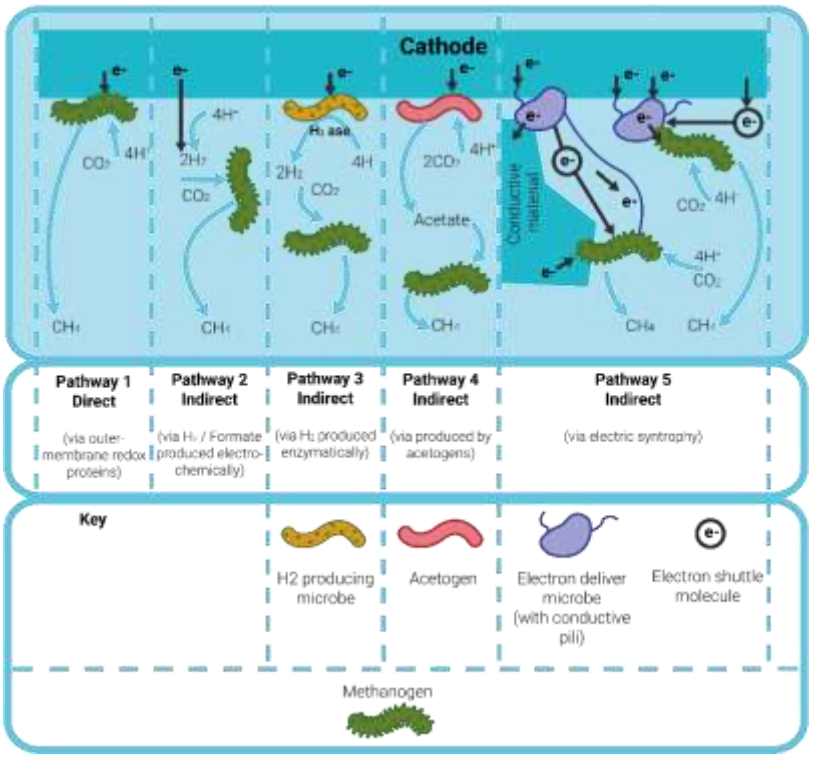

Figure 2-4: Schematic outlining the possible routes of methanogenesis for methane production. Pathway 1: direct electron transfer, Pathway 2: indirect electron transfer via electrochemically produced H_2, Pathway 3: indirect electron transfer via enzymatically produced H_2, Pathway 4: indirect electron transfer via biologically produced acetate and Pathway 5: indirect electron transfer via electric syntrophy. Schematic adapted from (Blasco-Gómez et al., 2017).

Direct Methanogenesis

There is one pathway for direct methanogenesis, as shown in the first pathway in Figure 2-4. In the pathway, methane is directly produced from CO_2 via outer membrane redox proteins that are in direct contact with the electrode (Blasco-Gómez et al., 2017).

Indirect Methanogenesis

Alternatively, indirect electron transfer methanogenesis proceeds via the production of an intermediate. Indirect methanogenesis takes place either via pathway 2, 3 or 4, as shown in Figure 2-4. Pathway 2 involves the intermediate production of hydrogen either electrochemically or bioelectrochemical, to produce methane through hydrogenotrophic methanogenesis (Villano et al., 2010). Pathways 3 and 4 involve biologically produced formate or acetate, producing methane via acetogenic methanogenesis (Nevin et al., 2011). Pathway 5 involves the interspecies electron transfers by electron carriers or nanowires (Blasco-Gómez et al., 2017).

Thermodynamically, methane can be produced by direct electron transfer at relatively low voltages (Anirudh Bhanu, 2019). However, in practice, this is very energy-intensive due to the high electrode potentials and the lack of an appropriate catalyst to reduce electrode overpotentials (Cheng et al., 2009). Methane generated in anaerobic digestors mainly originates from acetate (~70%) via acetotrophic methanogenesis where acetate is produced as an intermediate. However, analysis of the microbial consortium present at the cathode in an EMR, indicated that intermediate hydrogen production was favoured (Saheb-Alam et al., 2018). Villano *et al.* demonstrated that only a fraction of methane produced was via direct electron transfer with the majority from H_2-mediated methanogenesis via hydrogenotrophic methanogens (2010). The route to methane production is a crucial factor to consider when evaluating cathode materials. If H_2-mediated methanogenesis is favoured, then the hydrogen evolution ability of a material is crucial. Cathode materials, therefore, can be seen as acting as both catalysts and biocatalysts, by enhancing electrode-microbe electron transfer which improves the rate of formation of products (Zhang et al., 2013).

2.3.2 Review of MECs for Wastewater Treatment

The promise of MECs has led to an increase in research within the field. Table 2-1 shows various studies that are progressing to larger-scale systems. A full table of all experiments analysed in the research is in appendix 13.1, Table 13-1. The studies can be split into two groups; larger benchtop systems (8-100L) and pilot-scale (>100 L). The benchtop and pilot systems show different performance characteristics with no system excelling in all areas. The highest COD removal (%) was 78% for benchtop and 65.6% for a pilot (Escapa et al., 2016b), although there where multiple pilots showing above 60% efficiency (Cotterill et al., 2017a; Cusick et al., 2011a; Escapa et al., 2016b). The highest hydrogen purity reached 98% in benchtop systems (San-Martín et al., 2019) and 100% at pilot scale (Heidrich et al., 2014). The highest cathodic efficiency was 78 – 84% at benchtop scale (San-Martín et al., 2019) and 55% at pilot scale (Escapa et al., 2016b; Heidrich et al., 2013b).

The smaller systems generate higher energy output per volume when normalised compared to larger pilot systems. For easier comparison, the gas production rate, composition (H2% and CH4%) and the net calorific value of gases present are used to calculate the normalised net energy production. For urban wastewater, the benchtop study generated a normalised net energy production of 25.96 kWh/day/m3 with an unknown electrode to volume ratio (Carlotta-Jones et al., 2020). The pilot-scale system generated a normalised net energy production of 0.011 kWh/day/m^3 at a scale of 130L with an anodic surface area of 1.63 m^2/m^3 and a cathodic surface area of 2.72 m^2/m^3 (Baeza et al., 2017). There is a large difference, and it is difficult to understand if the reactor design is a contributing factor if the wastewater varied in some aspects due to some information not within the articles.

Higher-strength feedstocks lead to an increase in energy production. Normalised net energy production of 76.2 kWh/day/m^3 was achieved for pig slurry at a 16 L scale with an anodic and cathodic surface area of 11.25 m^2/m^3 (San-Martín et al., 2019). At a 1000L pilot scale, the net energy production was calculated to be 2.11kWh/day/m3 for winery wastewater with a cathodic surface area of 18.1 m^2/m^3 (Cusick et al., 2011a). It is difficult to compare studies with different substrates due to the substrate containing varying compounds that may or may not be easily digestible by the microbial consortium.

There is still a lot to learn about scaling up benchtop systems towards the pilot scale and then industrial scale. One barrier to scaling up is the difficulty in comparing different setups in the research accurately. The reactor size is only one parameter and does not give an accurate representation of the system scalability. Including details in the research such as organic loading rate and the electrode surface area to reactor volume ratio can help in providing a more comparative context between studies, aiding research-informed MEC scale up.

Table 2-1: Large Benchtop and Pilot MEC's Overview

Substrate / Feedstock (inoculum Source)	*Scale (L)*	*Anode (Specific Anode Surface Area (m^2/m^3))*	*Cathode (Specific Cathode Surface Area (m2/m3))*	*HRT (hrs)*	*Voltage Applied (V)*	*Temp (C)*	*Normalised Volumetric gas Production (m^3 gas/m^3 reactor volume/day)*	*Energy Production (MJ/d/m^3)*	*Cathodic Coulombic Efficiency (%)*	*COD Removal (%)*	*Author*
Urban WW	Estimated - 8	Carbon Fibres & Titanium plate +	SS Wool	8	1.0		0.0198	21.41		24.55	(Carlotta-Jones et al., 2020)
Urban WW	Estimated - 8	Carbon Fibres & Titanium plate +	SS Wool	8	1.0		0.0000	0.00		24.63	(Carlotta-Jones et al., 2020)
Urban WW	Estimated - 8	Carbon Fibres & Titanium plate +	SS Wool	8	1.0		0.0668	72.11		27.40	(Carlotta-Jones et al., 2020)

Urban WW	Estimated - 8	Graphite Felt	SS Wool	8	1.0		0.0037	3.94		13.05	(Carlotta-Jones et al., 2020)
Pig Slurry (Urban WW Digestate)	16	Graphite Felt (0.18)	SS Mesh (0.18)	48 - 124	1.0	19.2	0.2	211.68	78 - 84	-	(San-Martín et al., 2019)
Urban WW (Urban WW)	30	Graphite Felt (32)	SS Wool (13)	5	0.9	9 - 16	0.041		-	62.5	(Cotterill et al., 2017a)
Urban WW (Urban WW + Acetate)	120	Carbon Felt (16.4)	SS (3.4)	24	1.1	1 - 22	0.007	0.07	41	44	(Heidrich et al., 2014)
Urban WW (Urban WW + Acetate)	120	Carbon Felt (16.4)	SS Wool (3.4)	24	1.1	13.5 - 21	0.015	0.16	55	34	(Heidrich et al., 2013b)
Glycerole (AD Sludge+)	130	Graphite Fibre Plate + (1.63)	SS Wool + (2.72)	48	1.5	18-22	0.013	0.21	30	26.3	(Baeza et al., 2017)
Synthetic WW + (AD Sludge+)	130	Graphite Fibre Plate + (1.63)	SS Wool + (2.72)	48	1.5	18-22	0.028	0.48	23	36.8	(Baeza et al., 2017)
Urban WW (AD Sludge+)	130	Graphite Fibre Plate + (1.63)	SS Wool + (2.72)	48	1.5	18-22	0.031	0.38	28	25	(Baeza et al., 2017)
Urban WW (Urban WW)	175	Graphite Felt (34)	SS Wool (13)	5	0.9	9-16	0.005	0.05	<10	63.5	(Cotterill et al., 2017b)
Winery WW (Raw WW + Sludge)	1000	Graphite Fibre Brush +	SS Mesh (18.1)	24	0.9	31	0.190	5.85	-	62	(Cusick et al., 2011a)

2.3.3 System Architecture

The substrate is the source of chemical energy but optimising the reactor design is crucial to maximising efficiency. Reducing internal resistance can increase efficiency as well as increasing mixing, to make sure all the substrate encounters the anode. There are a variety of reactor designs. The main two configurations are single-chamber and dual-chamber systems that are typically used for MECs and EMRs, respectively. The main difference between the designs is that in dual-chamber systems, a membrane separates the anode and cathode. MECs for hydrogen production are usually dual-chamber as the membrane inhibits methane production from hydrogen via hydrogenotrophic methanogenesis. Additionally, the membrane also stops short-circuiting from the anode and cathode

touching (Kadier et al., 2016b). The effectiveness can be seen in some of the scale-up and pilot systems where multiple studies have shown 95%+ in hydrogen purity (Cotterill et al., 2017a; Heidrich et al., 2014, 2013b) compared to the single-chamber design by Cusick et al. which had 0% hydrogen and 86% methane (Cusick et al., 2011a). These studies highlight the benefits of membranes when trying to produce pure hydrogen. However, there are many cases where hydrogen purity is below 95%, and improvements need to continue.

Membranes

As well as acting as a separator to stop short-circuiting, membranes also limit bacteria crossover to the cathode (Kadier et al., 2016c; Lu and Ren, 2016). The membrane selection needs to allow the transfer of H+ ions through, and a variety of membranes have been tested including: Proton Exchange Membranes (PEM) (Liu et al., 2005a; Rozendal et al., 2006b; Selembo et al., 2009a), Anion Exchange Membranes (AEM) (Cheng and Logan, 2007; R. A. Rozendal et al., 2008; Rozendal et al., 2007), bipolar membranes (R. A. Rozendal et al., 2008) and charge mosaic membranes (R. A. Rozendal et al., 2008; Rozendal et al., 2007). Two issues arise with membranes, the first is due to the cations transferring over to the cathode chamber through the membrane which then creates a pH gradient that increases internal losses (Rozendal et al., 2007). If the system is continuous, the cathodic chamber will become more acidic as the pH gradient increases becoming more problematic, whereas in a batch system the catholyte can be replaced each time equalising the system (Premier et al., 2016). Over time the pH increases and can reach almost 13. Flowing CO_2 through the cathode chamber can decrease the pH reducing the overpotentials and increase the system performance (Ki et al., 2016).

Overcoming pH gradient adds complexity to the system, whilst removing the membrane avoids these issues. Removing the membrane increases the simplicity of the system and reduces the cost, which is essential for systems that are being used in under-served communities. There will still be a variation in pH in the solution, especially at the surface of the cathode, which can hinder performance (Ki et al., 2016). Increasing the mixing within the reactor can help reduce these pH concentrations building up at the cathode, which will increase overpotentials. Adding CO_2 to the catholyte has also been shown to reduce the pH and significantly reduce the overpotential (Ki et al., 2016). However, this will then mix with the hydrogen gas and increases complexity, so alternative methods need exploring.

Single chamber systems have a lower internal resistance due to the removal of the membrane allowing the easier transfer of H^+ ions from the anode to the cathode. At the anode CO_2 is produced and removing the membrane means that this will mix with the hydrogen and reduce the purity. A lot of the research has focused on creating high purity hydrogen as they envisage the system being coupled with Hydrogen Fuel Cells (HFCs). However, HFCs are expensive and aren't currently suitable for under-served communities or remote regions, where the end-use for the hydrogen will likely be cooking (Topriska et al., 2016, 2015). Alternatively, if electricity is required, another option is to use low-cost biogas generators, such as biogas engines developed by OakTec, which can operate using a wide range of gases. With the removal of the membrane, you also increase the susceptibility of the hydrogen being consumed by methanogens which grow on the anode (Call and Logan, 2008a; Kadier et al., 2016c). Exposing the anode to oxygen helps to reduce the methanogen's activity, as they are

strictly anaerobic bacteria. Oxygen exposure can only be utilised in batch operating systems in between the energy recovery; otherwise, the hydrogen will react with the oxygen to produce water and reduce the efficiency (Call and Logan, 2008a). In the case of using the gas for cooking or in a biogas generator, having methane in the mix does not necessarily impede the end-use. The introduction of a methane/hydrogen mix can create value, increasing the theoretical energy output (Rousseau et al., 2020). Measuring the effect of introducing methane into the mix is an interesting route for exploring and assessing system efficiency through the route of gas combustion.

Electrode Design & Placement

The electrode placement is also another consideration. Reducing ohmic losses in the electrodes and system architecture is critical as it is inevitable to generate losses due to the low conductivity of wastewater (René A Rozendal et al., 2008). The ohmic losses can be calculated in relation to the electrode spacing and the wastewater conductivity, as shown in Equation 2-20 (Barth et al., 2013). $\Delta V_{\Omega wastewater}$ is the ohmic loss in wastewater, d is the distance between the electrodes (m), j is the current density (A/m^2), and σ is the conductivity of the substrate (S/m). Placing electrodes closer together can reduce the internal resistance within the cell (Call et al., 2009a). However, biological factors such as the consumption of hydrogen for methanogenic activity are able to take over and deteriorate the performance.

Equation 2-19

$$\Delta V_{\Omega wastewater} = \frac{dj}{\sigma}$$

Reducing the electrode distance from 4-1cm increased coulombic efficiency by 18.2% (Rivera et al., 2017). However, Cheng and Logan found that a 2cm distance was optimal as it allowed the use of a brush anode which increased the biofilm surface area. Whereas, at a 1cm distance, a brush anode was not feasible because it could short circuit the system. At the 1cm distance, the current decreases showing that a high biofilm surface area is more important than a shorter electrode spacing (2011b). Ideally, a 1cm distance is preferable if a high surface biofilm can be achieved. Rivera et al. also explored the effects of electrode distance but found 4cm to be better than 1cm due to the higher hydrogen consumption and methanogenic activity at 1cm (Rivera et al., 2017). The theory and reasoning behind all of these results support each other.However, they all suggest different routes. The diversity in results shows the complexity and effects that other factors can have on the systems. The complexity makes it challenging to optimise designs with such a range of materials and methods being used.

Rivera et al., explored the different cathode surface areas in relation to the $60cm^2$ anode. They found that the smallest cathode (71cm2) had the highest overall efficiencies. It is believed that larger electrodes increase the electric resistance, which hinders the electron flow that stimulated methanogenic activity (Rivera et al., 2017). When it comes to scaling due to these electrochemical limitations, having multiple small cells stacked together will be the most suitable approach. Researching the resistance within the reactor also shows that a larger anode to cathode ratio is preferred. A concentric design performing better compared to flat plate designs (Rousseau et al., 2020).

Cheng *et al*. found that the biofilm surface area should be favoured over electrode spacing (Cheng and Logan, 2011b). For higher hydrogen recovery, greater electrode spacing can reduce hydrogen consumption and methanogenic activity (Rivera et al., 2017). The theory and reasoning behind all of the research support each other. However, the different options for system architecture show the complexity and the interconnected effects that the various components have on each other. The architecture should be informed by whether hydrogen or methane production is favoured. Focusing on the desired route to capture energy will inform the design of the MEC and EMR. For example, in EMRs it is not suitable to use membranes, and the electrode spacing should be reduced to favour hydrogen consumption for methane production.

Operational Considerations

Other aspects to consider in the architecture is sludge build-up and extraction. Carlotta-Jones *et al*., found that the COD reduction was hindered because of the build-up of sludge in the reactors. Future designs need to consider either sludge recirculation or extraction in-line with other wastewater treatment technologies (Carlotta-Jones et al., 2020). The end of life of MECs is also important from a cost and environmental perspective. Aiken *et al.,* found that the recovery of materials at the end of life had the largest effect on the Net Present Value (NPV) and systems should be designed to incorporate reusability (Aiken et al., 2019).

2.3.4 Electrode design in MEC

Anode

The MEC anode serves the same purpose as an MFC anode, as both systems rely on the development of an active biofilm which can effectively transport the electrons to the anode. Therefore, the same anode can be used for MFCs and MECs to give the same performance.

The anode is a limiting factor for the MEC's performance (Lim et al., 2017). A biofilm forms on the anode's surface containing EAM. Organic species are oxidised to CO_2, which is led by the EAM. Bond et al., found that the rate of electrical current produced by the anode increase exponentially when *Geobacter Sulfurreducens* microbes are introduced (Bond and Lovley, 2003b). The current increase highlights the importance of EAM activity, supporting the need for the anode to have excellent biocompatibility. Therefore, the anode material and surface treatment are one of the defining parameters of designing the anode to increase efficiency. The efficiency of the anode and biofilm can be measured by the current density, coloumbic efficiency (CE) and COD removal efficiency (Barbosa et al., 2018). Rousseau argues that research should focus on increasing current density as a high current density is crucial to industrial scalability (Rousseau et al., 2020). The current density is directly linked to the oxidation of the organics and the EAM's ability to perform EET to the anode, supporting the argument that the anode is a crucial component.

Presently, carbon materials are the most widely used electrode material as a result of their strong bio-adhesion, low cost, high surface area and availability (Jung and Pandit, 2018). The majority of papers reviewed showed that carbon-based materials are the most populous material (Table 2-1). Carbon materials increase the interfacial microbial colonisation accelerating the biofilm formation on the anode. Compared to other materials such as metals, carbon can have a relatively low conductivity.

New areas of research have shown very high electrical conductivity in certain carbon-based materials such as graphene and carbon nanotubes (Wang and Weng, 2018). However, commercial applications are limited, making them a less attractive option for low-cost electrodes. Due to the lower conductivity of commercially available carbon-based materials, metal current collectors are used as electron acceptors instead. Titanium wire is used due to its corrosion resistance (Cusick et al., 2011a; Escapa et al., 2016b), but stainless steel is also common in plate designs and has a lower cost than titanium (Carlotta-Jones et al., 2020; Cotterill et al., 2017b; Heidrich et al., 2014). Effective current collectors provide the conductive micro environment for EET can reduce losses from unfavoured reactions and enhance the current density (Li et al., 2017).

Due to its higher conductivity graphite is also one of the most widely used electrode materials (D. Liu et al., 2018). Similar to carbon anodes, various forms of graphite electrodes are used, including brushes, granular, rods, felts and foams (Li et al., 2017). Table 2-1 shows that graphite is used ten times in the research papers examined using systems above 8L. Graphite structure is generally planar, resulting in a lower porosity surface for bacterial attachment compared to other carbon materials.

The surface area of the anode is an important aspect of the design as it can increase the area of biofilm and the biofilm's contact with the substrate. With the majority of studies focusing on 3-D porous carbon materials including carbon foams, meshes, felts and brushes (Guo et al., 2015). Carbon fibre (CF) electrodes are considered one of the best options as they have a high surface area and offer customisability. However, they can be expensive (Pötschke et al., 2019). To reduce costs, recycled CF could be an alternative and performed well in pilot research (Carlotta-Jones et al., 2020). However, recycled CF is often non-uniform mats which pull apart easily. Mesh CF anodes tend to produce higher current densities than plate-shaped anodes due to better mass transfer, surface area and biofilm formation. Carbon brush electrodes have a high surface area, contributing to high current densities (Feng et al., 2010) and can also reduce clogging due to their free form. Despite CF performing well in the lab, they are rarely used in any large-scale BES partly because of their high cost, even though they have some of the highest pilot performances based on energy production (Cusick et al., 2011b).

Analysing the pilot studies shown in Table 2-1, carbon-based materials have been used in the form of brushes, felt and fibres. Cotterill et al. found that the EAM form a heterogeneous biofilm on anodes even if they use the same materials and construction. It was found that the biofilm in two pilot systems (130L and 45L) only contained an average biofilm coverage of 5%, with a maximum of 16% coverage in one region (Cotterill et al., 2018). The cost of the anode, is a significant part of the MEC construction (Carlotta-Jones et al., 2020). Utilising only 5% is not economically viable, and efforts to increase biofilm adhesion will likely lead to more significant improvements than increasing the surface area of the anode.

It is likely that effective electrode materials increase the biofilm adhesion and growth rather than supporting different microbial communities and is likely why surface treatments have been effective as they affect the surface charge (Guo et al., 2013). Multiple surface treatments have been successfully used, including heat treatment (Wang et al., 2009), acid soaking (Zhu et al., 2011) and electrochemical oxidation (Tang et al., 2011). Surface treatments can reduce startup time by providing ideal environments for biofilm formation, which can be applied to both anodes and cathodes. Research into surface treatments to change the surface charge of glassy carbon anodes found treating with $-N^{+}(CH_3)_3$ had the lowest startup time of 23 days and the highest current density of 0.204 mA/cm^2. This is likely a resulting from the fact that bacteria are usually negatively charged at neutral pH making the $-N^{+}(CH_3)_3$ treated surface more effective due to electrostatic forces (Guo et al., 2013). Surface topography increases the bacterial adhesion at the microscale and EET at the nanoscale (Champigneux et al., 2018). However, surface structures on electrodes with a mature biofilm did not show any sign of improvement from micro-scale surface adjustments (Moß et al., 2019). Increasing coulombic efficiency and hydrogen production can be achieved by doping activated carbon with calcium sulphide. Calcium sulphide showed the most significant improvement over Magnetite (Fe_3O_4) or iron sulphide (FeS), and it can attract biota, even though it has low conductivity. These results strengthen the argument of using bio-adhesion over other parameters, such as increasing the conductivity (Yasri and Nakhla, 2017). Colloidal forces have also been shown to be one of the most influential aspects of biofilm formation and increasing surface features of the electrode such as random surface roughness, micropillars, nanoparticles and extra-porous materials increase cathode and microbe interaction (Noori et al., 2020). The research highlights the need for a combination of bio-adhesion and the ability of the biofilm for EET to increase system performance.

Metals are also universally considered suitable electrode materials. Metals are typically 2 to 3 times more conductive than carbon-based materials (Santoro et al., 2015). Research into other materials is being conducted at a lab-scale, where a higher conductivity can aid in the extracellular electron transfer from the biofilm to the circuit. A review of 45 metal-based anodes both treated and untreated showed that molybdenum anodes had the maximum power densities (307-344 mW/m^2). Compared to platinum, molybdenum is cheap, with a price comparative to copper and nickel (Yamashita and Yokoyama, 2018). Molybdenum anodes also displayed good durability, not corroding or reducing in current production over 350 days. The durability of electrode materials is also a key factor to consider. There is a lack of data in the literature regarding the durability of the electrode with most experiments lasting no longer than a year.

Stainless steel (SS) is another possible anode material as it is readily available, has good mechanical properties and corrosion resistance (Dumas et al., 2008). As mentioned, SS is used as a current collector on various carbon cathodes. If it is possible to remove the need for the carbon, it could simplify the construction of the electrodes offering a promising scale-up opportunity. SS has advantages over carbon with increased conductivity, lower costs, and extensive manufacturing options (Guo et al., 2014). Although it offers excellent physical properties that would lend itself to EET, the biocompatibility is questionable due to a relatively smooth surface. Surface treatments such as flame spray oxidation create an iron oxide film on the surface, increasing the biocompatibility of iron-reducing bacteria and surface roughness (Guo et al., 2014). Heat treatments are relatively easy to scale-up. However, the longevity of SS is questionable, and further research is needed into metal anodes.

The anode material represents a high cost; in some cases, equating to 69% of pilot system cost (Cotterill et al., 2017a). For MECs to become economically viable, is it discussed that a 90% reduction in cost is required (Aiken et al., 2019). Two possible routes could be reducing the cost or reducing the size or number of the anodes. To make this feasible, increasing biofilm coverage will be crucial and ensure the reactor architecture forces the wastewater over the anodes. Exploring chemical surface treatments is one way to increase biocompatibility, but most research has not led to a commercially viable option (Rousseau et al., 2020). The other option is to explore lower-cost materials. Research shows that carbon-based anodes seem to be the path to the most economically viable option, even though they represent a high cost. Going forward, a cost-benefit analysis should be used in conjunction with the development of the anode, which takes into account the material availability and its corrosion resistance.

Cathode

In a MEC, the cathode needs to be an active catalyst for the hydrogen evolution reaction (HER). Other reactions can take place to produce other value-added products such as methane, but hydrogen production is the foundation for these reactions. Whereas previously mentioned, a membrane-less single chamber will likely produce methane as the hydrogen will be consumed during the reaction (Cusick et al., 2011b). With hydrogenotrophic methanogens producing methane via the intermediate production of hydrogen (Villano et al., 2010). The hydrogen evolution ability of the cathode should be the primary focus, irrespective of the energy production pathway. MEC cathode materials require physical properties for high conductivity; specific surface area, corrosion resistance, mechanical properties, and if methane is desired, good biocompatibility (Wang et al., 2019), in order to reduce large overpotentials of hydrogen evolution. Alongside the physical properties, cathodes need low cost, readily available materials that can use standard manufacturing techniques; increasing the feasibility for scalability.

Typically, materials with excellent catalytic properties for hydrogen evolution like platinum have a high cost. If used in MECs, the cathode could equate to 47% of the construction costs and to become economically viable the cathode needs to decrease by at least 10% (René A Rozendal et al., 2008). The cost reduction means that new low-cost catalysts and materials need to be explored. Researchers have explored platinum coatings on the surface of lower-cost materials to reduce costs (Call and Logan, 2008a; Rozendal et al., 2008). Although research shows, platinum is susceptible to irreversible poisoning from contaminants found in wastewater such as H_2S (Rozendal et al., 2008). The cost and potential for poisoning mean cathodes should look to remove platinum and search for other materials with similar HER performance. To find low-cost alternatives, research has explored various materials including; Stainless Steel (SS) plates (Selembo et al., 2009a) SS brushes (Call et al., 2009a), SS wool (Heidrich et al., 2014), SS and nickel mesh (Ki et al., 2016), nickel foam (Kuntke et al., 2014), nickel foam with graphene (Cai et al., 2016) and bio-cathodes using carbon and graphite (Croese et al., 2014). If methane production is desired, then the cathode wants to promote biofilm adhesion near to the catalytic surface. The biofilm would not want to completely cover the electrode surface as this may affect system performance.

SS is a relatively inexpensive metal and is commonly used for electrodes, and is a popular choice in MEC research used 33 times in a study of 63 papers shown in the appendix 13.1. With the majority of the research into pilot MEC using meshes (Cusick et al., 2011b; Escapa et al., 2016b; San-Martín et al., 2019) and wool (Baeza et al., 2017; Cotterill et al., 2017a; Heidrich et al., 2014, 2013b) creating low-cost, high surface area cathodes.

Research into SS with a high specific surface area can perform similarly to a carbon-containing platinum catalyst electrode for H_2 production (Zhang et al., 2010). The availability of SS means that there are many options to create high specific surface areas designs. Stainless steel brushes showed an overall energy efficiency of 221 ± 8%, comparable to using platinum (Call et al., 2009b). SS meshes have good ohmic resistance and electron transport resistance from the conductivity of SS (Ma et al., 2017). SS offers promise as a commercial cathode material due to the low cost and performance, especially in the forms of meshes and brushes.

Other materials offer opportunities, such as nickel, which exhibits excellent corrosion resistance and HER activity (Kellenberger et al., 2007). The comparison of SS, nickel and copper mesh cathodes from methane production showed that nickel outperformed SS and copper, increasing performance of AD by 42% (Sangeetha et al., 2016). The study found that nickel mesh was also the most durable, an essential factor for an economically viable electrode. Cai et al., explored the use of graphene on Nickel Foam (NF+G), the addition of the graphene increased the surface area three times and reduced the resistance. The NF+G cathode performed similarly to platinum-coated carbon cloth at an applied voltage of 0.8, whereas with lower voltages, it did not perform as well (2016). Biocathodes have received attention, as they generally exhibit lower overpotentials and can utilise low-cost materials, making them an attractive option for upscaling (Rozendal et al., 2008). Battle-Vilanova, found that a biocathode had higher energy efficiency (53-175%) compared to abiotic systems (7-96%) (2014).

The size and shape of the cathode play a role in the performance. Call et al., found that a SS brush anode that was 50% loaded was prefered over one fully loaded with bristles. The benefit was because of hydrogen bubbles were getting trapped in the high-density brush. The trapped bubbles led to increased overpotentials from the reduced surface area for HER and increased the opportunity for hydrogen consumption from methanogens (2009).

Other researchers have looked at meshes and foams to increase the active area for HER or use two cathodes on either side of the anode (Bajracharya et al., 2016). Going forward, SS seems to show the most promise, although further research into nickel should be explored. Both the materials can be relatively interchangeable as they are both available as plates, meshes and foams and can use similar fabrication methods. Similar to the research route of the anode, a cost-benefit analysis will help shine a light on the material selection for the cathode

Biocathodes are an alternative to the majority of research focused on abiotic systems. Biocathodes in MECs have been shown to utilise energy more efficiently than abiotic systems in MECs using graphite granules and graphite plate anode and cathodes (Batlle-Vilanova et al., 2014a). However, this study compared abiotic and biotic systems using carbon cathode materials that were chosen for biofilm growth. Compared to other literature graphite cathodes are unlikely to have the same catalytic properties of SS which are widely used in abiotic systems.

Compared to cathodes in abiotic systems, biocathodes rely on an effective biofilm formatting on the surface to act as the catalyst. Research suggests that biocathodes should possess biocompatibility, hydrophilicity, positive surface charge, and an extensive surface area (Noori et al., 2020). In the case of methane production, the biofilm must contain hydrogenase methanogenic microbes to maximise methane production. For methane production 3D structured graphitic/carbon materials have been exhibited increased performance over metal electrodes (Noori et al., 2020). Nano coated carbon electrodes have exhibited increased performance due to their increased conductivity which is a limiting factor to plain carbon electrodes. The study was focused on MFCs but showed that Fe_2O_3 doped anode and cathodes produced higher current densities than plain cathodes. However, Pt cathodes with doped anodes had the highest current densities (Nandy et al., 2019).

Most research into biofilm formation on BES electrode materials is focused on the anode and not the cathode. Research into anode materials can be applied to biocathodes, but further research into the optimal conditions are going to be required as different microbial species are required at each.

2.3.5 Operation Parameters

Within the operational parameters, various conditions affect the performance of the system; biofilm, temperature, applied voltage (V_{app}), pH, catholyte, flow rate and Organic Loading Rate (OLR).

Inoculation Biofilm Formation

System inoculation is still proving to be difficult at a larger scale system with full system inoculation taking 25-90 days (Saheb-Alam et al., 2018). There have been various research into testing multiple inoculum sources (Cusick et al., 2011a) and using additional chemicals such as acetate to expedite the start-up times (Escapa et al., 2015). From the articles reviewed, the mean start-up was 43 days.

Biofilm growth is likely to be a stochastic process. Therefore, BESs can be used to treat different types of wastewater. The inoculum should be derived from the wastewater that is to be treated, to ensure that bacteria will survive in the influent (Cotterill et al., 2018). The start-up period for the research focuses on how long it takes the system to start generating hydrogen or biogas. The start-up of the pilot-scale systems is longer, taking 50-90 days before biogas production is recorded (Baeza et al., 2017; Escapa et al., 2016b). However, in many cases, COD reduction may have higher or equal importance to biogas production, but the start-up of COD reduction is not recorded. Research into the start-up period for COD reduction should also be explored. The start-up is essential as it can affect the suitability of the technology as long start-up times might not be acceptable. More research into the right start-up conditions will increase the attractiveness of the technology working towards commercialisation of MECs for global wastewater treatment.

Biofilm Formation in MECs

Biofilm formation is complex and has multiple parameters that affect the formation and growth on surfaces. Bacteria have macromolecular structures on their cell walls to interact with surfaces and adapt/modify their cell walls to respond to different environments (Ploux et al., 2010).

There are typically four stages of biofilm formation;

1. Bacteria Transport
2. Bacteria Adhesion
3. Biofilm matrix synthesis
4. Maturation and detachment

There are two stages of adhesion within the second phase, "Reversible Adhesion" and “Irreversible Adhesion". The first reversible adhesion phase is a result of colloidal effects that result in physical and chemical forces taking place at the surface and cell walls. The forces result from repulsive /attractive electrostatic, van der Waals and hydrophobic and hydrophilic effects. The second irreversible adhesion is a strengthening of the microbial surface bond where short-range forces, including covalent and hydrogen bonding occur (Ploux et al., 2010).

The third growth phase is to form biofilm matrixes, through the cloning of cells to form microbial colonies. The microbes spread across the surface through different motion effects such as 'twitching' and 'swarming (Kaiser, 2007). During the mature phase of the biofilm, it has been shown that microbial colonies can form complex 3D architectures to create channels for nutrients and other support elements (Anderson and O’Toole, 2008). Biofilms can also communicate with each other using Quorum Sensing, which can allow the mature biofilm to detach, allowing them to colonise other surfaces (Ploux et al., 2010). The first five cycles of growth are shown to be fast, resulting in drops of charge transfer resistance (1404 Ω to 30 Ω) and high current generation. During the maturity of the biofilm (cycles 12-30), it was shown that dead cells accumulated increasing the diffusion resistance (53 Ω to 120 Ω) (Sun et al., 2016).

Anode surface charge has been shown to affect the biofilm formation, with positively charged and hydrophilic surfaces being more selective of electroactive microbes. Hydrophilic surfaces reduced startup time on average 9 days compared to Hydrophobic surfaces. Hydrophilic surfaces are likely to be more important than surface charge for effective biofilm formation in BES (Guo et al., 2013). The anode potential also affects the biofilm growth and microbial community.

Inoculation is an essential step in BES as it can affect multiple aspects at both the anode and cathode. Anodes initially poised at -0.25 V vs Ag/AgCl before increasing to -0.5 V vs Ag/AgCl were found to have a quicker startup time (current generation) and a higher concentration of *Geobacter* than those poised at -0.36 and -0.42 V vs Ag/AgCl. The study found that after the electrode potentials were all increased to -0.5 V vs Ag/AgCl the maximum power density was similar 270 mW/m2 (-0.25 V) and 250 mW/m2 (-0.36 V) (Commault et al., 2013). The study did not reduce the potential below -0.5 V vs Ag/AgCl due to limitations of the potentiostat. As studies reduce potentials to below -1.2 V there is further scope to understand if it does affect performance at these electrode potentials. The research also found that inoculating in batch vs continuous reduced treatment time. However, other

parameters also changed making it difficult to determine the exact cause (Batch – nitrogen sparging 10mins, temperature 18^{o}C and phosphate buffer – 0.1M, pH 7.5, Continuous – continuous nitrogen sparging, temperature 31^{o}C and phosphate buffer – 0.2M, pH 6.8).

The anode is predominantly populated by *Geobacter* species irrespective of the inoculum source for both MFCs and MECs when inoculated with bog sediment and AD waste at different solid to medium ratios (0.01, 0.1, 1, 10, and 25%). However, the inoculum source did affect multiple outputs. COD removal was better with AD inoculum, but bog inoculum had higher methane production. The bod sediment did require an inoculum solids content of at least 10% but best results occurred at 25%, whereas the AD solids content did not make a noticeable difference (Siegert et al., 2014a).

Within EMR the biofilm on the anode and cathode differ with different species populating the surfaces due to the availability of nutrients and organics favouring their metabolic pathway. Compared to the anode on the cathode in EMRs methanogens utalise the release of electrons to create methane via electro-methanogenis (Lohner et al., 2014). The presence of ammonia affects the methane production pathway altering the system to hydrogenotrophic from acetoclastic. The dominant methane production pathway highlights the dominance of hydrogenotrophic microbes for waste streams that contain higher ammonia content (Yang et al., 2018). Within faecal sludge, there are high volumes of urea that hydrolyses into ammonia, making the microorganisms within EMR more suitable to treat this waste stream than AD which can be adversely affected if concentrations are too high.

The consortium of microbes on the biocathode is diverse with different organism providing different pathways to energy generation. The growth of hydrogenase methanogenic microbes (*Methanococcus*. Maripaludis) on the cathode was found to reduce overpotentials due to the microbes supporting electron uptake; which increases current and hydrogen formation (Lohner et al., 2014). *A*nother study found the main microorganisms present on a biocathode were *Hoeflea* sp. and *Aquiflexum* sp. (Batlle-Vilanova et al., 2014b). For hydrogen production one of the main pathways on a biocathode is through sulphate reducing bacteria. Community analysis of a biocathode found *Desulfovibrio* spp. A the dominant species and are able to produce hydrogen (Croese et al., 2011). Whilst research into microbial communities within MECs for methane production found that the presence of Archaea of the hydrogenotrophic genera *Methanobacterium* and *Methanobrevibacter* are the most important microorganisms (Siegert et al., 2014a).

The activation and biofilm formation has been found to be quicker at the anode than the cathode (days vs weeks), and incremental increases can support the biofilm growth starting at 0.3 and increasing to 1.0V (Lim et al., 2020). The slow cathode biofilm growth indicates that it is important to ensure methanogens are present in the bulk liquid initially. In this case, following a flow rate similar to AD systems will be crucial to reduce bacterial washout.

Biofilm Architecture

Biofilm thickness also has a significant impact on the performance where the highest electrochemical performance was recorded at ~20 μm after which performance drops and a maximum biofilm of ~45

µm is reached (Sun et al., 2016). Although biofilm thickness affects performance, it has been shown that metabolic activity is occurring throughout the biofilm and likely supporting the current generation.

Research suggests the biofilm formation creates pillar structured biofilms across the anode surface, where low shear and turbulent forces produced similar complex structures as other studies (Franks et al., 2010). The maximum current density was recorded when biofilm pillars were at greater than 50 µm. Further research into mixing and shear forces on the electrode surface may help remove dead cells and reduce the biofilm thickness to reduce the charge transfer resistance and increase current generation.

When methane production is inhibited within the BES through limited hydrogen availability, it has been shown that the electron release at the cathode is used to create formate (Lohner et al., 2014).

Organic Loading Rate

OLR is one of the defining aspects of energy production from the system. With a low OLR, the system will not be able to generate any significant volumes of hydrogen. With low OLR, alternative technologies may be better suited to treat the wastewater as the main aim will shift towards COD removal over energy production. Escapa et al., found that with low strength wastewater and decreasing the OLR significantly increased the energy demand, and the V_{app} needs to be adjusted accordingly to ensure the system is energy efficient. During the study, an OLR of 441 mg/L/d with a V_{app} of 0.75 V showed optimal performance (Escapa et al., 2012a).

Applied Voltage

The applied voltage play a significant role in the operation and performance of MECs and EMRs. Out of 51 tests reviewed in appendix 13.1 Table 13-1, the applied voltage ranged from 0.13 (Guo and Kim, 2019) - 1.5V (Baeza et al., 2017). Both the mean and mode showed a V_{app} of 0.8, which was performed across 9 of the experiments. By increasing the $V_{app,}$ the cell potential will also increase, resulting in higher energy production; however, there is an upper limit. The cell potential needs to be controlled to stop it increasing above the threshold where oxygen and chlorine are generated, which would affect the biofilm (Rousseau et al., 2020).

Work conducted by *Ding et al.* showed that when there was no voltage supplied, the COD removal efficiency was 54.4%, whereas when 1.0V was supplied, the efficiency increased to 80.6% (Ding et al., 2015). The research shows that an applied voltage does increase performance for COD removal. The correlation indicates that the voltage promotes the growth of a biofilm which can more effectively breakdown the organics in the waste.

A study analysing the effects of the applied voltage of found that maximum hydrogen production and energy efficiency occurred at an Vapp of 1.0 V, which provided a cathode potential of -1.1 V. At a Vapp of 1.0 V the energy recovery is 30.2% oxidation of acetate and 69.8% from the external power supply. Whereas the maximum coulombic efficiency peaked at an Vapp of 0.7 V reaching 322% (Lim

et al., 2020). Similar studies also found an Vapp of 1.0 V to be optimum (Batlle-Vilanova et al., 2014b; Lim et al., 2018). Research suggests that a MEC using biotic cathodes to generate energy is more efficient than an abiotic cathode (Batlle-Vilanova et al., 2014b). In a dual-chamber system design to limit methane formation at the cathode found that higher electrode potentials increase methane concentrations, although minimal compared to hydrogen (<0.04 CH_4 L/m^2 vs 3-7.8 H_2 L/m^2 at an Vapp of 1.0 - 1 .9 V) (Lim et al., 2020). Although for biotic cathodes, one study found that applied potentials need to be more negative than -0.8 V vs SHE to produce hydrogen (Lim et al., 2018).

Ohmic Losses

MEC exhibit multiple losses from ohmic, mass transfer and activation losses. Activation losses are linked to the microbial activity of the biofilm. Mass transfer relates to the capacity of the feedstock to reach the biofilm within the anode. Ohmic losses are relate to the ions transfer from the anode and cathode and the electrical conductivity of the electrodes.

One of the most predominant is the ohmic resistance creating losses within the system and have multiple variations due to the biofilm on the anode and interact differently compared to electrochemical cells. The Nernst equation represents the relationship between the reduction potential of an electrochemical cell reaction to the standard electrode potential, temperature and chemical reactions undergoing oxidation and reduction. The Nernst equation is shown in Equation 2-20.

Equation 2-20: $$E_{cell} = E^{\ominus}_{cell} - \frac{RT}{zF} InQ_r$$

- E_{cell} is the cell potential (electromotive force) at the temperature of interest,
- $E^{\ominus}_{cell}$ is the standard cell potential,
- R is the universal gas constant: R = 8.31446261815324 J K^{-1} mol^{-1},
- T is the temperature in kelvins,
- z is the number of electrons transferred in the cell reaction or half-reaction,
- F is the Faraday constant, the number of coulombs per mole of electrons: F = 96485.3321233100184 C mol^{-1},
- Q_r is the reaction quotient of the cell reaction

The Nernst Equation has been adapted for BES use, by creating the Nernst Monod equation (Marcus et al., 2007), which has subsequently been built upon to include the resistance in a steady-state biofilm (Lee et al., 2016) and mechanisms of extracellular electron transfer (EET) as shown in Equation 2-21 (Lee, 2018).

Equation 2-21: $$j = 0.14 f_e^0 q_{max,\ app} X_f L_f \frac{S_d}{K_{sd,\ app} + S_d} \left(\frac{1}{1 + exp\left(-\frac{F}{RT}\left(E_{anode} - \Delta E_{EET} - E_{KA,EC}\right)\right)} \right)$$

- j is the current density (A/m^2)
- f_e^o is the fraction of electrons used for catabolism
- S_d is donor substrate (g COD/m3),
- $q_{max,app}$ is the apparent maximum specific substrate utilisation rate (g COD/g VS/d)
- X_f is the biofilm density of active exoelectrogens (g VS/m^3)
- L_f is the biofilm thickness (m)
- $K_{sd,app}$ is the apparent half-saturation concentration of electron donor (g COD/m3),
- q ¼ specific rate of electron donor utilisation (mmol-ED mg-VS)
- E_{anode} is the anode potential (V)
- R is the ideal gas constant (8.3145 J/mol-K)
- F is the Faraday's constant (96,485C/mol e^-)
- T is the temperature (298.15, K)
- n is the number of electrons transferred (assumed to be 1)
- ΔE_{EET} is an average energy loss in conductive EET of the third electron-transfer step (V)
- $E_{KA,EC}$ is a rate-limiting EC potential at which current density is half of the maximum current density (V) and $E_{KA,EC}$ is equal to E_{KA} in the original Nernst-Monod (Marcus et al., 2007) when ΔE_{EET} = 0, indicating no potential drop in the biofilm anode

ΔE_{EET} is a combination of measurable parameters, including biofilm thickness and conductivity using Ohms's law and the current density from the MEC shown in Equation 2-22 (Lee, 2018).

Equation 2-22: $$\Delta E_{EET} = \left(\frac{j}{2}\right)\left(\frac{L_f}{2}\right)\frac{1}{K_{bio}}$$

K_{bio} is the biofilm conductivity (S/m), $L_f/2$ is the mid-point of biofilm thickness, and $j/2$ is an estimate of the current density at the biofilm's mid-point. The ΔE_{EET} can be inserted into the Nernst Monod equation as shown in Equation 2-22 (Lee, 2018).

The ohmic losses can be considerable on the cathode at the interfacial electron transfer due to the conductivity of the electrolyte (Yasri et al., 2019). It is found that ohmic losses increase linearly with current production and equate up to 21% of the total voltage at 1.0 V (Guo et al., 2017). GAC electrodes have been found to incur greater losses due to the low conductivity. Studies have shown that the Vapp was 1.5 V, but the actual voltage received at the electrode was 1.0-1.2 V (Hussain et al., 2018). Whereas Stainless Steel (SS) is likely to reduce ohmic losses due to it's higher conductivity (Guo et al., 2017).

It has also been shown that intermittent power supply can increase the longevity of the MECs and increase the COD reduction and overall efficiency. In the research, the GAC acted as a capacitor and when powered was not applied the voltage drop at the cathode was from 1.2 to 0.9V (Hussain et al., 2018). Combing carbon-based materials for biofilm growth and conductive metals such as stainless

steel offers an attractive cathode option for future research to reduce over potentials and ohmic resistance whilst also creating opportunities for intermittent power supply.

Temperature

Temperature is another essential factor to consider and has a significant effect on the bioanode (Rousseau et al., 2020). Typically, AD systems are operated at 35-40^{o}C with low temperatures leading to the inhibition of methanogens and therefore low methane production. Evidence suggests that EMRs can be operated at much lower temperatures, especially when hydrogen is desired, and that lower temperatures can suppress methanogenic activity. However, when the temperature rises above 20^{o}C methane production resume (Chae et al., 2010; Lu et al., 2012b). In another study, it was also found that the optimum temperature for hydrogen production was 30^{o}C which would increase methanogenic activity in a single chamber reactor (Kyazze et al., 2010).

The operating temperature has a direct effect on the activity of methanogens, with temperatures above 35^{o}C, significantly improving the activity of methanogens (Yongtae Ahn, 2017). As previously explained, research conducted by Villano *et al*. found that in EMRs hydrogenotrophic methanogens are more abundant, producing methane via the intermediate production of hydrogen (Villano et al., 2010). So if methane production is the desired energy route, then higher temperatures would be required. Although in some cases, EMRs have been able to perform as effectively as AD systems at temperatures as low as 10^{o}C (D. Liu et al., 2016). Low-temperature methane production could increase efficiency and remove the need to heat reactors in cold climates.

Pressure

Pressure has a minimal effect on the equilibrium cell voltage, with 40mV lost with a pressure jump from 1 to 10 atm (Rousseau et al., 2020). The energy loss with the increased pressure is minimal compared to the addition of a compressor further down the line (Rousseau et al., 2020). In other industries, such as food preservation, pressures above 1000 atm are required to destroy microorganisms (Arroyo et al., 1997).

pH

pH is one of the main parameters that affect the biological community and activity within the cell. Neutral-alkaline conditions are preferable for operation with a pH of 8 being the optimal condition for biofilm formation at anode (Sun et al., 2019). However, within the reactor, to increase the performance, electrolytes are required to aid in the H^{+} ions moving towards the cathode. Electrolytes used for water electrolysis are generally very acidic or have high alkalinity making them unsuitable an increasing the difficulty of the electrochemical performance of the system (Rousseau et al., 2020). Lower pH in the cathodic chamber can increase hydrogen production and may be required to reduce potentials (Kyazze et al., 2010). The addition of salts may inhibit the system, even though it increases the ionic conductivity of the electrolyte, it reduces the ability to reduce acidification at the anode. (Rousseau et al., 2020).

2.3.6 Measuring MEC Performance

There are key parameters that need to be measured to determine the performance of the MEC including; Electrical Energy Efficiency (η_E), Substrate Efficiency, Coulombic Efficiency (CE) and Total Energy Efficiency (η_{E+S}) (Cotterill et al., 2016).

Electrical Efficiency

η_E (Equation 2-23) is a measurement to compare the electrical energy input to the amount of recovered in hydrogen. η_E is measured as a percentage, and if it is over 100% then the MEC is producing energy from the chemical energy present in the substrate (Cotterill et al., 2016).

Equation 2-23

$$Electrical\ Energy\ Efficiency\ = \frac{Energy\ Recovered\ in\ H_2}{Electrical\ Energy\ Input\ (Current\ x\ Applied\ Voltage\ x\ Time)}$$

$$\eta E = \frac{W_{out}}{W_E}$$

Electrical Energy Input (W_E) Equation 2-24 is given in kWh and is calculated by integrating the voltage added at each measured voltage (E) and external resistor R_{ex} $(I=E/R_{ex})$. E_{ps} is the applied voltage of the power supply, that should be adjusted for the losses caused by the external resistor (I^2R_{ex}), with integration over n data points measure over timer intervals Δt (Cotterill et al., 2016). In the case where systems are heated the W_E will also contain the heating power (H_p) requirements expressed in Equation 2-24.

Equation 2-24

$$(W_E) = \sum_1^n \left(IE_{ps}\Delta t - I^2 R_{ex}\Delta t\right) + (Hp\ \Delta t)$$

The Energy recovered in H_2 (W_{out}) is calculated from the moles of hydrogen produced (N_{H_2}) and the standard heating value of hydrogen (ΔH_{H_2}) as shown in Equation 2-25. The higher heating value (285.83kJ/mol) is used when it is presumed that the hydrogen will be used for industrial applications or in a fuel cell. The lower heating value (241.83kJ/mol) should be considered if the hydrogen will be combusted. The lower heating value includes the heat loss through the combustion and heat loss from the production of water vapour needs to be considered. The kJ are then converted into kWh using the 3600kJ/kWh conversion (Cotterill et al., 2016).

Equation 2-25

$$W_{out} = (\Delta H_{H_2} N_{H_2})/3600$$

Substrate Efficiency

Substrate efficiency (SE) (Equation 2-26) is the comparison of the amount of hydrogen moles (N_{H_2}) produced to the theoretically amount possible based on the substrate removed (N_S) from the MEC (Equation 2-27). SE is expressed as a percentage and indicates the substrate conversion efficiency (Cotterill et al., 2016).

Equation 2-26

$$Substrate\ Efficiency = \frac{Moles\ of\ H_2\ recovered}{Theoretical\ moles\ of\ H_2\ in\ the\ substrate\ removed}$$

$$SE = \frac{N_{H_2}}{N_s}$$

Equation 2-27

$$N_S = 0.0625 \Delta COD \Delta t$$

COD is the amount of oxygen required to oxidise an organic compound. 0.5 mol of oxygen is required to oxidise 1 mol of hydrogen . 0.5 mol of oxygen = 16g so the COD to oxidise 1 mol of hydrogen is 16g, therefore 1g of COD is 0.0625 mol of hydrogen (Equation 2-28). The COD removal is measured to give ΔCOD over the time interval of the experiment.

Equation 2-28

$$2H_2 + O_2 \rightarrow 2H_2O$$

Coulombic Efficiency

Coulombic Efficiency (CE) (Equation 2-29) is the amount of hydrogen produced compared to the amount which is theoretically possible based on the current or total charge passing through the cell. CE is shown as a percentage and cannot exceed 100% (Cotterill et al., 2016). Equation 2-29 is relevant in the case where only hydrogen is the fuel produced and, as demonstrated within the literature review, is often combined with other biofuels such as methane. Equation 2-30 shows the full CE for reactors that do not contain membranes and will likely operate as EMR.

Equation 2-29

$$Coulombic\ Efficiency = \frac{Moles\ of\ H_2\ Recovered}{Theoretical\ Moles\ of\ H2\ in\ the\ Current\ Produced}$$

$$CE = \frac{N_{CE}}{N_{H_2}}$$

Equation 2-30

$$Coulombic\ Efficiency = \frac{Moles\ of\ H_2{+}CH_4\ Recovered}{Theoretical\ Moles\ of\ H_2{+}CH_4\ in\ the\ Current\ Produced}$$

The theoretical moles of hydrogen based on current (N_{CE}) can be calculated through Equation 2-31.

Equation 2-31

$$N_{CE} = \frac{\sum_1^n I\Delta t}{2F}$$

I is the current calculated from the measured voltage and the resistance, Δt is the time interval, 2 is the number of electrons in the hydrogen evolution reaction and F is the Faraday's constant (96,485 C/mol e^-) (Cotterill et al., 2016).

Total Energy Efficiency

The Total Energy Efficiency (η_{E+S}) for MECs is shown in Equation 2-32. The total energy efficiency is the energy recovered in hydrogen compared to the electrical and substrate energy inputted into the system. η_{E+S} is calculated as a percentage. The substrate potential energy is calculated as chemical energy and not free energy which is lower especially in wastewater (Cotterill et al., 2016).

Equation 2-32

$$Total\ Energy\ Recovery\ = \frac{Energy\ Recovered\ in\ H_2}{Electrical\ and\ Substrate\ Energy\ Input}$$

$$\eta_{E+S} = \frac{W_{out}}{W_{E+S}}$$

Calculating the substrate energy (W_S) is shown below in Equation 2-33.

Equation 2-33

$$Ws\ =\ \Delta COD \Delta H_{WW/COD}$$

ΔCOD is the difference between the influent and effluent COD measured in grams. The energy content per gram of COD ($\Delta H_{WW/COD}$) is the internal energy of the substrate measured in kJ per mole in thermodynamic tables (Cotterill et al., 2016). As previously discussed, wastewater is a complex substrate with various chemicals. The complexity makes it difficult and time consuming to find a specific thermodynamic value. Gathering an accurate sample to use in a calorific bomb is difficult and time consuming, with both heat drying and freeze-drying methods loosing volatile fatty acids present within the wastewater, which can have a significant chemical energy. It is presumed the minimum energy content of wastewater can be 13-14 kJ/gCOD, however it could be much higher with results of 17.7 kJ/gCOD and 28.7kJ found in the same study (Heidrich et al., 2011).

This method of calculating the total energy efficiency is based on Hydrogen being the only energy output. However, depending on the type of MEC system there may be other gases present like methane. Most studies exclude methane as they are looking to produce high purity hydrogen so it can be used in the chemical industry or for PEM fuel cells. This research is looking to use the gas for combustion and this circumstance the methane is significant and should be considered within the total energy efficiency. Therefore, total energy efficiency will be calculated as Equation 2-34.

Equation 2-34

$$Total\ Energy\ Efficiency\ = \frac{Energy\ Recovered\ in\ H_2\ and\ CH_4}{Electrical\ and\ Substrate\ Energy\ Input}$$

2.4 Challenges for Scaling BES

One of the challenges with the progress of BESs is the slow progress to upscaling, where there are a few examples of pilot systems. For industries to adopt BESs, increasing the amount of pilot data is the next step. Both MFCs and MECs offer opportunities for economic scalability, but MFCs can offer higher energy returns compared to MECs producing hydrogen (Cusick et al., 2010). Due to the nature of MFCs, they are unable to compete with chemical fuel cells, and their application as an energy provider is limited (Kitching et al., 2017). However, assessing it from the perspective of a wastewater treatment process with small amounts of energy recovery and reducing sludge content, it shows promise (Song et al., 2015). MFCs can result in significant energy savings as the aeration process is the most energy-intensive part of wastewater treatment, and any energy production has significant commercial value (Heidrich et al., 2014).

Scaling up BES has difficulties because in increasing the reactor and electrode size, the internal resistance is also increased; making it difficult to directly scale up lab performance. Many researchers have looked at using multiple cell stacks in a parallel and series combination to increase the current and voltage of the system to more useable levels, as discussed previously. However, in MFCs, voltage reversal can take place if an MFC does not produce a current (Ieropoulos et al., 2010). Voltage reversal presents operational issues for MFCs when they are in series, because the power production will decrease as the substrate is consumed. Power management systems can be introduced to stop this happening, although they are expensive and create further losses (Butti et al., 2016). These operational factors make MFCs challenging to scale up compared to MECs where the applied voltage removes reversal possibilities (Oh and Logan, 2007). The reactor design of MECs can also be simplified compared to MFCs, which must have an aerobic cathode. The combination of the biocatalysts with external electrical input makes MECs one of the most attractive routes for scaling up, as they can increase the output level and potential applications (Kitching et al., 2017).

One of the factors faced with scaling up MECs is the limited number of large-scale and pilot systems. There is a significant gap in research of lab system and pilot-scale research, as shown in Figure 2-5. The focus of lab-scale research makes it challenging to assess factors important to commercial applications such as the operational requirements around maintenance, and component longevity that all impact the economic viability of the technology.

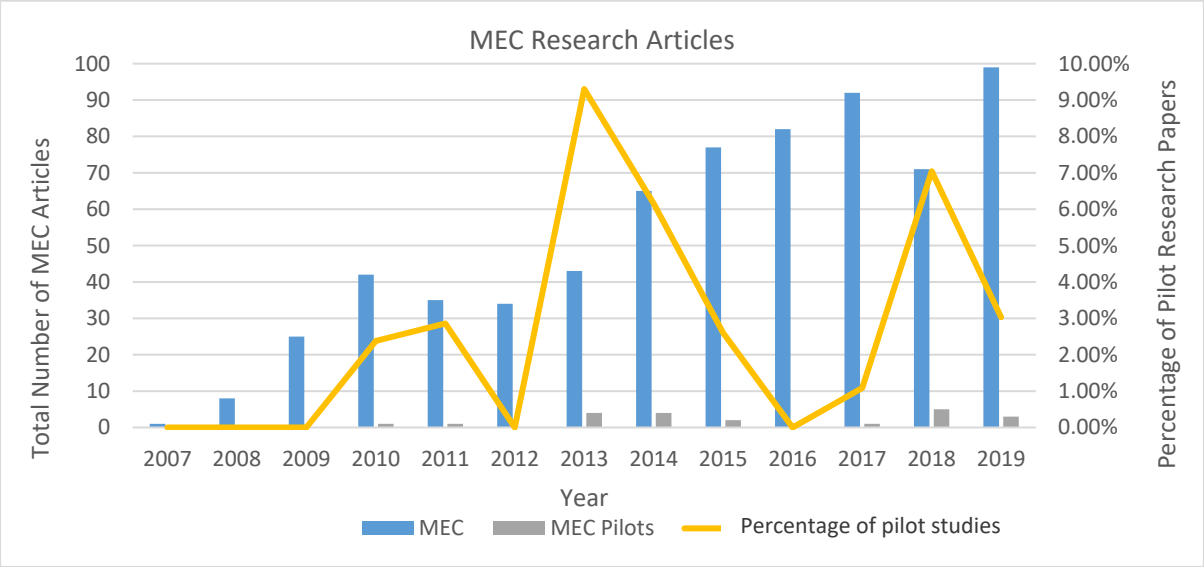

Figure 2-5: Representation of the number of published research studies into benchtop and pilot-scale MECs.

To find the total number of articles for MEC a Google Scholar Search was carried out to include (allintitle: "Microbial Electrolysis"). For pilot scale, MEC research a second Google Scholar Search was used (allintitle: Scaleup OR Scale-up OR Scaling OR Pilot "Microbial Electrolysis").

Testing the technology at scale is one of those challenges, but the systems need to be implemented in the correct way to maximise the impact and reducing barriers to entry. One route could be exploring the integration of MECs into existing infrastructure. Anaerobic Digestion (AD) is a widely adopted and accepted waste to energy technology. AD is used within the water sector for sludge treatment and other industries to produce methane from organic waste. Studies have shown that integrating MECs into AD can increase energy output by 40% and reduce COD a further 14.3% (Hassanein et al., 2017), and an increase in methane yields of 30% (Xu et al., 2019). Focusing on integrating MEC electrodes into existing AD systems could enable a smoother route to commercial adoption with fewer barriers to entry. An integrated approach will enable the technology to be tested at lower costs with the majority of the CAPEX already in place with existing AD systems. MEC integration could provide other benefits from increases in the system capacity by reducing the treatment time, and increased methane production. The modularity of the electrodes also lends itself to integrate into small and large AD facilities as the technology matures. Modular cells that can integrate into large reactors could dramatically reduce costs and enable retrofitting. Developing a flexible platform to integrate into existing infrastructure could lead to increasing the commercial application of the technology. Although consideration of the technical aspects that may affect integration need to be considered.

2.5 Conclusions

BES offers an attractive opportunity to generate energy from wastewater that could propel the circularity of the wastewater sector forward. The additional control parameters of the applied voltage in MECs and EMR offer extra stability compared to MFCs. Even though it may increase the construction cost, the additional flexibility in operational control could prove beneficial in the field. One of the challenges going forward is developing an effective strategy for scale-up. Without research into low-cost materials and large pilot systems, the technology will continue to remain an academic endeavour to make incremental system performances.

The focus of the PhD research is to explore opportunities of commercialising MECs. With the industrial adoption focus, the research will centre on three areas:

1. Assessing the suitability of the technology to treat different waste streams
2. Assessing the economic viability of the technology
3. Assessing the scaleup testing of the MECs which will lead to the implementation of the technology by industry

3 Chapter 3 - Feedstock Composition

The feedstock composition is one of the main factors in determining the energy output of BESs. The feedstock requires an adequately high COD, conductivity and substrate assimilation to have a significant power output, with temperature, pH and concentration playing a role (Premier et al., 2016).

BES have been tested on a broad spectrum of feedstocks including acetate, wastewater, brewery wastewater and swine slurry, showing the versatility of the technologies. Acetate is used often in principle investigations due to its simple structure and ease of degradability (Rivera et al., 2017). However, Heidrich et al., found that wastewater and acetate perform differently, and acetate may not give an accurate representation of how the system will perform with more complex substrate such as wastewater (2017).

Depending on the composition of the substrate, there may be other factors that affect the performance. MFC operating temperature has little effect between 23-31˚C for acetate and butyrate, but at higher temperatures, propionate and wastewater increased power densities 27% and 10% respectively (Ahn and Logan, 2010). The performance increase could be due to the higher temperatures being favourable to microbes that are more effective at breaking down more complex organics. However, the theory is not proven, and further research is required. Heidrich et al. found that high temperatures may not be as critical depending on the source of bacteria used to inoculate (2017). Wastewater is a complex substrate with a multitude of organic compounds that will vary in quantity depending on the location. The complexity of substrates used in research makes it difficult to compare the performance of different BES that operate on wastewater.

Understanding the energy content of the substrate can help determine the different compounds within the wastewater and understand the system performance. COD is a good indicator; however, as previously mentioned the energy per gram of COD can widely vary from 17.7 kJ/gCOD to 28.7 kJ/gCOD. The energy per gram of COD can vary due to presence of compounds that do not oxidise like urea which undergoes hydrolysis reactions, meaning that it will not affect the COD but will contribute to the energy value. Urea hydrolyses to ammonia and carbon dioxide. Ammonia is shown to affect methanogens in AD systems, where a 20% reduction in methane is shown ammonia if concentrations are above 2 g/L in mesophilic reactors and 5g/in thermophilic (Yang et al., 2018). Understanding the different compounds and energy value can help determine the most effective treatment. This is due to some compounds are energy rich per gram of COD resulting from their lack of hydrogen. In these cases extraction of the energy through hydrogen and methane (MECs) may not be as suitable as extracting the electrons directly (MFCs) (Heidrich et al., 2011). A quick categorisation of the feedstock may lead to the most suitable treatment or combination of multiple technologies combined in series to recover the maximum available energy. A step to progress this further would be to developing a simulation model. Simulations can help understand the different characteristics and compounds of wastewater and the reactions that take place during different treatment methods. The development of simulations will allow practitioners to test a variety of different technologies in sequence to maximise energy recovery and COD removal.

Domestic wastewater typically has low conductivity and COD, resulting in lower power BES performance. The wastewater will require an increase in electrolytes to aid in the electrochemical reactions within the wastewater streams (Rousseau et al., 2020). The organic compounds within the waste dilute as surface water and other low COD water sources mix with waste in our sewers. Low strength wastewater (< 250 mg/L COD) is usually challenging to treat economically with MECs. With slightly higher COD concentrations (360-400 mg/L COD), the system performance improves (Escapa et al., 2016b). Waste streams with high organic loads can increase energy production due to the higher chemical energy present in the wastewater. Depending on the waste stream that requires treating the economic viability of using MECs and EMRs will vary. This study is exploring the use of MEC and EMR for decentralised wastewater treatment for both industrial uses and under-served regions where the composition of waste varies for urban municipal wastewater.

3.1 Black Water - Composition

The composition of wastewater found in pit latrines is more like a slurry and will have a higher COD than wastewater found in the UK. The faecal sludge in pit latrines will likely be more comparable to sludge collected at wastewater treatment plants. Further analysis is required as human excrement quantity, and calorific value will vary from different locations due to the variety in lifestyles.

Understanding the expected volume and composition of human excreta will help increase resource recovery and design functionality. Excreta rates are approximately 1.2-1.5L of urine per day and 250g-350g of faeces a day (Feachem et al., 1983; Rose et al., 2015). Urine is 91-96%, and faeces is 75% water (Rose et al., 2015). Alongside energy recovery nutrients are also an important factor to generate organic fertilisers that can be reintroduced into the food cycle. Table 3-1 shows the nutrient content found in urine and faeces.

Table 3-1: Yearly Nutrient Values for an Individual adapted from (Rose et al., 2015)

Nutrients	Urine (kg/Person/Year)	Faeces (kg/Person/Year)
Nitrogen	2.5-4.3	0.5-0.7
Phosphorus	0.7-1.0	0.3-0.5
Potassium	0.9-1.0	0.1-0.2

3.2 Industrial Wastewater

In high strength wastewater, the high organic load increases the chemical energy present. Industries produce a variety of high strength waste streams Table 3-2 identifies the COD of the different wastewater streams and research into using BES to treat the waste. Further research into the performance of MECs and EMRs effectiveness to treat different wastewater streams will provide

valuable insights. Where, in some cases, the research suggests that the bacteria present are not able to breakdown the waste. Such as in the case of cheese whey where no gas was generated possibly due to the feedstock inhibiting the methanogens (Montpart et al., 2015).

A MEC could be optimised for hydrogen production with an OLR greater than 1000-2000 mg COD/L/d and become competitive with activated sludge treatment (Gil-Carrera et al., 2013b). Equation 3-1 describes how the OLR is calculated. Using the higher OLR value of 2000 mg COD/L/d, the theoretical HRT for the different waste streams is calculated in Table 3-2. The average HRT of the research previous presented in Table 2-1 is 30 hours. The theoretical HRT shown in Table 3-2 shows that it is possible to increase the HRT and still be competitive against activated sludge. Increasing the HRT could see an increase in COD removal but may affect energy efficiency and will need to be explored for the different waste streams.

Table 3-2: Industrial Wastewater COD Range adapted from (Doorn et al., 2006)

Industry	*COD Range (mg/L)*	*Required HRT to obtain OLR of 2000mg COD $^{-1}$ L^{-1} D^{-1} (Hrs)*	*BES Research Papers*
Urban WW	300 - 500 (Doorn et al., 2006)	5 -6	(Baeza et al., 2017; Carlotta-Jones et al., 2020; Cotterill et al., 2017a, 2017b; Escapa et al., 2016b; Heidrich et al., 2014, 2013b)
Alcohol Refining	5,000 – 22,000 (Doorn et al., 2006)	60 - 264	(Escapa et al., 2016b), (Cusick et al., 2011a)
Beer & Malt	2,000 - 7,000 (Doorn et al., 2006)	24 – 84	(Sangeetha et al., 2016)
Coffee	3,000 - 15,000 (Doorn et al., 2006)	36 – 180	(Nam et al., 2010)
Dairy Processing	1,500 – 5,200 (Doorn et al., 2006)	18 – 62	(Rago et al., 2017a)
Meat & Poultry	2,000 - 7,000 (Doorn et al., 2006)	24 – 84	(Mohammed and Ismail, 2018) (Int ; Prabowo et al., 2016)
Fish Processing	2,500 (Doorn et al., 2006)	30 – 30	(Noori et al., 2016)
Swine waste	18,300 (Taiganides, 1992)	220	(San-Martín et al., 2019; Wagner et al., 2009)
Crude glycerol	925,000 – 1,600,000 (Viana et al., 2012)	11,112 – 19,200	(Baeza et al., 2017; Chookaew et al., 2014; Escapa et al., 2009; Selembo et al., 2009b)
Cheese Whey	50,000 - 102,100 (Kolev Slavov, 2017)	600 - 1230	(Montpart et al., 2015; Moreno et al., 2015)
Activated Sludge	Dependent on waste stream	Dependent on waste stream	(Liu et al., 2012)(Wang et al., 2014) (Lu et al., 2012a)

Equation 3-1 *OLR ($kg/m^3/d$) = Feed Concentration (COD kg/m^3) x Hydraulic Retention Time (d)*

3.3 Compositional Analysis of Wastewater

For the assessment of this research, a compositional analysis of brewery wastewater and faecal sludge was carried out. The analysis shown in Table 3-3 can provide information to assess the application of treating both industrial and sanitation wastewater. Samples 1,2 and 4 were collected from WASE Limited research facility which has a microbrewery to produce waste samples and a non-flush toilet to collect faecal sludge. Sample 3 was made using three different brewery grains crystal malt: chocolate malt: cara malt at a ratio of 2:1:1. To make the sample a total of 40 g of dried and milled grains were added to 500 ml of deionised water. The grains were stirred for 30 minutes at 80°C to simulate brewery spent grain waste. The Residual Biogas Potential (RBP) used for AD waste stream analysis was carried out on the different waste streams. The RBP calculates the total gas yield, total methane content, total methane per tonne and methane mass per tonne of waste as shown in Table 3-3.

Table 3-3: Wastewater and Sludge Nutrient and Theoretical Biogas Analysis

	Brewery Tank Bottom	*Brewery Boil Water*	*Brewery Spent Grain*	*Faecal Sludge*	*Method*
Sample	1	2	3	4	
Compositional Analysis					
COD (mg/L)	18,189.5	17,698.5	N/A	10,137.4	
Crude Protein	2.40%	1.20%	<0.3%	2.30%	Outsourced NRM Labs
Crude Fibre	<0.1%	<0.1%	0.20%	0.10%	NRM Labs
Total Solids	8.80%	13.80%	3.10%	3.80%	NRM Labs
Moisture	91.20%	86.20%	96.90%	96.20%	NRM Labs
Ash	0.40%	0.50%	<0.2	0.80%	NRM Labs
Oil-B	<0.3%	<0.3%	<0.3%	<0.3%	NRM Labs
Theoretical Energy Analysis					
Total Gas Yield [Fresh Material]	43.7 m^3/t	71.4 m^3/t	16.2 m^3/t	15.1 m^3/t	NRM Labs
Total Methane Content	55%	51%	53%	66%	NRM Labs
Total Methane per tonne	24.03 m^3/t	36.41 m^3/t	8.59 m^3/t	9.97 m^3/t	
Methane Mass (kg/tonne)	17.21 kg/tonne	26.07 kg/tonne	6.15 kg/tonne	7.14 kg/tonne	
Energy per tonne (Gross Calorific Value)	265.02 kWh	401.52 kWh	94.67 kWh	109.89 kWh	
Energy per tonne (Net Calorific Value)	239.21 kWh	362.41 kWh	85.45 kWh	99.19 kWh	

3.4 Discussion

From the total gas yield and methane percentage of the different waste streams, the gross and net calorific energy value of each sample was calculated per tonne of waste. Figure 3-1 compares the biogas composition and the gross calorific value. Brewery boil water and tank bottom have the highest energy value per tonne, with spent grain has the lowest. However, the spent sample contained only 80 g/L of dried grains which are 4.5 times fewer solids than brewery boil water. Industrial spent grain waste from breweries could contain more solids. At the same total solids content, the spent grain would be in a similar region with a gross caloric value of 420.43 kWh/tonne. Faecal sludge had one of the lowest energy values per tonne, but it produced the highest methane content within the biogas at 66%.

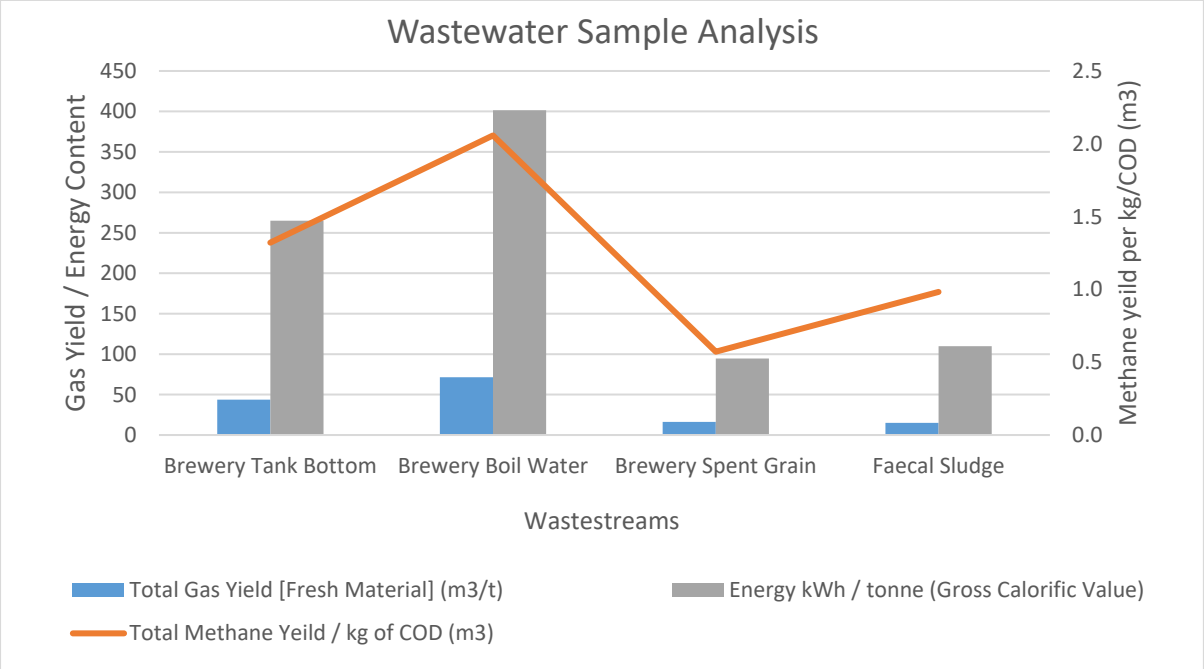

Figure 3-1: Wastewater and Sludge Biogas and Energy Value

From the theoretical biogas and energy potential analysis of faecal sludge, you could generate approximately a net energy value of 161,283 GWh of energy per year globally from untreated waste (Table 3-4). The energy value is based on the average human excrement values and the 2.4 billion people that do not have access to sanitation (WHO, 2019). The energy produced just from the faecal sludge could provide roughly enough energy for 51.5 million people using the average global energy demand per capita.

Table 3-4: Global Biomethane Energy Value from Faecal Sludge

		References
Daily personal faecal sludge production	1.65 kg/day	
Yearly personal faecal sludge production	0.60225 tonnes/year	
Global untreated Faecal Sludge	1,626,075,000 tonnes/year	
Global Net Energy Value	161,283 GWh/year	
Average Global Energy (electricity) per capital	3132 kWh	(World Bank, 2014)

Table 3-5 shows the estimated theoretical energy production for different breweries sizes and the estimated waste production (SIBA, 2020). The average energy value for brewery tank bottom, boil water and spent grain was used (229 kWh/tonne) to calculate the theoretical net energy production. The theoretical biogas calculation for brewery wastewater treatment also offers significant benefits with it's higher energy value. The breweries also have the benefit of offsetting their high volumes of heat and electrical energy required for the brewing process.

Table 3-5: Brewery Biomethane Energy Value per size

Brewery Size *Annual production levels*	*Average combined waste (tonnes/year)*	*Combined Theoretical Energy Production (Brewery tank bottom, boil water & spent grains)*
0-999HL	196	45 MWh
1,000-4,999HL	928	213 MWh
5,000-29,999HL	3,207	734 MWh
30,000-59,999HL	11,920	2730 MWh
60,000-200,000HL	50,825	11640 MWh

3.5 Conclusion

Multiple wastewater streams offer attractive feedstocks for treatment using MEC and EMR. Both could provide energy production or energy-efficient wastewater treatment, offering a more sustainable solution than current solutions. Table 3-2 gives a quick estimation of the expected treatment time for MEC treatment to be competitive with current aeration systems. The feedstock analysis also indicates that both faecal sludge and brewery wastewater could benefit from bioenergy recovery through conventional AD systems. Further analysis into both waste streams is needed to understand what benefits MEC could bring compared to alternate technologies. Such as AD which is used for energy recovery but has long treatment times and aeration which is used for quick organic removal but is energy intensive.

MEC and EMR offer different configurations and operational parameters that make some more suitable than others in certain situations. Assessing which technology is most suitable for decentralised wastewater treatment is dependent on the application. The research focus on access to safely managed sanitation and onsite industrial wastewater treatment to help define a route to commercialisation.

4 Chapter 4 - The Route to commercialisation

For any technology to progress from the laboratory to the field, it needs to be cost-effective. A Technological Economic Analysis (TEA) is essential to advance this technology for commercial use. More information is required for a detailed examination of the technology, the investment required, and market conditions to assess the suitability of the technology for widescale use.

4.1 Economic & Cost Analysis

The economic analysis of energy technologies include a Life Cycle Costing (LCC) analysis to allow the identification and evaluation of operational and capital costs (OPEX and CAPEX). Output results will include financial service values (revenue streams) and Levelised Cost of Energy (LCOE) targets (expressed as £/kWh, £/m2 and £/kWh/cycle). LCOE is a measure of the average net present cost of electricity generated from a facility over its lifetime. Assessments should include figures on the possibility of cost reduction through operational optimisation of services and collocation synergy (with renewables and energy storage solutions), as well as other economic figures such as Net Present Value (NPV) and Return of Investment (ROI). The LCC assessment should be performed in parallel to the Life Cycle Assessment (LCA), making the same assumptions. Using these calculations will help to define future costs, business models, economic strategy and risks for MECs.

Obtaining low CAPEX is crucial, and lower manufacturing costs are needed to make MECs economically viable (Escapa et al., 2012b). With the main costs associated with the anode and current collectors which can equate to 94% of the total system (Aiken et al., 2019). In Table 2-1, only two papers show the cost of the system, and the full energy demand of the system is not shown in any of the systems. The limited data highlights a crucial gap in the research hindering the commercialisation of MECs for wastewater treatment. A case study of MECs to treat urban wastewater in Saudi Arabia showed that there is potential for commercialising MECs even with their current limitations (Khan et al., 2017). However, further analysis and pilot studies are required.

Traditional wastewater treatment is energy-intensive, requiring approximately ~1 kWh to oxidise 1 kg/COD through activated sludge, therefore, treating 1 m^3 of wastewater would require ~0.5 kWh (30 kWh per capita per year) (Rabaey and Verstraete, 2005). In the current UK market, 1 kWh of electricity is £0.144 or $0.186. The electricity cost of treating 1 m^3 of urban wastewater is approximately £0.072/$0.093. Activated sludge treatment generates 0.4 kg of sludge per 1 kg of COD treated, resulting in further processing which is commonly anaerobic digestion (AD) (Rabaey and Verstraete, 2005). MECs offer an attractive option to reduce COD and generate energy, although currently most of the systems do not achieve >100% energy efficiency. Using MECs to reduce the COD and BOD of wastewater more efficiently compared to activated sludge is an attractive proposition for water utilities to have energy savings and reduce carbon emissions. Alternatively, MECs could be used to treat the sludge independently or integrated into AD. However, before MECs can be widely used commercially, the CAPEX will need to be reduced as current systems are approximately 248 times more expensive than activated sludge systems (Aiken et al., 2019). Even with reduced OPEX, the current cost will be a barrier for many financers globally.

Escarpa et al. developed three case studies assessing the economic costs of integrating MEC systems into a wastewater utility to identify the purchase price for the MEC per m^3. MECs have improved in performance since the research, and only scenario's 2 and 3 are included in Table 4-1. The analysis is based on individual cassette MECs stacked together and shows a purchase cost of £396 to £1149 [*1] per m^3 (Escapa et al., 2012b). From literature, reaching the higher purchase price seems feasible when compared to current pilot system costs. Where the construction cost of Cotterill et al's system was £1308/m^3 (Cotterill et al., 2017a) and Heidrich et al.'s £2344/m^3 (Heidrich et al., 2013b), when considering the economies of scale through mass manufacturing the lower purchase price may be possible. Along with the purchase cost, the system performance is crucial and, in this case, neither of the studies were able to achieve both a 44% COD reduction and 50% CCE. However, the targets seem obtainable with both studies close to meeting the performance requirements. The low-cost system with a working volume of 175 L using graphite felt anodes, stainless steel wool and rhinohide membranes achieved a 63.5% COD reduction. The system failed to get high coulombic efficiency getting below 10% at an applied voltage of V_{app} = 0.9V and 5h HRT (Cotterill et al., 2017a). The high-cost system had a higher coloumbic efficiency of 55% but a COD reduction of 34%. The system had a working volume of 120 L using carbon felt anodes, stainless steel wool and rhinohide membranes at an applied voltage of V_{app} = 1.1V and 24h HRT (Heidrich et al., 2013b). Both systems were operating on urban/municipal wastewater. However, the high cost system had a lower organic loading rate at 140 g/m^3/day compared to the scenario, which is set at 8800 - 17,500 g/m^3/day. These values were set by Escarpa et al., to allow the systems to a current density of 2.5 A/m^2 and 5 A/m^2 that would be in line with moderate and optimistic system improvements respectively (2012b).

Table 4-1: Estimation of MEC costs integrated into WWTP Parameters – Table adapted from (Escapa et al., 2012b).

Parameters	*Escarpa et al., Scenario 2 - 3*
COD Removal	44%
Energy Consumption	1.0 - 0.9 kWh kg/COD
Cathodic Coulombic Efficiency (CCE)	50%
Hydrogen Production	0.6 – 0.8 m^3/m^3/day
Organic loading rate	8800 - 17,500 g/m^3/day
MEC Volume	2200 – 1100 m^3
MEC Purchase Price	396 to 1149 [*1] £/m3

**1 converted from EUR at current EUR:GBP exchange rate of 1:0.8*

Aiken et al., built on Escarpa et al.'s previous work simulating seven scenarios using real-world conditions, pilot data and lower operating temperatures (1°C to 22°C) (2019). The study used Heidrich et al.'s pilot study that had a higher cost of £2344/m^3 as the baseline system performance (2013b). The different scenarios explored in the research changed market conditions and the MEC performance to guide future research and create targets for researchers. The comparative study used Activated Sludge (AS) for the competing technology. The NPV was calculated for the MEC to see at

what stage the organic loading rate made the technology more economically viable than AS (Aiken et al., 2019). The NPV shows the difference between the present value of cash inflows and the present cash outflows and is used in budget planning to assess the profitability of a project. The baseline assumptions are indicated in Table 4-2 and the other six scenarios were built around these. The paper found that MECs at the current design will have a CAPEX of £42.7 million compared to the £172,000 for activated sludge. However, the energy demands are £11,000 and £106,000 respectively. The material cost was the most significant part of the system equating to 99% of NPV for MECs. For MECs to become economically viable, the system costs need reducing by 84% to £375/m^3 with an OLR between 800-1400 g-COD/m^3/d and reaching a current density of 2-3 A/m^2 (Aiken et al., 2019). One of the challenges both of the studies highlighted was that systems need to achieve higher OLR. Using MECs for municipal wastewater treatment means that a lower HRT are required with a maximum HRT of 8.5h based on a COD of 500 mg/L. From the studies in Table 2-1 two of the MECs had an HRT below 8.5hr (Carlotta-Jones et al., 2020; Cotterill et al., 2017a). Carlotta-Jones et al, system had a 44.5 times higher normalised HRT reaching 0.0668 m^3-H^2/$m^3_{reactor}$ in an 8L MEC with carbon fibre and titanium plate anodes and stainless steel wool cathodes at a Vapp = 1.0V (2020). The only other study that achieved an OLR above 1400 g/m^3/day with non-urban wastewater was Cusick et al.'s system. The MEC was fed winery wastewater with an HRT of 24hrs and a COD range of 700-2000 mg/L (Cusick et al., 2010).

Table 4-2: Baseline Parameters for MEC vs Activated Sludge Analysis – Table adapted from (Aiken et al., 2019).

Parameters	
Price of Electricity	£0.1 kWh
Input Power	1.1V, 0.3A
Cathodic Coulombic Efficiency (CCE)	50%
Hydrogen Production	0.015 m^3/m^3/day
Organic loading rate	140 g/m^3/day
Hydrogen Purchase Price	£3.55/kg - £2.66/kg

Cusick et al., found that the value of energy recovered (hydrogen) in MECs is £0.15±0.05/kg-COD (*2) (Cusick et al., 2010). A 1m^3 MEC treating urban wastewater with a COD of 400 mg/L at an OLR of 2000 mg COD/ L/ D^{-1} would treat 5 m^3 a day. The MEC would treat 2 kg of COD generating £0.30 of energy a day or £109.50/year. The energy demands of an activated sludge treatment would equate to approximately £0.72/day or £262.80/year. If MEC systems are designed to have comparable power consumption, then they could see a significant reduction in OPEX as they will create value through energy generation.

**2 converted from USD at an $:£ exchange rate of 1 : 0.77*

Escapa et al. 's analysis show that MEC's become economically viable when the cost is reduced to 1038 £/m^3 (*1), energy consumption is 0.9 kWh kg/COD and current densities of 5 A/m^2. However, these costs are based on lab-scale systems and operational temperatures of 30°C. A system cost of £375/m^3 with an OLR between 800-1400 g-COD/m^3/d and applied voltage of Vapp = 1.0V provides

researchers with a target based on a real-life case study. Currently, only a few economic studies on MECs are presented base on urban wastewater treatment. Further analysis of EMR and MEC-AD integration and alternative waste streams should be explored. Building on techno-economic assessments of AD systems can provide insights into the economic benefits of EMR over standard AD systems as well as the technical improvements that have been reported in multiple studies (Yu et al., 2018). Creating a standardised TEA and life cycle assessment is crucial to allow comparative and reproducible analysis that can guide investors and policymakers (Rajendran and Murthy, 2019). Both of TEA and LCA's do not always capture all of the social impact and effects. A Social Organisational LCA is a new approach to capture the social impact over a products lifetime (Martínez-Blanco et al., 2015).

4.2 Hydrogen or Methane Production as the route to industrial implementation

The potential of hydrogen as an energy carrier is becoming more economically viable. The need for integrated energy storage is increasing with the demand to store renewable energy (Pandev et al., 2017). Most of the research focuses on recovering H_2 rather than CH_4. In an ideal situation, the aim would be to generate pure hydrogen, for use to manufacture other chemicals or used in the various energy recovery technologies. Otherwise, the gas will likely require post-processing to remove impurities which can increase the cost of the systems. Generating pure hydrogen has proved difficult in MEC studies with only Heidrich et al. achieving 100% purity but at low volumes ($0.015 m^3$ gas^{-1} m^3 reactor $volume^{-1}$ day) (Heidrich et al., 2013b).

Research has been led down the route for hydrogen as it has a higher energy content than CH_4 (Katuri et al., 2019). The net heating value of H_2 is 120 MJ/Kg and the high gross heating value is 142 MJ/Kg, and CH_4 is 50-55.5 MJ/kg respectively. The majority of assumptions are also based on the hydrogen being used in fuel cells and the relevant Gibbs free energy. If the gas is used for combustion then the standard enthalpy must be taken into account and this is when gas mixes (H_2 + CH_4) can add value and can see a 20% increase in energy yields (Rousseau et al., 2020).

Hydrogen also adds complexity to the system design and operation. Hydrogen requires sophisticated storage and processing equipment which is often costly. For energy generation, CH_4 offers an attractive alternative as there is extensive infrastructure to store and convert CH_4 into electrical and thermal energy. Most research does not indicate the full composition of the gas but from the data collected in Table 2-1 clearly shows that at the pilot-scale Cusick et al. 's system generates the highest amount of energy (11.31MJ/day) (Cusick et al., 2011a), where methane is the energy carrier. The paper with the highest energy production is San- Martin et al (462.56 MJ/Day) through hydrogen production at 98% purity (San-Martín et al., 2019). However, the system is a scaled-up bench system (16L) which often prove to have higher performance than pilot systems.

Bastidas-Oyanedel and Schmidt found the average prices of Methane to be £308/t^{*2} and hydrogen production costs to be (£462–1386/$t\_H_2^{*2}$) based on the production costs of hydrogen from natural gas (Bastidas-Oyanedel and Schmidt, 2018). Hydrogen is 1.5 – 4.5 times more valuable if it is required for the manufacture of other chemicals. In the case of onsite energy generation, then the value for

both methane and hydrogen will come down to the LCOE and Levelised Cost of Heat (LCOH) that is generated and utilised onsite. Cusick et al. found that an MEC was able to generate hydrogen at £3.47/kg[*2] (Winery WW) and £2.31/kg-H_2[*2] (Urban WW) (Cusick et al., 2010), which is significantly higher than when produced from natural gas.

Gas storage will play a significant role in the commercial viability of the system and reducing the storage complexity, cost and parasitic energy requirements are key for global hydrogen economy structure. It has been proposed that MECs can be coupled with renewable power sources (Chae et al., 2009; Wan et al., 2015), where the gas could be used stored as chemical energy and utilised when there is no wind or sun. CH_4 also has a higher energy density than hydrogen, making it a more viable option to be stored in bladder bags at low pressure removing the need for compressors which will significantly reduce the system efficiency. However, storing low-grade biogas (50-60% CH_4 and 40-50% CO_2) from AD is not attractive due to the energy input to store the gas at (250psi) equating to 10% of the energy value (Bastidas-Oyanedel and Schmidt, 2018). MECs produce higher quality biogas with methane concentrations reaching 86 +/- 6 % (Cusick et al., 2011a), making long term storage a more attractive option.

ADs generate hydrogen sulphide (H_2S) which needs to be removed as it is a toxic gas and can produce sulphuric acid in the presence of water. For long term storage, water vapour and hydrogen sulphide will need to be removed to stop corrosion of the storage vessels, and the cost of removal can increase the CAPEX of AD facilities (Bastidas-Oyanedel and Schmidt, 2018). Sulphides also need to be removed from wastewater. MECs are capable of removing sulphides in wastewater between 57-62.5% (Y. Jiang et al., 2014). With continuous systems removing sulphide 11 times faster than batch processing systems (Luo et al., 2014). With an applied voltage of 0.8 - 0.9V, Liu et al showed that sulphates were converted into HS^- (22%), S^{2-}(36%) but H_2S was the dominate product (2014). When MECs are designed to produce pure hydrogen, the cathode will be in a separate chamber with a catholyte to increase hydrogen production efficiency, meaning it is less likely to produce H_2S. However, the construction costs will increase with the added cost of the membrane and the increased complexity of the system design.

There is a range of technologies and manufacturers of energy production systems that can utilise biogas that range from kWh to MWh capacity including; reciprocating engines, microturbines, fuel cells, gas turbines, steam turbines and combined cycle systems (Trendewicz and Braun, 2013). Biogas can also be upgraded to biomethane for injection back into the grid if the system once it reaches a particular scale (Bastidas-Oyanedel and Schmidt, 2018). Fuel cells have high-efficiency low pollution emissions compared with the other technologies mentioned. Higher efficiency results from the direct chemical energy conversion into electricity instead of combustion. However, with any emerging technology fuel cells have a high CAPEX (Trendewicz and Braun, 2013). Solid Oxide Fuel Cells can operate with mixed fuels including methane and hydrogen and offer an attractive option for both hydrogen and/or methane production from MECs and EMRs.

4.3 Discussion & Outlook

The research into MECs and EMRs is growing for wastewater treatment. However, there is not yet an obvious route towards commercialisation. Future research should include new parameters to guide system design and material selection. As shown in appendix 13.1 Table 13-1, there is a lack of consistency in data reporting. The lack of information makes it challenging to compare studies and the data cohesively, in order to determine what parameters improve performance. Researchers should, as a minimum, record feedstock (type and COD content), inoculum source, system design (batch/flow, architecture, scale, electrode materials and surface area, cost), operational factors (HRT, duration, start-up period, applied voltage, temperature) and outputs (gas production and composition, energy production, cathodic coulombic efficiency, COD removal (%) and COD output).

One of the main factors indicated is the cost-effectiveness of a system, which currently has high manufacturing costs. There are many ways to improve system performance; however, this can lead to a considerable increase in complexity and cost. Researchers need to optimise the system using readily available materials and manufacturing techniques to reduce cost as the CAPEX is a crucial factor for the viability.

In terms of electrode materials, untreated carbon anodes and stainless-steel cathodes are currently the most viable option and are used consistently in research. A cost-benefit analysis needs to be carried out on anode and cathode materials including availability of material and its life span. Corrosion resistance is of particular importance to the longevity of the electrode, which will directly affect the OPEX. Electrodes should ideally last multiple years to reduce downtime for maintenance and operational cost for new components. There is little research on longevity beyond a year in the pilots and this will be an area of interest for the industry in determining the commercial viability of MECs or EMRs . The research also indicates that there is a lack of knowledge in the best practice to scale the electrode size which impacts the commercialisation of these technologies. Research shows that electrode materials and designs that perform well in the lab may not be effective when implemented at scale..

Comparing MEC and EMR systems to alternative wastewater treatment systems, both in terms of cost and efficiency, is imperative when getting the industry to adopt the new technology. When comparing BESs to AD, further research regarding the start-up period for COD reduction should be explored as long start-up times are a drawback of AD. The start-up is crucial as it can affect the suitability of the technology. Long start-up times may not be possible in some commercial applications, where waste needs to be treated straight away to avoid pollution. Future research about the start-up period for waste removal along with effective start-up procedure will increase the attractiveness of the technology.

Another area to explore is how we implement technologies and in what markets. Both can give new insights into the economic benefits and business cases for adoption. One possible route could be to focus on the possibility of MECs and EMRs to create hydrogen and methane respectively, and store the energy for later use. In some countries, renewable energy production is exceeding consumption. It is becoming more common to see headlines like "German renewables meet 100% of power demand for the second time ever" (Clean Energy Wire, 2018) or “Costa Rica's electricity generated by

renewable energy for 300 days in 2017" (Embury-Dennis, 2017). During the low peak, energy demand periods excess solar or wind energy could be converted into chemical energy and stored. Methane and hydrogen can both be stored without degrading, unlike battery storage. Using a chemical energy storage option is another route to assess the economic viability of MECs and EMRs.

There are several factors that determine whether hydrogen or methane production is favoured, including the scale and location of the site. Currently, due to the maturity of the methane and biogas infrastructure, electro-methanogenesis may be the most feasible route to market. Methane infrastructure is mature, and methane can be easily stored. Therefore, bio-electrochemically generated methane can be directly connected to existing gas infrastructure for use in cooking and transportation. However, the hydrogen economy is predicted to become a significant part of decarbonising our energy network with extensive research being conducted worldwide to make hydrogen a viable fuel. There are great challenges in both hydrogen storage and end of use. Therefore, EMR and methane production can then act as a stepping-stone for MECs and hydrogen production, as the market matures.

4.4 Summary

Bioelectrochemical wastewater treatment provides an opportunity for sustainable and efficient wastewater treatment method with promising results in many lab-scale studies. There is, however, a discrepancy between lab-scale studies and pilot-scale studies that is hindering the commercialisation of this technology, indicating that more pilot-scale research is critical. It is yet to be fully understood how electrode design, influent and inoculation, are affected when systems are significantly scaled up. Through economic analysis, it can be concluded that the high CAPEX acts as a significant barrier and dramatic reduction in costs are needed to make these technologies economically viable for use in industry. Electrode materials account for the most considerable capital cost and, therefore, optimised biofilm formation is paramount to minimise the electrode costs. Research in low-cost materials, manufacturing methods and component lifetime should become a focus of future research.

Assessing the practical implementation should also be a focus. Comparing other wastewater treatment methods such as aeration and anaerobic digestion with the CAPEX, OPEX and efficiency of MEC and EMR systems will help justify the use of the technology in the industry. Focusing methane production may be the most viable route to the commercialisation of this technology in the interim. The research will focus on the route of methane production using EMR, combining both an academic and industrial focus to accelerate the commercial adoption.

5 Chapter 5 - EMR Brewery Wastewater Treatment Methodology

5.1 Introduction

The chapter discusses the scale-up of electro-methanogenic systems to treat brewery wastewater. With changing regulation within developing parts of the world, regulatory barriers are increasing, putting greater restriction on business discharging their effluent. The National Environment Management Authority of Kenya (NEMA) recently shut down multiple businesses that are polluting into local environments (Onyango, 2019). EMR offers an attractive way to treat brewery wastewater and wastewater from the food and beverage industry, which is high in organics and is produced at a significant quantity.

The research were to validate EMR technology to provide decentralised wastewater treatment and energy production for breweries. The project developed an understanding of the EMR capabilities to treat brewery wastewater to meet regulatory standards and what tertiary treatment is required post-treatment. The research informed future collaborations with Forest Road Brewery that is interested in implementing both wastewater treatment and bioenergy production from their different waste streams. Currently, the wastewater that is produced consists of tank bottoms and effluent from reverse osmosis. The tank bottoms are comprised of various organic molecules from the yeast, beer and trub, which can be treated with EMR. Effluent from the reverse osmosis portion of brewery wastewater does not contain organics and will not be assessed during the study. Forest Road Brewery also produces 275 tonnes of spent grain per year which is high in organics and is a prime feedstock for biogas production at the brewery.

5.1.1 Method

The section explains the experimental methodology for the lab research into series and batch EMR treatment. Figure 5-1 shows the reactors setup. The reactors are heated to increase methanogenic activity using a Lerway 17.5W Heating Mat, and insulated using Thermo Wrap Insulation with an R Value of 1.455 m^2 K/W from tool station. The influent flows upwards from the bottom to increase mixing and solid retention within the reactor. All the reactor ports are below the water level to reduce any gas leaks. Both the gas and water outlets have tubes that go up to the top of the tank illustrated in Figure 5-1. The temperature was measured within the reactor using a Diymore 5PCS DS18B20 Waterproof Temperature Sensors Probe. Each reactor contains 4 electrodes, 2 cathodes and 2 anodes that are connected in series to a HULKIN SPS-3005D 30V 5A variable DC power supply. The reactors have a total volume of 2.5L, with a liquid volume of 2.3L and a gas volume of 0.2L.

The anodes are carbon fibre brushes, and the cathodes are stainless steel GAC pockets. Both the anodes and cathodes were connected using 0.1 mm titanium sheet that is connected to 1mm titanium wire. Outside the reactor, a terminal connector connects the titanium wire to a copper wire that connects to the power supply.

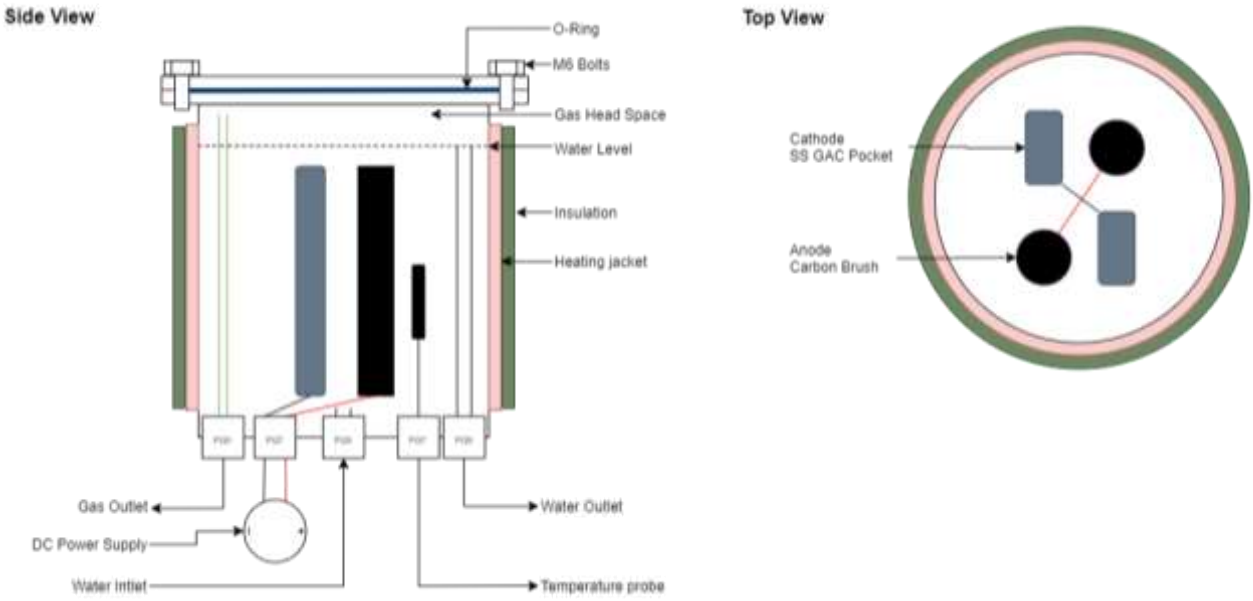

Figure 5-1: EMR Reactor Setup

5.2 Operational Conditions

The reactors are heated to 30^{O}C to maintain mesophilic temperatures.

For experiment 1 synthetic brewery wastewater continuously flows through the reactors at an 84 mL an hour to give a 24, 48, 72 and 96 hour HRT for reactors 1, 2, 3 and 4 consecutively which are connected in series. Within the batch experiments 2 and 3 the wastewater is recirculated within the reactors, at a set rate of 24 hour.

Experiment 1 ran for a total of 30 days with waste being flowed into the system and then left for a further 14 days. Experiment 2 ran for a total of 21 days using the pre-inoculated electrodes from experiment 1. Experiment 3 ran for a total of 28 days using the pre-inoculated electrodes from experiment 1 and 2.

The reactors had an Up-flow Velocity (V_{up}) of 0.00125 m/hr. The V_{up} is calculated using Equation 5-1.

Equation 5-1

$$Upflow\ Velocity\ (V_{up}) = \frac{Reactor\ height\ (m)}{HRT\ (hr)}$$

The optimum cathode potential for methane production was found to be -1.1 V which was achieved with 1.0V (Lim et al., 2020). The study used a potentiostat to analyse the voltage potential at the electrodes. However, this research is unable to understand the exact voltage potential achieved as a potentiostat is not available. With this in mind and with research suggesting methane concentrations

increase at high Vapp's an initial Vapp of -1.1 V was used. The applied voltage was reduced to 0.8 V after 29 as further analysis into MEC-AD systems operating on brewery wastewater were found to be optimal (Sangeetha et al., 2016). Although the study found the most efficient system to be a nickel cathode over stainless steel used for this research.

5.2.1 Feedstock Composition

The experiments use different feedstocks as detailed below.

Synthetic Brewery Wastewater

Synthetic brewery wastewater is used to create a controlled waste stream that will simulate tank bottom wastewater generated during the brewing process which contains yeast (60-70%), Beer (25-30%) and trub (5-10%) which contains sediment and hops after the fermentation phase. The compounds used to make the synthetic waste are shown in Table 5-1, and the substrate composition is in Table 5-2.

Table 5-1: Synthetic Brewery wastewater recipe – method for 1L at a low and high concentration

Chemical	*Formula*	*Concentration*		*Justification*
		Low Strength	*High Strength*	
Yeast Extract		1000 mg/L	2000 mg/L	Carbon Source
Malt extract		4000 mg/L	8000 mg/L	Carbon Source
Sodium hydrogen phosphate	NaH_2PO_4	80 mg/L	160 mg/L	Phosphorus source & buffer
Disodium hydrogen phosphate	Na_2HPO_4	140 mg/L	280 mg/L	Phosphorus source & buffer

The reactors are fed 2.3 L of synthetic brewery wastewater a day with a VS content of 94.1% and a pH ranging between 5.6 and 6.5. The VS loading rate was set at 2.7 g/L/day using the low strength brewery wastewater for the first reactors in the series for the first 10 days. The effluent from reactor 1 flowed in reactor 2 and continued across the series of four reactors to have a total 96 hour HRT. For the duration of the experiment, the VS loading rate was increased to 5.1 g/L/day using the high strength brewery wastewater and continued to flow in series through the reactors.

Table 5-2: Synthetic Brewery wastewater composition

	TS (g/L)	*VS (g/L)*	*VS (%)*	*COD (mg/L)*
Synthetic Brewery Waste (Single strength)	5.05	4.75	94.1%	3903 ± 137
Synthetic Brewery Waste (Double strength)	9.5	8.85	93.2%	8816 ± 1412

Spent Grains

Breweries generate significant volumes of spent grain, which could become a valuable resource to generate bioenergy onsite that can be used for heating and electricity production. The research uses a combination of three different grains, Crafty Brews crystal malt: chocolate malt: cara malt at a ratio of 2:1:1. The VS loading rate was calculated to assess the correct loading for the digestors. In practice the grains will need to be broken down in a macerator and chopper pump.

The VS for dried spent grains are approximately 96.1% (Panjičko et al., 2017). Typical loading rates of AD systems are between 1.6 - 3.2 kg VS/m^3/day. An upper VS loading rate for a wet digester is 5-6 kg VS/m^3/day, with a majority of ADs operating between 3-4.5 kg VS/m^3/day (ADBA, 2017). The United States Environmental Protection Agency's AD calculation tool 'Introduction to the Anaerobic Digestion - Project Screening Tool (AD-PST)' suggests a VS loading rate of 1.6-3.2 kg VS/m^3/day (US-EPA, n.d.). A total of 33.12 g of VS was added to each reactor equivalent to 6 times a VS loading rate of 2.4 g/L/day to establish a VS concentration of 14.4 g/L. The experiment was continued for 21 days to ensure the full breakdown of the organics during the experiment.

Brewery Boil

Brewery boil water was collected from the production of a dark brown ale brewed at WASE. The boil water was then blended to reduce the size of the solids allowing them to be circulated through a peristaltic pump. Below Table 5-3 shows the substrate analysis.

Table 5-3: Brewery Boil Substrate Analysis

	Turbidity (NTU)	*TDS g/L*	*TSS g/L*	*TS g/L*	*VS g/L*	*VS (%)*	*COD mg/L*
Brewery Boil	18400	95	200	206.9	202.6	97.92	81455.1

The brewery boil have a VS content of 97.92%, the reactors each had 240mL of boil added to the digestate. A total of 48.6 g of VS were added, increasing the VS concentration by 45% to 21.1 g/L.

5.2.2 Inoculation

Each EMRs had 2L of digestate from a 50L lab AD system that was operating on food waste to inoculate the systems. The digestate was filtered to remove any large particles from the digestate to reduce any sludge build-up within the system. After the digestate was inserted into the reactors the system was sparged with nitrogen and left for 7 days with an applied voltage of 1.1V. The seven-day period was to allow the biofilm to start developing on the anode and cathode with the set differentials. The seven day period also allows the organics in the digestate to be broken down further, and all the methane and carbon dioxide has off-gassed. Nitrogen sparging for 1-minute was to ensure an anaerobic environment by removing dissolved oxygen and oxygen in the reactor headspace. After the 7 days, the synthetic brewery wastewater was flowed through the system. After seven days of flowing the synthetic brewery wastewater into the reactors, an additional 1L of digestate from an AD system was flowed directly into each reactor to increase the micro-organisms within the bulk liquid. After the first 30 days of the first experiment spent grain was added to the reactors and left for 14 days to increase the biofilm growth and reduce microbial washout.

For the subsequent experiments comparing EMR to AD, the same EMR electrodes from reactor 2-4 in experiment 1 were re-used in the EMR to remove the need for long inoculation periods. To bolster the micro-organisms within the bulk liquid of the EMR and AD system the effluent from the first experiment was mixed together and 2.2 L of effluent was redistributed to each of the 3 EMR and 3 AD reactors. The reactors were sparged with nitrogen to remove any dissolved oxygen. After sparging the reactors were left for 7 days to off-gas after the reinoculation to breakdown any remaining organics within the effluent. After the seven day period the spent grain waste was added to the reactors.

For experiment 3, the reactors were emptied from experiment 2 and the AD, and EMR effluent was mixed. 1.3 L of the effluent was then added to each of the EMR and AD systems to ensure an even spread of the micro-organisms across the reactors. The reactors were sparged with nitrogen to remove any dissolved oxygen. After sparging the reactors were left for 7 days to off-gas after the reinoculation to breakdown any remaining organics within the effluent. After the seven day period, the brewery tank bottom waste was added to each of the reactors.

5.3 Electrode Preparation

Carbon fibre brush electrodes were prepared using carbon fibre (bare carbon fibre string, Fibraplex) cut into 87 x 5cm lengths; this made a brush with a TPI of 200,000 per inch. The brushes were trimmed to have a radius of 20mm. Brushes had a total of 1,040,000 strands with a total surface area of 11,438.6 cm^2 per brush. Grade 1, 0.8 mm Titanium wire was used as the core of the brush, which also acted as a current collector (Figure 5-2 and Figure 5-3).

The research used a combination of both SS and GAC for the cathode to increase the conductivity and the surface area. The 3D GAC provides a bed for methanogenic bacteria to form near to the surface where hydrogen production occurs. The cathode pockets are fabricated using 304 stainless steel 40 mesh (Figure 5-2 and Figure 5-3). The mesh is seam welded to create a pocket for the GAC (15 x 4 cm)

with a total surface area of 120 cm^2. The pockets are filled with 27g of GAC (Chemviron Carbon - Environcarb 207C). The GAC creates a fixed bed for a methanogenic biofilm to form at the point of hydrogen production to accelerate methane production. The GAC has a surface area of 21,600 m^2. The total specific surface area of the cathode is 92,991.3 cm^2/ cm^3.

Table 5-4: Electrode Characterisation

Electrode	***Electrode Specific Surface Area (cm^2/cm^3)***	***Dimensions (mm)***
Carbon Fibre Brush	4.92	130 x 30
Stainless Steel GAC Pocket	92991.27	150 x 40

Figure 5-2: Carbon Brush Anode & Stainless Steel Pocket & GAC Cathode - Front View

Figure 5-3: Carbon Brush Anode & Stainless Steel Pocket & GAC Cathode - Side View

5.4 Experimental Setup

Figure 5-4 shows the system flow diagram for one of the series treatment setups. The setup is duplicated for a repeat experiment. The synthetic brewery wastewater is mixed and inserted into a 5L storage tank. A peristaltic pump flows the wastewater into the bottom of the first reactor. The four reactors connect in series with the wastewater flowing out the top reactor and into the bottom of the next. A T-connector is in between the reactors with a ball valve for wastewater sample collection between the reactors. Each reactor has a separate DC power supply for the electrodes.

The batch experiments use the same reactors and electrodes from the series setup to simulate the operation of an EMR with a mature biofilm. The wastewater flows out the top and into the bottom of the same reactor to agitate the bulk liquid. There is a sampling port on both the outlet and inlet for

samples to be taken during the experiment shown in Figure 5-5. Pictures of the experimental setup are shown in Figure 5-6 and Figure 5-7.

The operational conditions for the three experiments and feedstocks is shown below Table 5-5.

Table 5-5: Operational Conditions:

Feedstock	*Inoculum*	*COD Input Range (mg/L)*	*Scale (L)*	*Specific Anode Surface Area (m2/m3))*	*Specific Cathode Surface Area (m2/m3))*	*HRT (hrs)*	*Duration (days)*	*Voltage Applied (V)*	*Temp (C)*
Synthetic Brewery wastewater	Digestate from a food waste AD system	3903 - 8816 mg/L	10L Series 4 x 2.5L	22877.2 cm^2/ cm^3	92,991.3 cm^2/ cm^3	24, 48, 72 & 96	60 (+7 inoculation)	1.1 (0-30days) 0.8 (31-45 days)	≈30
Spent Grains	Effluent from EMR synthetic brewery wastewater		2.5L 3x2.5L EMR 3x2.5L AD	22877.2 cm^2/ cm^3	92,991.3 cm^2/ cm^3	Batch	21 (7 days starving beforehand)	0.8	≈30
Brewery Boil	Effluent from EMR & AD spent grain		2.5L 3x2.5L EMR 3x2.5L AD	22877.2 cm^2/ cm^3	92,991.3 cm^2/ cm^3	Batch	28 (7 days starving beforehand)	0.8	≈30

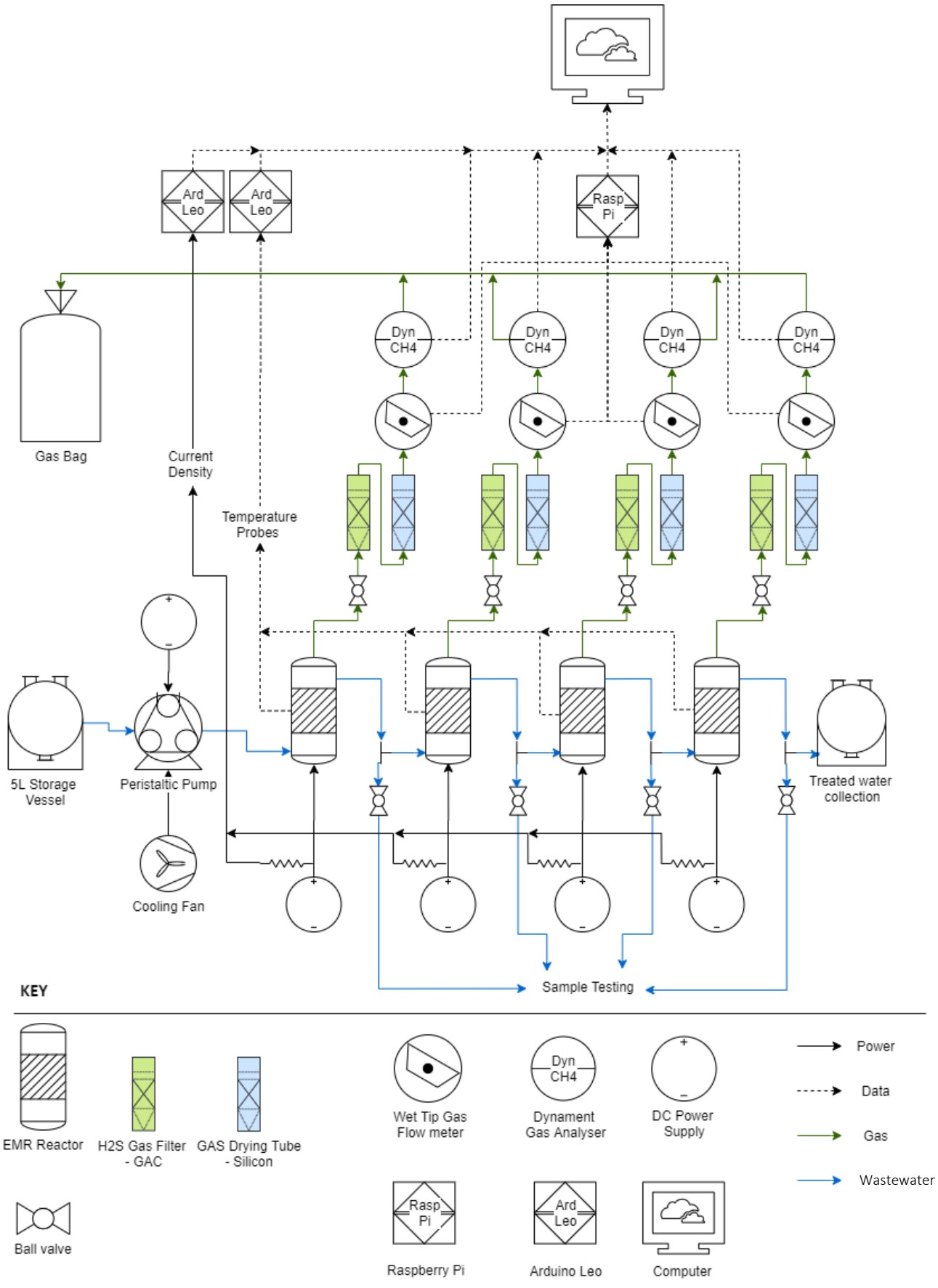

Figure 5-4: Brewery wastewater series EMR analysis - System Flow Diagram showing 1 of 2 identical setups

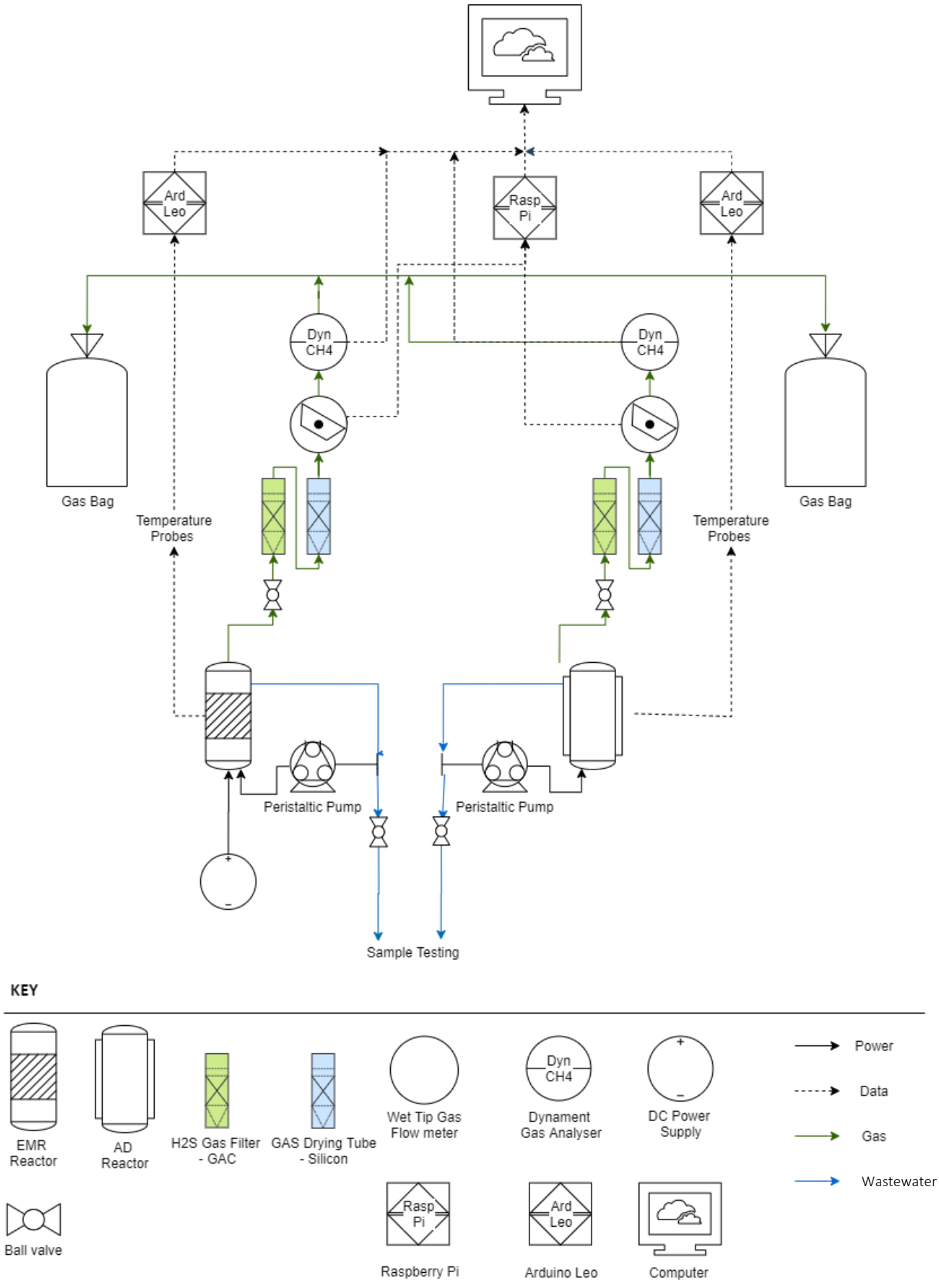

Figure 5-5: Upflow EMR & AD Batch Analysis - System Flow Diagram showing 1 of 3 identical setups

Figure 5-6: Brewery wastewater series (Duplicates) and batch EMR and AD analysis – Experimental setup

Figure 5-7: Brewery wastewater series (Duplicates) and batch EMR and AD analysis – Heating jackets removed

5.5 Analytical Measurements

Below are the various parameters measured to analyse the system performance at treating the different waste streams. The experimental data is duplicated twice for the series experiments and three times for the batch experiments to reduce errors. Multiple samples were taken and stored to enable repeats if the experimental error of the analysis was great than 5% using a set standard.

5.5.1 Gas Analysis

The biogas flows through two filtration columns; the first is to remove H_2S and is filled with GAC (Chemivron Carbon-STIX). The gas then flows into the second column filled with silicon beads to remove any moisture from the gas. The biogas flows through a wet-tip gas flow meter calibrated to record in 10mL increments. When 10mL of gas is collected the flow meter tips closing a switch, the Rasberry Pi records the signal, counting the number of tips to calculate the gas flow rate. The biogas composition is analysed using a Dynament Dual-Gas High-Resolution Methane / Carbon Dioxide Sensor (CH_4 0-100%, CO_2 0-100%, Other Hydrocarbons 0-4%).

5.5.2 Temperature

The temperature probes connect to an Ardunio Leo connected to a PC that records the temperature within the reactor every 30 minutes.

5.5.3 Current Density

The current was measured every day using a multimeter (Standard st-920). Each power supply connects to a circuit with a 1-ohm resistor. The circuit measured the current generation for each EMR, as shown in Equation 5-2.

Equation 5-2 $$Current = Voltage / Resistance$$

5.5.4 Wastewater Analysis Parameters:

Different wastewater tests were taken at the four sampling points between the series experiments and between the out and inflow of the batch recirculation. For the series, experiment the samples were taken before treatment and at the four sampling points after each reactor shown in Figure 5-4. A 4mL sample was taken when only the pH, COD and turbidity tests were measured, and a 30mL sample for the full analysis. Eight parameters are measured listed in Table 5-6 with the schedule of the tests in Table 5-7.

Table 5-6: Wastewater Analysis - Equipment

Parameter	*Instrument*	*Units*
pH	SciQuip Portable precision Multi-Parameter Water Quality Meter(SQ-7052) P11 pH Electrode	
Total Dissolved Solids (TDS)	SQ-7052 - K10 Conductivity Cell	mg/L
Turbidity	HANNA Instruments - LP2000 Turbidity Meter	NTU
Chemical Oxygen Demand (COD)	Camlab Cw2000 colormeter HACH LangeLT200 – Heating block HACH COD Vials 0-1500mg/l and 0-15,000 mg/L	mg/L
Total Suspended Solids		mg/L
Sludge Volume Index		mL/g
Batch Settling Curve		mL/L
Volatile Solids		mg/L

Table 5-7: Wastewater Analysis Schedule

Sampling Point	*Test*	*Frequency*
Pre Treatment from storage container	pH	The wastewater produced to a specific methodology. The analytical tests were carried out 3 times to assess the baseline wastewater quality pre-treatment.
	Total Dissolved Solids (TDS)	
	Turbidity	
	Chemical Oxygen Demand (COD)	
	Total Solids (TS)	
	Total Volatile Solids (VS)	
Post Treatment	pH	Exp1& 2. Every day (Mon-Fri) Exp3. Every day
	TDS	Exp1. Every day (Mon-Fri) Exp2 & 3. End of experiment
	Turbidity	Exp1. Every day (Mon-Fri) Exp2 & 3. End of experiment
	COD	Exp1& 3. Every day (Mon-Fri) Exp3. Every day
	Total Suspended Solids	Exp2& 3. End of experiment
	Batch Settling Curve	Exp2. End of experiment
	Sludge Volume Index	Exp2. End of experiment

COD Reduction Percentage

The COD reduction percentage is shown over time and is calculated in Equation 5-3

Equation 5-3: $$COD\ Reduction\ (\%) = COD_{in} - \frac{COD_{in} - COD_{out}}{COD_{in}}$$

Total Suspended Solids

Total Suspended Solids (TSS) are calculated using Hach AE grade Filters. The filters are recorded and then placed into Burcherner funnel. A 20ml sample is placed into the funnel and pulled through a vacuum filter paper. The filter paper is placed into the oven at 105°C to dry the sample. The mass of the sample is then measured, and the mass of the filter paper is taken away to calculate the sample TSS.

Total Dissolved Solids

Total Dissolved Solids (TDS), the liquid portion that is pulled through the filter paper from the TSS is poured into a petri dish. The petri dish is placed into the oven at 105°C to dry the sample so the mass can be calculated. Equation 5-4 is used to calculate the TDS (mg/L) from the sample mass

Equation 5-4 $$TDS\ (\frac{mg}{L}) = \frac{mass\ of\ solids\ (mg)}{volume\ of\ sample\ (L)}$$

Volatile Solids

The Volatile Solids (VS) is calculated using a 1mL sample; the liquid is dried in a crucible in the oven at 105°C to dry the sample. The mass of the crucible is measured with the dried solids. The weighed sample is put into a furnace at 550°C for 1 hour to burn off the volatile solids. Equation 5-5 is used to calculate the VS (mg/L) from the sample mass:

Equation 5-5 $$VS\ (\frac{mg}{L}) = \frac{mass\ of\ ovendried\ solids\ (mg) - \ mass\ of\ ash\ (mg)}{volume\ of\ sample\ (L)}$$

Batch settling curve

To measure the sludge settling curve, a 500mL sample is required from the tanks. The sample is poured into a 500ml graduated cylinder showing 50ml increments. The sludge settling is then recorded every 0.5, 1, 2, 3, 4, 5, 10, 15, 20, 30 and 45 minutes.

Sludge Volume Index

The Sludge Volume Index (SVI) describes the settling ability of the sludge from the treatment system. SVI is calculated using the TSS and the 30-minute sludge volume from the batch settling curve using Equation 5-6.

Equation 5-6

$$SVI = \frac{Settled\ sludge\ volume\ \left(\frac{mL}{L}\right)}{Total\ Suspended\ Solids\ \left(\frac{mg}{L}\right)}\ x \frac{1000mg}{gram}$$

5.5.5 Operational Analysis

The section below has adapted the system performance equations from section 2.3.6 changing the formulas from hydrogen to methane.

Energy Production

The energy production is calculated using the biogas volume of biogas produced multiplied by the concentration of methane and the net energy value of methane to get the kWh, as shown in Equation 5-7. The Dynament sensor measures - both methane (0-100%) and hydrocarbons (0-4%). For the analysis, the methane and hydrocarbons have been combined to create a total combustibles percentage. For the analysis, the total combustibles are presumed to be methane for energy production values.

Equation 5-7:

$$Energy\ Production = Biogas\ Production\ (m^3)\ x\ Methane\ Concentration\ (\%)\ x\ Methane\ Net\ Calorific\ Value\ (10.087\ kWh/m3)$$

Electrical Efficiency

η_E64 is a measurement to compare the electrical energy input to the amount of recovered methane (Equation 5-8). η_E is measured as a percentage, and if it is over 100%, then the EMR is producing energy from the substrate potential energy (Cotterill et al., 2016).

Equation 5-8

$$Electrical\ Energy\ Efficiency = \frac{Energy\ Recovered\ in\ CH_4}{Electrical\ Energy\ Input}$$

$$\eta E = \frac{W_{out}}{W_E}$$

Electrical Energy Input *(W_E)* Equation 5-9 is given in kWh and is calculated by integrating the voltage added at each measured potential (*E)* and external resistor R_{ex} *(I=E/*R_{ex}*)*. E_{ps} is the applied voltage

(potential) of the power supply, that should be adjusted for the losses caused by the external resistor (I^2R_{ex}), with integration over n data points measure over timer intervals Δt (Cotterill et al., 2016). In the case where systems are heated the, W_E contains the heating power (H_p) requirements expressed in Equation 5-9.

Equation 5-9 $$(W_E) = \sum_1^n \left(IE_{ps}\Delta t - I^2R_{ex}\Delta t\right) + (Hp\Delta t)$$

The Energy recovered in CH_4 (W_{out}) is calculated from the moles of methane produced (N_{CH_4}) and the standard heating value of methane (ΔH_{CH_4}). The gross heating value of methane (39.8 MJ/m^3) is used if the electrochemical conversion of methane to electricity is through a fuel cell. In the case of the experiments being carried out the lower heating value (35.8 MJ/m^3) needs to be considered as it is likely that methane will be combusted. The lower heating value includes the heat loss through the combustion and heat loss from the production of water vapour needs to be considered. The MJ are then converted into kWh using the 0.278 MJ/kWh conversion (Cotterill et al., 2016).

Equation 5-10 $$W_{out} = \frac{\Delta H_{CH_4} N_{CH_4}}{3600\ Joules}$$

Substrate Efficiency

Substrate efficiency (SE) (Equation 5-11) is the comparison of the number of moles of methane (N_{CH_4}) produced to the theoretically amount possible based on the substrate removed (N_S) from the EMR. N_S is calculated with Equation 5-12. SE is expressed as a percentage and indicates the substrate conversion efficiency (Cotterill et al., 2016).

Equation 5-11 $$Substrate\ Efficiency = \frac{Moles\ of\ CH_4\ recovered}{Theoretical\ moles\ of\ CH_4\ in\ the\ substrate\ removed}$$

$$SE = \frac{N_{CH4}}{N_S}$$

Equation 5-12 $$N_S = 0.0136 \Delta COD \Delta t$$

Equation 5-13 $$CH_4 + 2O_2 \rightarrow CO_2 + 2H_2O$$

From Equation 5-13 it can be assumed that two moles of oxygen (64g) is required to oxidise 1 mole of methane (22.4L). Meaning that 1g of COD is equivalent to 0.35L of methane at 0°C and 760mm Hg pressure (STP) at higher temperatures of 35°C and 1 atmosphere the CH_4 equivalence is 0.395L (Speece, 2007). One mole of methane is 28.96L, so at higher temperatures 0.395L is 0.0136 moles. The COD removal is measured to Equation 5-13 give ΔCOD over the time interval of the experiment.

Coulombic Efficiency

Coulombic Efficiency (CE) is the amount of methane produced compared to the theoretical maximum amount of electrons produced based on the current or total charge passing through the cell (Equation 5-14). CE is shown as a percentage and cannot exceed 100% (Cotterill et al., 2016).

Equation 5-14 $$Coulombic\ Efficiency\ = \frac{Moles\ of\ CH_4\ Recovered}{Theoretical\ Moles\ of\ CH4\ in\ the\ Current\ Produced}$$

Equation 5-15 $$CE\ = \frac{N_{CE}}{N_{CH_4}}$$

The theoretical moles of methane-based on current (N_{CE}) can be calculated through Equation 5-16.

Equation 5-16: $$N_{CE} = \frac{\sum_1^n I\Delta t}{4F}$$

I is the current calculated from the measured voltage and the resistance, Δt is the time interval, 2 electrons are required for the hydrogen evolution reaction, and 2 hydrogen molecules are required for methane. Therefore 4 electrons are required, and F is the Faraday's constant (96,485 C/mol e-) (Cotterill et al., 2016).

Total Energy Efficiency

Total Energy Efficiency (η_{E+S}) Equation 5-17 is the Energy recovered in methane compared to the electrical and substrate energy inputted into the system. η_{E+S} is calculated as a percentage. The substrate potential energy is calculated as chemical energy and not free energy which is lower, especially in wastewater (Cotterill et al., 2016).

Equation 5-17 $$Total\ Energy\ Efficiency\ = \frac{Energy\ Recovered\ in\ CH_4}{Electrical\ and\ Substrate\ Energy\ Input}$$

Equation 5-18 $$\eta_{E+S}\ = \frac{W_{out}}{W_{E+S}}$$

Calculating the substrate energy (W_S) is shown below in Equation 5-18

Equation 5-19 $$Ws\ =\ \Delta COD \Delta H_{WW/COD}$$

ΔCOD is the difference between the influent and effluent COD measured in grams. The energy content per gram of COD ($\Delta H_{WW/COD}$) is the internal energy of the substrate measured in kJ per mole in thermodynamic tables (Cotterill et al., 2016). As previously discussed wastewater is a complex substrate with various chemicals. The research assumes the energy value is 17.7 kJ/gCOD and will be used for the $\Delta H_{WW/COD}$ of wastewater.

5.5.6 Statistical Analysis

Statistical assessments can help identify the correlations between measured parameters alongside the statistical importance of the correlation.

Pearson's Coefficient

Pearson's coefficient (r) will identify the degree of a negative or positive linear correlation between two variables and can be calculated with Equation 5-20. n is the sample size, x_i and y_i are sample points indexed by i. $\bar{x}$ *and* $\bar{y}$ and the sample mean values. Peason's coefficient show values between 0 and 1. 0 shows no correlation whilst 1 shows a perfect correlation. The correlation can be either positive or negative, indicated by positive or negative values (Patten, 2018). Figure 5-8 shows the correlation strength from 0 no correlation to 1, which is a perfect correlation.

Equation 5-20

$$r = \frac{\sum_{i=1}^{n}(x_i-\bar{x})(y_i-\bar{y})}{\sqrt{\sum_{i=1}^{n}(x_i-\bar{x})^2}\sqrt{\sum_{i=1}^{n}(y_i-\bar{y})^2}}$$

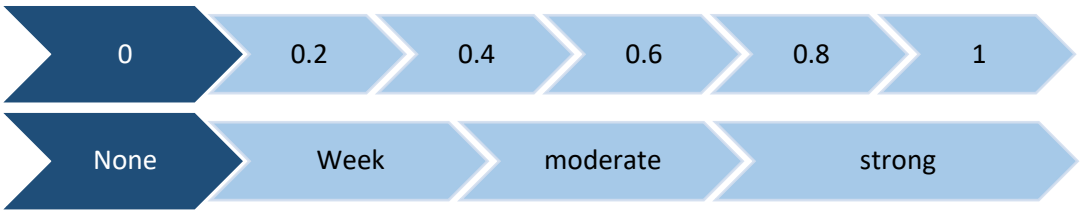

Figure 5-8: Pearson's Coefficient Relationship adapted from (Patten, 2018)

To understand the statistical importance of the correlation, the P-Value is calculated. The P-value uses the t-distribution value shown in Equation 5-21. The P-value indicates whether or not the correlation is significant <0.05 or not significant >0.05 (Patten, 2018).

Equation 5-21:

$$t = \frac{r\sqrt{n-2}}{\sqrt{1-r^2}}$$

6 Experiment 1 - Series EMR Results

During the experiment, a couple of issues arose with the pumping and flow of the system.

a) On day four, the continuous flow was causing issues with gas lines flooding. The water was not flowing from one reactor to the next correctly. It was decided to change the system to a run as a sequential batch system allowing someone to be present for the duration of the pumping and to stop any faults occurring.
b) On day seven, the reactors 1-8 were fed with 1L of additional digestate directly to increase the bacterial loading. It was speculated that the high flow rate could have washed out the bacteria reducing the ability of the biofilm to form.
c) On day nine, Reactor 5 (R5) failed due to a crack forming around the system. The fault meant that the system drained overnight. A replacement reactor was fitted, and the previous electrodes where inserted. Fresh digestate was fed into the R5 after setup.
d) On day 17, it was suspected that the dynament sensor housing could be leaking as the gasbags were not filling up, but the flow meters were registering gas production—new housings where gas tested and fitted.
e) On day 23 the systems were still producing small volumes of gas and low methane concentrations. 100g of spent grains were added to the brewery wastewater, to understand how the EMR would react to an increase in the OLR.
f) On day 29, the reactors where not fed and the applied voltage was lowered from 1.1V to 0.8V and left to stabilise before batch tests.

6.1 Reactor Conditions

Over the 30 days, the total organic loading was 0.58 kg across the two setups with each system receiving 0.29 kg. The operational conditions of the reactors for the duration of the experiment are below in Table 6-1.

Table 6-1: Series EMR Operational Conditions

Reactor number	*Reactor Series*	*HRT (hours)*	*Operating Temperature (°C)*	*Avg. pH*
1	First	24	28.1	5.37
2	Second	48	29.7	5.61
3	Third	72	31.6	6.35
4	Fourth	96	30.2	6.40
5	First	24	30.6	5.54
6	Second	48	30.6	5.80
7	Third	72	32.2	6.52
8	Fourth	96	30.1	6.71

6.1.1 Water Quality Measurements:

One of the main parameters to assess for EMR is the ability of the systems to treat wastewater. Below the different water quality measurements throughout the experiment are shown.

pH

Figure 6-1 shows the pH for the different reactors from the first to fourth. Throughout the experiment, there is a clear indication that the pH increases towards neutral (pH) from the first to the fourth reactor. The experimental setup changed from a continuous low flow rate to a sequential batch system, due to pumping issue. The setup change meant that 2.5L of wastewater flowed through the system in 1 hour instead of over 24 hours. The changed pumping schedule resulted in an increased flow rate from 1.6 mL/min to 38 mL/min. As a result, the reactors would undergo a quick change in the composition of the wastewater. For the duration of the experiment, the pH of the feed was between 6 and 7.2 apart from day 3. As the waste was continually pumped at this point it is likely the wastewater underwent fermentation before entering the reactors causing the low pH. The reactors all show a lower pH, which does increase from the first to fourth in the series. The high flow rate of feed could have shocked the microbial community compared to a continuous system. A small, steady flow of untreated wastewater would mix with existing wastewater within the reactor, creating a buffer to help stabilise the pH. In reality, the systems had a high VS loading in a short period resulting in a high concentration of VFA to form, causing the pH to drop. We can see on day 16 that there is a significant pH drop from the feed where we see within the first 24 hours the pH decrease to 3.96 just below the optimum pH range for the first acid formation stage. Only reactors R7 and R8 reach the lower optimum pH range for methanogenesis of 6.5 to 8.2.

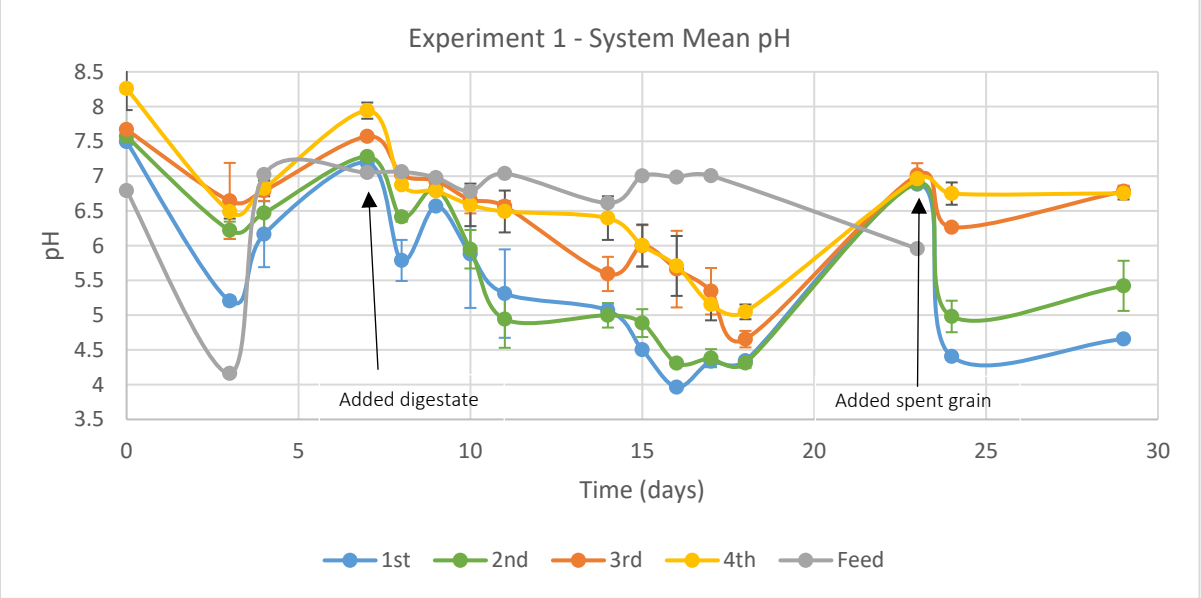

Figure 6-1: Series EMR - Brewery Wastewater mean pH with error bars representing the range across the duplicated experiments and arrows illustrating points of additional feed.

Chemical Oxygen Demand

Below, Table 6-2 shows an overview of the COD removal and Figure 6-2 and Figure 6-3 shows the COD effluent and the COD percentage reduction throughout the experiment. On day 7, additional digestate was added to the digesters to increase the bacterial loading, which is why the effluent COD is higher than the feed. On day 23, 50g of spent grains were also added to the brewery wastewater, which caused the COD of the first and second reactors to increase above the feed COD. From around day eight, they follow a trend that the COD reduction increases from the first to the fourth reactor as expected. The COD removal did not take into account the initial inoculum. During the start of the test with the lower OLR, the effluent would have contained a higher proportion of sludge within the reactors that would affect the COD measurements and is likely to have caused the irregular COD reduction shown in Table 6-2. The final effluent has an average 51.7% COD reduction, reaching an average COD effluent of 4458 mg/L. The effluent still has a very high COD content and would require further treatment to reduce it to below 125 mg/L to meet EU discharge regulations. The negative COD values shown in Figure 6-3 are likely due to the spent grain added to the reactors. Additionally spent grain is not represented in the feed COD as it is a solid waste and would not translate directly into COD.

Table 6-2: Mean Series EMR COD including the Range (±)

Reactor Series	*Average COD Reduction*	*Avg. Low OLR– COD Reduction*	*Avg. High OLR – COD Reduction*	*Avg. Percentage increase*	*Avg. Cumulative Percentage Increase*	*Average (Avg.) high OLR COD Effluent (mg/L)*
First	33.6 *± 6.9%*	32.0 *± 2.7%*	34.0 *± 8.1%*	-		5839 *± 736*
Second	35.0 *± 5.8%*	21.3 *± 2.7%*	38.7 *± 6.6%*	+ 1.4%	+ 1.4%	5517 *± 595*
Third	38.0 *± 6.2%*	7.8 *± 8.7%*	46.2 *± 5.3%*	+ 3.0%	+ 4.4%	4884 *± 461*
Fourth	47.5 *± 3.8%*	31.9 *± 5.3%*	51.7 *± 4.2%*	+ 9.5%	+ 13.9%	4458 ± 383

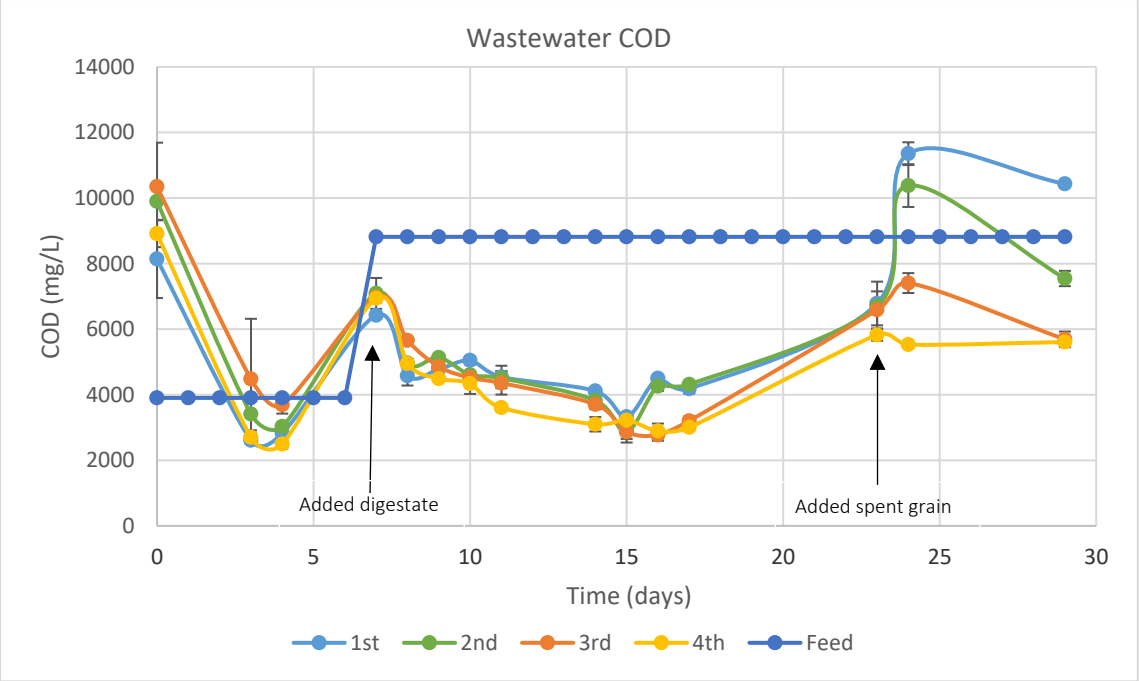

Figure 6-2: Series EMR - Brewery Wastewater COD Reduction, with error bars representing the range across the duplicated experiments and arrows illustrating points of additional feed.

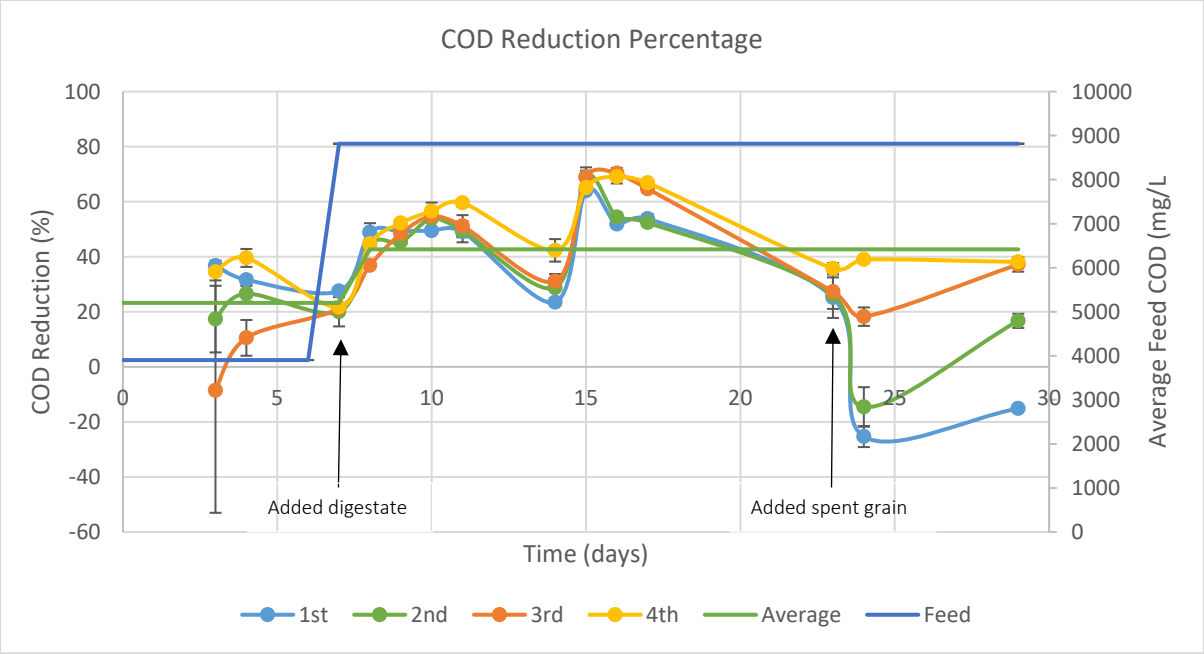

Figure 6-3: Series EMR - Brewery Wastewater COD Percentage Reduction, with error bars representing the range across the duplicated experiments and arrows illustrating points of additional feed.

The pH can affect the system performance by inhibiting certain micro-organisms such as methanogens. Figure 6-4 to Figure 6-8 compare the pH against the COD reduction to analyse any correlation between the two. The data within the graphs do not show any correlation, with a Pearson's coefficient of -0.12 and p-value of 0.23.

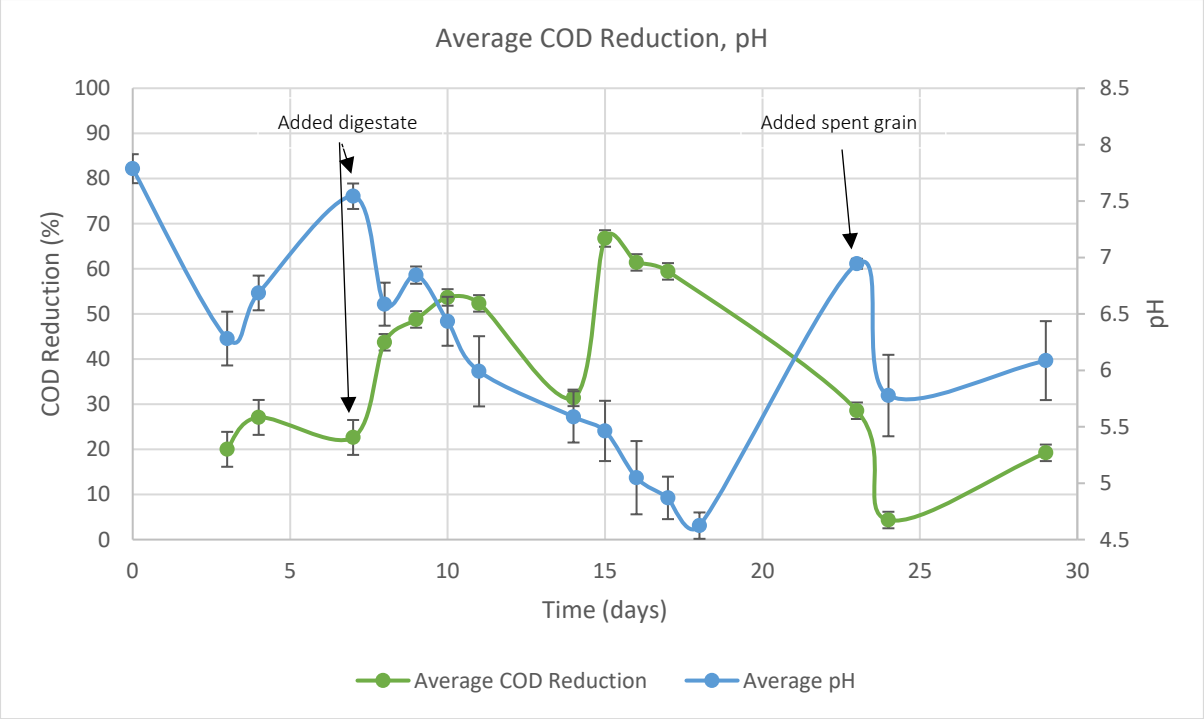

Figure 6-4: Series EMR - Brewery Wastewater COD Percentage Reduction compared to pH, with error bars representing the range across the duplicated experiments and arrows illustrating points of additional feed.

Turbidity

Below Figure 6-5 shows the turbidity from each of the reactors; the data did not provide any insights as the turbidity was significantly higher than the feed. The reason is likely due to the digestate inoculation that was also being flushed through the system. As a result, the data was not collected continuously throughout the experiment.

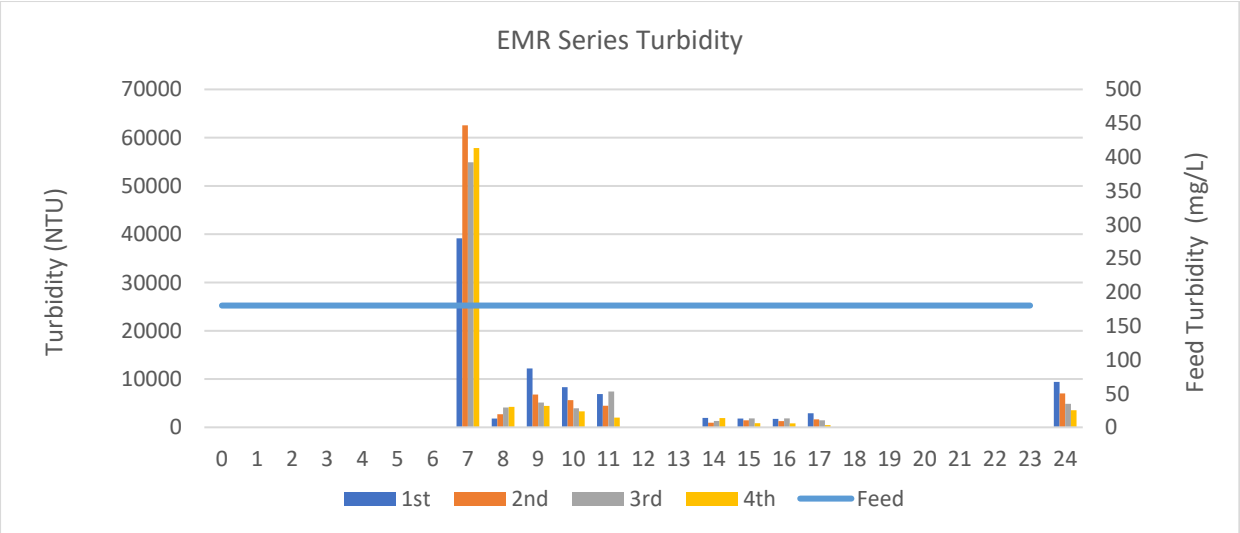

Figure 6-5: Series EMR - Brewery Wastewater Turbidity compared to the mean feed turbidity

6.1.2 EMR Biogas and Energy Performance

Below shows the energy analysis of the series reactors comparing the biogas production, biogas composition to calculate the energy production from each reactor. Over the first 30 days, reactors in the first to the third position in the series had similar gas production, but the first reactor had the highest total energy production. From days 31-44, the systems were left to stabilise with no flow between them. There was a significant change with the second reactors, which is due to R6 showing a significant increase in both biogas production and the percentage of combustibles.

Table 6-3: Series Reactor Biogas and Energy Composition for the first 30 days with continuous feeding and the last 14 days in batch mode.

Reactor Series	*Biogas production 0 -30 days (ml)*	*Biogas production 31 - 44 days (ml)*	*Avg. Combustibles 0- 30 days (%)*	*Avg. Combustibles 31- 44 days (%)*	*Energy Production 0-30 days (Wh)*	*Energy Production 0-44 days (Wh)*
First	4578 ± 393	10,485 ± 1264	4.27 ± 2.50	1.15 ± 0.55	7.03 ± 0.014	4.54 ± 0.14
Second	4424 ± 1633	15076 ± 7514	2.78 ± 1.09	20.79 ± 19.84	5.02 ± 1.00	28.72 ± 28.46
Third	3442 ± 197	8807 ± 176	4.52 ± 1.88	15.36 ± 5.32	5.75 ± 1.76	7.59 ± 3.90
Fourth	459 ± 239	1924 ± 404	2.60 ± 0.64	1.42 ± 0.59	0.33 ±0.13	0.08 ± 0.01

Biogas Production

Figure 6-6 to Figure 6-9 show the mean daily biogas composition to assess the carbon dioxide and the combustible portion of the gas. The individual biogas composition and gas production is shown in Figure 13-1 to Figure 13-8 in appendix 13.3. The cumulative biogas production is shown alongside the gas composition. All the reactors responded to the first feed where there is a small spike in methane production as the systems start to produce biogas. The gas production drops off after a few days, which coincides with a drop in the pH. The reduced pH is likely due to fermentation taking place within the reactors producing organic acids like acetic or butyric acid, which is common in the brewing process. One of the reasons could be due to the synthetic wastewater containing yeast and sugars that have not been processed and could be competing with the exoelectrogens and methanogenic micro-organisms.

The pH continues to drop until around day 17. The pH drop corresponds with the gradual reduction in methane as shown by the arrows in Figure 6-6 and Figure 6-7. The reduction in methane is apparent in the first reactor, which had the lowest pH decreasing to 3.94 on day 16 (R1). The second reactors show a less steep reduction in combustibles which reached the lowest pH of 4.24 on day 18 (R2) and 4.29 (R6) on day 16. As previously discussed the pH increases as the water flows through the series, and by the third reactor, we see a higher methane content and the dips in methane peaks corresponding with pH drops. The fourth reactor shows minimal biogas production throughout the experiment, indicating that most of the easily digestible soluble organics have been broken down in

the first three reactors. However, the COD reduction increases by 13.9% from the third to fourth reactors implying that there should be biogas generated. The fourth reactors could be exhibiting leaks resulting in the low gas production and methane concentration being recorded. Alternatively, another cause of the lower COD could be a result of the series flow acting as baffles increasing solids retention in the first three reactors.

The reactors all show a spike in CO_2 and biogas production on day 23 when the spent grains were added to the system to ascertain whether a higher OLR was required to increase methane production. On day 23 all the reactors had a neutral pH ranging from 6.85 (R3) to 7.16 (R7). The pH then drops in all the reactors on day 24. The pH did not recover in the first reactors, but the second to fourth had increased to the lower limit of where methanogens are active, which is when you see the sudden rise in methane and biogas when the systems where left in the second and third reactors. The system setup likely provided good solids retention with the reactors acting as baffles. The baffling effect is likely to have caused the second and third reactors to retain more solids reducing the OLR to the fourth reactors which did not show a spike in methane production even though the pH was between 6.64 - 6.84.

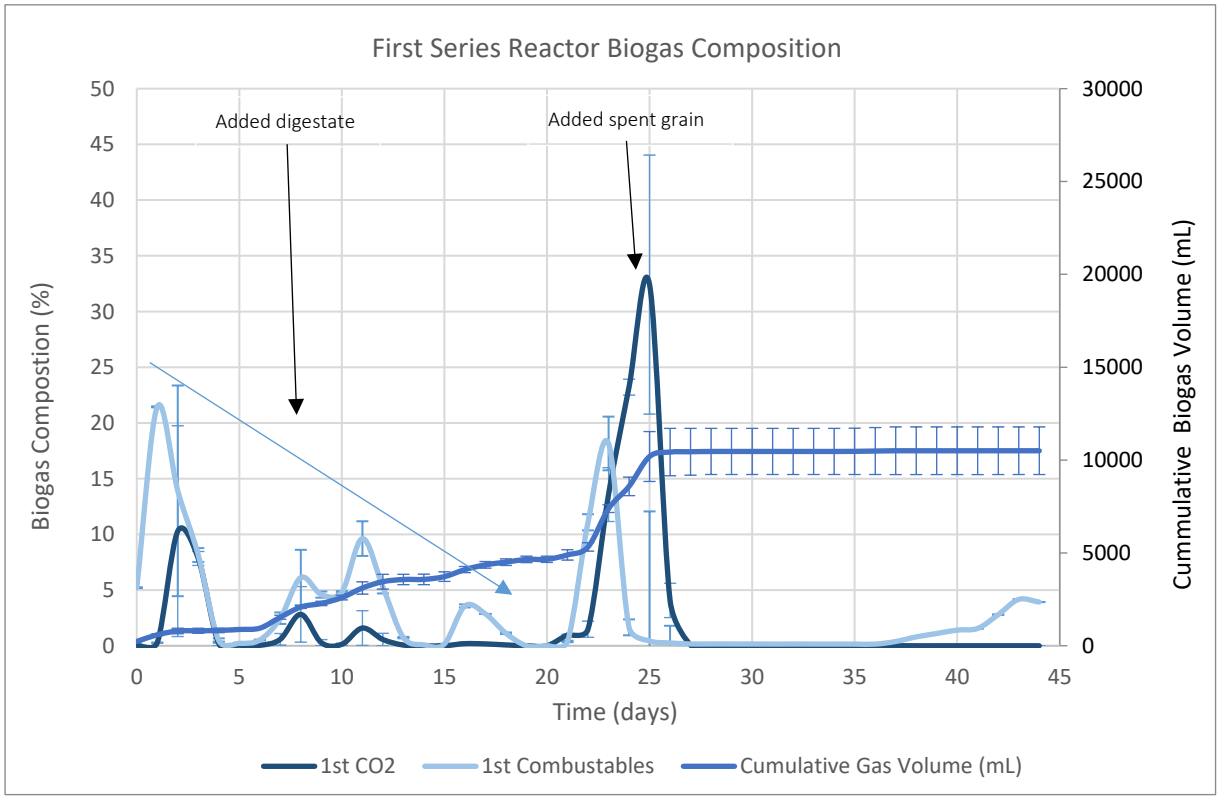

Figure 6-6: First Series EMR (R1 & R5) - Brewery Wastewater Biogas Composition and Production, with error bars representing the range across the duplicated experiments and arrows illustrating the decline in combustibles and points of additional feed.

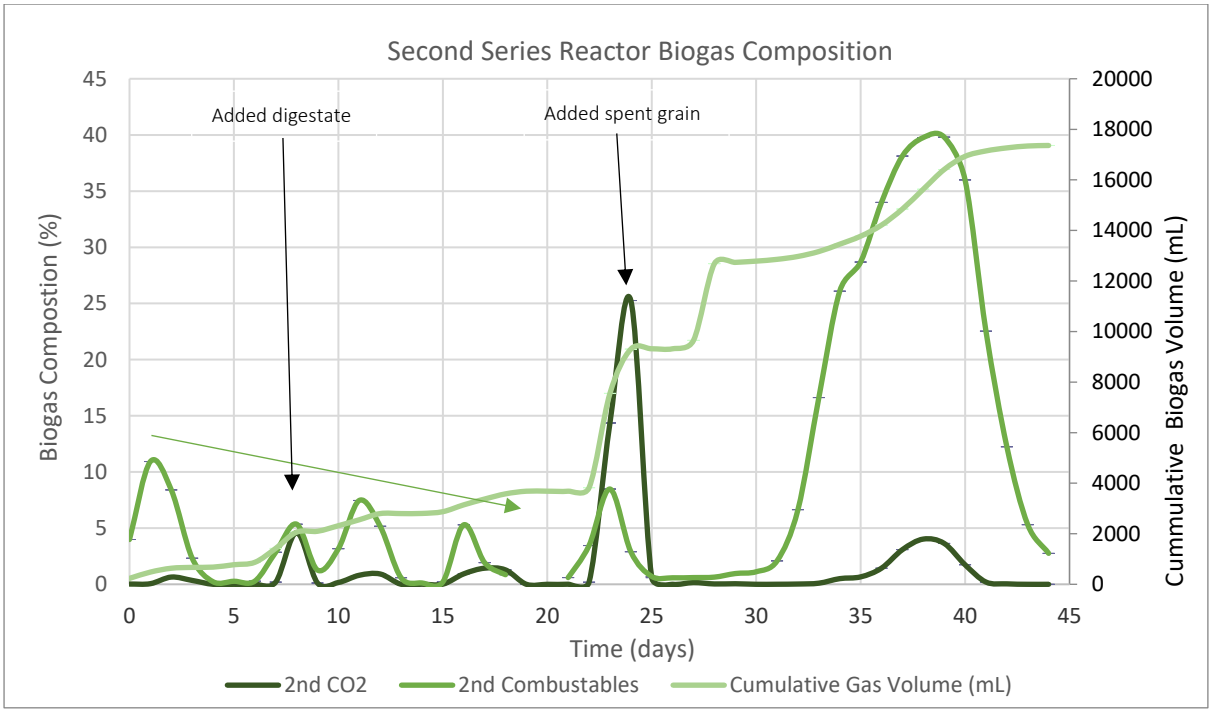

Figure 6-7: Second Series EMR (R2 & R6) – Brewery Wastewater Biogas Composition and Production, with error bars representing the range across the duplicated experiments and arrows illustrating the decline in combustibles and points of additional feed.

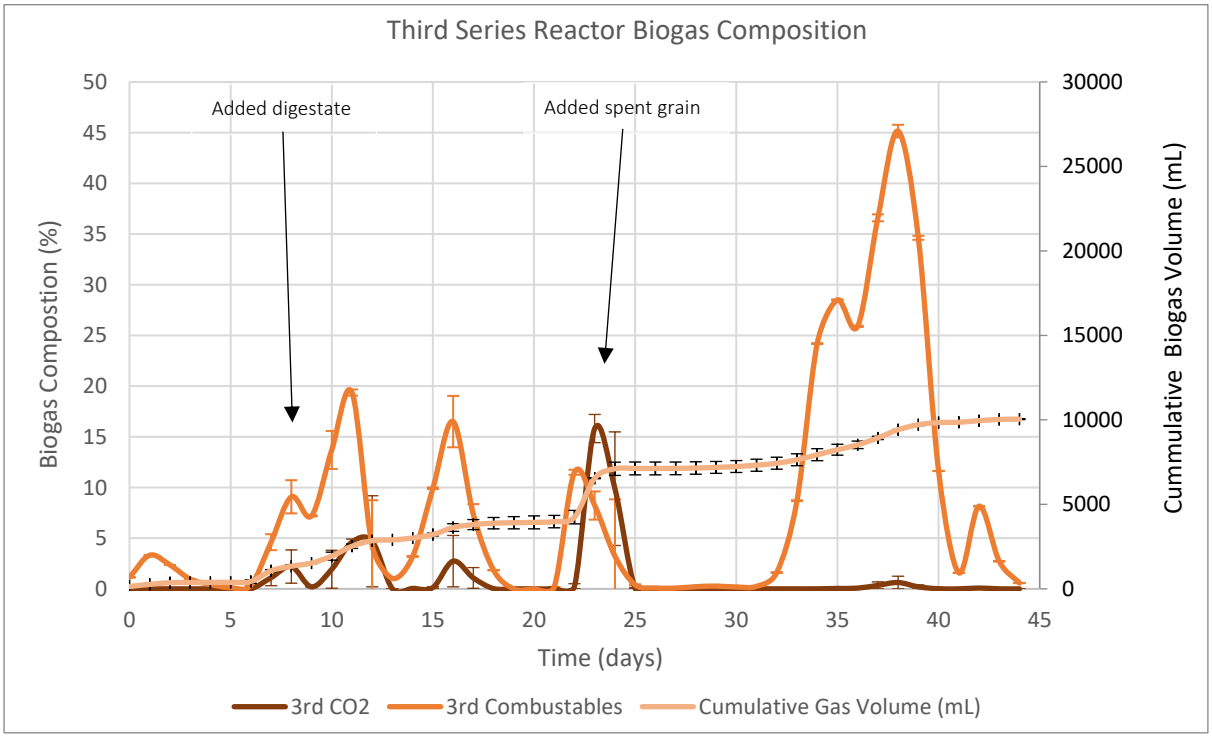

Figure 6-8: Third Series EMR (R3 & R7) – Brewery Wastewater Biogas Composition and Production, with error bars representing the range across the duplicated experiments and arrows illustrating points of additional feed.

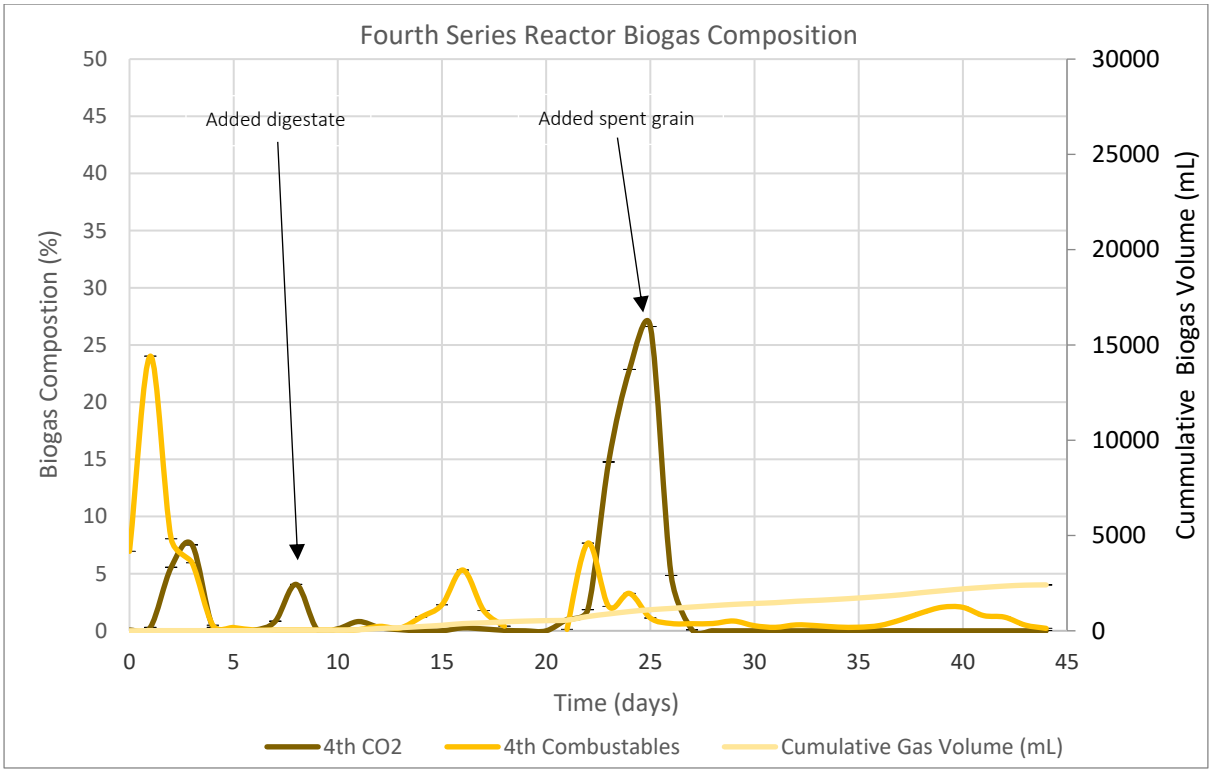

Figure 6-9: Fourth Series EMR (R4 & R8) – Brewery Wastewater Biogas Composition and Production, with error bars representing the range across the duplicated experiments and arrows illustrating points of additional feed.

The Dynament sensors are limited in what gases they can detect and measure. Throughout the experiment, the biogas composition never reaches 100%. During AD hydrogen is produced during the acidogenesis phase. From the literature, MEC's and EMR's increase the hydrogen production rate. The aim within EMR is that hydrogen scavenging bacteria will convert the hydrogen and carbon dioxide into methane. However, the pH is often below the optimum range for hydrogenotrophic methanogens. If the hydrogen is not converted into methane, then the system cannot detect the hydrogen in the biogas composition accounting for energy losses. In other research into EMR, hydrogen production up to 17.4% was recorded alongside methane production (Hassanein et al., 2017). More information on the complete biogas composition is required to give an accurate indication of the total systems energy performance, which could be achieved through gas chromatography.

Energy Production

Using the biogas composition and biogas production, we could calculate the daily (Figure 6-10) and cumulative (Figure 6-11) net energy production. Over the 30-day experiment, the first reactors had the highest energy production, which could be due to the most easily digestible organics being broken down in the first 24 hours. However, from days 30 - 44, the second reactor showed a significant increase in energy production, and it gave time for the micro-organisms to breakdown the less digestible organics.

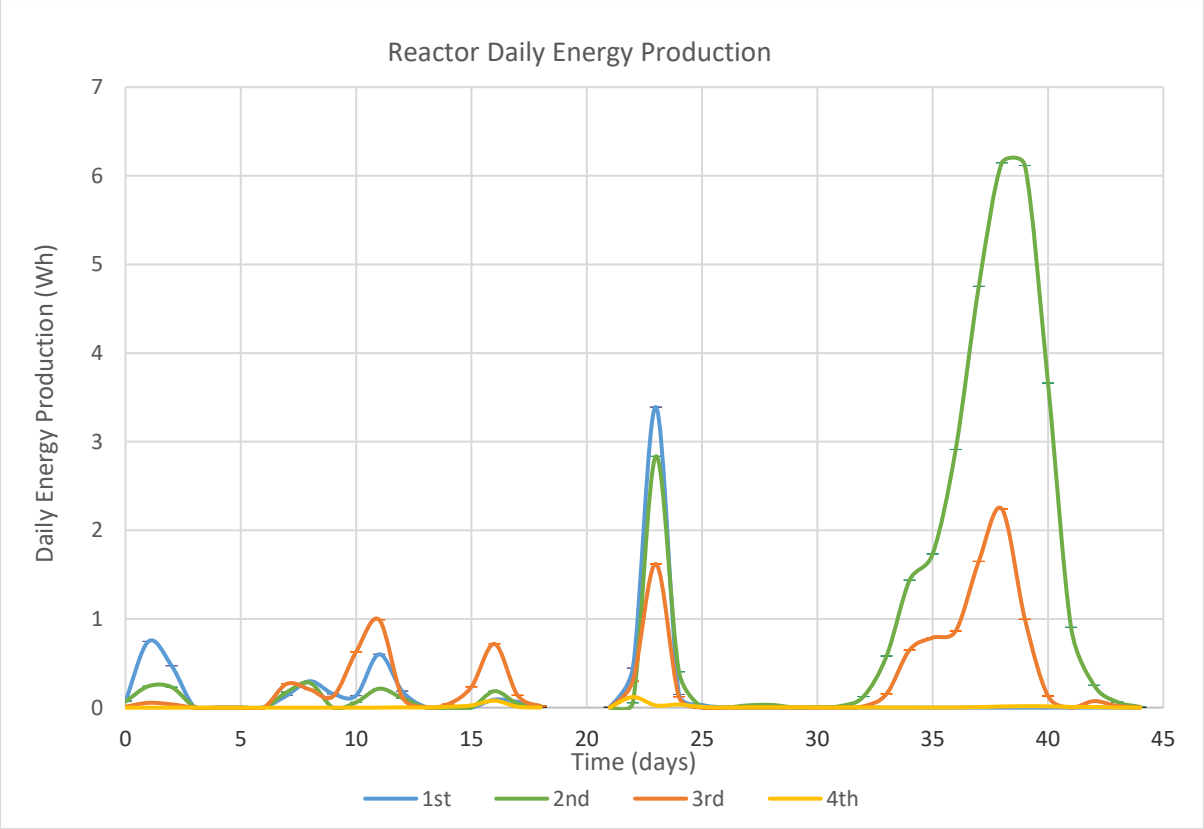

Figure 6-10: Series EMR - Brewery Wastewater Daily Energy Production with error bars representing the range across the duplicated experiments.

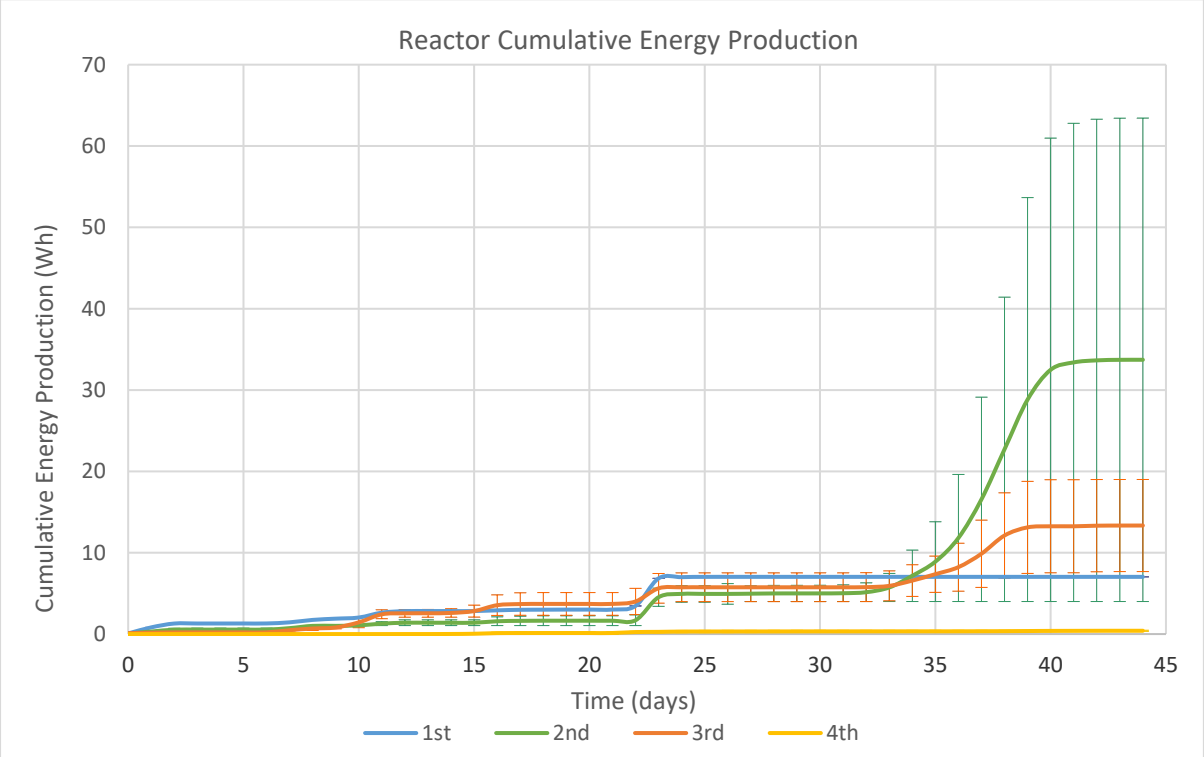

Figure 6-11: Series EMR - Brewery Wastewater Cumulative Energy Production with error bars representing the range across the duplicated experiments.

6.1.3 System Efficiency

Table 6-4 shows the overall system efficiency at different stages of the experiment.

Table 6-4: Series EMR System Efficiency showing the total amount of methane produced compared to a theoretical maximum based on COD.

Days	*Total Energy Recovery (kWh)*	*Substrate Efficiency (%)*	*Electrical Efficiency (%)*	*Total Energy Efficiency (%)*
0 - 23	0.017 ± 0.028	0.58± 0.03	0.11± 0.02	0.097
0 - 30	0.018 ± 0.003	0.63 ± 0.03	0.09± 0.01	0.091
0 - 44	0.109±0.035	-	0.18± 0.11	-

Substrate Efficiency

The substrate efficiency is low as the EMR were unable to convert the COD removed into methane. It was noted that there was significant sludge build-up at the bottom of the reactors, that could have meant that the non-soluble COD was not broken down and could have affected the substrate efficiency. The moles of recovered methane is shown in Table 13-2 in appendix 13.3.

Electrical Efficiency

The current was recorded at intervals, and the mean current produced was 89.32 mA, the recorded current is shown in appendix 13.3. The current was used to calculate the mean power requirements for the electrodes, as shown in Equation 6-1 to Equation 6-3. Over the 30 days the total power electrode requirements equated to 0.53 kWh Equation 6-4. To maintain the temperature of the reactors, the heating jackets used 0.007 kWh using a total of 40.32 kWh over 30 days. The overall electrical efficiency was 0.09% (Equation 6-5).

Equation 6-1: $\text{Electrode Power Requirements (EPR)} = \text{Voltage x Current}$

Equation 6-2: $\text{Higher Voltage } (EPR_{HV}) = \text{Voltage } (1.1V) \text{ x Current } (0.083A) = 0.0913 \text{ W}$

Equation 6-3: $Lower\ Voltage\ (EPR_{LV}) = Voltage\ (0.8V)\ x\ Current\ (0.083A) = 0.0664\ W$

Equation 6-4: $$Total\ EMR\ Power\ Requirements\ (kWh)_{30\ days} = \frac{EPR_{HV}(0.0913W)\ x\ hours\ (720)}{1000}\ x\ 4\ EMR$$

$$= 0.26\ kWh$$

Equation 6-5 $$\eta E_{30} = \frac{0.018}{0.26 + 20.16}\ x100 = 0.09\%$$

Coulombic Efficiency

CE is the amount of methane produced compared to the amount of theoretically possible based on the current or total charge passing through the cell (Equation 6-6). CE is shown as a percentage and cannot exceed 100% (Cotterill et al., 2016). The system had a low coulombic efficiency of 0.21% over the 30 days as a limited amount of methane was generated Equation 6-7 to Equation 6-9.

Equation 6-6 $$Coulombic\ Efficiency\ = \frac{Moles\ of\ CH_4\ Recovered}{Theoretical\ Moles\ of\ CH4\ in\ the\ Current\ Produced}$$

The theoretical moles of hydrogen-based on current (N_{CE}) can be calculated through

Equation 6-7: $$N_{CE} = \frac{\sum_1^n I\Delta t}{4F}$$

Equation 6-8: $$N_{CE} = \frac{\sum_1^4 0.083\ A\ x\ (30x24x60x60)}{4\ x\ 96{,}485} = \frac{860544}{385940} = 2.2297$$

Equation 6-9 $$CE\ = \frac{0.0046}{2.2297} = 0.21\%$$

Total Energy Efficiency

The system showed a low total energy efficiency of 0.63% (Equation 6-11). Each system required 40.32 kWh to heat the system and power the electrodes. The energy value within the substrate equated to 3.208 kWh as shown in Equation 6-10.

Equation 6-10 $$Ws_{30\ days} = \Delta COD\Delta H_{WW/COD} =$$ *652.49g x 17.7 kJ = 11549.07 kJ = 3.208 kWh*

Equation 6-11 $$\eta_{E+S\ (30days)} = \frac{0.0362}{0.53 + 39.8 + 3.208} = 0.63\%$$

6.2 Discussion

The system energy conversion performance for the first 30 days is low with the systems on average performing a substrate efficiency, electrical and total energy efficiency all under <1%. One of the reasons for the low conversion could be due to competing reactions such as fermentation. The pH drop is likely to be from the fermentation as the system goes through the acidogenesis phase where the simple monomers are being converted into fatty acids when the pH is >5. When the pH is <5, then it is likely that ethanol production is occurring (Bajpai, 2017). The pH does increase from the first to fourth reactors, showing that the systems are breaking down the fatty acids into acetate (pH 5.5) that produces hydrogen as a by-product. Typically, the hydrogen is scavenged by methanogens to produce methane; however, during the 96 hour retention time, methane production is low. Increasing the

retention time, as shown in day 31-44, does increase in methane production. The methane production indicates that the systems do contain methanogenic microorganisms which are converting the acetate and hydrogen into carbon dioxide and methane. The EMR systems do recover from low pH ranges, further analysis into EMR's ability to recover from low pH could provide valuable insights in how to stabilise anaerobic wastewater treatment and anaerobic digestion where methanogenic bacteria are active in a small pH range for 6-8.

Fully understanding the composition of the gas is vital in understanding the system performance. During the hydrolysis and fermentation stages of anaerobic digestion, hydrogen production occurs. Continuous Stirred Reactors (CSTR) have shown significant improvements by having a pre-acid phase before the main reactor (Speece, 2007). During the experiment, the four reactors would have performed in different phases. However, understanding the time intervals for the different stages of organic conversion into methane is not understood due to the low HRT. Further analysis into the time intervals for the different stages that EMR goes through compared to the AD systems, are required to design and optimise electro-methanogenic systems.

The experimental design was developed to simulate baffling to create four distinct phases of treatment that could simulate the four stages of anaerobic digestion. However, from the off-gasing period of days 31-45, it showed that the system was likely overloaded with organics and could not effectively convert the organics into methane due to a build-up of volatile fatty acids. The biogas sensors were unable to measure hydrogen, and if the system was going through the acetogenesis stage but not reaching the methanogenesis stage, then it is likely that some of the chemical energy produced by the system was not able to be recorded.

From the individual analysis of the reactor, R6 highlighted promise in EMR reaching above 70% methane concentrations during the 31-45 day period. R7 also showed higher methane production during this period reaching between 55-60% methane. The two systems showed a variation between them both with R5-R8 performing in a more typical AD biogas production curve shown in batch experiments as shown in the appendix MR Series Brewery Wastewater Analysis Figure 13-1 to Figure 13-8 (pg.240).

The irregularity in the system performance could be due to multiple factors, including the inoculation period, temperature and the OLR. After the re-inoculation, a spike of energy was produced. The increase in energy indicates that the inoculation period was likely too short to allow a biofilm to develop or the high flow rate caused a microbial washout and required a longer period to establish itself. To understand biofilm development and inoculation more clearly periodic analysis of biofilm growth on the anodes would provide new knowledge.

The temperature is below the typical AD operation range of 35-38^{o}C however methanogenic microorganisms do operate at lower temperatures. Further analysis of the temperature could inform the optimal system range. The varying energy production between the four reactors indicates there is a difference in the breakdown of organics within the 24-hour segments, indicating further analysis into the HRT of EMR and the stages of treatment are an essential step in optimising the system.

6.3 Next Steps

When the system was left in batch mode (days 31-45) it identified that the system is sensitive to VS concentrations and the OLR may have been too high and affected the microbial activity. Establishing a correct OLR and HRT is a vital part in understanding the operational parameters for EMR. Going forward, a batch test system will provide information about the optimum VS concentration to inform OLRs and HRTs. Through a batch system, it will be easier to see the different phases the system is undergoing from the changes in pH and biogas composition.

Understanding the correlation between COD reduction and pH can help to optimise the system performance and organic loading rates so that the reactors have time to adjust their pH. Exploring EMR's ability to reduce the build-up of VFA's could provide new knowledge into the operation of AD systems that are sensitive to VFA's and the resultant low pH. Using EMR to stabilise pH between 6-8 could reduce the need for buffering solutions simplifying the operation of AD systems and making them more robust to changes in waste composition. The ability to increase and stabilise pH also opens up opportunities to treat other waste streams that are too acidic for anaerobic digestion.

7 Experiment 2 - Batch Tests Results

The experiment aims to compare AD and EMR to understand if the addition of electrodes and an applied voltage demonstrate an improvement in system performance. During the experiment, a couple of issues arose with the recirculation. The small-bore peristaltic pump kept getting clogged from particulates in the substrate. Due to the frequent blockages, the pump was not run after the first 2 hours removing any mixing within the system.

The experiment used an assumption based on previous research to calculate the percentage of VS due to the furnace requiring maintenance. After the experiment was completed the VS of the spent grains was measured. The actual VS was 92.5%, which meant the VS concentration was 1.3 g lower than the initial estimate at 32.3 g. The change in VS meant that the VS concentration was 14.04 g/L instead of 14.4 g/L.

7.1 Reactor Conditions

Over the 21 days, the operational temperature for the systems was 32.13 ± 0.45°C. The reactor operational conditions throughout the experiment are below in Table *7-1*.

Table 7-1: Series EMR Operational Conditions

Reactor number	*Reactor Type*	*Stirred*	*Operating Temperature (°C)*	*Avg. pH*	*Total Power Consumption (kWh)*
3	AD	NO	32.22	4.94	0.01
4	AD	NO	31.44	4.98	0.01
5	AD	NO	32.58	5.00	0.01
6	EMR	NO	32.58	6.54	0.04
7	EMR	NO	32.53	6.47	0.04
8	EMR	NO	31.44	6.31	0.04

7.1.1 Operational Water Quality Measurements:

One of the main parameters to assess for EMR is the ability of the systems to treat wastewater. For the batch test, the change in pH and COD was taken Monday to Friday, and then a full analysis was carried out at the end of the experiment. The section below shows the different water quality measurements throughout the experiment.

pH

Figure 7-1 shows the change in pH over the experiment. The influent samples were spoiled and were removed from the analysis to remove errors. There is a clear difference between the pH change in the EMR systems compared to the AD systems. Both the AD and EMR's pH dropped to between 5 and 5.5. The pH in the EMR systems increased above 6 between days 6-9. By the 21st day, all three EMRs reached neutral conditions of 7.03 ± 0.05. The systems operating as AD did not show the increase and in some cases, dropped below 5. The low pH in the AD systems indicates that there is a possible build-up of VFA's within the reactor, and the pH drop below 5 could indicate that ethanol is being produced. At the end of the 21 days, the pH across the AD systems was 4.92±0.09.

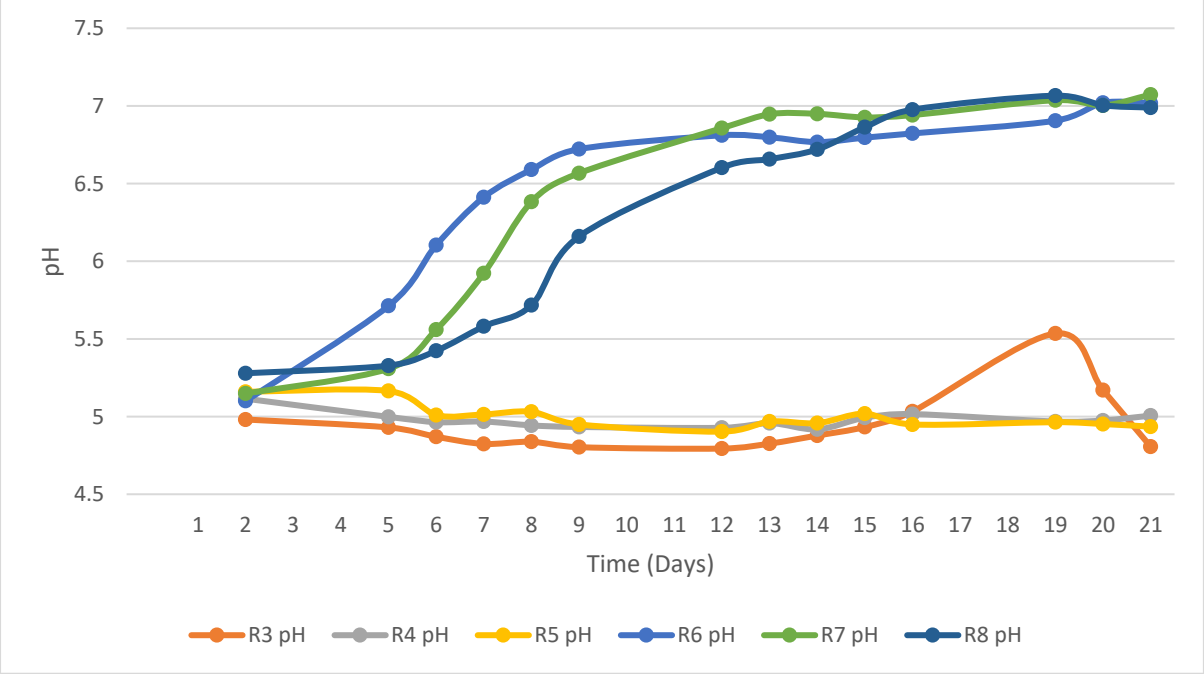

Figure 7-1: AD (R3-5) and EMR (R6-8) - Brewery Wastewater pH over the 21-day duration

Chemical Oxygen Demand

Table 7-2 shows an overview of the COD removal for the EMR and AD systems, and Figure 7-2 show the COD effluent and the COD percentage reduction throughout the experiment. Overall, the AD showed no decrease in COD throughout the experiment, remaining around 10,000 mg/L. The EMR system overall showed a 42.37 ± 2.05% reduction in COD. The EMR effluent was still considerably high at the end of the 21 days with a COD of 5130 ± 403 mg/L and would require tertiary treatment to lower the COD. *Figure* 7-3 shows both the pH and the COD reduction. The EMR systems show a continual decrease in the COD throughout the experiment and do not show any substantial increase as the pH increases. A statistical analysis of the pH and daily COD reduction using Pearsons Correlation Coefficient (r) does not show any correlation between the two values. AD r = -0.097 (p-value = 0.542) and EMR r = -0.085 (p-value = 0.344). It is likely that the AD would have undergone

some COD reduction, but the reduction may be minimal and within the error range of the COD analysis.

Table 7-2: Spent Grain Batch COD for EMR and AD

Reactor Series	*Average COD Reduction*	*Average COD Effluent (mg/L)*
EMR	*42.37 ± 2.05%*	*5130 ± 403*
AD	*-2.04 ± 4.39%*	*10387 ± 361*

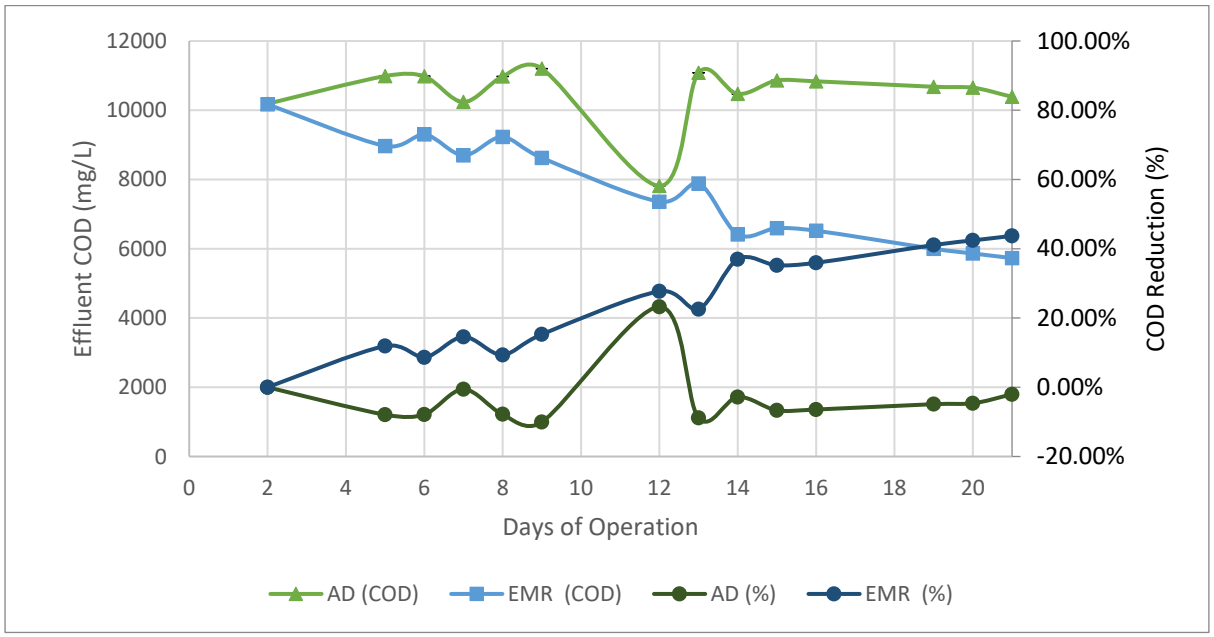

Figure 7-2: Batch EMR (R6-8) & AD (R3-5) –Spent Grain COD Effluent and Reduction

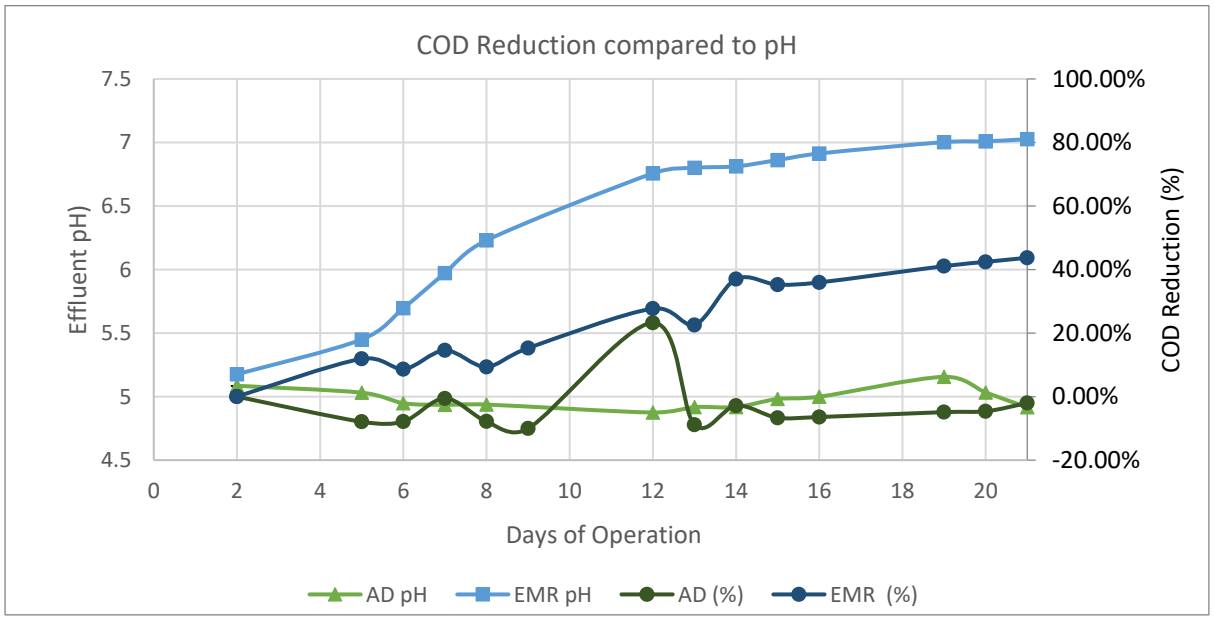

Figure 7-3: Batch EMR (R6-8) & AD (R3-5) - Spent Grain Wastewater COD Percentage Reduction compared to pH

7.1.2 EMR Biogas and Energy Performance

Table 7-3 shows the overall energy analysis for both the AD and EMR systems over the 21 days. The EMRs all produced biogas throughout, whereas the AD systems only produced biogas initially and stopped once they became too acidic (<5.5). The EMR lab test produced 64% less energy than the theoretical maximum amount calculated from the feedstock analysis. The full breakdown of each reactor can be seen in the appendix Figure 13-10 to Figure 13-16.

Table 7-3: Batch Spent Grain Biogas and Energy Composition

	Total Energy Production (kWh)	*Total Biogas Production (mL)*	*The Proportion of Combustibles over 21 days (%)*	*Expected Energy Production per Tonne(kWh)*
AD	0.001 ± 0.0008	2353 ± 1407	5.2 ± 1.0	1.0
EMR	0.039 ± 0.0039	10567 ± 703	37.9 ± 2.3	34.0
EMR/AD % Difference	97%	349%	628.4%	
Theoretical Max			53	93.5
EMR/Theoretical % Difference			-28%	-64%

Biogas Production

Figure 7-4 and Figure 7-5 shows the mean daily biogas composition and gas volume production to assess the carbon dioxide and the combustible portion of the gas. Both the AD and EMR systems show a spike in CO_2 production in the first two days as the systems undergo the hydrolysis phase. Both of the systems then drop on biogas production on day 3. The EMR then picks up in gas production from day four whereas the AD system flat lines and does not produce any more biogas for the duration of the 21 days.

The difference in biogas production is clearly seen in Figure 7-6 and Figure 7-7, which compares both the daily and cumulative biogas production. The methane concentration with the EMR peaking on the daily average of 59.39% on day ten whilst the AD system peaked on the first day at 5.84%. Both the systems have a higher gas production on day one with the EMR system producing on average 47% more biogas, indicating an accelerated breakdown of the organic compounds due to fermentation of the hydrolysis phase.

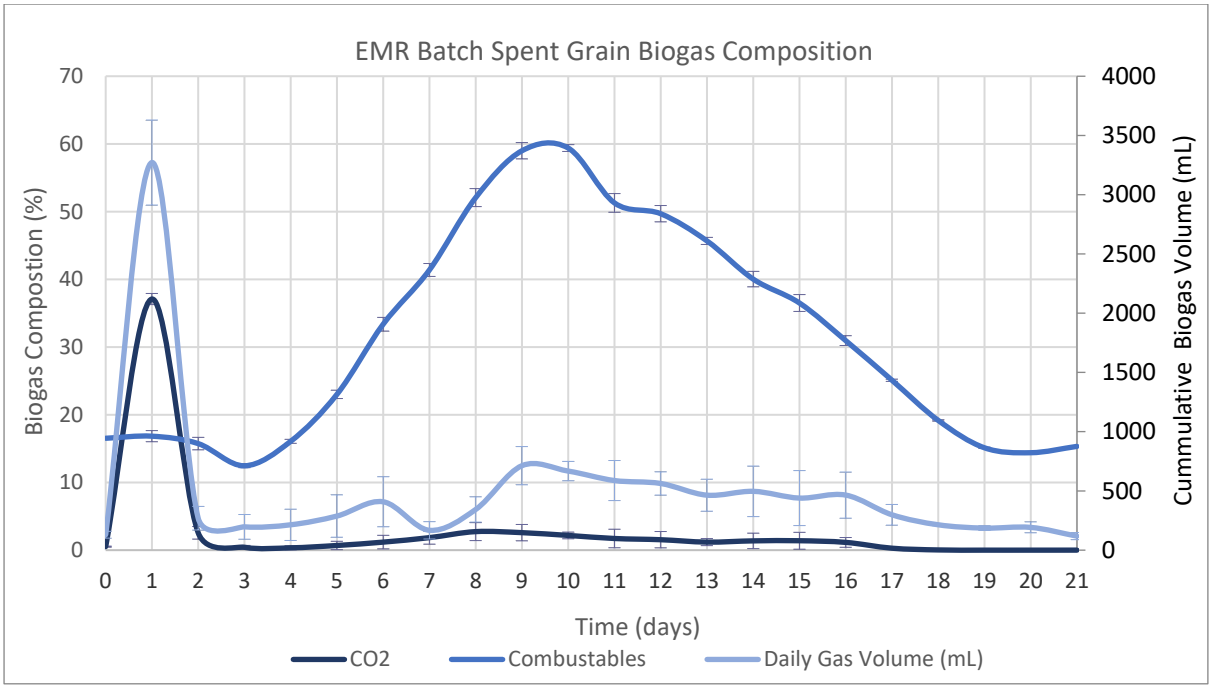

Figure 7-4: Batch EMR –Spent Grain Biogas Composition and Production, with error bars representing the range across the duplicated experiments.

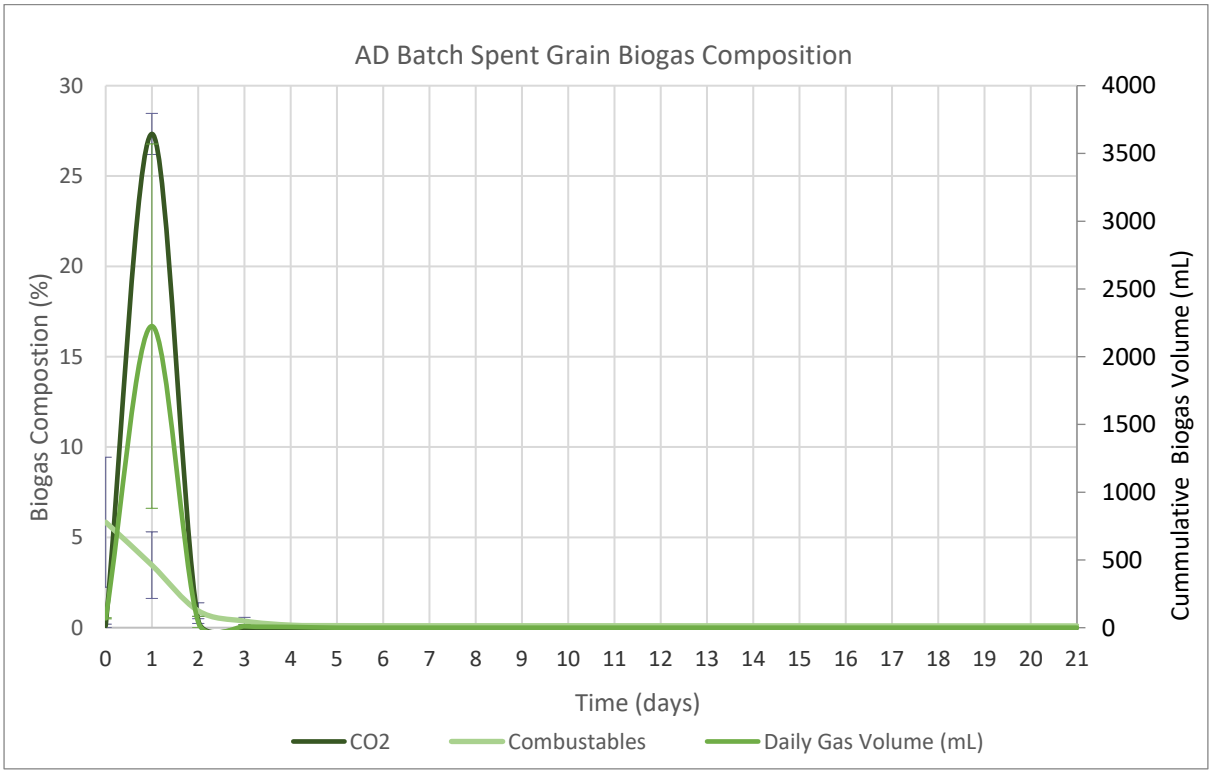

Figure 7-5: Batch AD –Spent Grain Biogas Composition and Production, with error bars representing the range across the duplicated experiments.

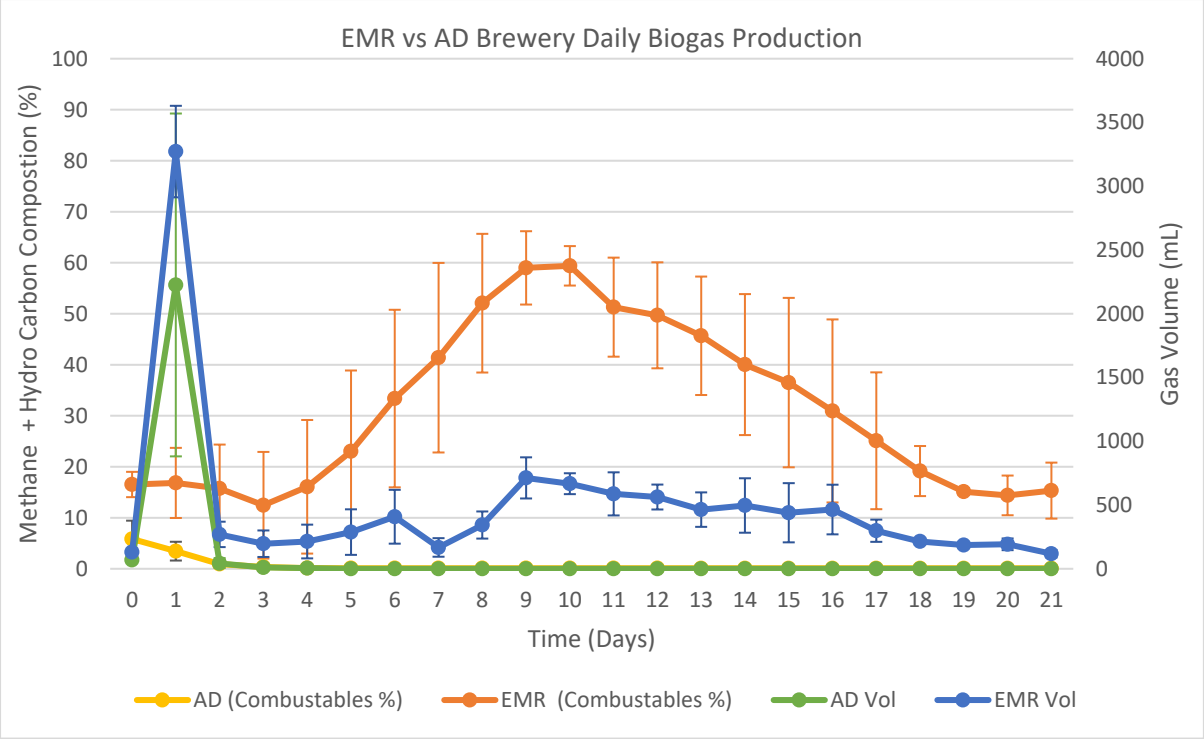

Figure 7-6: Batch EMR & AD – Spent Grain Daily Biogas Production and CH_4 Percentage, with error bars representing the range across the duplicated experiments.

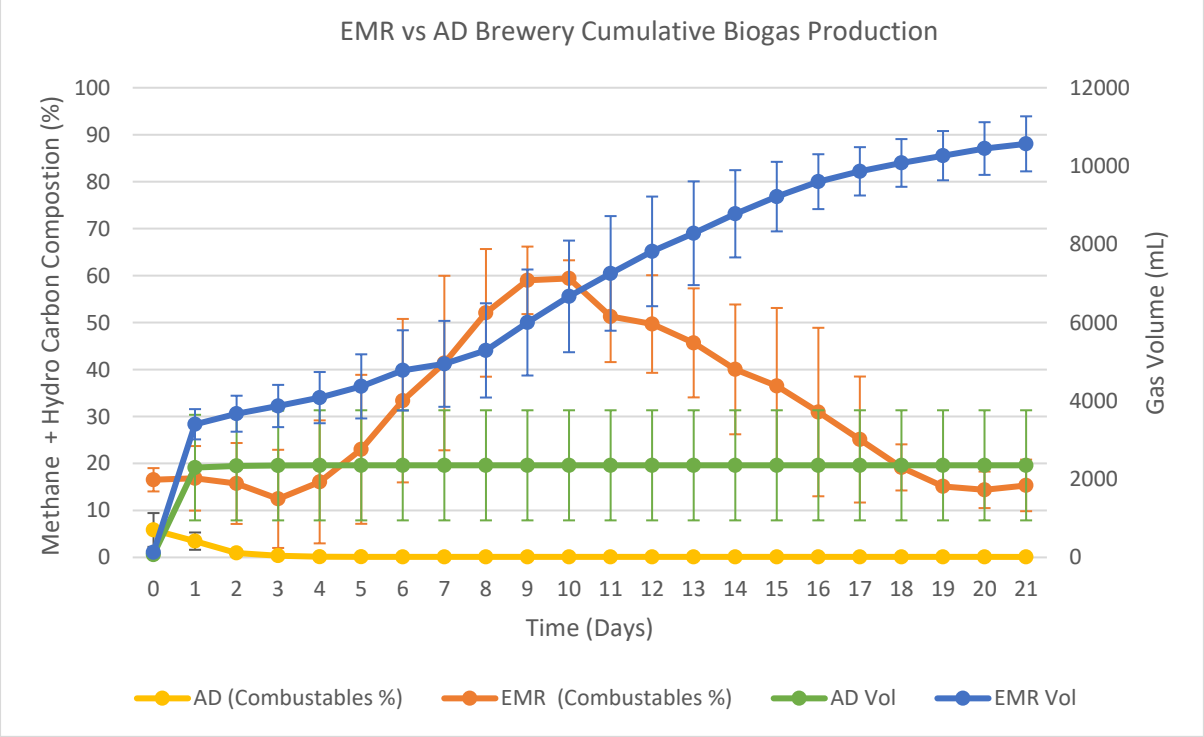

Figure 7-7: Batch EMR& AD–Spent Grain Cumulative Biogas Production and CH_4 Percentage, with error bars representing the range across the duplicated experiments.

During the experiment, the total biogas composition reached just over 60% between days 9-10, indicating a high proportion of other gases that could be present (Figure 7-8).

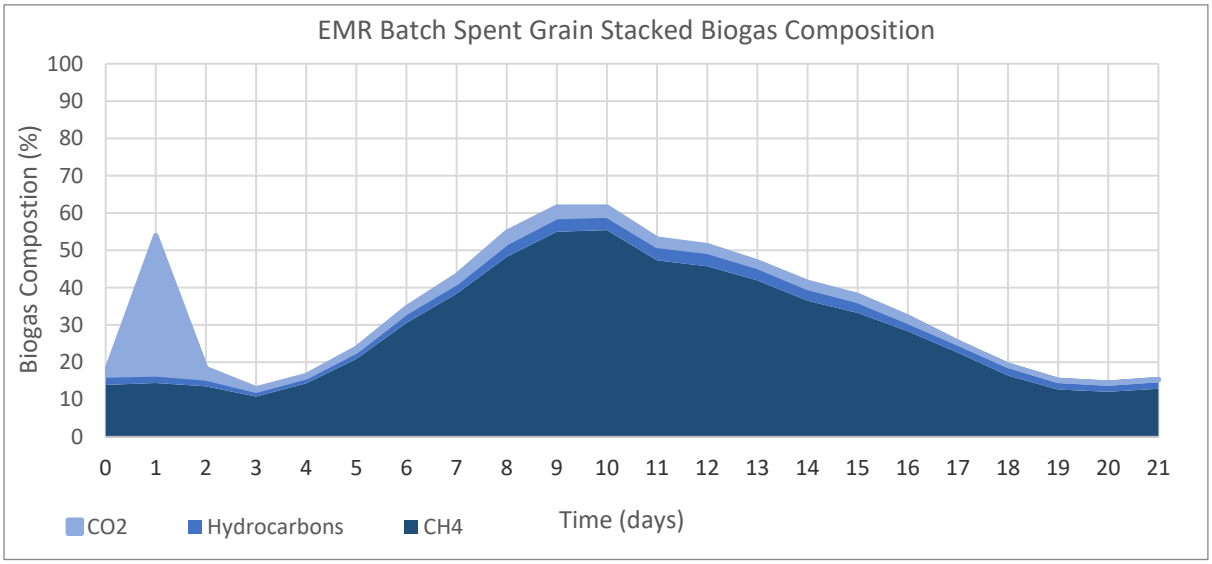

Figure 7-8: Batch EMR –Spent Grain Stacked Mean Biogas Composition.

Energy Production

Using the biogas composition and biogas production, we could calculate the daily (Figure 8-8) and cumulative net energy production (Figure 7-10). Throughout the experiment, the EMR systems had the highest energy production. The highest daily energy production was on day 1 when there was below a 20% methane concentration, but the systems had the highest biogas production rate. The mean energy production of the systems started to plateau on day 17 to 18.

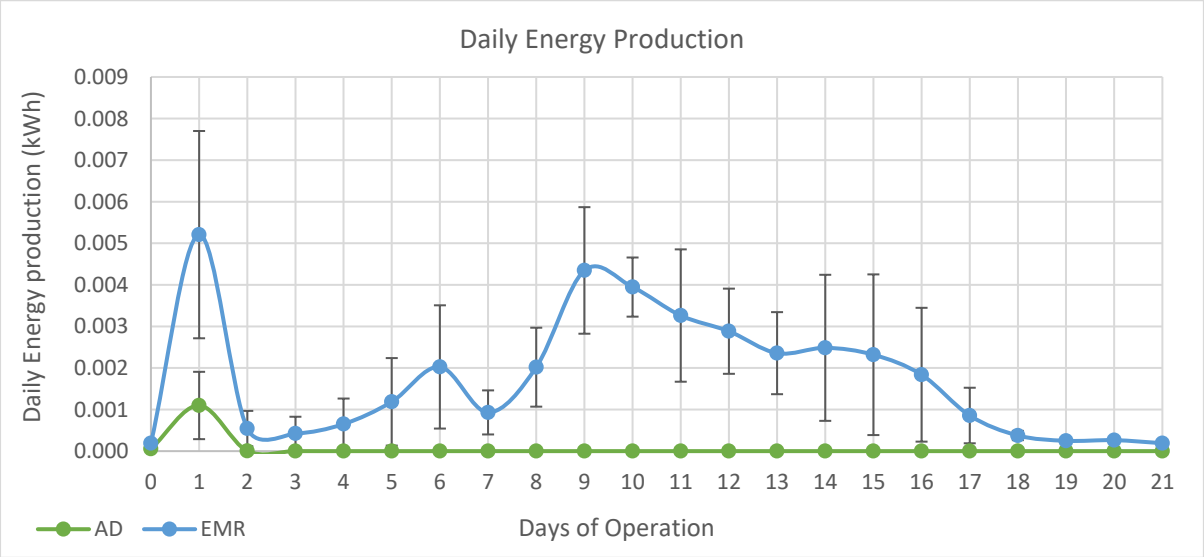

Figure 7-9: Batch EMR & AD –Spent Grain Daily Energy Production, with error bars representing the range across the duplicated experiments.

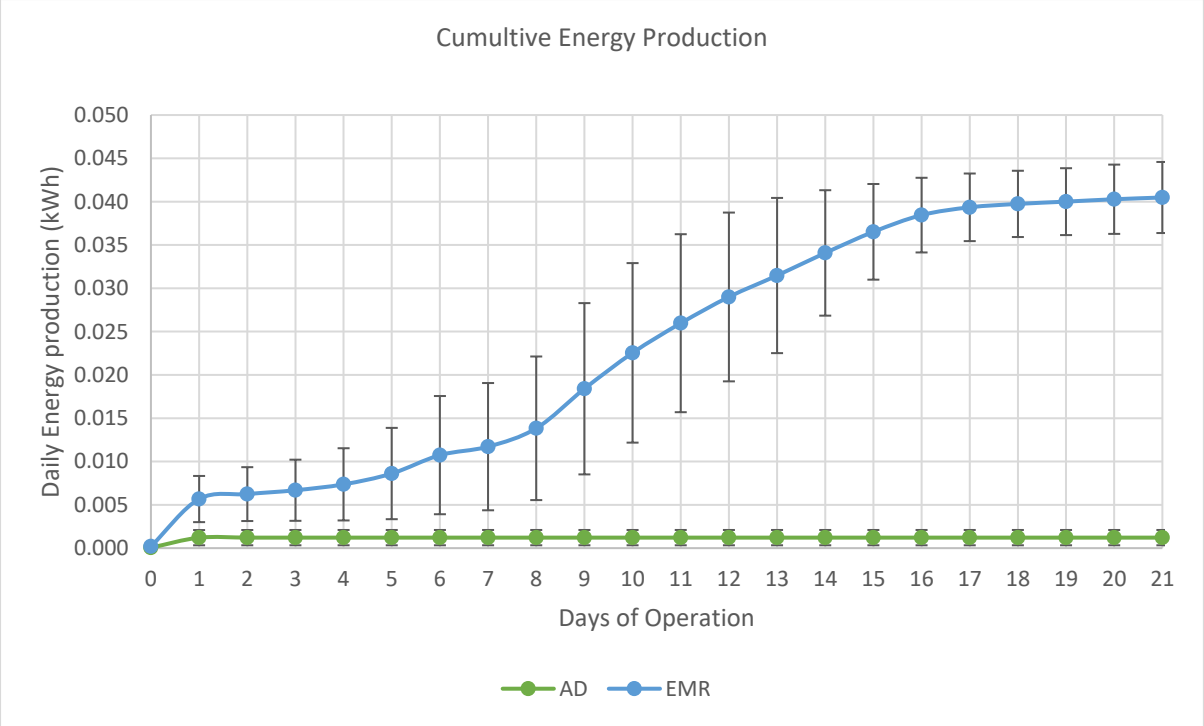

Figure 7-10: Batch EMR & AD –Spent Grain Cumulative Energy Production, with error bars representing the range across the duplicated experiments.

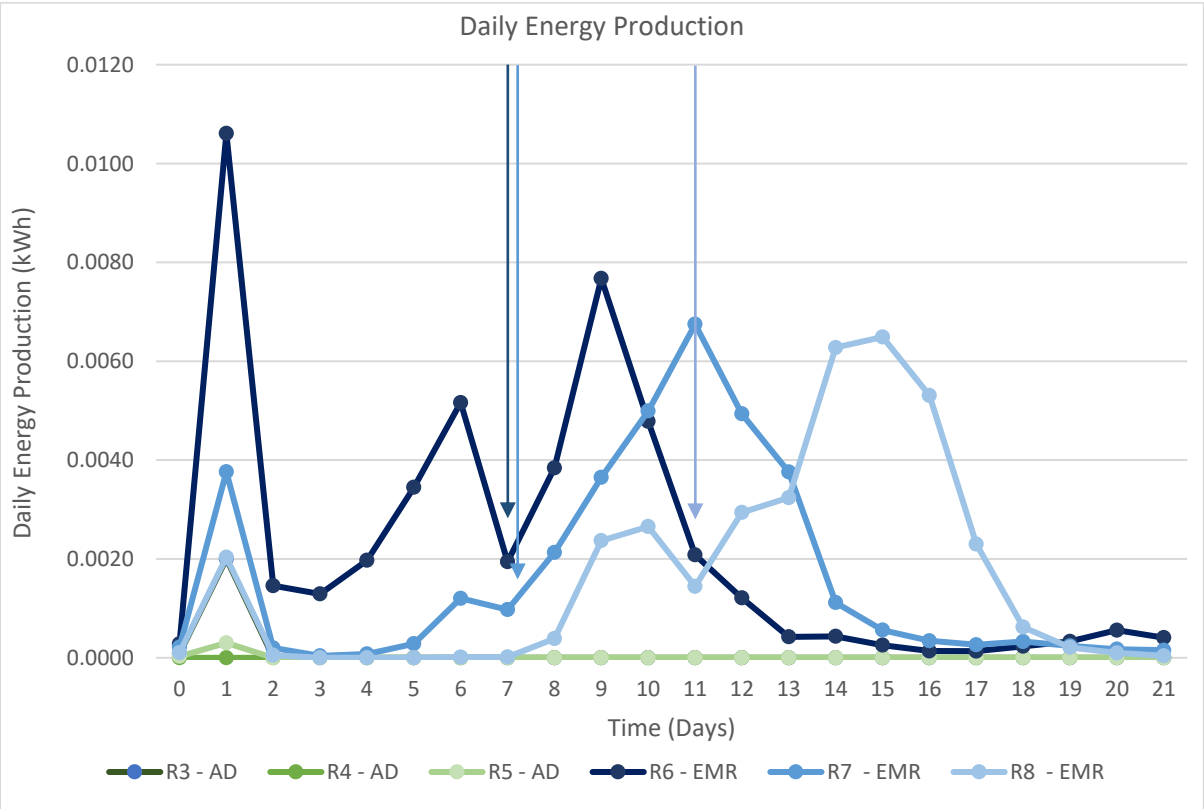

Figure 7-11: AD (R3-5) and EMR (R6-8) Daily Biogas Production, with arrows indicating dips in the daily energy production.

Figure 7-11 shows the daily biogas production for the different reactors, after the initial peak on day one the energy production does not follow a smooth curve. All three of the EMR reactors start to increase and then drop in energy production as indicated by the three arrows. The drop could be due to a build-up of some intermediaries that can inhibit biogas production such as propionate, although low concentrations of propionate are typical in well-functioning bioreactors (Speece, 2007).

Below Figure 7-12 shows the energy comparison against the pH within the reactors. The pH and the energy production show a correlation as would be expected for the methanogenic phase. A closer look into the changes in pH for the EMR systems indicates the effect on energy production, as shown in Figure 7-13. Where R6, R7 and R8 increase the pH at different rates, they also peak in energy performance in the same sequence as the reactors increase in pH.

Pearson's correlation coefficient (r) of the pH and biogas production and the methane concentration shows different values depending on the time frame. Initially, over the 21 days, the pH and methane concentration showed a weak positive correlation. The AD systems had an r of 0.196 (p-value = 0.215) and the EMR system has an r of 0.171 (p-value = 0.278). The correlation returned p-values that were not statistically significant, which is likely due to the pH stabilising but the methane percentage dropping once the organics have been digested. Changing the period to the first half of the experiment where there was the greatest rate of change in the pH showed a coefficient. The AD r was 0.436 (P-value = 0.004) a moderately positive correlation, and the EMR r was 0.863 (P-value = $1x10^{-13}$) showing a strong positive correlation of the methane increase with the pH. The strong correlation is to be expected with methanogenic microorganisms favouring pH between 6-8. The correlation between the biogas production was not as strong, showing similar week correlations over the 21 days but moderate correlation over 10. AD r = 0.523 (p-value =0.0004) and EMR r = 0.629 (p-value = $8x10^{-6}$).

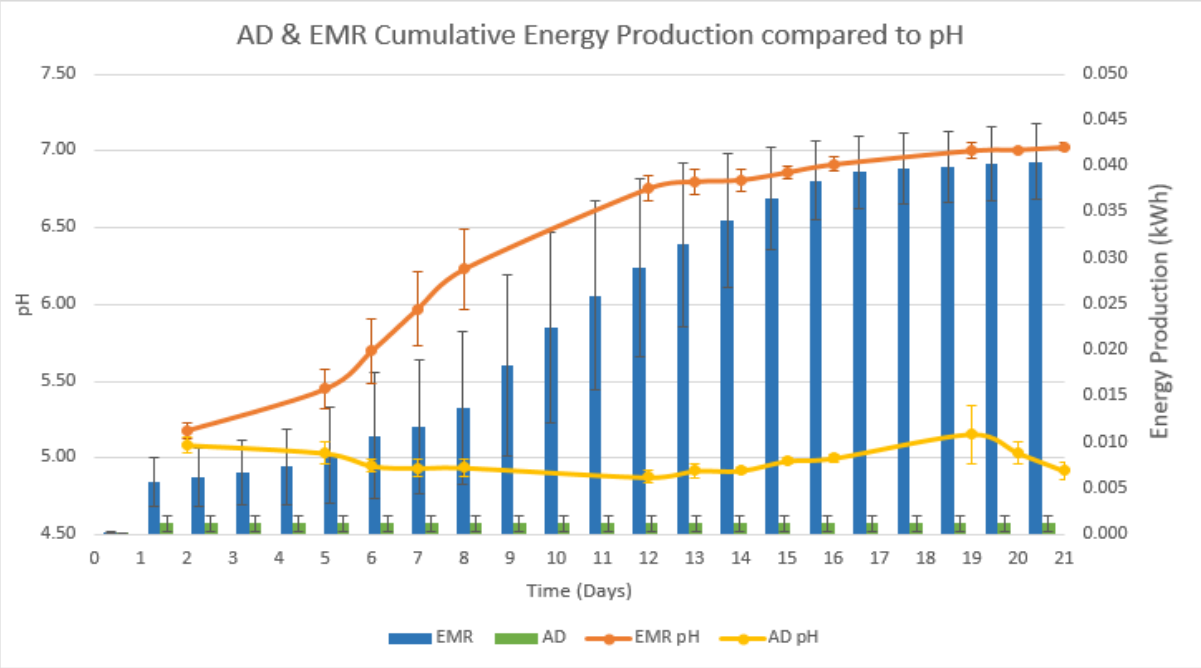

Figure 7-12: Batch EMR (R6-8) & AD (R3-5) Spent Grain – Cumulative Energy production compared to pH, with error bars representing the range across the duplicated experiments.

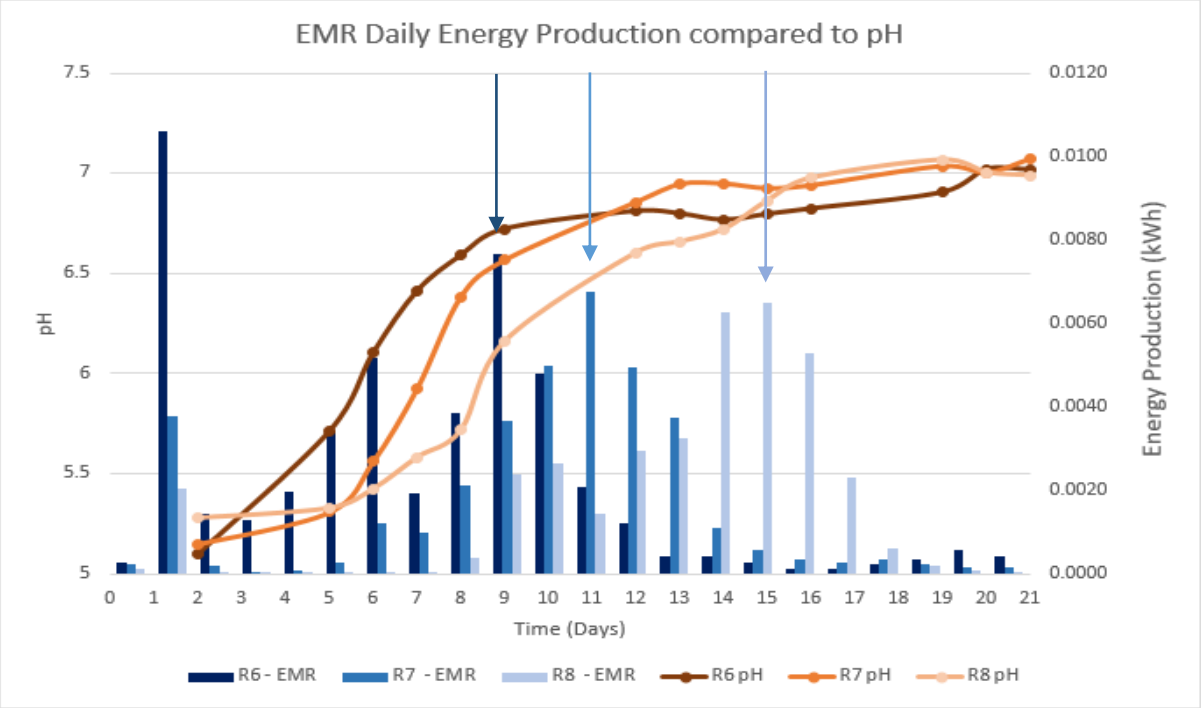

Figure 7-13: Batch EMR Spent Grain – Daily Energy production compared to pH, with arrows indicating the peak daily energy production.

7.1.3 Effluent Analysis

The effluent analysis of the AD and EMR systems showed some significant differences between the different systems that can be seen in Table 7-4. The EMR showed higher performance in most of the wastewater quality analysis apart from the Sludge Volume Index (SVI) and the batch settling curve (Figure 7-14) but had a lower variation than AD. The lower variation shows that the system had a good consistency and will support the design of post-treatment systems, including sedimentation of non-degradable organics. The TSS also saw a marginal increase, with a 3.88% increased reduction.

Table 7-4: Batch - EMR & AD Spent Grain Effluent Analysis

	Turbidity (NTU)	***TDS (mg/mL)***	***TSS (mg/mL)***	***Total Solids (mg/mL)***	***Volatile Solids (mg/mL)***	***COD (mg/L)***	***Sludge Volume Index***	***pH***
AD	3513 ± 77	6.83± 0.67	4.30± 1.15	13.70± 3.60	4.20± 1.70	*10387 ± 361*	70.60± *10.56*	4.92± *0.09*
EMR	2057 ± 233	5.17± 0.83	4.13± 0.67	7.87± 0.63	2.53± 0.27	*5130 ± 403*	79.35 *±25.65*	7.03± *0.05*
EMR % Difference	41.46%	24.39%	3.88%	42.58%	39.68%	44.83%	-11.26%	42.93%

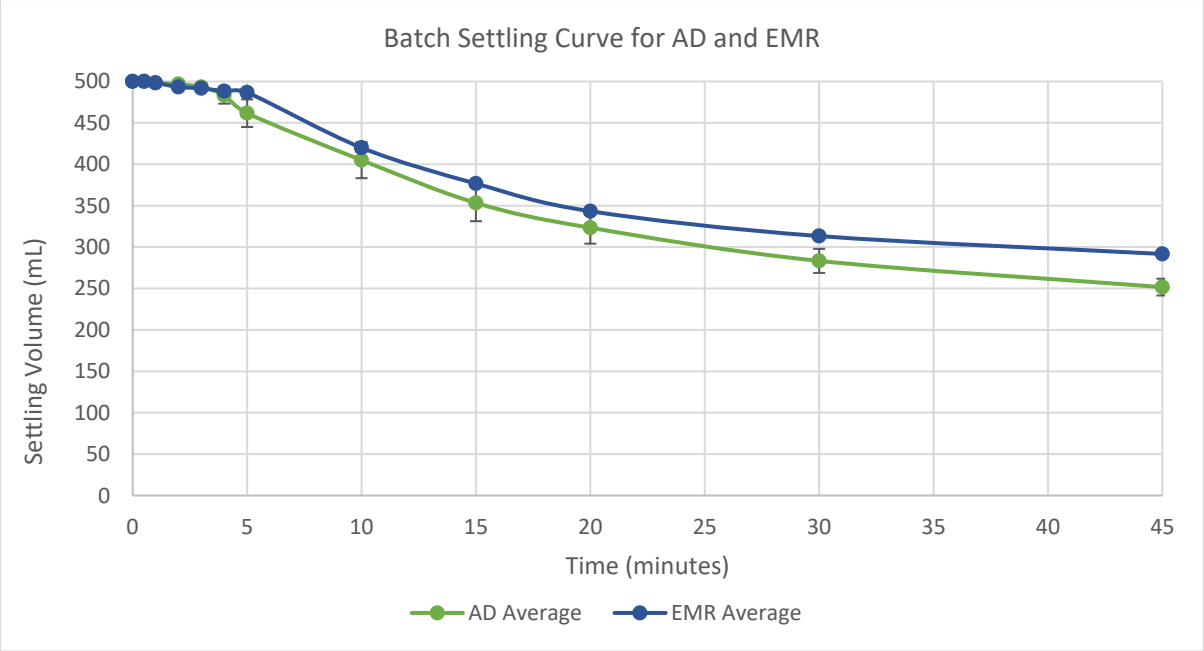

Figure 7-14: Batch EMR (R6-8) & AD (R3-5) – Batch Settling Curve, with error bars representing the range across the duplicated experiments.

7.1.4 System Efficiency

Table 7-5 compares the AD and EMR system efficiency at different stages of the experiment.

Table 7-5: : Batch EMR (R6-8) & AD (R3-5) System Efficiency

	Electrical Efficiency (%)	*Substrate Efficiency (%)*	*Total Energy Efficiency (%)*	*Coulombic Efficiency (%)*
AD	8.0 ± 12.8%	33.4 ± 74.4%	8.1 ± 7.6%	N/A
EMR	100.4 ± %	99.2 ± 15.3%	25.2 ± 11.3%	53.2 ± 11.1%
EMR % Difference	1150.6%	197.3%	211.0%	N/A

Electrical Efficiency

The power consumption for the EMR electrodes was 0.03kWh over the 21 days with a mean current of 0.075A. The heating power requirements were 0.01kWh equating to a total 0.04kWh and 0.01kWh for EMR and AD consequently. As the AD system was not able to recover from the build-up of VFAs, the electrical efficiency was low. However, the mean EMR electrical efficiency reached 99.2 ± 15.3%. One of the reasons the EMR efficiency dropped is due to the 21-day experimentation period. Figure 7-15 shows the change in the systems energy production compared to energy consumption. By the second day, the consumption was greater than production. On the 10th day the systems were

producing more energy until the last day. By the 21st day, the consumption overtook the production, which started to plateau on the 16th day.

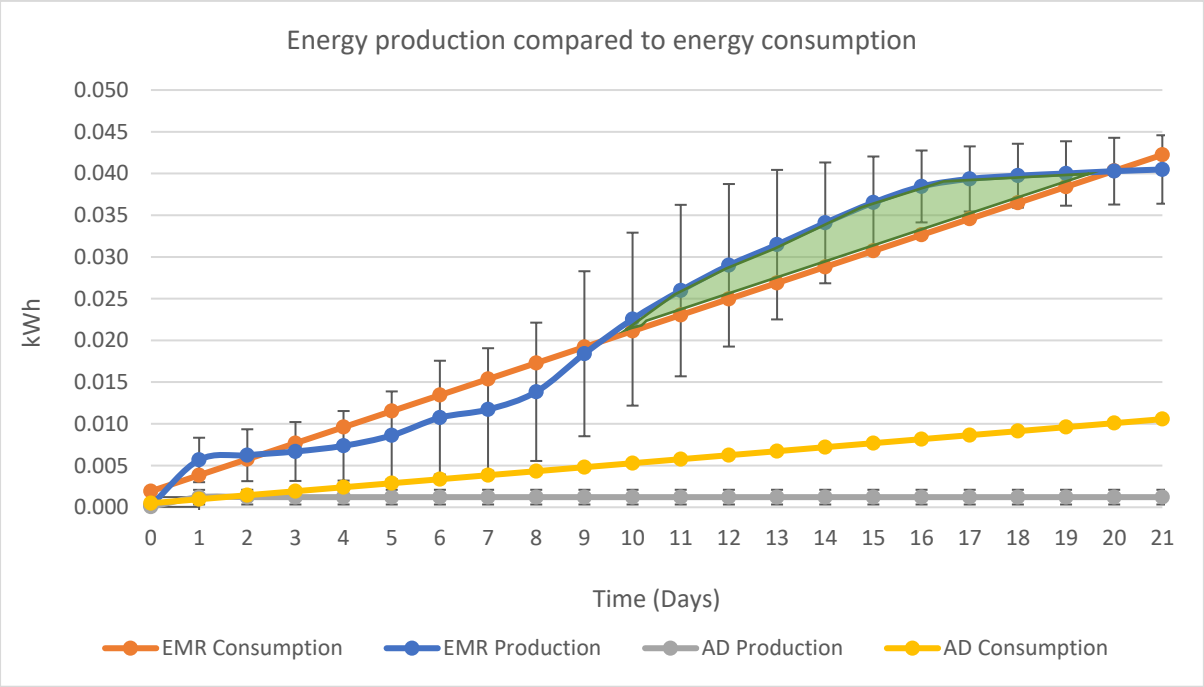

Figure 7-15: Batch EMR (R6-8) & AD (R3-5) Energy Production vs Consumption, with error bars representing the range across the duplicated experiments and a green highlighted area indicating the positive energy generation.

Substrate Efficiency

The mean substrate efficiency shows that the EMR system is effectively converting the organic compounds within the wastewater into methane. The disparity with the EMR reaching over 100% efficiency could be a result of two factors. One could be due to some of the solids portion of the breakdown of the organics that settled in the bottom of the reactor not being accounted for within the COD analysis. The second and more likely option is due to error and/or variations in the COD analysis. The mean AD system was low, but the standard error showed a significant difference between the three systems, where the energy generation varied considerably.

Total Energy Efficiency

The total energy efficiency is higher in the EMR due to the increased ability for the system to convert the organic compounds into the production of methane.

Coloumbic Efficiency

The coulombic efficiency is slightly lower than the average efficiency (69.9%) of the MECs reviewed in appendix 13.1.

7.2 Discussion

The continual pH increase in the EMR suggests that the biofilm on the anodes are still active at lower pH levels compared to the microbial community within the AD system. However, biofilm mass is shown to decrease sharply at pH levels of 5 and 6 (Sun et al., 2019). Exo-electrogens are known to grow in similar pH ranges to methanogens of 6 to 8.5 but at a larger temperature range of 15-42^{o}C (Sun et al., 2014). Optimal conditions for biofilm growth and enrichment were found to be at a pH of 8 (Sun et al., 2019). Rapid drops in pH could cause irreversible impairment to the exo-electrogenic micro-organisms on the anode, where the pH<4 in a MEC did not show signs of recovery within 24 hours after the pH was neutralised (Wang et al., 2010).

The correlation of the EMR systems energy production and pH shows the importance of increasing the pH after the acidification phase. The reactors and electrodes were continually used from the series reactors allowing time for de-gassing. The reactors all flowed into each other and the batch test shows a correlation for the systems to recover from the changes in pH at different rates. During the series test, R6 was fed with more acidic waste streams from R5 (pH 5.5) than R8 was receiving from R7 (pH 6.5). From the batch analysis, it indicates that it is likely the microorganisms on the electrodes adapted to the different pH ranges and could be the reason why R6 recovered at a faster rate than R8. Different stage testing can show a performance increase within AD, including separating the hydrolysis and acidic phases from the methanogenic phase as they require different optimal pH ranges (Speece, 2007). The EMR also showed a greater performance to recover from low pH. It suggests that some exo-electrogenic microorganisms present in EMR can accelerate the breakdown of the VFAs compared to the dominant microorganisms in the AD system. Increasing the breakdown rate could stop the formation of a high VFA concentration. As a result, the pH would decrease rapidly impeding performance, and in this case, stopping the AD from producing biogas.

EMR showed a significant increase in the effluent characteristics compared to AD. Both of the systems are likely to see a significant increase in performance if mixing took place in the reactors. Mixing is a crucial part of commercial AD and wastewater treatment as it increases mass transfer increasing energy production and the breakdown of organic compounds. Increasing the mixing of a two-stage AD system to 90 RPM showed the maximum hydrolysis and acidification efficiency (Ma et al., 2019). As a result, EMR is likely to benefit from mixing. The introduction of the electrodes already shows performance increases in operational conditions through pH stabilisation, effluent quality and energy production. However, the surface area of the electrodes is only in contact with a small portion of the liquid volume. If the performance increase is due to the electrodes, then mixing will increase the organic contact time with the electrode biofilm that should see an increase in performance.

Even though the EMR showed a significant drop in the total solids of 42.58 %, the TSS only reduced by 3.8%. The marginal difference in the TSS could be due to the particle sizes being reduced, increasing the solids in liquid suspension. Going forward, analysing the first 1L from the effluent tube may provide different results compared to the analysis of the whole reactor wastewater. The AD system also failed to reduce any of the COD within the reactor, it is unlikely that no organics would have been broken down within the reactor. The inoculum source could have been one reason as there would

have been a lower concentration of methanogenic organisms. With the addition of the waste to the inoculum lowering the pH it would then not have provided the optimum conditions for the methanogens to grow and increase in concentration. For future tests combing both the EMR effluent with fresh AD sludge would provide a better inoculum source if it is to be used to compare both systems.

7.3 Next Steps

The final analysis used a sample of wastewater from the total reactor liquid. However, in practice, the effluent would not contain the sludge blanket and solids that settle at the bottom of the reactor. Future analysis should compare the effluent from the outlet to understand effluent quality as well as the mixed wastewater to understand the total organic removal.

The batch tests have a high initial loading of organics and can show the pH curve as the VFAs are broken down. Increasing the OLR and VS could indicate how effectively EMR's can handle the build-up of VFAs and understand if EMR systems can recover from low pH (<4) over a prolonged period and not just 24 hours as was reported previously (Wang et al., 2010). Understanding the OLR, VS and pH limits of EMR can be used to optimise continuous flow systems.

Implementing a smart flow control system can indicate the points at which the biogas drops and increase the influent liquid flow rate accordingly. A smart flow system can ensure the system continues to have a higher than 100% electrical energy efficiency if the system is targeted towards energy production. When the organics drop below a point where energy consumption is higher, the system optimisation could shift. The system can be tailored towards energy efficiency, where the system measures the energy required to remove COD. The EMR energy demand can be compared to alternative technologies such as aeration, activated sludge and membrane bioreactors to optimise the wastewater treatment process.

Achieving total energy efficiency is not feasible, and the main aim for the system should be targeted towards an electrical efficiency above 100% to ensure the system can create value.

8 Experiment 3 - Batch Tests Results

Previous batch experiments showed that EMR could outperform AD efficiently breaking down VFAs and stabilising the pH. The aim of the experiment is understanding the effect of EMR to withstand increases in the VS load. Originally the experiment was planned to run for 21 days. The experiment was extended due to the systems taking longer to increase the pH and show biogas production. The final water quality analysis was on day 28. The pH and Biogas composition was measured until day 30 after the system exhibited an increase in biogas production and a rise in the pH.

The experiment came across the same technical issues of recirculation as the first batch test system. Steps were taken to reduce blocking that was caused within the first experiment: (i) the wastewater was blended and filtered, (ii) a mesh was added to the effluent pipe. However, the steps taken to reduce blockages were not successful, and the peristaltic pump was turned off after a couple of hours. An error occurred when adding the brewery boil to the reactors which meant that R8 had 300mL of brewery boil pumped into the reactor instead of 240 mL. The higher flow rate meant the VS loading rate was 60.75g instead of the 48.6g VS in R6 and R7. The increase in VS meant that R8 had a 88% increase from the second batch experiments and a 25% increase in VS compared to R6 and R7. The average EMR results below have removed R8 to remove errors. The R8 results are discussed separately due to the performance variation resulting from the higher VS loading rate.

The COD was planned to be taken daily for the duration of the 21 days. Due to Covid-19 the reagents required to perform the analysis were on an order backlog. After day 15, the testing schedule was reduced to ensure that measurements could be performed at the end of the experiment.

8.1 Reactor Conditions

Over the 28 days, the operational temperature for the systems was 31.45 ± 1.64^{o}C. Table 8-1 shows the operational conditions of the reactors throughout the experiment. The heaters are all controlled by one system; the variation in temperature could be due to the position of the thermocouple and how close it is to the reactor wall. Some reactors may also be exhibiting more significant thermal losses. The higher power consumption of R8 was due to current drawn being 10 - 50 times higher than R6 and R7. It is unlikely that a difference of that magnitude in current is due to changes in the substrate or biofilm and is likely due to a short circuit with the anode and cathode touching.

Table 8-1: *Batch AD (R3-5) and EMR (R6-8)* Operational Conditions

Reactor number	*Reactor Type*	*Stirred*	*Operating Temperature (^{o}C)*	*Avg. pH*	*Total Power Consumption (kWh)*
3	AD	NO	31.20	3.56	0.0139
4	AD	NO	29.69	3.64	0.0139
5	AD	NO	32.52	3.62	0.0139
6	EMR	NO	32.52	4.57	0.0140
7	EMR	NO	33.09	4.51	0.0140
8	EMR	NO	29.69	4.31	0.0184

8.1.1 Operational Water Quality Measurements:

Table 8-2 shows the starting wastewater quality measurements. The AD systems R3-R5 show, on average a higher solids and organics content that the EMR. The difference is due to the off-gassing period before the brewery boil was added where the EMR systems produced more biogas than the AD systems resulting in a lower COD. R7 also has the highest VS, one reason could be due to poor mixing of the samples compared to the other reactors as a result of the pump blocking.

Table 8-2: Batch AD (R3-5) and EMR (R6-8) brewery boil - Day 0 wastewater quality analysis

	Turbidity (NTU)	*TDS (g/L)*	*TSS (g/L)*	*TS (g/L)*	*VS (g/L)*	*VS (%)*	*COD (mg/L)*
R3	5800	11.0	6.5	32.0	29.7	92.81%	16290
R4	6720	12.0	4.7	26.4	26.3	99.62%	16061
R5	5910	7.5	6.5	33.2	31.4	94.58%	16231
R6	5120	7.0	4.9	23.7	22	92.83%	14051
R7	6370	6.5	4.7	48.8	46.9	96.11%	13735
R8	5930	3.5	4.9	27.5	24.9	90.55%	15120
Feed	18400	95.0	200.0	206.9	202.6	97.92%	81455

pH

Figure 8-1 shows the change in pH changes over the 28 days. The systems initial pH was between 6.5 and 7. During the fermentation phase, all the reactor exhibited a drop in pH due to the production of VFAs. The EMR systems reached their lowest pH on days 2-3, reaching 3.83 ± 0.01. The EMR showed a slow increase up to 4.92 ± 0.08 on day 28 and then accelerated at a quicker rate in a further two days to 5.33. R8 did not increase the same way as R6 and R7, which could be due to the higher VS loading rate or because of a possible short circuit. The short circuit would inhibit hydrogen production on the cathode that would directly impact the pH as H^+ are removed. The AD system dropped below 3.5 on day 4 and did not increase until the 30th day. On day 30 the pH increased to 4.03 ± 0.19 from 3.39 ± .05 on day 29.

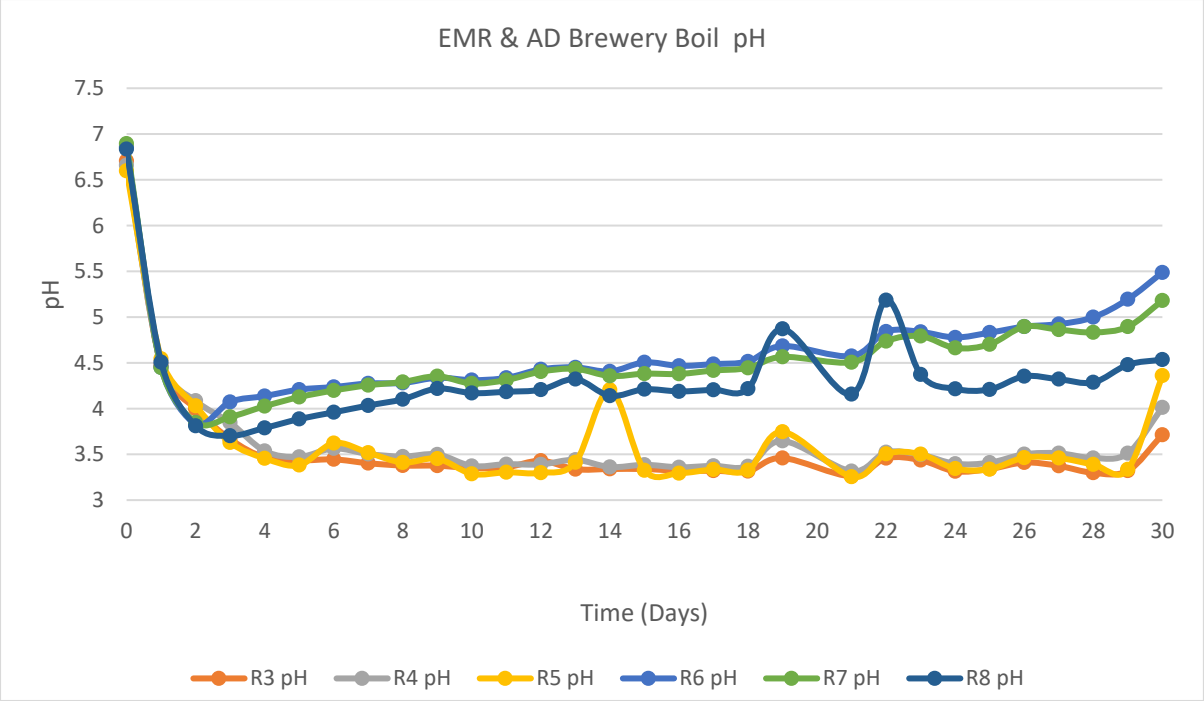

Figure 8-1: Batch AD (R3-5) and EMR (R6-8) - Brewery Wastewater pH

Chemical Oxygen Demand

Figure 8-2 shows an overview of the COD removal for the EMR and AD systems. Both the AD and EMR showed a quick drop in the COD up until day 3, after which the COD reduction rate reduced. From day 4 to day 28, there was a less significant change. AD showed a higher COD reduction of 36.17 ± 0.99% partly due to the higher initial COD. The AD system had a higher starting COD as the EMR produced higher volumes of biogas in the off-gassing phase before the start of the experiment. The EMR showed a lower COD reduction of 34.40 ± 3.98%. The EMR COD effluent was lower than AD but is still higher than EU discharge standards at the end of the 28 days with a COD of 8650 ± 441 mg/L. At the end of the experiment, the systems were still producing biogas, indicating that the COD could reduce further.

Table 8-3: Spent Grain Batch mean AD and EMR COD Analysis, showing the range (±)

Reactor Series	*Average COD Influent (mg/L)*	*Average COD Effluent (mg/L)*	*Average COD Reduction*
EMR	14302 ± 419	8651 ± 442	36.17 ± 0.99%
AD	15248 ± 68.2	9870 ± 153	34.40 ± 3.98%

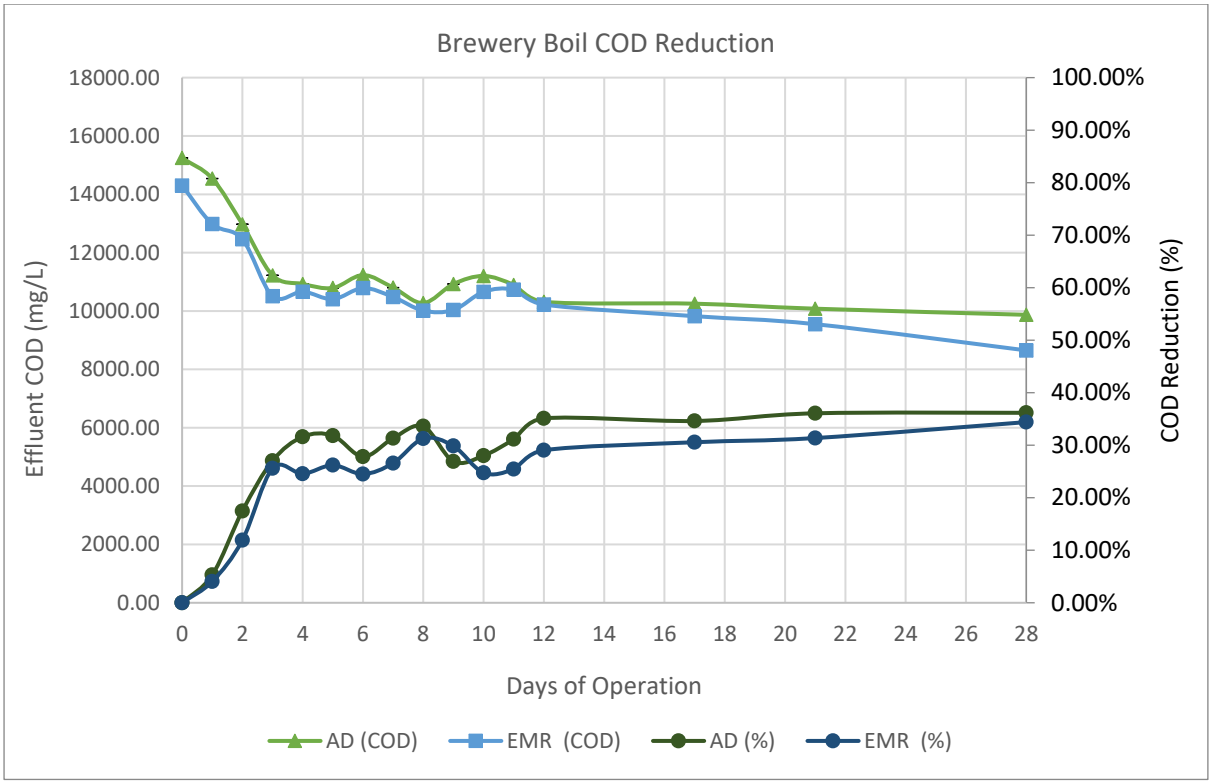

Figure 8-2: Batch AD (R3-5) and EMR (R6-8) – Spent Grain COD Reduction

8.1.2 EMR Biogas and Energy Performance

Table 8-4 shows the overall energy analysis for both the AD and EMR systems over the 28 days. The EMRs all produced biogas initially, however, R8 quickly stopped after day 5. In contrast, R6 and R7 continued to produce small volumes of biogas and energy until day 28, after which there was a small spike until day 30. The AD systems initial produced gas but then stopped after a couple of days. The EMR lab test produced 94% less energy than the theoretical maximum amount calculated from the feedstock analysis obtained in chapter 4. The full breakdown of each reactor is in appendix 0, Figure 13-17 to Figure 13-22.

Table 8-4: Batch Brewery Boil Reactor Biogas and Energy Composition (30 days)

	Total Energy Production (kWh)	*Total Biogas Production (mL)*	*The Proportion of Combustibles over 30 days (%)*	*Expected Energy Production per Tonne(kWh)*
AD	0.003 ± 0.003	5636 ± 5442	5.2 ± 1.3%	2.6
EMR	0.023 ± 0.001	15924 ± 1234	24.2 ± 3.5%	22.7
EMR/AD % Difference	+ 766%	+ 192%	+ 366%	+ 766%
Theoretical Max				401.5
EMR/Theoretical % Difference				-94%

Biogas Production

Figure 8-3 and Figure 8-4 shows the mean daily biogas composition and gas volume production to assess the carbon dioxide and the combustible portion of the biogas. Both the AD and EMR systems show a spike in CO_2 production in the first two days as the systems undergo the hydrolysis phase. Both of the systems then drop on biogas production on day 3. The EMR does not pick up in gas production until day 20 whilst the AD systems continue to flatline and do not produce any more biogas for the duration of the 30 days.

The biogas production difference is clearly shown in Figure 8-5 and Figure 8-6 that compares both the daily and cumulative biogas production. The methane concentration with the EMR peaking on the daily average of 26.74 ± 3.73% on day 27 whilst the AD system peaked on the first day at 4.90 ± 3.37%. Both the systems have a higher gas production on day one as carbon dioxide is produced due to fermentation. On day 6 the reactors show a spike that drops off the next day. The spike does not correlate with any operational change, including temperature or a change in voltage and is likely to be an anomaly. The EMR does not start to generate biogas again until day ten where it increases slightly and peaks at a max biogas production on day 28 at 1094 ± 84 mL/day. R8, however, did not follow the same pattern as R6 and R7 with the biogas and methane production stopping on day 3. R8 followed a similar pattern to the AD systems, suggesting that R8 was overloaded with VS inhibiting the microorganisms within the reactors and on the biofilm. From day 17-27 R6 and R7 had a low average energy production of 0.6 – 0.7 Wh/day, which then increased on day 28 to 33 Wh/day.

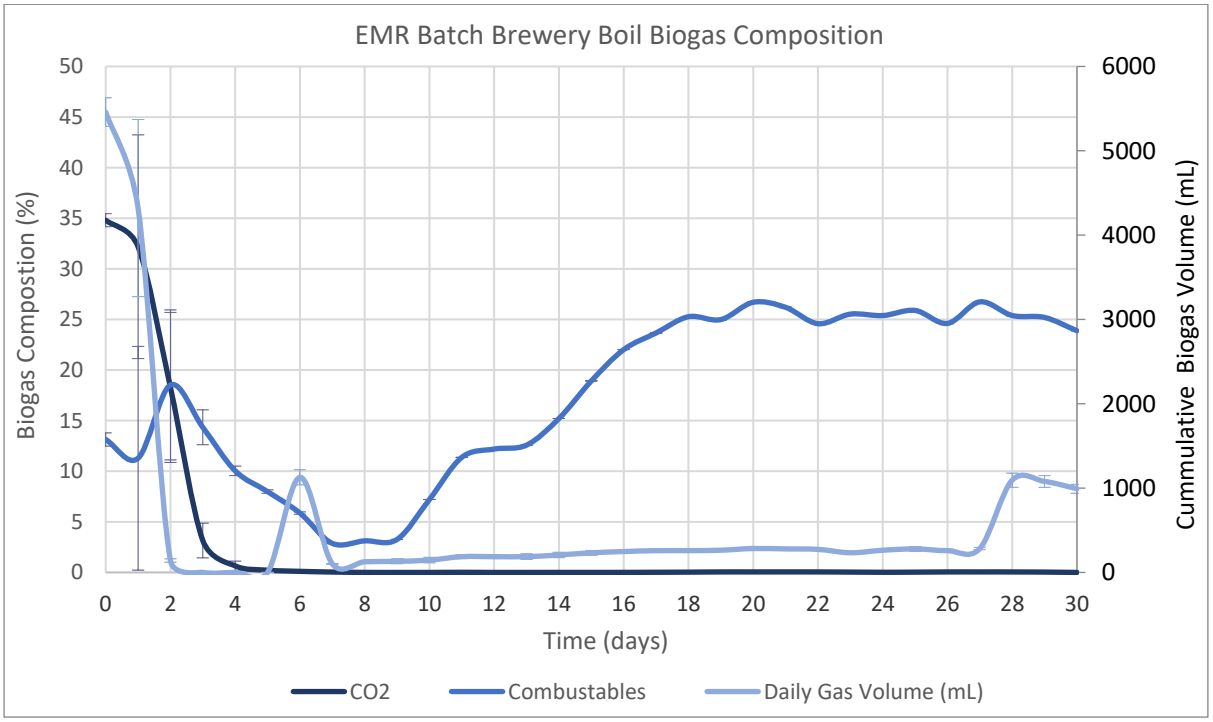

Figure 8-3: Batch EMR – Brewery Boil Biogas Composition and Production, with error bars representing the range across the duplicated experiments.

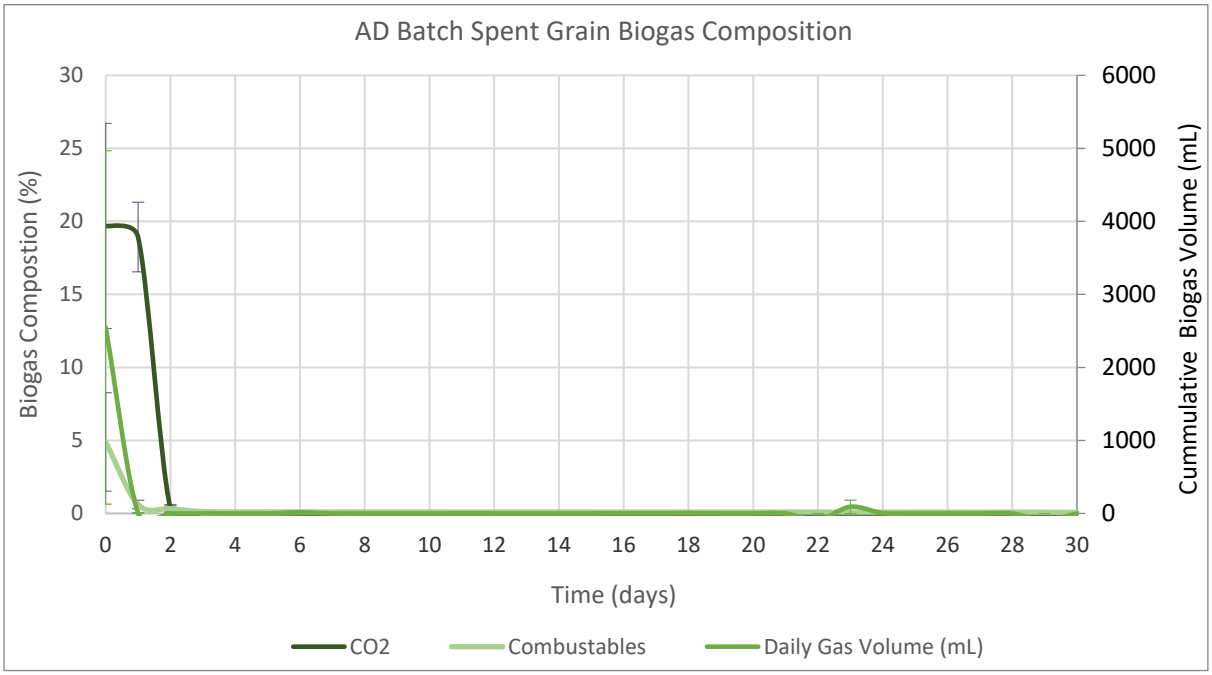

Figure 8-4: Batch AD – Brewery Boil Biogas Composition and Production, with error bars representing the range across the duplicated experiments.

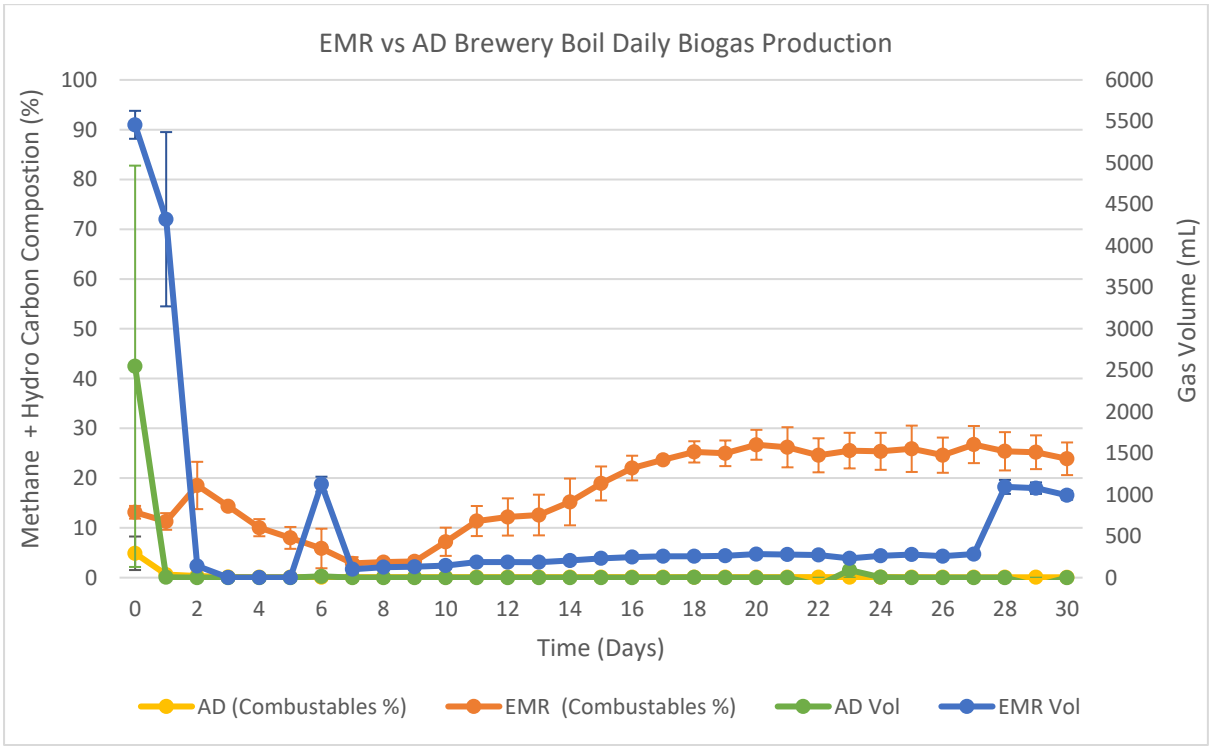

Figure 8-5: Batch AD (R3-5) and EMR (R6-8) – Brewery Boil Daily Biogas Production and CH_4 Percentage, with error bars representing the range across the duplicated experiments.

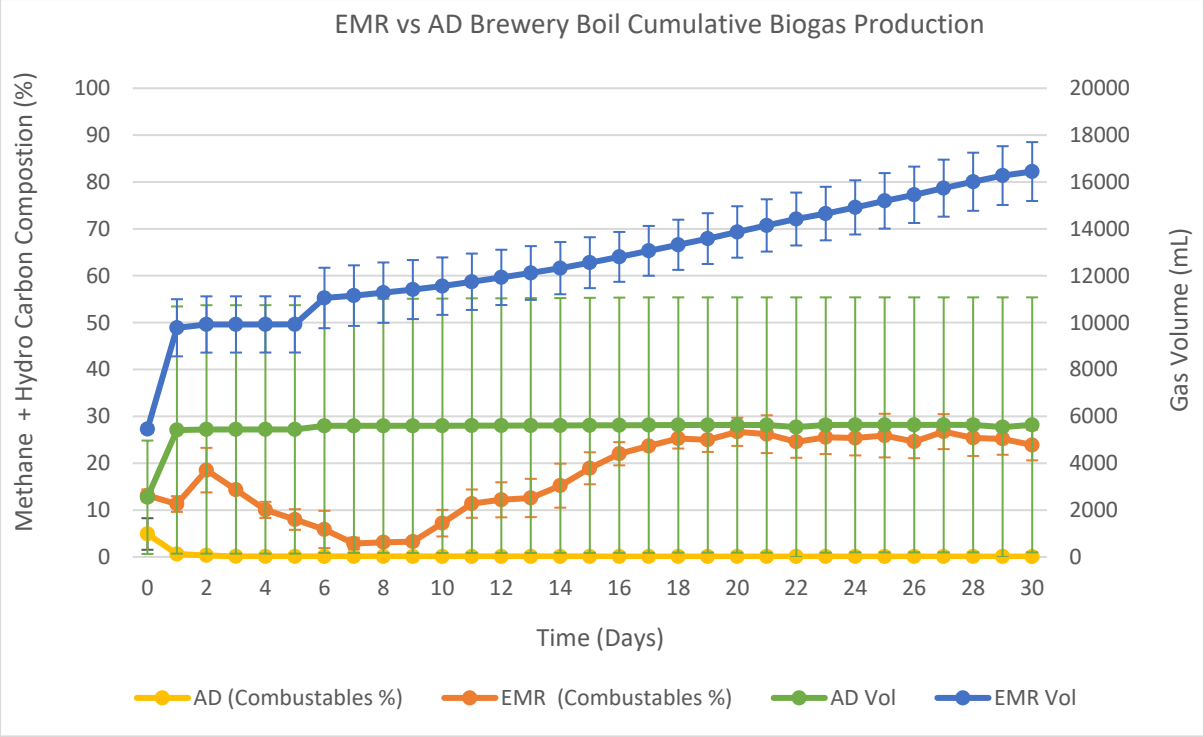

Figure 8-6: Batch AD (R3-5) and EMR (R6-8) – Brewery Boil Cumulative Biogas Production and CH_4 Percentage, with error bars representing the range across the duplicated experiments.

During the experiment, the total biogas composition reached just under 50% at the start of the experiment, after which the majority of the biogas could not be accounted for (Figure 7-8).

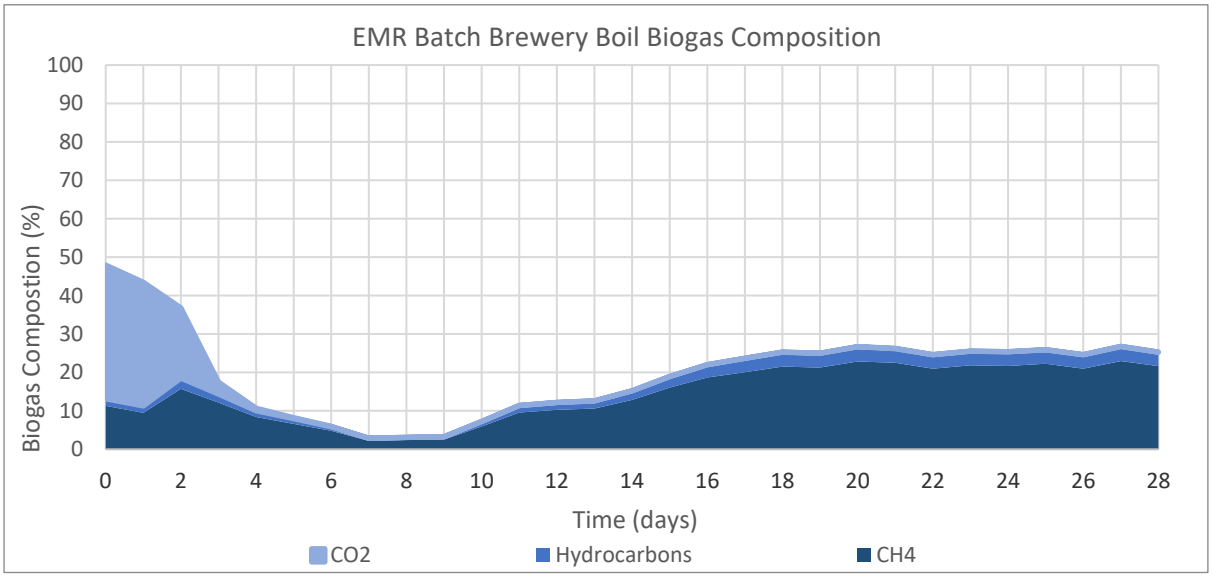

Figure 8-7: Batch EMR – Brewery Boil Stacked Mean Biogas Composition.

Energy Production

The daily and cumulative net energy production are shown in Figure 8-8 and Figure 8-9. Throughout the experiment, the AD failed to generate any energy whilst the EMR started to generate small

volumes of energy on day ten until day 30. The highest daily energy production was on day 0 that quickly dropped off. Even though the methane percentage was only 13.14 ± 1.28%, the higher biogas production meant the energy production was approximately three times higher than the final days.

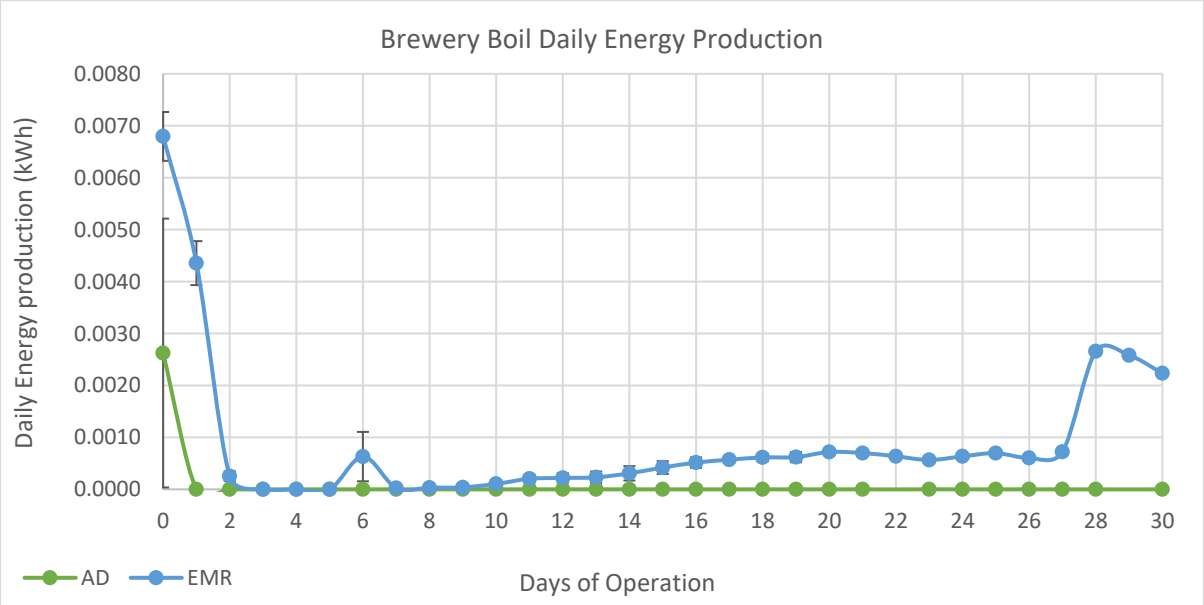

Figure 8-8: Batch AD (R3-5) and EMR (R6-8) –Spent Grain Daily Energy Production, with error bars representing the range across the duplicated experiments.

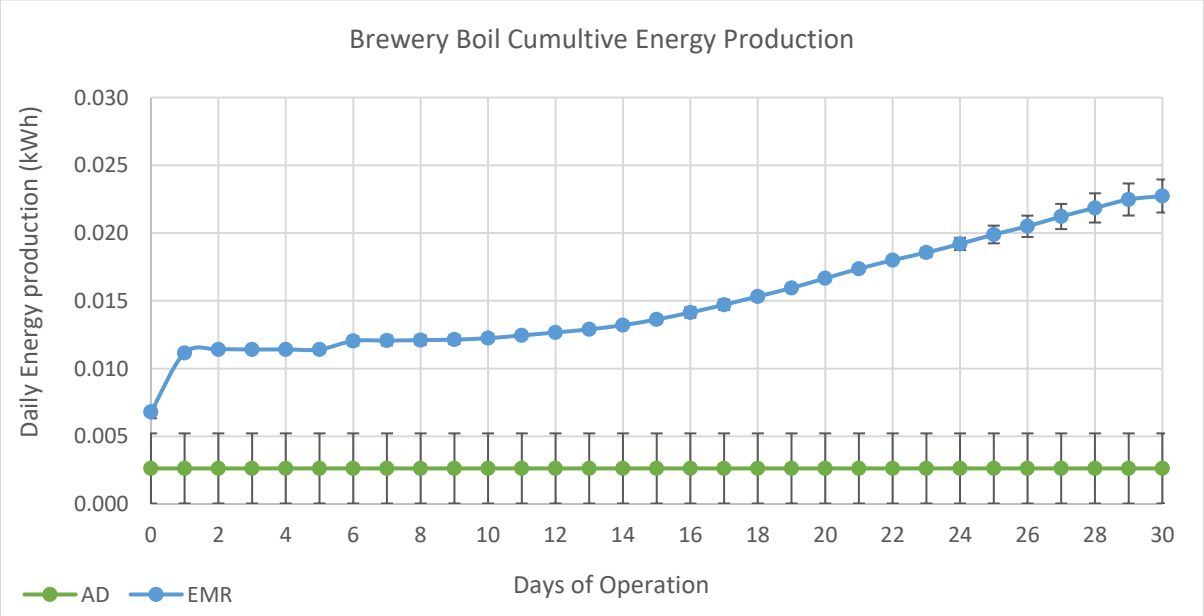

Figure 8-9: Batch AD (R3-5) and EMR (R6-8) – Brewery Boil Cumulative Energy Production, with error bars representing the range across the duplicated experiments.

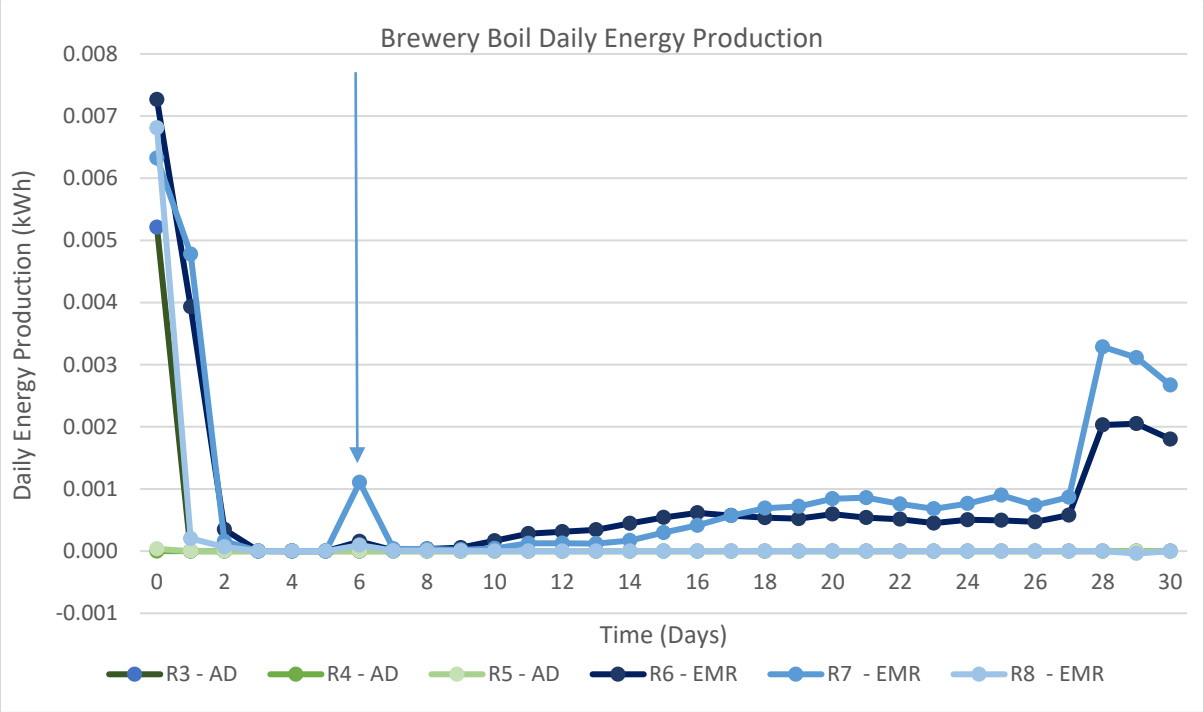

Figure 8-10: Batch AD (R3-5) and EMR (R6-8) - Brewery Boil Reactor Daily Biogas Production, with an arrow showing the anomaly in R7 daily energy production

Figure 8-10 shows the daily biogas production for the different reactors. The graph clearly shows the effect of the rapid pH drop due to the high OLR. The EMR systems show slight signs of recovery from day 10, producing a low amount of energy until day 27. The energy production increases from day 28-30.

Below Figure 8-11 and Figure 8-12 shows the daily and cumulative energy production compared against the pH within the reactors. Similar to the spent grain batch results, the pH and the energy production show result indicate a correlation for energy production. The peak in energy production in R6 and R7 correlates to a quicker increase in pH as it starts to surpass a pH of 5, increasing towards 5.5.

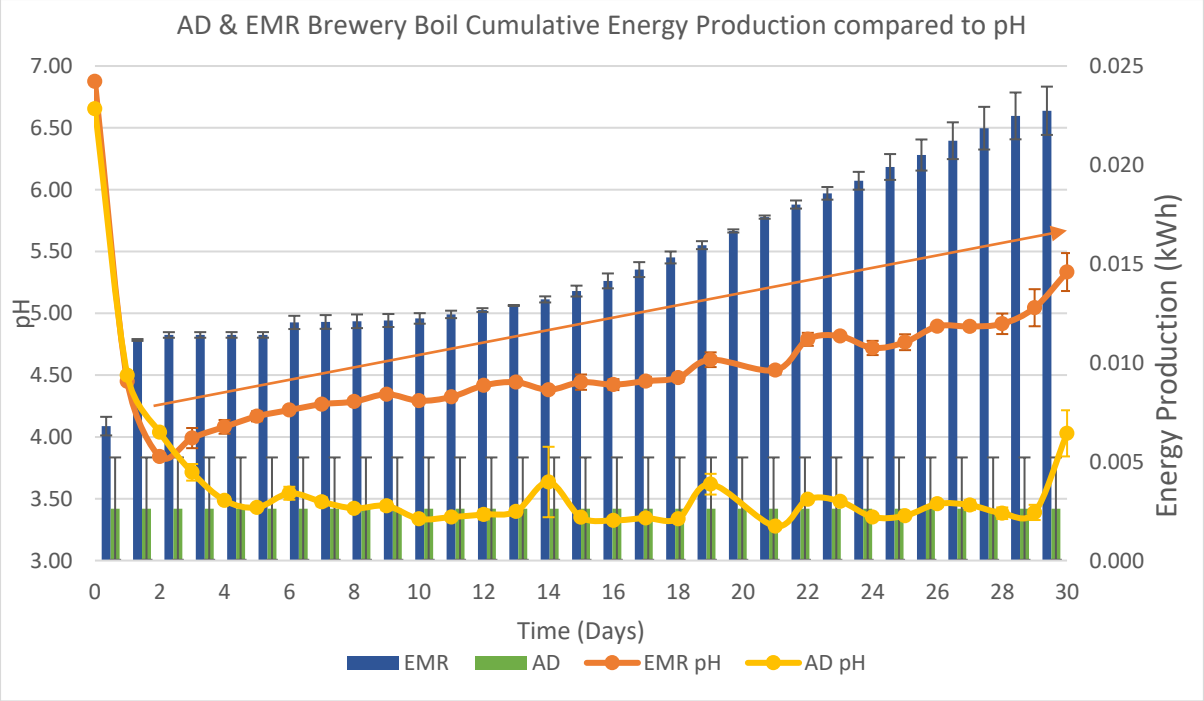

Figure 8-11: Batch AD (R3-5) and EMR (R6-8) Spent Grain – Cumulative Energy production compared to pH, with error bars representing the range across the duplicated experiments and arrow showing the EMR pH increase.

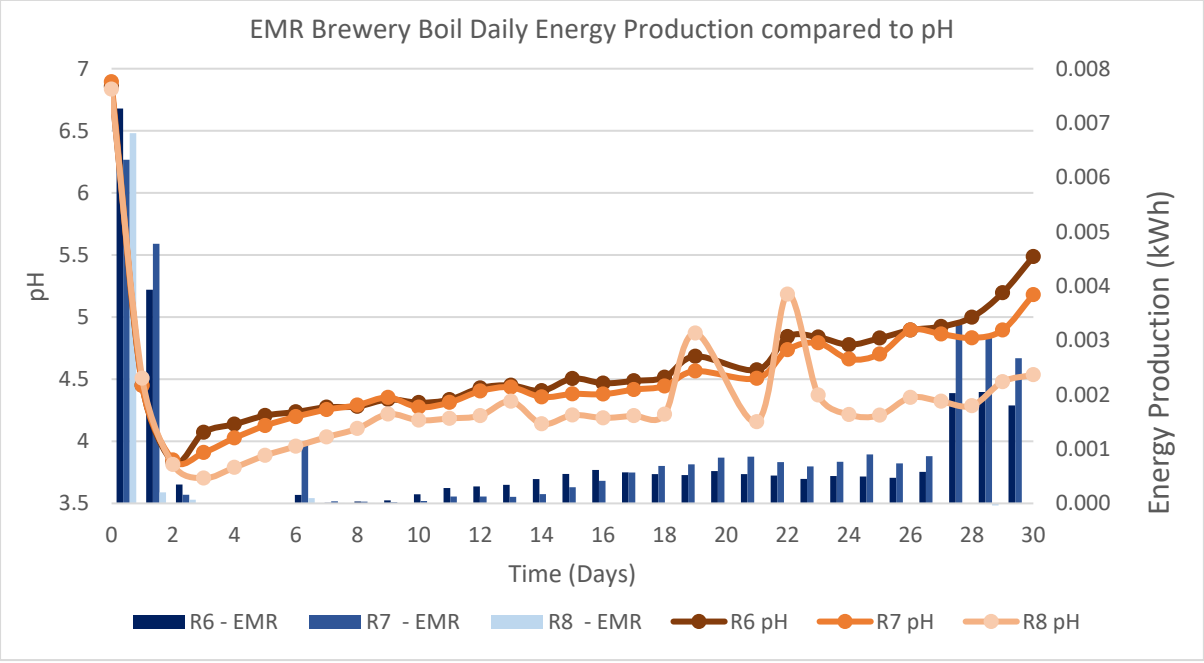

Figure 8-12: Batch EMR Spent Grain – Daily Energy production compared to pH

Table 8-5 shows the statistical analysis to understand the correlation of the pH and the systems ability to generate energy. To be expected, r shows a strong positive correlation between the pH and the energy production that is statistically significant for EMR. The pH and daily energy production have a weak correlation that is not statistically significant for AD. However, AD has a moderate to strong

positive correlation when it comes to methane concentration, whereas the EMR has a week positive correlation.

Table 8-5: Batch AD (R3-5) and EMR (R6-8) Brewery Boil – Pearson's Correlation Coefficient pH Analysis

	pH & Methane (%)		*pH & Daily Biogas*		*pH & Daily energy production*	
	AD	EMR	AD	EMR	AD	EMR
Pearson's Coefficient (r)	0.659	0.366	0.537	0.593	0.159	0.813
p Value	0.000	0.000	0.000	0.000	0.134	0.000

8.1.3 Effluent Analysis

The effluent analysis of the AD and EMR systems showed some significant differences between the two systems that can be seen in Table 8-6. The EMR showed higher performance in most of the wastewater quality parameters apart from the turbidity and TSS. From the previous batch experiments, the AD effluent had a better sludge settleability compared to EMR. The analysis is taken from the effluent with most of the solids settled at the bottom of the reactors. The only mixing would be from gas production at the bottom, causing solids to rise, which may be happening in the EMR but not the AD. Overall the EMR had over 80% lower total solids, volatile solids and total dissolved solids compared to AD. The VS percentage is still at 55% within the EMR, indicating that there are still organics present within the waste that can be converted into methane.

Table 8-6: Batch - EMR & AD Spent Grain Effluent Analysis

	Turbidity (NTU)	***TDS (g/L)***	***TSS (g/L)***	***Total Solids (g/L)***	***Volatile Solids (g/L)***	***Volatile Solids (%)***	***COD (g/L)***	***pH***
AD	874 ± 66	14.7 ± 3.3	2.1 ± 3.0	9.7 ± 3.3	8.7 ± 2.8	89.9 ± 4	9870 ± 152	4.03 ± 0.19
EMR	1310 ± 170	1.5 ± 0.83	2.7 ± 0.2	1.5 ± 0.5	0.8 ± 0.3	55.5 ± 0.5	8651 ± 441	5.33 ± 0.15
EMR % Difference	-49.94%	89.77%	-29.27%	84.48%	90.42%	38.27%	12.35%	32.38%

Compared to the influent all the systems showed a reduction in the turbidity, TSS, TS and VS. The TDS was higher for all the AD systems and R8. The increase in TDS could be due to the breakdown of the suspended solids dissolving into the water as the boil water mixed with the inoculum.

Table 8-7: Batch AD (R3-5) and EMR (R6-8) Effluent Water Quality Percentage Reduction

	Turbidity	***TDS***	***TSS***	***TS***	***VS***
R3 Effluent	84%	-64%	79%	75%	76%
R4 Effluent	86%	-8%	53%	70%	71%
R5 Effluent	87%	-73%	60%	61%	63%
R6 Effluent	74%	71%	42%	92%	95%
R7 Effluent	80%	85%	46%	98%	99%
R8 Effluent	75%	-129%	22%	71%	73%

8.1.4 System Efficiency

Table 8-8 compares the AD and EMR system efficiency.

Table 8-8: Batch AD (R3-5) and EMR (R6-8) System Efficiency

	Electrical Efficiency (%)	*Substrate Efficiency (%)*	*Total Energy Efficiency (%)*	*Coulombic Efficiency (%)*
AD	11.8 ± 23.3%	3 ± 6.7%	2.1 ± 4.1%	N/A
EMR	152.8 ± 8.2%	65.6 ± 12.9%	20.5 ± 2.1%	150.4 ± 36.8%
EMR % Difference	1199%	1846%	894%	N/A

Electrical Efficiency

The power consumption for the EMR electrodes was minimal at 4.8 x 10^{-8} kWh with a mean current of 0.1 mA with heating power requirements of 0.014kWh. Similar to the previous batch experiments, the AD electrical efficiency was low, whilst the EMR reached a higher electrical efficiency of 152.8 ± 8.2%. Figure 8-13 shows the EMR daily energy production compared to the mean daily energy consumption. The high efficiency is due to the first two days and the last three where higher volumes of methane are produced. The EMR is energy negative at day two and does not become energy positive until day 16, where it is just above the consumption until day 28.

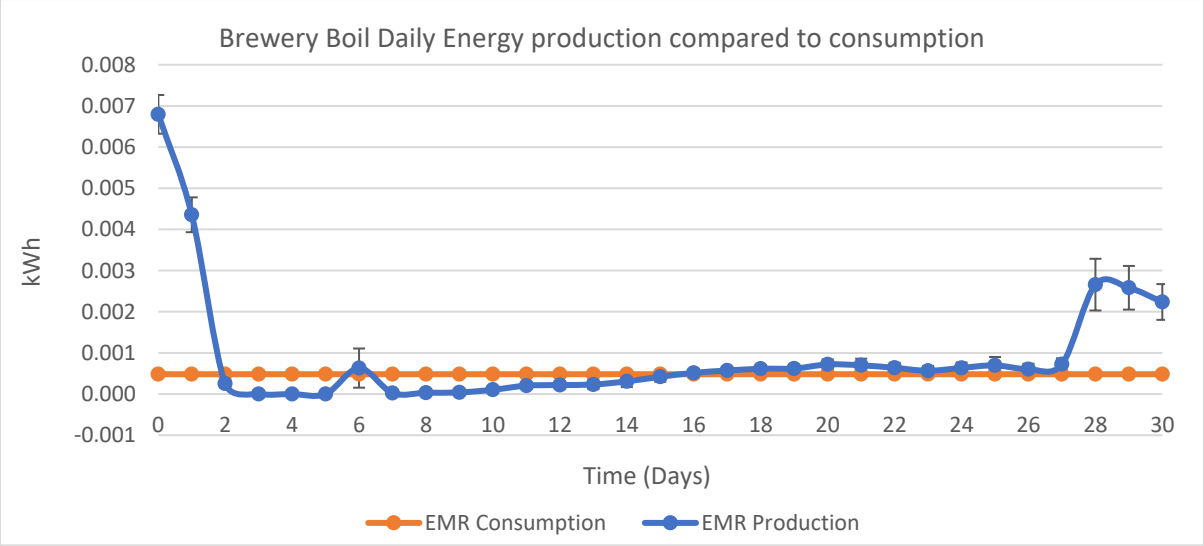

Figure 8-13: EMR Daily Energy Production vs Consumption, with error bars representing the range across the duplicated experiments.

Substrate Efficiency

The mean substrate efficiency shows that the EMR system is not effectively converting the organic compounds within the wastewater into methane. The mean AD system was low with the systems not generating energy after the first couple of days. R8 also had a low substrate efficiency that could be a result of the higher VS content causing a slower pH recovery.

Total Energy Efficiency

The total energy efficiency is higher in the EMR due to the increased ability for the system to convert the organic compounds into the production of methane. However, both of the systems have low total energy efficiency.

Coulombic Efficiency

The coulombic efficiency of the second system is higher than the previous batch even though the system is generating low methane concentration. Similar to the electrical efficiency the high coulmbic efficiency is likely to be a result of the reduce current being drawn from the systems.

8.2 Discussion

One of the aims of the research was to understand the limits of EMR to recover from an increase in VS. As previously discussed research had shown that a drop <4 in pH meant that MECs were not able to recover with 24 hours after buffering to a neutral pH (Wang et al., 2010). In the experiment, all the reactors fell below 4. Unlike the previous experiment, the pH within the EMR did not recover quickly and failed to reach a pH above 5.5 in 30 days which was the point where methane production started to increase. The AD control failed to increase the pH falling below 3.5 and showed no signs of changing. The low pH in all the systems indicates a high concentration in VFA's as a result of the increase in VS. The research showed signs of the EMR recovering without the need of buffering solutions. However, the rate of recovery is slow and for commercial systems, a quicker pH revival would be preferable to increase methane generation and COD reduction. The pH increase does show that the reactors do show signs of generating promising levels of methane and recovering from a pH below 4.

The methane concentration within the biogas is stabilising around 30%. In the previous batch research, the methane concentration did not breach 30% until day 6 when the pH was between 5.5-6. As methanogens do not like low pH and the AD systems fail to generate methane, there may be a localised pH difference around the electrodes. A localised change would explain the methanogenic pathway through hydrogenotrophic microbes. If there is a localised pH that would also explain a low methane concentration as the cathodes surface area is small compared to the reactor volume. With no mixing, it is affecting the mass transfer coefficient. Mixing would help reduce the liquid diffusion layer around the electrode biofilm and the bulk liquid. The agitation would increase the suspended and dissolved solids contact with the biofilm on the anode enhancing the organic removal and bioenergy production.

Continuing the duration of the experiment is likely to increase the pH to between 6 – 8, at a range that is optimum for methanogens. However, at the current rate of pH change, it would likely take around an extra ten days, which would be longer than the typical AD HRT of 30 days.

The peak of energy production was on day 0 however, the energy density of the biogas would be very low compared to typical biogas with a 50-60% methane concentration. At such low methane concentrations, it would affect the useability of the biogas and could render the energy recovery useless for practical application. It is crucial to understand the OLR to limit the VS content to optimise flow rate, pH, biogas production and methane concentration. Developing a computational model to assess the different OLR against the critical performance parameters would enable system optimisation for various feedstocks.

The brewery boil batch-test showed a high electrical efficiency compared to the spent grain. The main reason for this is due to the lower current drawn from the boil water experiment. It is unknown why a significantly lower current was being drawn, but it could be an error with the monitoring equipment.

The system showed a reduction in COD and VS content within the wastewater. However, neither the EMR nor AD were able to reduce the organics within the wastewater to levels where tertiary treatment would not be required. Although the systems did show a significant reduction, an increase

in mixing would aid in solids removal. Developing a model to simulate the removal of the organics will enable the EMR system to be integrated into multi-process simulations. The process simulation can then design appropriate tertiary treatment systems to ensure safe disposal or reuse of the wastewater.

8.3 Next Steps

The 55% increase in VS compared to previous batch experiments shows that the EMR system was not able to convert the organics into readily useable methane. The biogas contained minimal methane content which is not comparable to commercial AD (50-60%) or the previous batch experiments. Future research should focus on loading the organics in a daily batch or continual process that can optimise the EMRs ability to operate at higher VS loading rates.

System mixing has caused multiple issues that will affect the mass transfer coefficient. To increase efficiency for future pilot systems, exploring options for mixing the bulk liquid should be one of the priorities.

9 Chapter 9 – Pilot Scale Electro-Methanogenic Reactor

9.1 Introduction

The chapter discusses the scaleup of electro-methanogenic systems to treat blackwater from an ablution unit fitted with a male and female toilet. The aim is to validate EMR technology to provide decentralised wastewater treatment. The system offers opportunities to provide a circular approach, using wastewater as a resource to generate biogas, produce fertilisers and recover water for reuse. The technology can integrate into rural and urban communities as well as industrial applications, creating opportunities for onsite waste management and energy generation. The pilot research focus is to treat toilet waste (blackwater) directly. The aim is so that the system can then be scaled up for community decentralised wastewater treatment.

The United Nation World Food Program (WFP) supports schools through their schools' meal program and see the potential of the EMR technology to integrate into their work. Schools provide a cooked meal for the children with food supplied by the WFP. The schools currently cook the food using stoves run on firewood which is supplied for free, removing incentives for the school to reduce consumption and change behaviour to reduce the volume of wood they use for cooking. WFP has provided clean cooking stoves; however, the school still use the same volume of firewood, as shown in Figure 9-1.

Figure 9-1:Kenyan School Firewood Delivery & Fuel Efficient Stoves - Kakuma Refugee Camp

The schools have a large number of pupils, and septic tank construction and emptying costs can be high. In the two schools visited both were constructing or have constructed new latrines where previous ones were full and now not operational as seen in Figure 9-2.

Figure 9-2: Old School Pit Latrines and new pit latrine block in Kakuma Refugee Camp in Kenya

Figure 9-3 shows how the EMR system could be scaled up to treat wastewater at a school compound. The system could use solar power to convert the waste to provide biogas that can be used for the cooking within the kitchen — removing the need for firewood which is causing rapid deforestation. The treated water could then be used for irrigation with additional tertiary treatment.

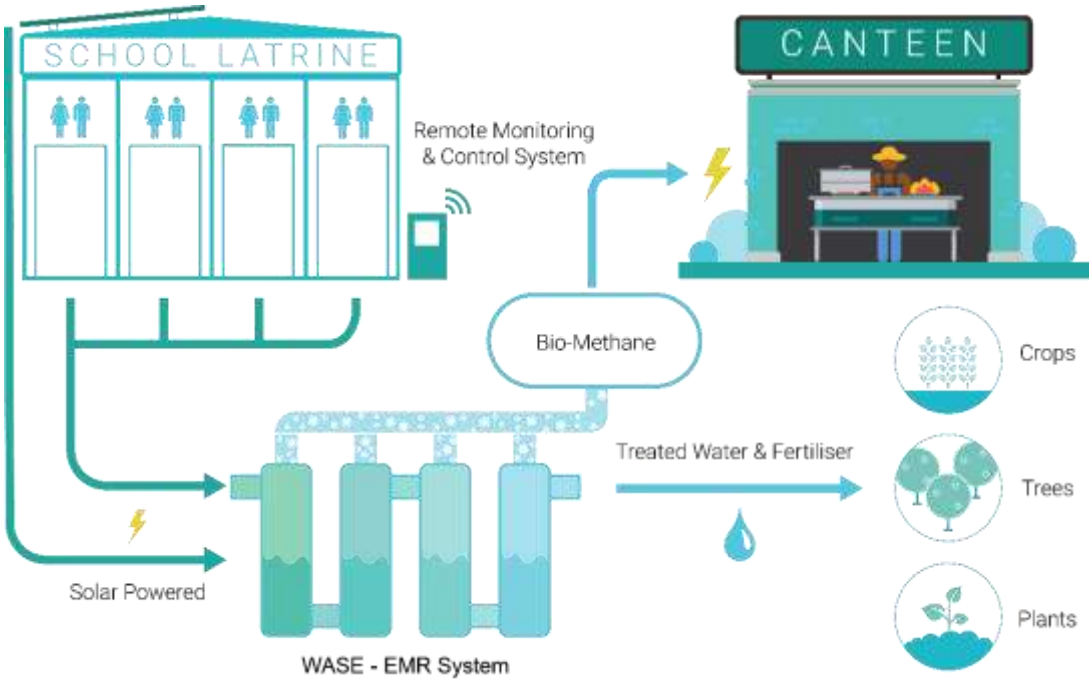

Figure 9-3: EMR Flow Diagram - School Implementation

The project offers developments in EMR, an emerging waste-to-energy technology. Through lab research, EMR has shown to improve the performance of AD by increasing the biogas output and stabilising the system. In other research, EMR has increased the content of methane in output biogas up to and beyond 80% (Cusick et al., 2011a), thus increasing its chemical energy density and heat capacity. The accelerated performance of the technology could create new opportunities for onsite blackwater treatment, where the system could create a real impact within underserved communities.

AD has been tested on blackwater and shows promise but requires higher HRT of 20 days to generate biogas effectively and reduce COD by 53-61% (Wendland et al., 2007). Lansing et al., found that the optimum HRT was 47 days for sanitation waste and requires grey water separation to maximise biogas yields and see a 99.9% reduction in E. coli (Lansing et al., 2016).

Both of these systems have significantly higher HRT than pilot tests on MECs, meaning the systems require a large amount of space. With urban populations continuing to grow and rural populations decreasing, space will become a premium, which means that reducing the size of decentralised wastewater treatment is a crucial concern. Even with MECs and EMRs being more expensive per m^3, where land is costly, the economics can shift by reducing the amount of space required and reducing the civil works.

The system requires small amounts of electricity to power the MECs, which can be powered by solar panels in areas where no electricity is available. The ability to produce biogas creates added value in areas where cooking fuels are scare. Where communities rely on solid cooking fuels such as firewood or coal, it leads to deforestation, severely affecting the environment (Bamwesigye et al., 2018). Cooking with both firewood and charcoal produces harmful emissions that cause 4 million premature deaths every year (WHO, n.d.). Indoor air pollution disproportionately affects women who tend to cook and also children, where both typically collect firewood (Amoah et al., 2019). Figure 9-4 shows a charcoal stove used in a restaurant within the Kakuma settlement in Kenya.

Figure 9-4: Coal Stove in Kakuma Refugee Camp in Kenya

The pilot is in collaboration with the United Nations World Food Programme (WFP) as part of a three-phase scaleup strategy to test the system in underserved communities. The research is the first phase of piloting using a controlled environment to assess technical performance. The system was installed in a UN Humanitarian Response Depot managed by WFP, in Brindisi, Italy. An EMR system was

designed, built and tested onsite. The pilot provides a testbed to trial the technology and identifies issues before deploying the system in the field.

The main goal of the first phase was to assess the performance of the EMR to treat toilet waste in a controlled environment directly. To measure, processing time, quality and quantity of outputs. Identify any issues that may arise, gaining feedback from users and operators to make adjustments for the second phase of testing in an operational environment. Additionally, the pilot offers a better understanding of implementing EMRs in humanitarian settings. EMR can be used for WFP staff in remote off-grid sub-offices as well as for beneficiaries were it can help to strengthen the wastewater and sanitation network.

The collaborative "Sprint Brindisi" project started in October 2018. The project timeline is below in Figure 9-5.

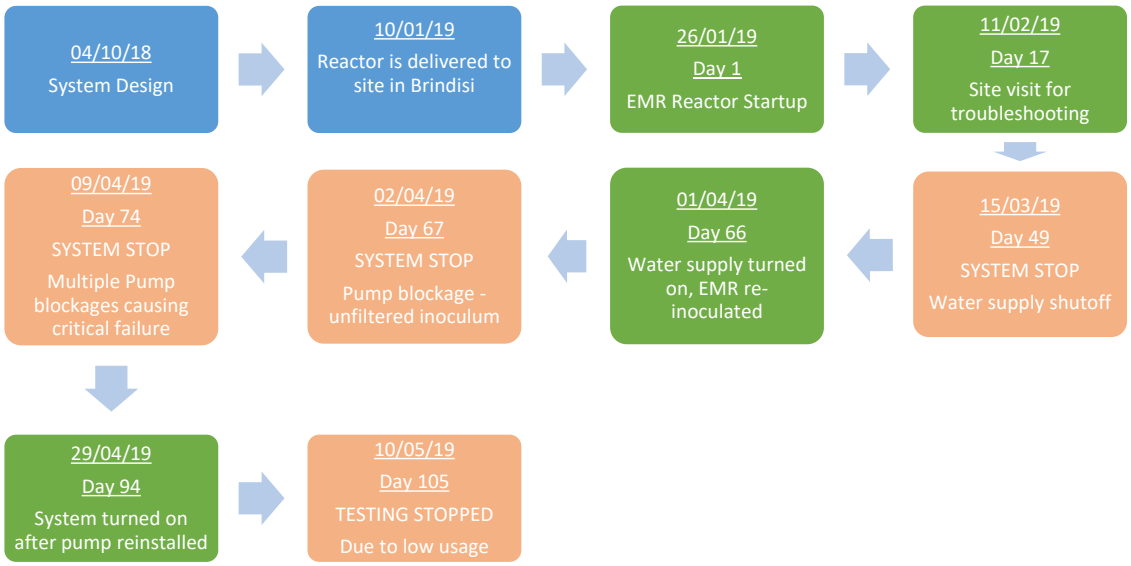

Figure 9-5: EMR Pilot Project Timeline

9.2 Method

In this section, the various methodologies surrounding the pilot are explained. The pilot was constructed for the site using one of the UNRD's ablution units that are a vital component in their first response kit. The first response kits are packages deployed to set up a UN base in emergency relief situations. The ablution unit contains two toilets with 8L flushes and handwashing facilities. The waste flowed into a holding tank (200L). From the holding tank, the waste is pumped using a Boyser AMP-16D Peristaltic Pump into the EMR. The effluent from the reactor flowed directly into a sewer system with sampling points to monitor.

The design and setup of the pilot are to simulate typical conditions within Kenya. The installation was in southern Italy during the winter, and two Heatrod Element Immersion heaters were inserted into the EMR at points TT2 and TT1 on Figure 9-8. The heaters were connected to a circuit with two

thermocouples 15cm from both of the heating elements. An Arduino Leo controlled the circuit recording the temperature at each point independently. The heaters turned off when the temperature reached 35°C and turned them on when the dropped below 34.5°C to stimulate methanogenic conditions.

Figure 9-6: EMR Brindisi Pilot 1

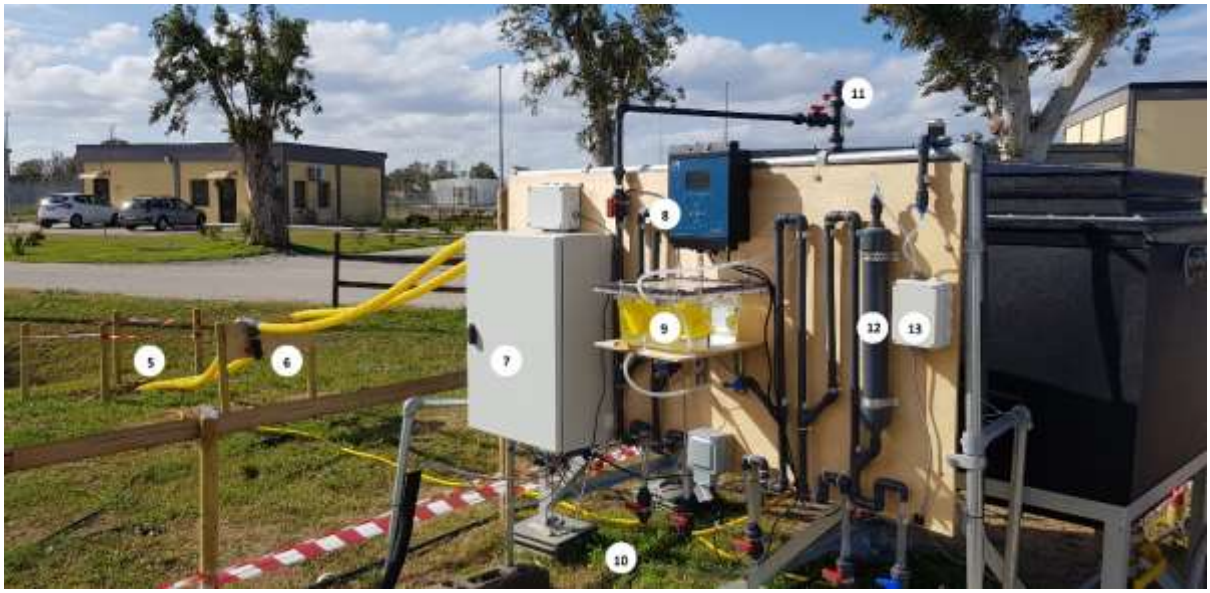

Figure 9-7: EMR Brindisi Pilot 2

9.2.1 Components

Figure 9-6 and Figure 9-7 show the component numbers listed below:

1. Ablution unit with a male and female toilet with eight-litre cistern flush and handwashing facilities.
2. Pump housing for Boyser AMP-16D Peristaltic Pump
3. Electromethanogenic Reactor
4. Biogas Bag Trellleborg B6060
5. Effluent exit port into a sewer
6. Effluent Testing point
7. Control and monitoring panel
8. Inline Process Instrument Crius pH and Temperature Monitoring Panel
9. Wet Tip Gas Flow Meter (wettipgasmeter.com)
10. Biogas water condensing columns (x4)
11. Biogas Testing Point B
12. Desulphurisation Column (Chemiviron Envirocarb Stix 4mm)
13. Dynament biogas analyser

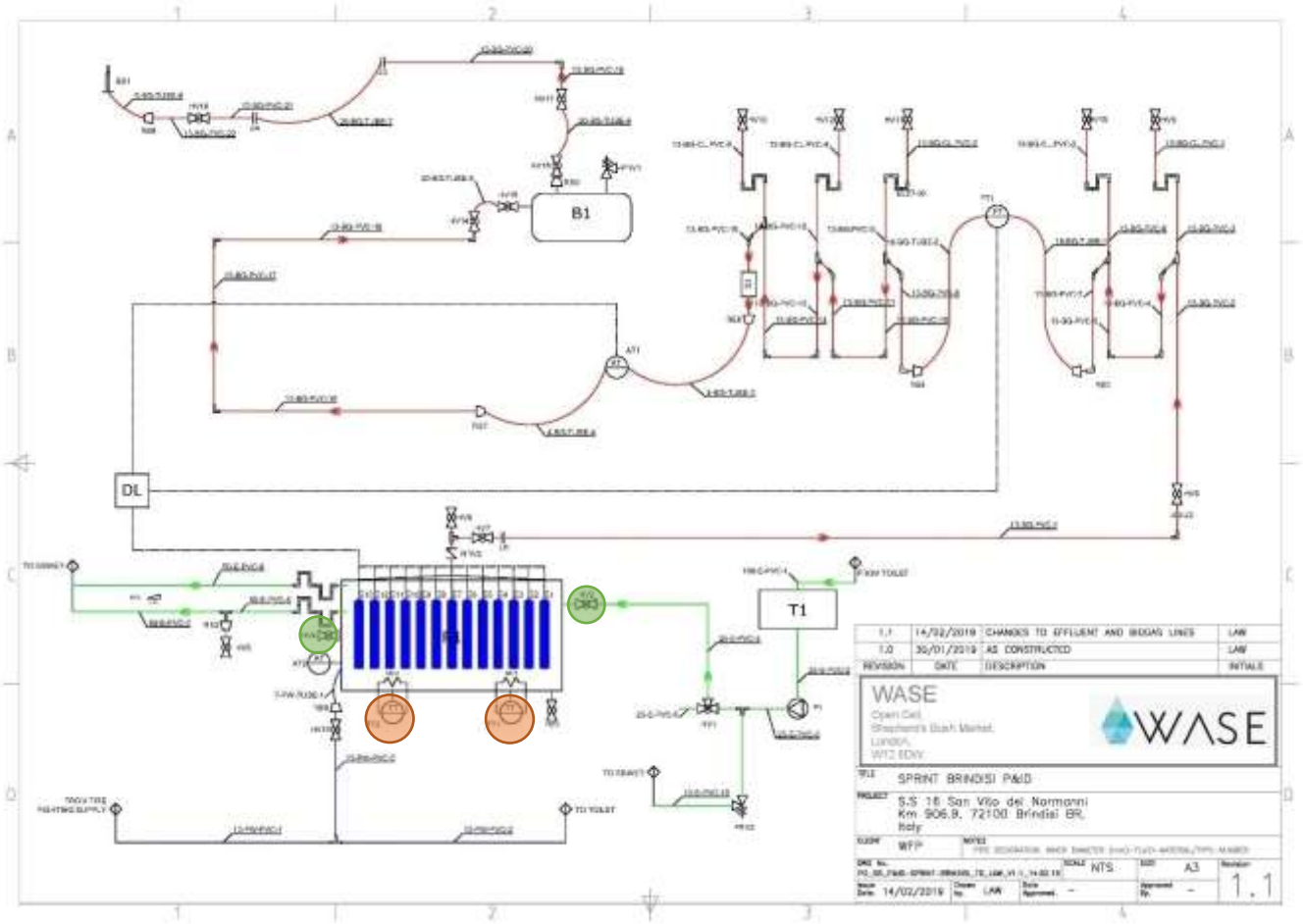

Figure 9-8: EMR Pilot Piping & Instrumentation Diagram (P&ID), highlighting TT1 and TT2 (orange) and HV1 and HV2 (green)

9.2.2 Tank Design

A 1.4m^3 tank was designed and built specifically for the pilot to allow easy insertion of the electrodes and for specific placement to increase the turbulence within the system, as shown in Figure 9-9. The fastening points allowed the panels to be positioned in a floating and standing orientation at 179 cm and 121 cm intervals. The electrode positions created a baffling effect to direct the flow of liquid in a continuous upward and downward motion. The baffling effect will reduce short-circuiting and increase the contact time of the organics in the electrodes. The front of the tank has a slope allowing sludge to be collected and drained from the bottom of the system. Baffled reactors can increase mixing within tanks without any mechanical or moving parts, as well as increasing sludge retention time (Barber and Stuckey, 1999).

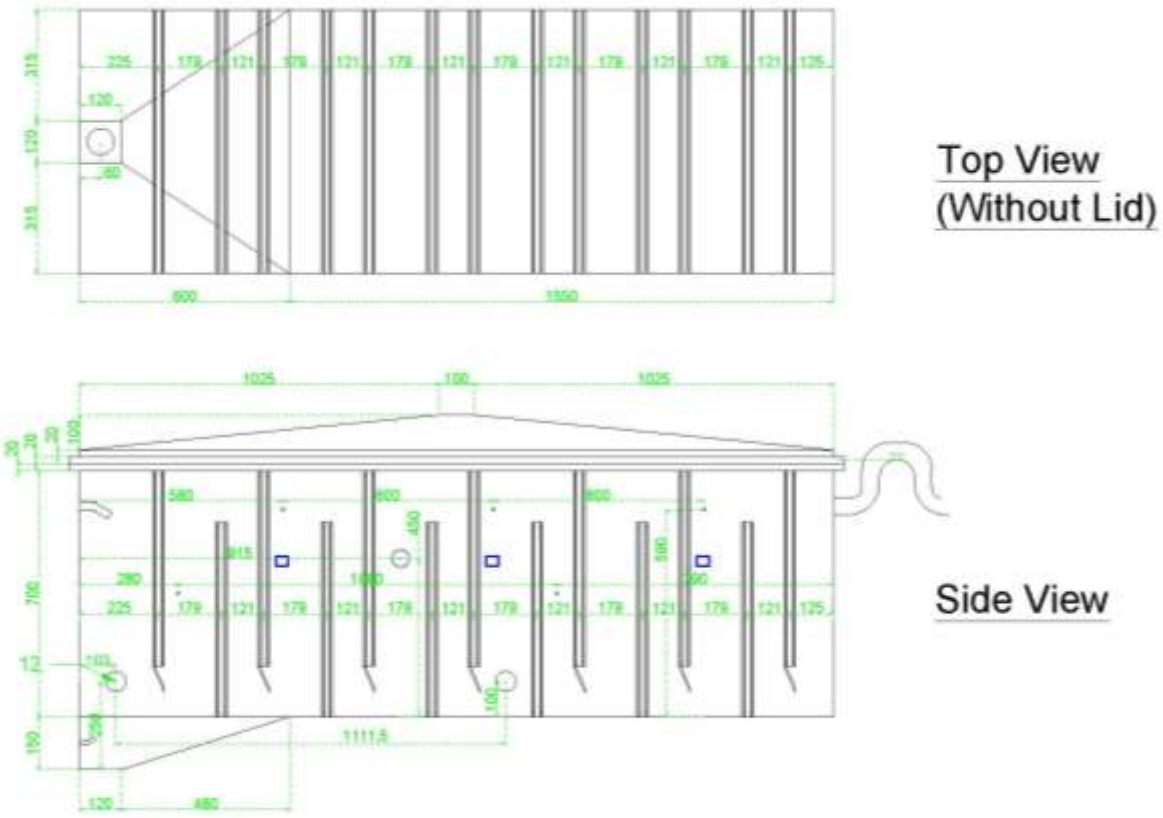

Figure 9-9: Brindisi Tank Technical Design

Anaerobic Baffled Reactors (ABR) have specific design parameters shown in Table 9-1. The parameters were used as a guide where the number of electrode plates needs to be significantly higher than the usual amount of 3-5 baffles in a typical ABR. The main parameter difference was in the up-flow to downflow ratio, where increasing the spacing would have reduced the number of electrodes. Reducing the number of electrodes would have a negative effecting on the organics and electrode contact time that will affect the mass transfer within the reactor.

Table 9-1: Design parameters for an ABR treating domestic wastewater adapted from (Maria and Bsceng, 2009)

Parameter	Symbol	Unit	Ratio / Equation	EMR Reactor Design
Flow Rate	Q	m^3/d		0.7
Number of compartments	N		4 - 6	14
Peak up-flow Velocity	V_p	m/h	0.5	
Design flow velocity	V_d	m/h	$Vp/\ 1.8\ =\ 0.28$	28
Compartment up-flow area	A_u	m^2	$Q/(V_D \times 24)$	60
Upflow to downflow area ratio	$R_{U:D}$	m^2:m^2	1:2-3	1:1.5
Compartment width to length ratio	$C_{W:L}$	m:m	1:3-4	1:3
Reactor Width	r_W	m	$\sqrt{\frac{V_W x C_{W:L}}{N x r_D}}$	750
Reactor Length	r_L	m	$\frac{N x r_W}{C_{W:L}}$	2150
Reactor Volume				$1.6m^3$
Liquid Volume				$1.4m^3$

9.2.3 Thermal Heating System Design

Two heaters were used in the pilot, one to raise the temperature and one to maintain the temperature. The heating requirements of the first heating element was calculated to heat up the wastewater to 35°C. Where Ahn et al., reports the maximum methane yields and current density for treating sewage sludge(Ahn et al., 2017). The second heater was then used to maintain the temperature within the tank at 35°C. Equation 9-1 was used to calculate the energy required to heat up the water shown in Equation 9-2 to Equation 9-4. The second heater requires less power as its function is to maintain the temperature as the wastewater flows through the reactor shown in Equation 9-5 and Equation 9-6. Foam insulation panels insulated the reactor to reduce heat loss - 50mm Xtratherm Safe-R Phenolic Insulation Board which provided an R-value of 2.46 (Insulation Shop, 2020).

Equation 9-1 $$Q = mCp\Delta T$$

Equation 9-2 $$Q\ =\ 113094g\ x\ 4.186\ J/g^{-1}deg\ C\ x\ \ 22^oC = 10415053J$$

Equation 9-3 $$Power\ requirements\ = \frac{Q}{T}\ x\ Safety\ Factor$$

Equation 9-4 $$Power\ requirements\ = \frac{10415053J}{135721.28\ s}\ x\ 1.2 = 920.92\ W$$

Equation 9-5 $$Q\ maintain = (Surface\ Area\ x\ (R - value\ of\ the\ insulation\ )x\ \Delta T\ x\ Safety\ factor$$

Equation 9-6 $$Qm = (4.06m^2\ x\ 2.46km^2W^{-1})\ x\ 35\ x\ 1.2\ =\ 78.4\ W$$

9.2.4 Electrode Design

One of the essential elements of the anode is the electronically active bacteria that form a biofilm on the surface of the anode. The adhesion of the biofilm is critical to system performance. Carbon-based materials can promote interfacial microbial colonisation, accelerating the formation of the biofilm (Li et al., 2017). As well as the biofilm, the anode needs to have an effective electron acceptor as carbon-based materials can have low conductivity compared to metals (Escapa et al., 2016a). Research has led to focus on the high surface area to volume materials looking towards 3D porous carbon electrodes, such as foams, meshes and brushes (Guo et al., 2015). As previously mentioned, the cost of the system is crucial to the economic viability. Carbon brushes were explored for the pilot; however, the cost to manufacture was too high for the pilot. Granular Activated Carbon (GAC) is widely available, relatively cheap and has a high surface area for biofilm formation offering an alternative anode material. GAC is biocompatible and biologically non-toxic (Zhu et al., 2019), and the high surface area for biofilm attachment increases the mass transfer between the electrode and wastewater solution (D. Liu et al., 2018). The cathode requires similar properties with the addition of hydrogen evolution. Cost considerations were vital when taking this project forward due to the aim for deployment in Kenya where CAPEX of systems needs to be relatively low. The electrode placement can be seen in Figure 9-10.

Figure 9-10: EMR Pilot Electrode Placement Images

The EMR contains thirteen electrode plates. Each electrode plate contained 12 anodes and 24 cathodes for a total of 156 electrode triplets. The electrodes anodes were constructed out of a HDPE frame with Granulated Activated Carbon (Chemviron Carbon - Environcarb 207C) inserted into the 12 channels. The anodes within the electrode plate were connected in series using a titanium plate that was inserted into the channels to act as the electron acceptor. The cathodes were constructed out of stainless steel 304 mesh, seem welded to create pockets. GAC (Chemviron Carbon - CARBSORB 30) was inserted into the pockets to create a bed for a methanogenic biofilm to form at the point of hydrogen production to accelerate methane production. The cathodes within the electrode module were connected in series by a stainless steel 316 solid bar along the length of the plate. Below Table 9-2 shows the operational conditions of the pilot system.

Table 9-2: EMR Operational Pilot Conditions:

Feedstock	Inoculum	COD Input Range (mg/L)	Scale (L)	Specific Anode Surface Area (m2/m3))	Specific Cathode Surface Area (m2/m3))	HRT (days)	Duration (days)	Startup (days)	Voltage Applied (V)	Temp (C)
Blackwater	Drainage water + cow manure	2276.7 mg/L	1300	1100	900	35	103 (58 days Operational)	-	1.1	40

The electrode plates where powered individually and in parallel using 5V power supplies. A circuit reduced the voltage, to supply 1.1 V across the electrode plates. Nine power supplies were used to power the electrodes. With electrodes 3 & 4, 7 & 8, 9 &10 and 12 & 13 being powered in parallel using one power supply for the electrode plate pairs. Electrode plates 1, 2, 5, 6 and 11 had their own power supply. Each power supply connects to a circuit with a 1-ohm resistor. The circuit measured the current generation for each electrode plate or pair of electrode plates depending on the power supply setup. An Arduino Leo was used to connect the circuits and calculate the current using Equation 9-7 and recorded the data every 15 minutes.

Equation 9-7 $$Current = Voltage / Resistance$$

9.2.5 Analytical Measurements

The system performance was monitored both remotely and onsite by WFP staff that were trained to take the different measurements. The remote data monitoring involved the use of 2 Arduino Leos and a Raspberry Pi2 system to collect data and transmit it. The computer control systems monitored the electrode's current, the volume of gas produced by the system and the gas composition. The gas was stored in a $4m^3$ gas bag (Trellleborg B6060). The biogas composition was measured using a Dynament Dual-Gas High-Resolution Methane / Carbon Dioxide Sensor (CH_4 0-100%, CO_2 0-100%, Other Hydrocarbons 0-4%). A secondary gas composition and pressure measurement were taken using RASI700-BIO-03 Gas Analyser, which measured for O_2, CO_2 and CH_4 (0-100%) and dual H_2S 0-5000 ppm

& H_2 0-50000 ppm and pressure up to 300 mbar. The gas volume was measured using a wet-tip gas flow meter (from wettipgasmeter.com) calibrated to record in 100ml increments. When 100ml of gas is collected the flow meter tips closing a switch, the Rasberry Pi records the signal, counting the number of tips to calculate the gas flow rate.

A manual tracker was used to record the daily amount of faeces and urine and to estimate the volume in the holding tank. The pump was turned on and off depending on the holding tank volume. The daily flow rate was calculated using Equation 9-8.

Equation 9-8: $Daily\ Flow\ rate = Pump\ Flow\ Rate\ x\ Time$

Three temperature probes recorded the temperature within the reactor. Two thermocouples connected to an Arduino Leo where 20cm away from the two heating rods. The third temperature probe was connected to a Process Instruments Crius which also recorded the pH within the reactor every 30 minutes.

9.2.6 Wastewater Analysis Parameters:

During the pilot study, various wastewater tests were taken at two sampling points. The samples were taken pre-treatment (HV1) and post-treatment (HV5), denoted on Figure 9-8: EMR Pilot Piping & Instrumentation Diagram (P&ID). Seven parameters where measured listed in Table 9-3 and the schedule of the tests indicated in Table 9-4.

Table 9-3: Wastewater Analysis - Equipment

Parameter	Instrument	Units
pH	SciQuip Portable precision Multi-Parameter Water Quality Meter(SQ-7052) P11 pH Electrode	
Conductivity	SQ-7052 - K10 Conductivity Cell	mS/cm
Total Dissolved Solids (TDS)	SQ-7052 - K10 Conductivity Cell	mg/L
Dissolved Oxygen (DO)	DO 100 Polarographic probe	mg/L
Turbidity	HANNA Instruments - LP2000 Turbidity Meter	NTU
Chemical Oxygen Demand (COD)	Camlab Cw2000 colormeter HACH LangeLT200 – Heating block HACH COD Vials 0-1500mg/l and 0-15,000 mg/L	mg/L
Coliform Presence (E.coli)	Camlab - Coliform bacteria check water quality tests	Absent/Present

Table 9-4: Brindisi Pilot Wastewater Analysis Schedule

Sampling Point	Test	Frequency
HV1	pH	Every Monday
	Conductivity	Every Monday
	Total Dissolved Solids (TDS)	Every Monday
	Dissolved Oxygen (DO)	Every Monday
	Turbidity	Every Monday
	Chemical Oxygen Demand (COD)	Once a month
	Pathogens	Never
HV5	pH	Every day
	Conductivity	Every day
	TDS	Every day
	DO	Every day
	Turbidity	Every day
	COD	Every Monday, Wednesday and Friday
	Pathogens	Every Tuesday
HV9, HV10, HV11, HV12 and HV13	Gas Water Traps – Volume Measurement	Every Monday, Wednesday and Friday
HV6	Gas measurement	Every day.

9.2.7 Reactor System Safety Tests

The system was pressure tested to test for leaks. The tank was filled with water and air was pumped into the system using a compressor to 0.100bar and was maintained for 30 mins. The heating system was tested before the installation. The lid was removed, and a portable temperature probe was used to check that the heaters turned off once the water reached 35^{o}C.

9.2.8 Operational Conditions

The section discusses the operational conditions achieved during the pilot. Table 9-5 shows the actual achieved operational conditions and how they differed from the design specification. The atmospheric temperature during the pilot changed throughout the seasonal change ranging from 3 – 28^{o}C, which would have affected the influent temperature significantly as the holding tank was only 200L. The specification of the holding tank had initially been 1.5m^{3} to hold two days worth of wastewater that would sustain continuous flow over the weekend. Due to issue with having to move the ablution unit, it was not possible to have a large holding tank. As a result, the pump was not operational from 4 pm – 8 am to ensure the pump did not run dry changing the operation of the pilot into a semi-batch system.

Previous pilot studies operating on wastewater stepped up Vapp from 0.6 to 1.1 V where the systems started generating hydrogen. At this point the potential difference was around 0.5 V between the

electrodes (Heidrich et al., 2013b). The study is the closets pilot scale system to the research and 1.1 V was used for the pilot system as hydrogen needs to be generated to then convert into methane.

9.2.9 Inoculation

The system was inoculated with 50L of digestate from LEAP Calthorpe Living LabAD system. A further 200L of sludge and water was added to the reactor to bolster the microorganism diversity from a nearby storm drain (Figure 9-11). To kick start the system 1kg of sodium acetate were added as the holding tank filled from the ablution unit, and the site would be closed for two days over the weekend. During this time, the first two days the temperature controller malfunctioned, resulting in the tank reaching 69.4^{o}C for 48 hours pasteurising the system. Due to the limited time available to spend on site, there was no opportunity to find an alternative inoculum source, to reinoculate. It was decided that the system should be turned on, and the wastewater from the ablution unit would flow into the reactor to see if biofilm could grow within the system from the blackwater.

Due to low performance during the pilot, the system was reinoculated with 200L of cow manure. The manure was mixed with water in a 1:2 ratio and pumped into the reactor on day 66.

Figure 9-11: Storm Drainage Channel

9.2.10 Wastewater Flow Rate

The daily flow rate of the system was significantly lower than the predicted 700L per day. Table 9-5 shows the daily flow rate of the wastewater entering the EMR system. The average daily flow rate was around 90L per day instead of the predicated 700L. The reason for the lower flow rate was due to staff being deployed to respond to an international emergency. The reduced staff meant fewer users, where only 2-3 people were using the toilet, and no one was authorised to use the site at weekends. During the pilot, the wastewater flow had to be turned off twice, as indicated in the two periods of zero flow in Figure 9-12 indicated by the red boxes. The reasons where due to the site's water being turned off for unplanned maintenance. The second period was due to the pump malfunctioning and requiring repairing during the pilot after the second inoculation. The aim of injecting agricultural waste into the system was to increase the microbial community within the reactor. The microorganisms would form a biofilm on the electrodes and break down the organic waste. Unfortunately, with the pump breaking down after the inoculation, the system was not operational

for 28 days. As a result, the bacteria would not have received any new organics and were not mixing within the tank.

Table 9-5: Brindisi pilot operational conditions

Parameter	*Expected*	*Achieved*
Operation Time	120 days	103 full duration 58 days operational
Down Time	5%	44%
Flow rate	700 L/day	90 L/day
Hydraulic Retention Time	2 days	35 days
Temperature	35°C	37.6 + 4.7/- 9.1 °C
pH	7.0 +/- 0.5	7.16 + 0.77/- 0.27
COD	3000 mg/L	2276.7 mg/L
Organic Loading Rate	2100 mgCOD/L/day	204.84 mgCOD/L/day

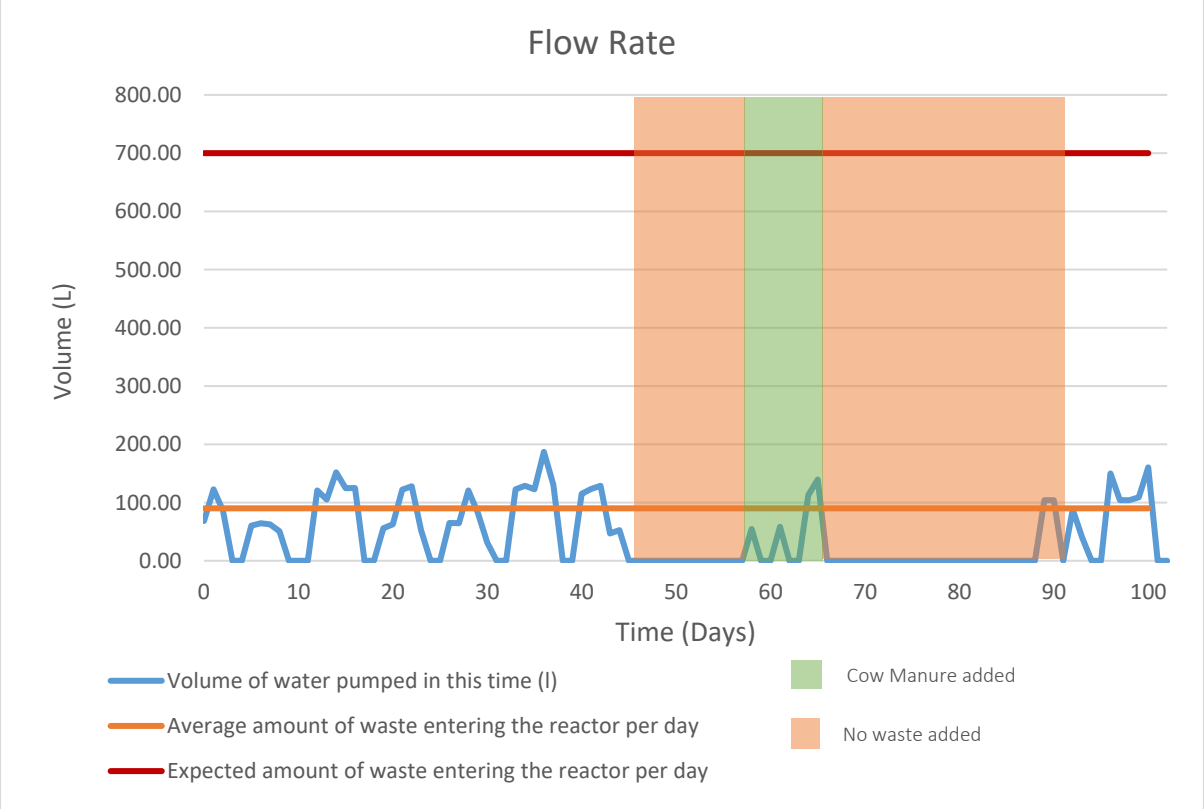

Figure 9-12: Comparison of daily flow rate to the predicted flow rate of wastewater, highlighting the periods when no waste was added or when cow manure was used as a waste stream and inoculant.

9.2.11 Debrief Focus Group

After the pilot, a focus group with the four operational staff involved with the pilot was carried out. The objective of the focus group is to ascertain the effectiveness of EMR to be implemented in the field. The staff involved are part of the WFP first response unit that is deployed in international emergency situations and will have informed expert opinions on different aspects of the technology. The focus group aims to gather insights into the effectiveness of the technology to be deployed in underserved communities in three areas. The first is around behaviour change to understand any social and cultural issues that may impact the use of the system. The second is around the operations of the pilot and the technology that need to be addressed before the system could be trialled in the field. The final area is around the maintenance of the technology that may limit its practicality within the field. The aim of using a focus group over survey data is to create an opportunity for discussion between the users allowing opinions to be challenged.

Usually focus groups would contain 8-12 people, with similar characteristics to ensure everyone is comfortable expressing their opinions (Grudens-Schuck et al., 2004). Due to staff limitation and participants within the trial, it was only possible to have four participants.

An interview guide was prepared for the focus group to help facilitate the session and provide open questions that the participants could build on. During the focus group, the session was recorded, to identify repeated themes and select quotations that will inform the analysis. Participants were encouraged to use a whiteboard to make notes during the discussion.

9.3 Results

In this section, the results of the pilot study show the system performance throughout the study.

9.3.1 Reactor Conditions

Figure 9-13 shows the internal temperature and pH within the reactor throughout the pilot duration. Both the pH and temperature recorded the environmental conditions within the reactor as both affect the activity of the microorganisms. After the temperature rose to 69.4^{o}C it took a couple of days to reduce to below 50^{o}C when the temperature was then recorded and shown below in Figure 9-13. The system 20 days before the temperature stabilised around 37.6 + 4.7/- 9.1^{o}C on day 14. During the first 20 days, there was a drop in temperature of 53.6^{o}C where the reactor fell to 15.8^{o}C. The high temperature and significant drop are likely to have affected the formation of biofilm during the first two weeks. The system temperature shock shows the effect on the pH within the reactor due to water at higher temperatures having a greater ability to ionise and increase hydrogen ions causing the pH to drop. Increases in temperature also improve volatile suspended solid removal causing the solution to increase in alkalinity (Ahn et al., 2017). Once the temperature stabilised after 14 days, the pH stabilised around 7.16 + 0.77/- 0.27. The pilot system was at an optimal pH range for microbial activity and did not show the same pH fluctuations as the lab experiments.

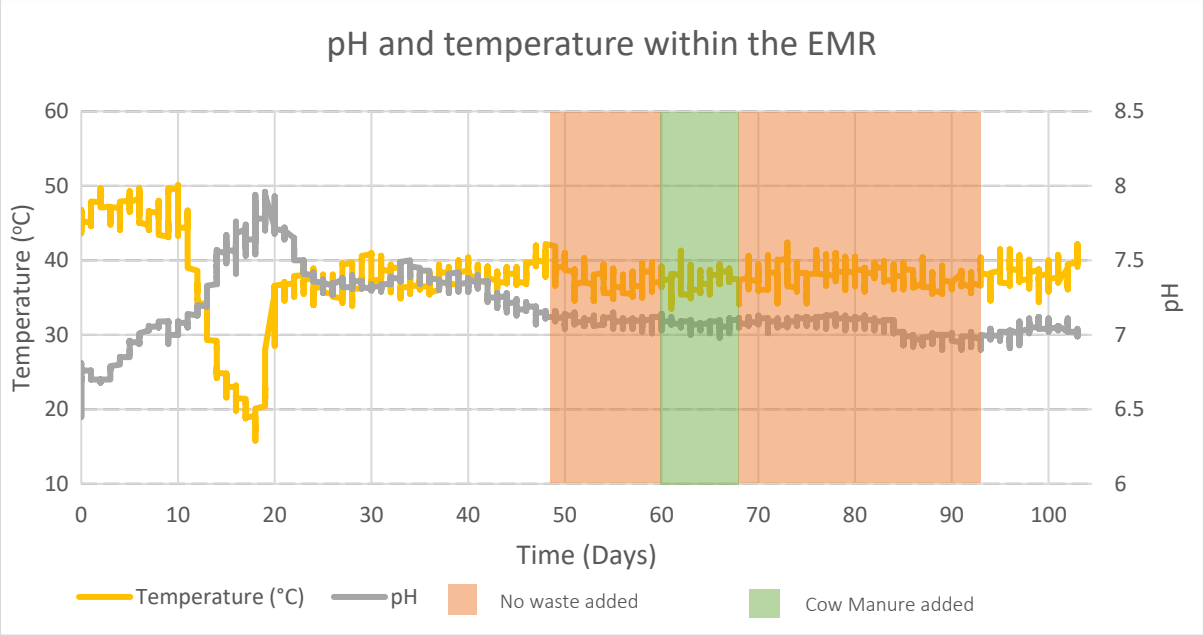

Figure 9-13: The pH and temperature within the reactor, highlighting the periods when no waste was added or when cow manure was used as a waste stream and inoculant.

9.3.2 Water Quality Measurements:

Table 9-6 shows the water quality analysis on the influent and the effluent and compares the test results to EU wastewater discharge standards.

Table 9-6: Water quality data comparisons

Test	Pre-Treatment	Post Treatment	Removal Efficiency (%)	EU Standard
pH	7.7 ± 0.1	7.6 ± 0.1	-	6.5 - 8
TDS (ppt)	3.9 ± 0.2	3.6 ± 0.1	12.7 ± 4.3	<450
COD (mg/L)	2276 ± 1188	1653 ± 196	46.9 ± 6.4	125
Turbidity (NTU)	398.4 ± 102.9	65.2 ± 7.5	83.6 ± 1.9	
Conductivity (µS)	4752.5 ± 1427.8	5469.4 ± 512.1	- 46.0 ± 2.9	
Dissolved Oxygen (%)	7.9 ± 0.0	5.5 ± 0.5	34.4 ± 7.0	

Below, Figure 9-14 and Figure 9-15 shows the fluctuations in the COD removal efficiency during the pilot. The efficiency is calculated using Equation 5-2 comparing the average influent COD to effluent. The HRT and disruptions during the pilot reduced the amount of comparable data for the COD removal efficiency. The results show an average COD reduction of 46.9%.

The average influent COD was used due to the high HRT and fluctuations in daily flow rate required to calculate the COD removal efficiency. The influent COD fluctuated significantly during the pilot. To calculate the average influent COD, a standard deviation of 0.5 was applied to the results to identify

any outliers. The influent COD fluctuated from 500mg/L to 13140mg/L, applying the standard deviation of 0.5 indicated three incorrect values show with red crosses on Figure 9-14. Resulting in a mean influent COD of 2276mg/L.

Due to spoiled COD effluent samples, the data collection intervals were not matched reducing the reliability of the data set. Figure 9-15 shows large fluctuations in removal efficiency during the pilot. The COD reduction is not in line with EU discharge standards. Even with the HRT of 35 days, the COD was not significantly reduced with operational AD outperforming the system. Part of the issue with the low performance is due to the inoculation of the system. With an ineffective biofilm and bio consortium within the reactor, the breakdown and removal of organics will be slower, and the results show that there has been ineffective COD removal for the treatment time. With an effective OLR of 204.84 mgCOD/L/day which is ten times lower than the 2000 mgCOD/L/day literature proposes as a rate that can compete with activated sludge (Gil-Carrera et al., 2013b).

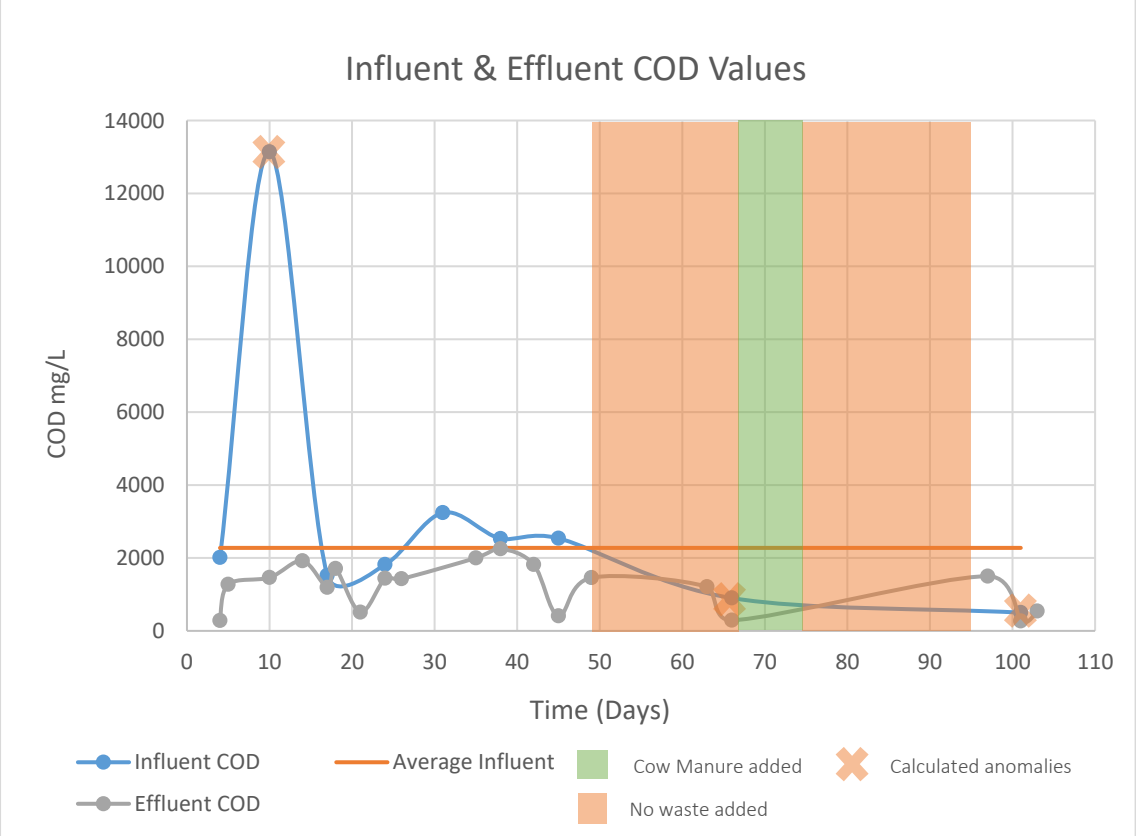

Figure 9-14: Influent & Effluent COD, highlighting the periods when no waste was added or when cow manure was used as a waste stream and inoculant and crosses indicating calculated anomalies.

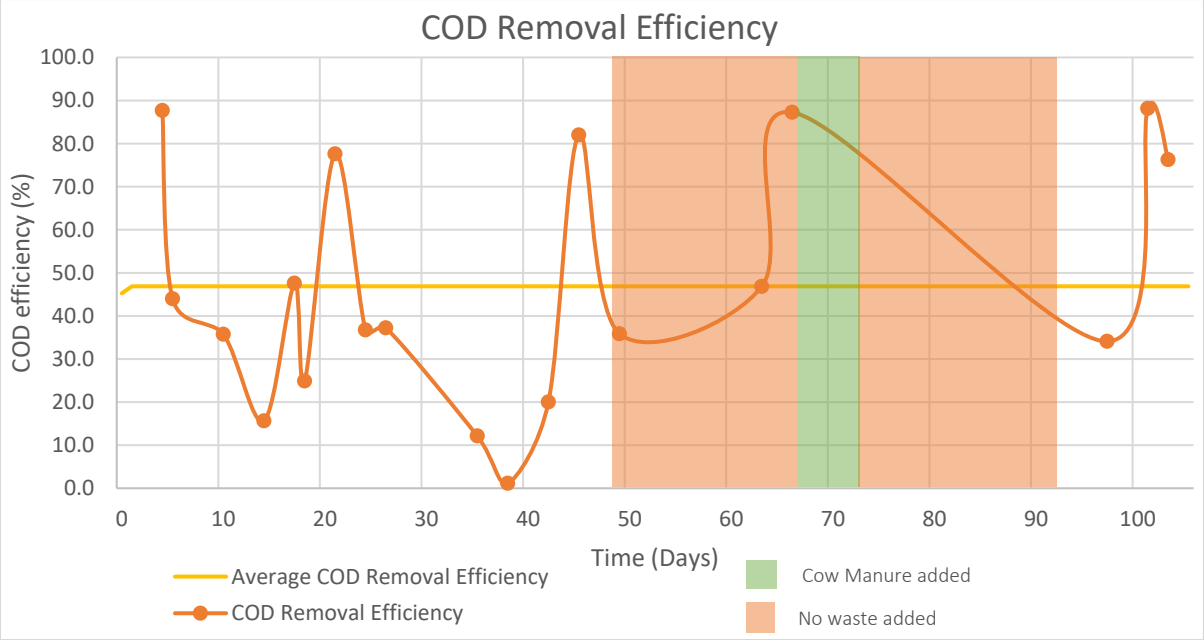

Figure 9-15: COD Removal Efficiency, highlighting the periods when no waste was added or when cow manure was used as a waste stream and inoculant.

The low organic loading rate was due to the reduced number of participants using the ablution unit resulting in a low flow rate. Figure 9-16 shows the toilet usage throughout the project. The system was operating on black water from the ablution unit, which reached a peak usage of 19 times a day but a mean usage of nine during the operational periods. The system was designed to operate with a minimum of 10 users but ideally 15-20 users to reach the predicted 700L/day. The COD of the influent wastewater was 24% lower than the predicted COD of 3000mg/L.

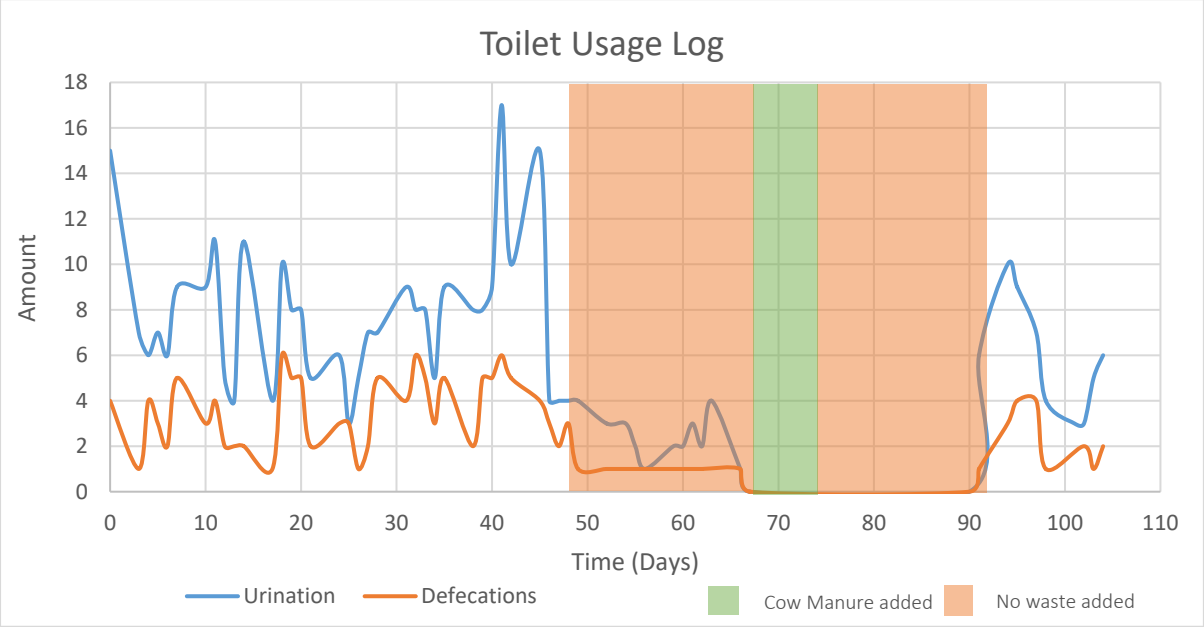

Figure 9-16: Stacked line graph showing toilet usage, highlighting the periods when no waste was added or when cow manure was used as a waste stream and inoculant.

The pH is a good indicator of reactor conditions, the pre, during and post pH is shown in Figure 9-17. As mentioned previously AD systems typically have a high build-up of Volatile Suspended Solids (VSS), causing the pH to drop significantly, which can inhibit the bacteria within the system (Logan, 2007). The stable pH within the reactor and higher pH at the effluent indicates that there is not a build-up of VFA within the wastewater. As the system is operating in ideal mesophilic conditions, the treatment will likely be following similar stages hydrolysis, acidogenesis, acetogenesis, and then methanogenesis. With no build-up of VFAs at any stage they have either gone through acetogenesis to produce acetate or in this case more likely carbon dioxide as there are low volumes of methane production. Another possibility is that the VFAs are used for electricity generation by the exoelectrogens present within the biofilm.

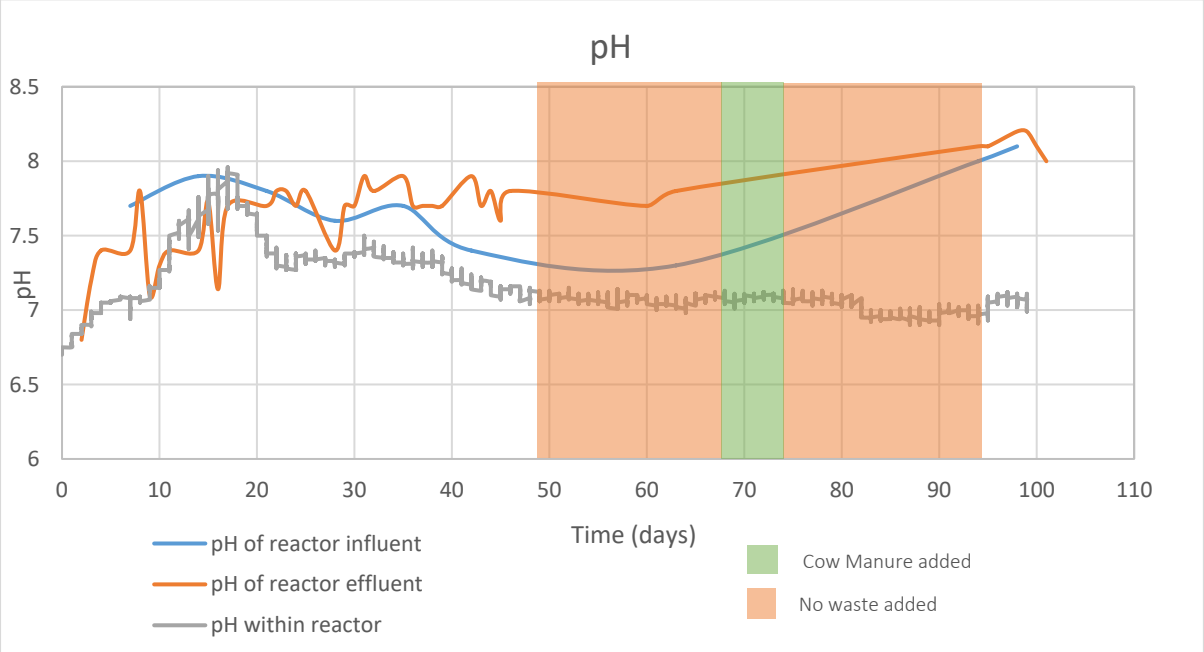

Figure 9-17: pH change pre, during and post-treatment, highlighting the periods when no waste was added or when cow manure was used as a waste stream and inoculant.

Figure 9-18 shows the reduction in turbidity pre and post-treatment. Overall, the pilot showed a significant reduction of 83.63%. The main reason for the reduction is due to the long HRT and the electrode plate baffles. The combination is allowing significant time for the solids to settle before the effluent leaves the system.

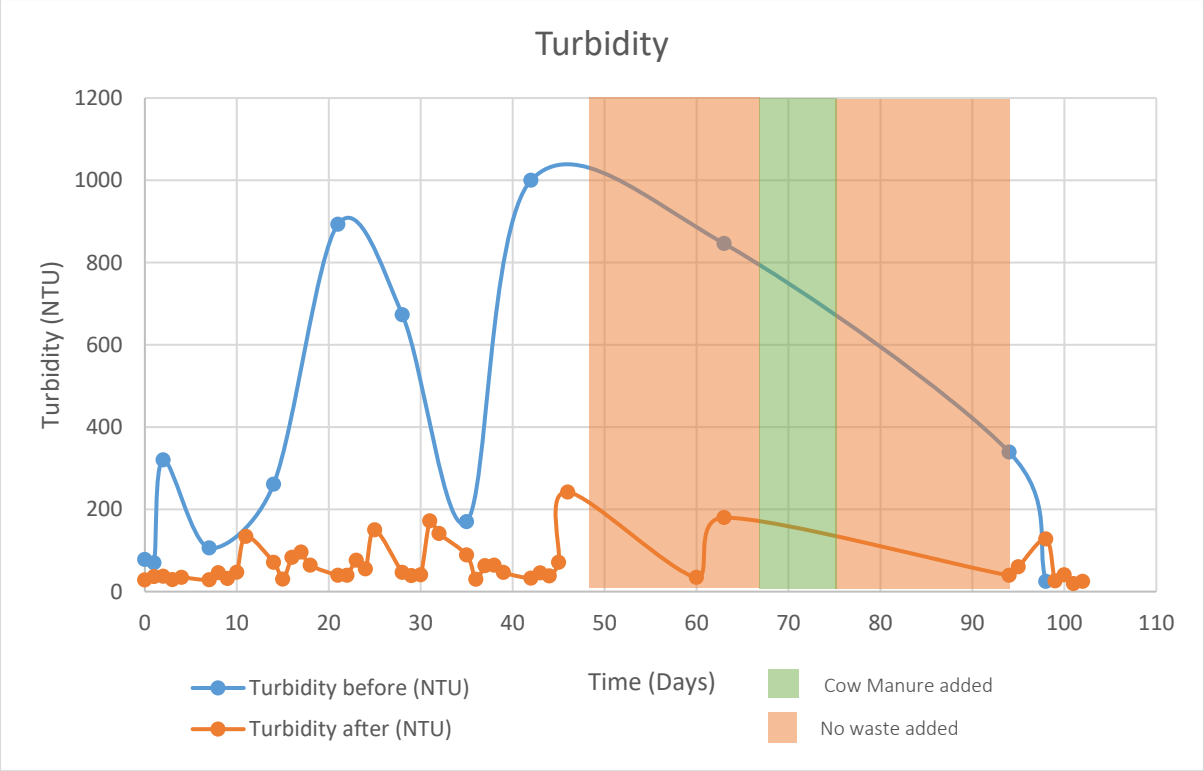

Figure 9-18:: Turbidity of wastewater before and after the reactor, highlighting the periods when no waste was added or when cow manure was used as a waste stream and inoculant.

Table 9-7 shows the presence of pathogens in the effluent of the system. EMR is unlikely to affect pathogen removal, especially at the intended HRT. A tertiary treatment will be required to remove coliforms and pathogens before it can be safe to discharge into the environment.

Table 9-7: Results of pathogen checks on the reactor effluent

Time (days)	*Pathogens Present*
4	No
11	Yes
18	Yes
25	Yes
32	Yes
39	Yes
46	Yes
102	Yes

9.3.3 EMR Performance

The pilot EMR failed to produce any significant volumes of biogas producing on average 1.3L of gas per day. The methane concentration volumes were on average 0.09% and carbon dioxide levels of 1.45% as seen in Table 9-8. Both are higher than atmospheric conditions indicating that there is bio

digestion taking place within the reactor. Due to the low methane and gas volumes, the energy efficiency of the system is not relevant as the pilot failed to start up and perform effectively as an EMR.

Table 9-8: EMR Pilot System Performance

Volumetric Gas Production (m3 gas/m3 reactor volume/day)	Gas Composition (%)				Gas Pressure (Pa)	Energy Production (MJ/day)	Cathodic Coulombic Efficiency (%)	Current Density (A/m^2)
	CH_4	CO_2	O_2	H_2S (PPM)				
0.001	0.09	1.45	20.78	0.11	-0.14	-	-	0.45

During the pilot, approximately 10.04kg of COD entered the system and 2.75kg was removed. A typical AD system generates around 1kWh from 1kg of COD and will typically operate with waste streams above 1g/L of COD (Pham et al., 2006). 1 kWh is 3.6 MJ; methane has a gross heating value of 40.34 MJ/m^3. Therefore, $1m^3$ of methane is 11.2 kWh. The theoretical maximum volume of methane with 100% conversion of COD in an AD would be 10.04kWh, which would be 895L. For 2.75kg of COD removed during the pilot, an AD system would have generated 2.75kWh or 2.3L of methane a day.

Biogas

Figure 9-19 shows the daily gas flow rate. The X indicates anomalies likely due to a faulty connection within the monitoring equipment as the flow rate rapidly drops. The flow rate was monitored after the pilot had stopped, and the wastewater was not pumped into the tank to see if gas was still generated. The system did generate low volumes of gas around 0.5L/day for 35 days after the pumps were stopped.

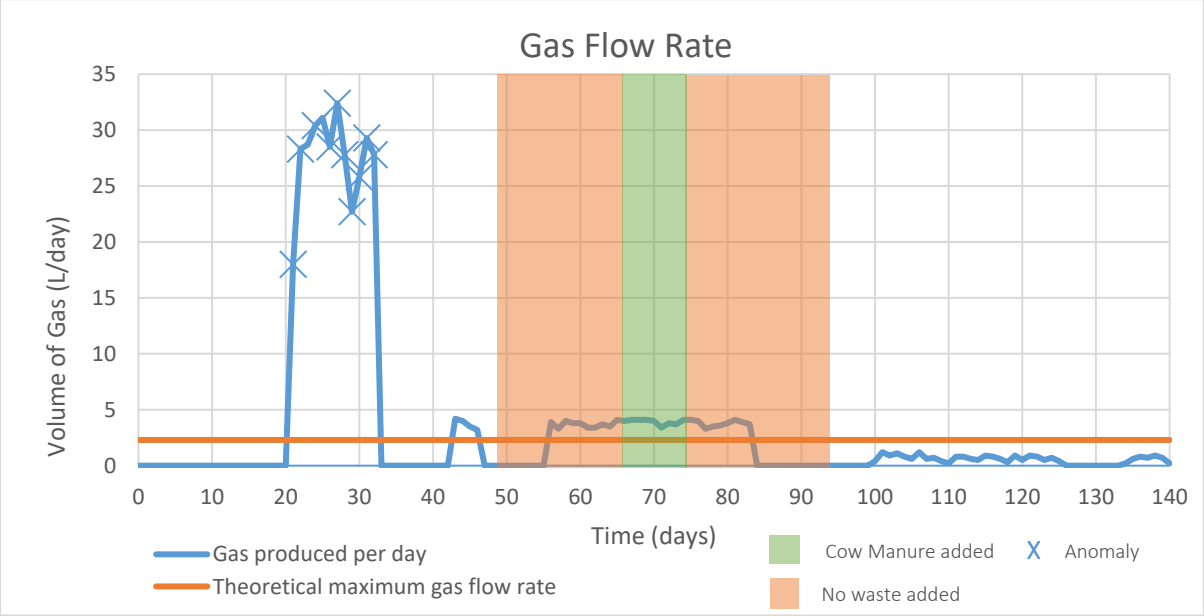

Figure 9-19: EMR Pilot Gas Flow Rate, highlighting the periods when no waste was added or when cow manure was used as a waste stream and inoculant and X indicating anomalies.

Figure 9-20 shows the gas composition throughout the pilot, with minimal change to the methane content that stay <0.1%. The system was not designed to operate with hydrogen, and the measuring instruments were not able to measure if hydrogen continuously. The gas storage is permeable and is not capable of storing hydrogen effectively. The portable biogas analyser used onsite was capable of measure hydrogen up to 5000 ppm. The results indicate that there was minimal hydrogen shown on the device. As limited gas was being produced, the system pressure was not optimal for the analyser, and the results have not been shown.

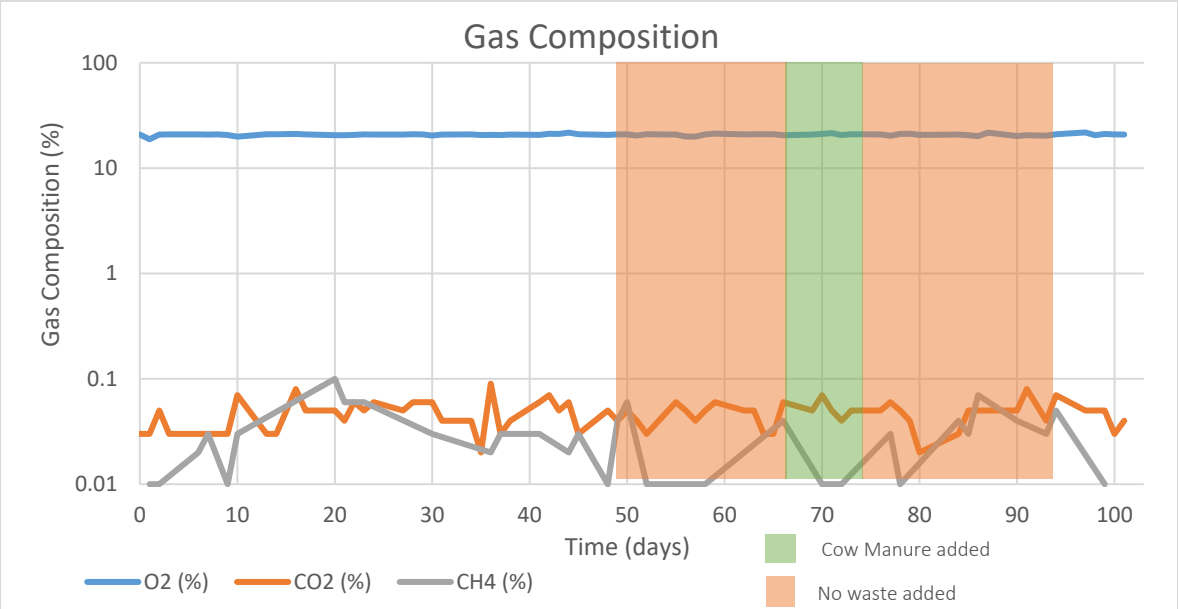

Figure 9-20: EMR Pilot Gas Composition, highlighting the periods when no waste was added or when cow manure was used as a waste stream and inoculant.

Current Density

BES cannot generate current at a higher rate than the biofilm on the electrodes can oxidise the organics within the waste (Logan, 2007). The current density is a measure of the biofilm growth and the ability of the exoelectrogenic bacteria's ability to oxidise the substrate. The current was recorded after the pilot finished to understand how the biofilm would reactor to no wastewater flowing through the system.

Figure 9-21 and Figure 9-22 show the current density for the electrode plates throughout the experiment. The current density fluctuates through the system during the experiment. The graphs show the drop in current density after the pump is turned off from day 49. The current density shows that it fluctuates between 58 and 84 with no significant drop or rise. Between days 84 and 99 the data that was remotely sent was corrupted. From the day 99 the current density shows a significant increase until day 116 when it sharply decreases and then builds until the decommission at 140 days. The increase at day 116 could be due to the substrate going through the acetogenesis stage, forming acetate. Multiple studies have shown that BES effectively oxidise acetate, which could have increased the current density. During the pilot, the current density increases by an average of 14% across all the electrodes. The rise indicates that an exoelectrogenic biofilm did develop on the electrodes, however the current was not converted into methane.

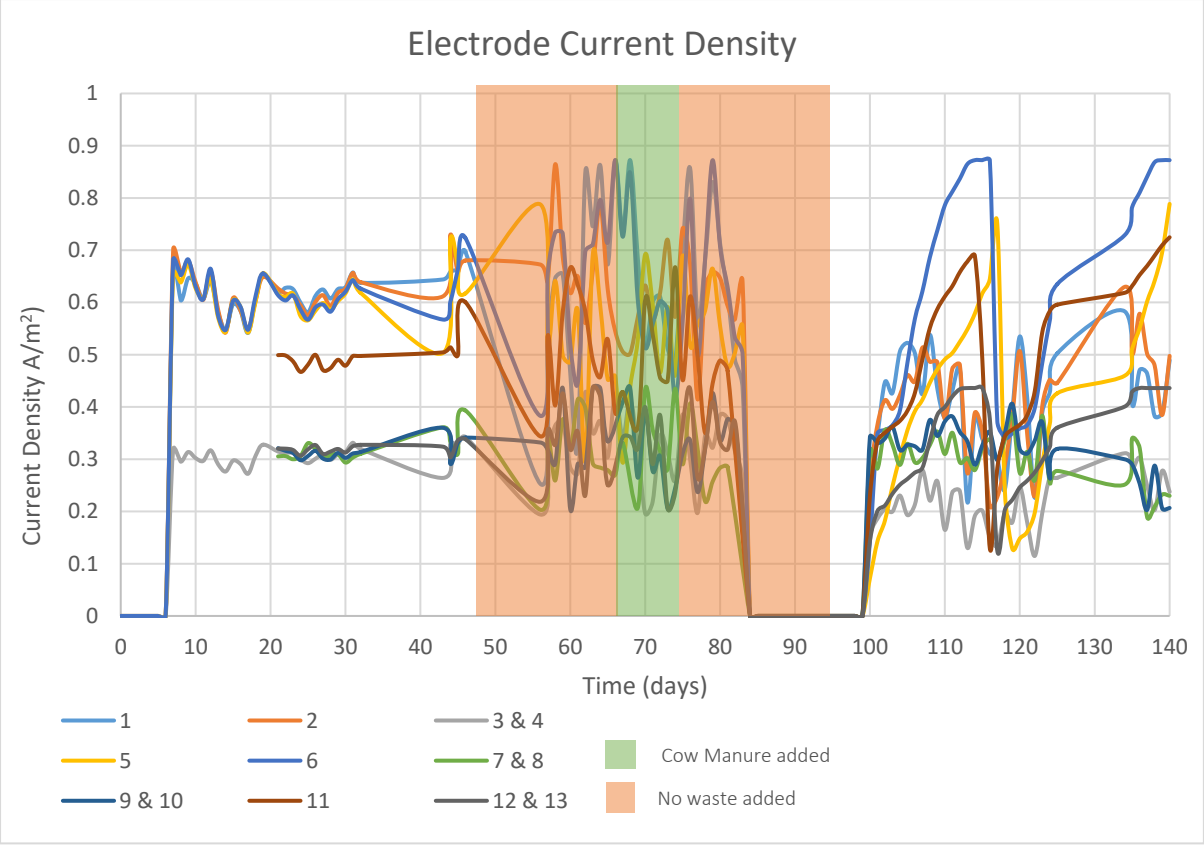

Figure 9-21: Electrode plate current density, highlighting the periods when no waste was added or when cow manure was used as a waste stream and inoculant.

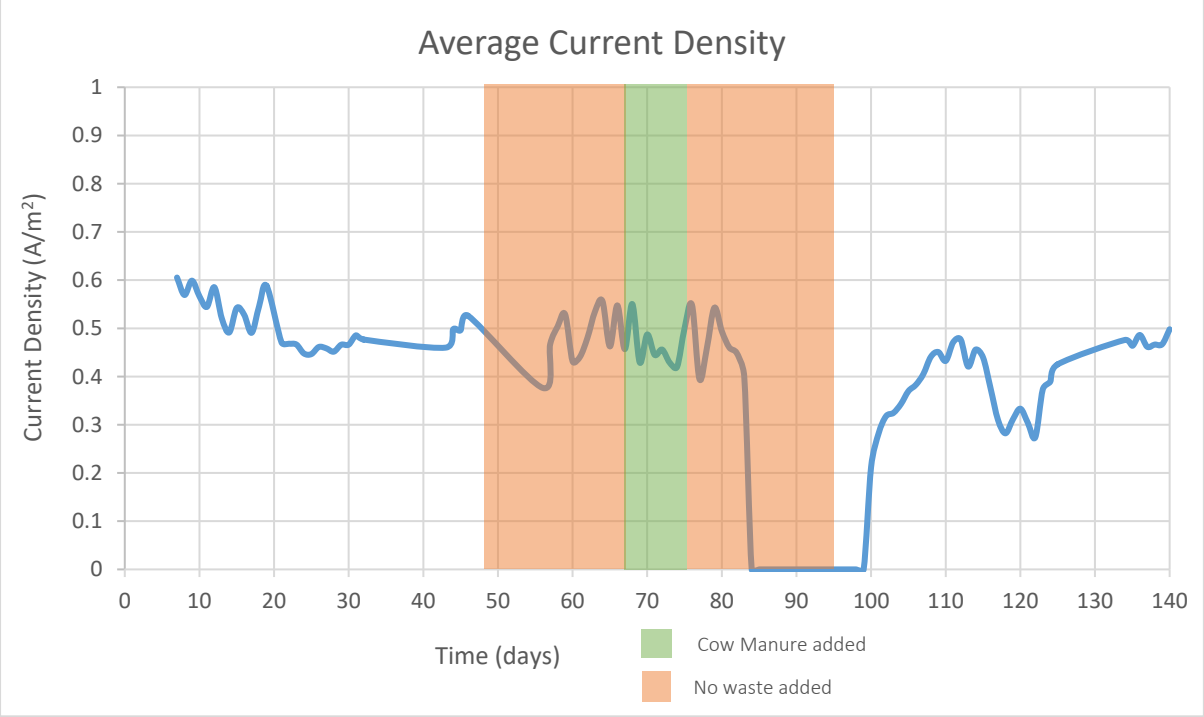

Figure 9-22: EMR Pilot Average Current Densities, highlighting the periods when no waste was added or when cow manure was used as a waste stream and inoculant.

Figure 9-23 shows the average current density of the electrodes and electrode pairs throughout the experiment in relation to the HRT of the wastewater within the tank. Figure 9-24 and Figure 9-25 show a clearer picture of the increase in electrode density, the longer the HRT. As the substrate within the wastewater oxidises, they break down into simpler organic chains such as acetate. Which as previously mentioned, is readily oxidised by exoelectrogens. The increase in current density could support the argument that the reactor was operating in the four stages of AD.

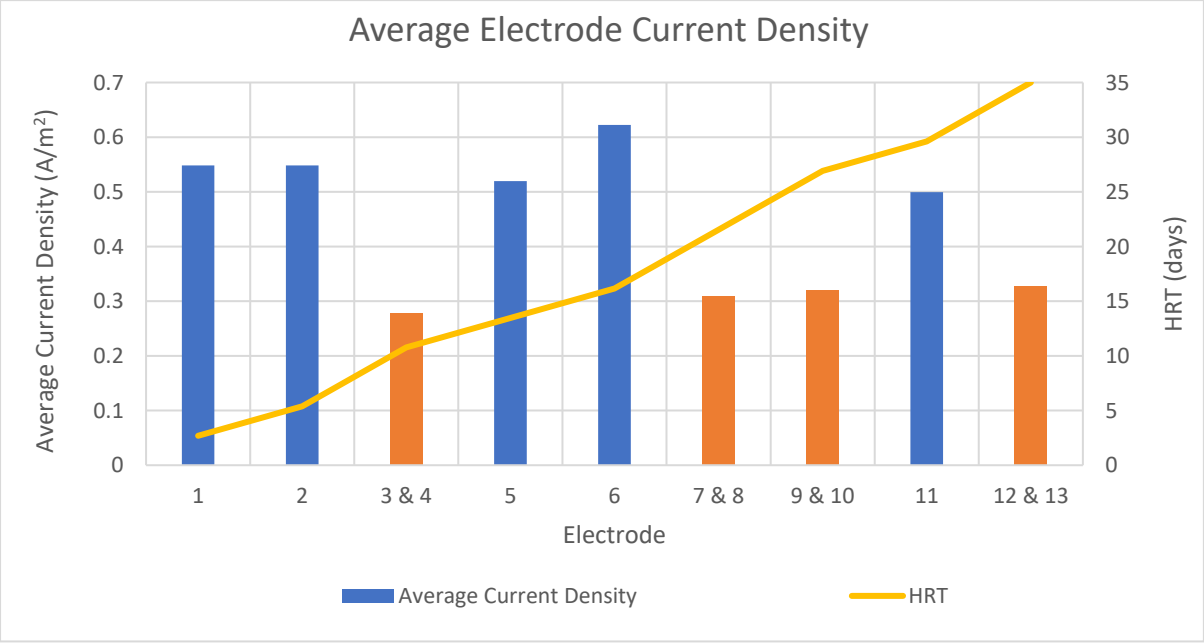

Figure 9-23: EMR Pilot Electrode Current Density in relation to treatment time

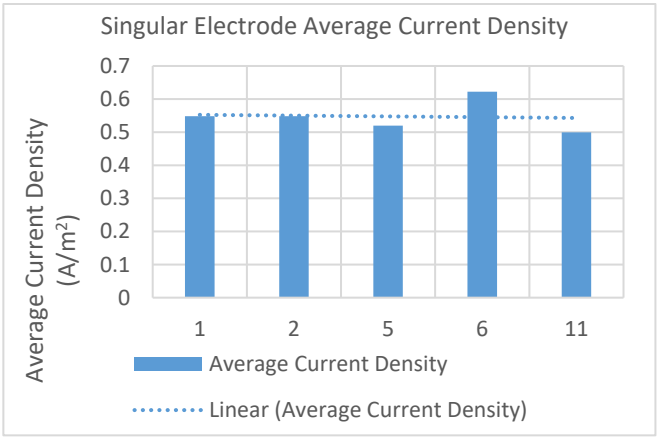

Figure 9-24: Singular Electrode Plate Average Current Density

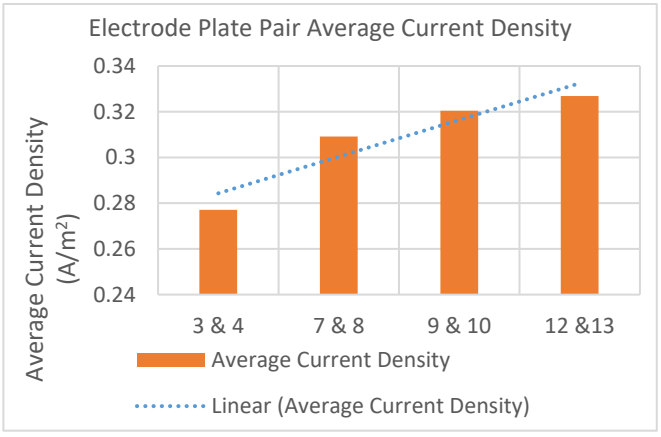

Figure 9-25: Electrode Plate Pair Average Current Density

9.3.4 Focus Group Analysis

A focus group with the WFP staff assessed the usability of the system from an operational perspective. The focus group aims to improve the design of the system to meet the needs of the WFP field staff. The focus group identified some critical insights into the operational performance of the pilot. Key themes continued to appear throughout the focus group around the social acceptability, required behaviour change, operations and maintenance. During the focus group, the participants used a whiteboard to facilitate their idea generation as shown in Figure 9-26.

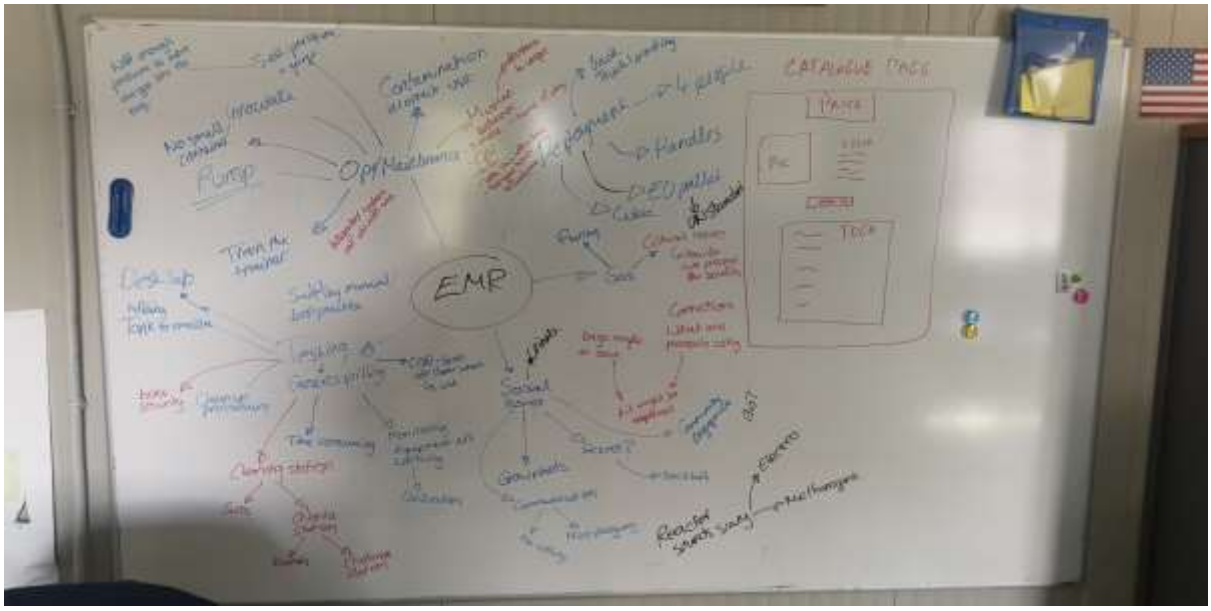

Figure 9-26: Focus group discussion whiteboard notes

1. How did users react to using the ablution unit and EMR pilot?

Due to the location of the ablution unit it was situated outside of the two offices involved in the trial. One set of users also had another toilet that was more conveniently located. During the group discussions it was clear that these users found the pilot to be more of an inconvenience quoting that "it is too far to go", "it is cold outside" and "it smells of faeces". Other comments about the aesthetics of the pilot were mentioned with one user commenting that one of the other users said: "it looks like a coffin". During the discussion, the EMR operating staff commented that they believed the second group of users made excuses not to use the system. They reported that the site did not smell even during maintenance where holding tanks where opened. The main reason they believed the users did not partake readily is due to the ease of their current toilet access that was connected to their office. User participation was one of the main reasons for failure during the pilot. One was related to staff being redeployed, and the other was participants using alternative washroom facilities. The comments could affect future deployment were interventions have to be convenient for the users.

The central theme to appear relates to behaviour change, with users not willing to change their habits. Behaviour change is a theme commonly linked to failed interventions within the humanitarian sector. During the pilot, there was limited space and ability to place the ablution unit in alternative locations that would be suitable for staff. The WFP staff chose the location and participants that would be using the ablution unit for the study. For future tests, further analysis of the site location is required to ensure that users do not have to change their behaviour significantly. The focus group

mentioned that increasing stakeholder engagement at every stage of the pilot would help. The stakeholder engagement will help inform users and help identify the various stakeholder's concerns and expectations early on in the design stage.

The theme around site aesthetics was mentioned to make the experience of using the system appealing to others. Unfortunately, the pilot was installed during the winter, meaning that weather was a significant barrier. Around the theme of aesthetics, users commented that the name "the name Electro-Methanogenic Reactor creates, scary and complex connotations". The comment made an insightful look into understanding how some of the participants saw the pilot as a complex science experiment than a possible immediate intervention. The views based on this meant they did not see the technology as an immediate solution to provide alternative wastewater management within the humanitarian context. Staff highlighted alternative names and marketing should be used to engage users with the project. Future projects should aim to make the site an attractive environment to increase staff and community wellbeing, along with increasing the acceptability of adopting new technologies.

2. How did users react to the concept of using biogas for cooking that has been produced from faecal sludge?

The operational staff were happy and prepared to use the biogas if the pilot had operated as planned. However, during the pilot discussions with other staff around the site, they had mixed reactions. One participant stating that someone commented to them "You're going to cook with the gas from that" indicating that they felt it was unsanitary. There were also concerns about religious views. Some participants commented that this could be in an area with religious and cultural practices and views that may present some issues. The focus group indicated a divide on views between the operational staff and the toilet users. The theme of behaviour change appeared again with operational staff commenting that they had a good understanding of the technology and how it produced biogas. However, other staff were less informed about how the system worked and the environmental and social benefits it could provide within the humanitarian context. Another theme appeared around education. It was mentioned that education is vital to inform the participants of how the system works and operates to create behaviour change.

Various educational practices are applied within the sanitation sector. Community-Led Total Sanitation (CLTS) is one methodology that has been used to scale up open defecation free zones in Kenya and other countries (Chambers, 2009). CLTS uses an approach that gets users to assess and decide if they want to go open defecate free. Using a similar approach around the acceptability of waste to energy could be used within the humanitarian context to ensure user buy-in before implementing the technology.

3. Where would you foresee issues around the installation of EMR technology in the humanitarian context?

Two themes emerged around the installation, the ability of quickly deploying the unit and quick start-up. The system took two weeks to install, the target was a one-week installation. The longer installation is partly due to weather issues making the ground unsuitable for some of the forklift

trucks used to position the ablution unit. The staff mentioned that in humanitarian and emergency settings, there is a need for quick installation and instant operation. Depending on the context, the importance of the two may differ, but in emergencies where the first response unit typically works the issues around inoculation and start-up presented significant concerns.

Other areas around the design of the system were identified about the ease of use and installation without the need of large machinery like forklift trucks, or pallet trucks may not be readily available to position and install the EMR. The group identified areas that would improve the design of the system. Modularity appeared as a theme throughout the discussion, with the concept of small moveable modules that could easily be positioned and scaled up to increase capacity.

The group identified two key design criteria for the next design iteration:

1. Allow four people to easily carry the EMR system so it can be positioned on-site without the need for any heavy machinery.
2. Alter the dimensions to match standard EU pallet sizes for easy distribution.

4. What concerns do you have around the operational aspects of the technology if it is to be successfully deployed in the field?

As previously mentioned in this chapter, multiple issues arose with the pump and the system start-up—both were brought up by the participants. A key theme around ease of use brought up, the pilot had a lot more technical aspects due to the nature of being a research project requiring a lot more control. To scale up the technology, the participants identified that it would need to be robust and can maintain itself with minimal staff input. The inoculation and start-up identified concerns to the staff as they had to re-inoculate with animal waste, which was time-consuming. These kinds of activities may present difficulties in the field. Participants were keen to see if the bacteria could be inserted before it is shipped or have an easy way to add them. The concept of plug and play was mentioned multiple times to simplify the installation and start-up.

When asked around the biogas aspects, the participants were not able to make many comments about the use of biogas/setup as the system failed to produce any. One concern the staff did mention was around the pressure not be sufficient to be moved around different sites. When asked if small transportable bags would be better, there was a mixed reaction and staff had concerns about complexity and the various fittings that would be required. Staff were more enthused by the idea of biogas pumps to transport the gas.

The staff identified four key areas to consider in the system redesign to ease operations and maintenance:

- Remove heaters to operate at ambient temperatures only
- Gravity-fed system to remove pump requirements
- Incorporate inlet works and filter to remove large media, which can be easily accessed to maintain
- Define Inoculation protocol for quick system start-up

9.4 Discussion

Overall, the pilot did not perform as was expected from previous lab research and literature. As previously discussed, multiple reasons could have affected the systems performance and its failure to produce biogas. The main two are ineffective inoculation and a low flow rate. The initial pasteurisation will have affected the performance, and it took a while to obtain another substantial source of waste.

The pilot was in effect, operational only for the first 49 days. After which, various issues with the site and pump caused the system to stop. The second inoculation on the 66th day would have boosted the methanogenic and exoelectrogenic bacteria within the reactor. However, a failure in the pump meant that wastewater could not flow into the reactor until the 94th day. The delay in being able to pump wastewater afterwards would have effectively starved the bacteria for 28 days which would have reduced the bacteria and its ability to form a biofilm on the electrodes. The project was initially planned for 100 days, the aim was to continue if possible due to the stops, but with the low flow rate, it was decided to stop the pilot after 105 days. Other pilots treating urban wastewater had a start-uptime of 50 to 90 days (Baeza et al., 2017; Cotterill et al., 2017b). These fall between the time when the site issues occurred, which would have hindered the performance of the system.

The reactor has a liquid volume of 1.4m3 and was designed to receive 700L of waste a day with a two-day Hydraulic Retention Time (HRT) to achieve an OLR of 2000 mg/L/day. However, the system was receiving 90L of wastewater a day and did not put the EMR under ideal testing scenarios. The design of the baffles was designed to increase mixing, but the limited flow would have meant that they were ineffective, with a flow rate as low as 0.2L/min. The low flow rate and intermittent pumping resulted in limited mixing allowing the solids to settle. As a result, the bacteria and organics would be encountering the electrodes at a significantly reduced rate. The reduced contact will affect the biofilm growth and the mass transfer within the reactor, both of which are vital to the start-up period and the system performance.

The reactor showed oxygen in the gas headspace, due to site safety restrictions we were not able to bring bottles of compressed nitrogen to flush the headspace. As a result, we were unable to ensure the reactor was in anaerobic conditions initially. Due to the small headspace and the predicted flow rate, it was assumed that the waste would degrade producing CO_2 initially. The CO_2 would effectively flush the headspace making the conditions within the reactor anaerobic. It is clear from the results that gases produced by the degradation of the waste were not able to flush the headspace. The presence of oxygen would affect the methanogenic bacteria and also mass transfer. Oxygen is an excellent electron acceptor. If hydrogen was being produced within the system water and not methane would be the likely route until the reactor became anaerobic. In this instance, CO_2 would also be produced as the organics are broken down in aerobic conditions reducing methane production. Going froward adding oxygen-scavenging chemicals into the reactor at the startup can help remove dissolved oxygen such as cysteine hydrochloride.

Another aspect affecting system efficiency was the electrode design. Spade fittings were used for the electrical connections increasing the electrical resistance. Using a bolt fixing would ensure good contact and reduce resistance. Even with the increase in current density, indicating biofilm growth,

the system has an issue with the mass transfer as the pilot failed to produce methane. The conductivity of the anode was also a contributing factor. GAC was chosen due to its low cost and high surface area for the biofilm to grow. However, carbon-based materials do have a relatively low conductivity compared to metals. BES can have mass transfer limitations, the thicker the biofilm on the anode resulting in a reduced current density (Logan, 2007). With a low flow rate, GAC pockets could limit the shearing force of the water to remove the dead or excess biofilm that could lead to reducing current density. It is unlikely a thick biofilm was the result of poor mass transfer during the pilot.

In previous pilot studies, the average biofilm coverage was only 5%, reaching a maximum of 16% in one part of the electrode (Cotterill et al., 2018). The GAC electrodes have severe limitations if no biofilm is present as the conductivity will be low due to the poor electrical contact between the carbon granules. An effective electron acceptor can alleviate lower conductivity and increase mass transfer. A titanium plate was water-jet cut to act as the electron acceptor. However, due to high costs of titanium, the titanium did not go down the full length of the plates and only covered the top 20%. With biofilm covering such a small proportion of the electrodes, it is likely that the bottom 80% of the electrodes were not functioning as intended. The design of the electron acceptor would have severely limited mass transfer and the ability of the exoelectrogenic bacteria to transfer electrons to anode effectively.

In many cases, there may have been more readily available electron acceptors within the wastewater causing the low system performance. A brush electrode design has all the carbon fibres connected to the electron acceptor and as a result has shown some of the most promising pilot results (Cusick et al., 2011a). To further develop GAC electrodes a more effective coverage of the current titanium collector is required but could be costly due to the materials. Stainless steel is an alternative material that has been used in multiple pilots (Carlotta-Jones et al., 2020; Cotterill et al., 2017b) although the corrosion resistance is lower, which may affect life span.

The pilot did not obtain the expected results. The effluent does not meet EU wastewater discharge regulations, and the system failed to generate biogas. The operational issues that appeared during the pilot limited the amount of data that could be collected. With the limited time frame of the pilot, there was not an opportunity to extend the pilot for the amount of time that would provide valuable data. With the results, it is hard to say how effective the technology would be at providing decentralised wastewater treatment in underserved communities. The operational issues did highlight areas that need to be considered for future tests, especially around removing un-necessary components such as heaters and pumps were possible.

9.5 Next Steps

From the pilot, it is clear that the EMR pilot requires further testing and a redesign of the electrodes. For future research, site location will be crucial where a guaranteed and controllable flow of wastewater is available. Exploring quick start-up is also crucial, especially in humanitarian contexts. Bacteria additives could provide an attractive option allowing a selection of crucial bacteria to be added into the reactor. Research is building on the strains of bacteria found on the electrodes (Sun et al., 2015). There are companies such as Drylet that can provide a custom selection of micro-organisms

embedded on a silica powder that can be stored for months at a time and used to inoculate the EMR systems. Building confidence for EMRs in the industry is crucial. One of the main ways to increase confidence is developing more reliable start-up periods, especially to attract users away from alternative technologies.

Another area to explore alongside the technical functionality of the system is the economic viability. Exploring new designs and the associated costs can be used to develop a Technical Economic Analysis (TEA) of EMR. The TEA can compare EMR to alternative solutions that are in use and the areas that need to be considered in future designs to ensure it is economically viable.

10 Chapter 10 - The Economic Assessment of Electro-Methanogenic Reactors for Under-Served Communities

A strategy for decentralised wastewater treatment is presented for schools in under-served communities. The study presents case studies using EMRs to treat wastewater from the school toilets. The scenario is based on blackwater treatment using a case study for a refugee setting.

EMRs, have made significant strides in research communities offering an exciting new way to treat wastewater quickly while also generating energy in the form of biogas. Unfortunately, there has been slow adoption by commercial organisations to move the research from the lab to field. The aim of the chapter is to explore the different parameters that affect the commercial implementation of EMRs.

The goal of the chapter is to compare EMR against AD, pit latrines and septic tanks to explore the economic viability of waste to energy systems compared to low-cost systems.

10.1 Introduction

With an increasing demand for energy globally and historically high levels of atmospheric carbon dioxide (Energy Agency, 2018), there is a need to develop and adopt renewable sources of energy. One of the issues for the slow adoption of renewable energy systems is the economic cost associated with new technologies requiring the first adopters to pay a premium price financially. As adoption increases, prices drop through economies of scale, making systems more affordable. We can see increasing adoption with the highest growth rate for investment in renewables, where bioenergy equated for approximately 10% of the investment (Energy Agency, 2018). A new route to sustainable living is to adopt a circular economy approach reusing resources and reducing waste going to landfills or our environment. One issue of implementing circular models is the difficulty to create value-added products due to waste being mixed, diluted and contaminated with other waste streams, which is common with current centralised infrastructure.

The economic assessment of any technology is crucial to its commercial viability. The chapter aims to assess the economic benefits of implementing EMR. The case study will review the cost to install and operate the system against the current operational costs and the potential savings from, water reuse and energy savings.

The scenario used in the analysis is a proposed live project with Peace Winds Japan to offer decentralised wastewater treatment to schools in Kalobeyei refugee camp. The aim if economically viable is then to scale up the system across the schools that the WFP operate in across Kenya.

10.2 Integrated System Design Methodology

The design for the system has been based around the improved development of a modular EMR system developed in partnership with WASE Limited. The system capacity will be assessed on a scale to assess the minimum functional size of the system to meet economic sustainability.

The study is based on EMR modules with a $1m^3$ liquid volume at an estimated retail price of £1634. The manufacturing costs have been calculated from material costs, manufacturers quotes and estimated assembly costs. A detailed manufacturing cost breakdown is in appendix 13.6, Table 13-5. The total cost breakdown is based on a previous study assessing the economic capabilities of microbial fuel cells by Powell and Hill (2009).

10.2.1 CAPEX

The Capital Expenditure (CAPEX) will include the material costs for manufacturing the facility as well as the installation costs Equation 10-1

Equation 10-1 $$CAPEX = Mc + Ic$$

Material Cost (Mc)

The material costs are based on commercially available products. The electrodes used for the EMR are based on manufacturing quotes with production volumes of 10,000 unit bundles, with each bundle containing enough electrodes for $1m^3$.

- Tanks
- Electrodes
- EMR assembly
- Control
- Pump
- Pre/post-treatment
- Gas Storage
- Gas reuse – biogas cooker, biogas engine, generator or CHP

Installation Cost (I_c)

The installation cost will vary for each case study, and a standard rate of 10% of the Mc is used for the study.

10.2.2 OPEX

The Operating Expenditure (OPEX) is key to the successful implementation of the technology for the case studies. Equation 10-2 shows the OPEX that include costs for labour, maintenance, spare components/materials, utilities. For service-based models, the $OPEX_S$ includes administration and marketing costs, as shown in Equation 10-3.

Equation 10-2: $$OPEX = L + M_C + U_C$$

Equation 10-3: $$OPEX_S = L + M_C + U_C + A_c + MK_C$$

Maintenance

EMR is an emerging technology, and the maintenance (M_c) of the system include labour and parts at 10% of CAPEX cost as shown in Equation 10-4.

Equation 10-4: $$M_C = X\% \; x \; CAPEX$$

Utility Cost

The main utility cost (U_C) is for electricity to power the electrodes (PW_E) as shown in Equation 10-5. Depending on the scenario heating (PW_H) may be required to optimise the system to reach temperatures of 35°C to generate methane. In some cases, energy may be required for pumping the wastewater (PW_P).

Equation 10-5: $$U_C = PW_E + PW_H + PW_P$$

Administrative Costs

Equation 10-6 shows the annual Administrative Costs (A_c). A_c includes salaries, materials, and benefits to all labourers and office running costs. Administrative salaries and wages are assumed to be 20% of maintenance materials. Other office operating costs are estimated at 25% of the plant's overall utility costs. These estimations have been developed and used in previous studies (Powell and Hill, 2009) and Ulrich and Vasudevan (2004).

Equation 10-6: $$A_c = 0.2M_C + 0.25\, U_c$$

Marketing

Marketing is required to launch new products and must be included in the economic assessment to make it suitable for commercial success. In particular, for new decentralised sanitation, the marketing will be crucial to develop behaviour change activities and workshops. The marketing costs have been set at 10% of the operating costs (Ulrich and Vasudevan, 2004), as shown in Equation 10-7.

Equation 10-7: $$MK_C = 0.1\ (M_C + U_C + A_c)$$

10.2.3 Levelised Cost of Energy

The Levelised Cost of Energy (LCOE) is the minimum cost of the energy for the project to break even and allows comparison across different energy generation systems. Equation 10-8 shows the standard LCOE where 8760 stands for the number of hours in a year, and PR is the rated biogas power output. The CRF is the capital recovery factor which is calculated in Equation 10-9. The capacity factor is a percentage of the maximum energy output. The capacity factor for AD has been steadily increasing with the maturity of the technology, and commercial systems are reaching above 86% (Grant et al., 2016). For the analysis, the capacity factor for EMR has been set at 86%. In Equation 10-9 *i* stands for the interest rate and *n* is the number of years of the loan.

Equation 10-8: $$LCOE\ \left(\frac{£}{kWh}\right) = \frac{((CAPEX\ x\ CRF)+Fixed\ Costs)\left(\frac{£}{yr}\right)+Variable\ O\&M\left(\frac{£}{yr}\right)}{PR\ (kW)\ 8760\ x\frac{h}{yr}\ Capacity\ factor\ (\%)} + \frac{Fuel\ Costs\ \left(\frac{£}{yr}\right)}{Energy\ output\left(\frac{kWh}{yr}\right)}$$

Equation 10-9: $$Capital\ Recovery\ Factor\ (CRF) = \frac{i(1+i)^n}{((1+i)^n)-1}$$

10.2.4 Levelised Cost of Wastewater Treatment

The Levelised Cost of Wastewater Treatment (LCOWT) is an adaptation of the LCOE. LCOWT is not typically used when assessing water infrastructure. In this study, the LCOWT is calculated to compare the cost per m^3 of wastewater treated with local charges faced by the organisations. Equation 10-10 shows the standard LCOWT where 8760 stands for the number of hours in a year, and the CRF is the capital recovery factor which is calculated in Equation 10-9. The capacity factor is a percentage of the maximum treated wastewater output. VR is the volume flow rate input of the wastewater to be treated in m^3/h

Equation 10-10: $$LCOWT\left(\frac{£}{m3}\right) = \frac{((CAPEX\ x\ CRF)+Fixed\ Costs)\left(\frac{£}{yr}\right) + Variable\ O\&M\ \left(\frac{£}{yr}\right)}{VR\ \left(\frac{m3}{h}\right)8760\left(\frac{h}{yr}\right)\ x\ Capacity\ factor\ (\%)} + \frac{Fuel\ Costs\ \left(\frac{£}{yr}\right)}{Wastewater\ volume\ treated\ \left(\frac{m3}{yr}\right)}$$

Monte Carlo Analysis

The Monte Carlo analysis takes the LCOE and simulates uncertainty and risk into the costs to create a quantitative analysis (Gu et al., 2018; Heck et al., 2016). A Monte Carlo analysis uses a simulation model that runs LCOE multiple times with each variable being recalculated using a set standard deviation and randomisation. Due to the performance of EMR varying substantially within literature due to the number of factors that affect the energy output, a Monte Carlo analysis will provide a more realistic expectation of the LCOE.

The Monte Carlo simulation is shown in Equation 10-11 where *j* represents the number of simulations. The analysis was run on Excel using 1000 simulation trials. Each input factor into the LCOE was calculated using the *NORM.INV* function in Excel and using the *RAND()* Excel function to calculate the probability randomly, as shown in Equation 10-12. The input stands for the different input values required to calculate the LCOE such as CAPEX and Energy Output.

Equation 10-11:
$$Monte\ Carlo = \begin{cases} LCOE_1 \\ LCOE_2 \\ \dots\dots \\ LCOE_j \end{cases}$$

Equation 10-12:
$$= NORM.INV(RAND(), input, (input * Standard\ Deviation)$$

10.3 Case Study 1 – School Wastewater Treatment

Figure 10-1: Kalobeyei Settlement, (UNHCR, 2020)

The economic assessment is focusing on installing and building decentralised Wastewater Treatment (WWT) facilities in the Kalobeyei refugee settlement, as shown in Figure 10-1. Kalobeyei settlement is in northern Kenya, which is currently hosting 183,000 individuals even though the designed capacity is 70,000 (UNHCR, 2020).

Humanitarian organisations are building households with accompanying communal latrines within Kalobeyei refugee settlement. Within the site, all new structures must be temporary under the current agreement with the local government.

Pit latrines are currently built with a 3-5m^3 pit depending on the soil type and is sometimes lined to store waste. As it stands, the site has no waste treatment facilities and the latrines are either covered, or the waste is left or dumped untreated in the surrounding environment. There is a growing need to implement wastewater treatment solutions within the camps, combined with the need for clean cooking fuels. Electro-Methanogenesis offers an attractive opportunity to build small, efficient WWT facilities that generate biogas for use as alternative cooking fuels—reducing the need for biomass which causes rapid deforestation (FAO and UNHCR, 2018) and indoor air pollution(de la Sota et al., 2018).

52 schools within the settlement currently use pit latrine blocks shown in Figure 10-2. Once the latrines are full they are often abandoned, and new facilities are built. The current method has low a CAPEX; however, the costs rapidly increase, and space becomes limited. The case study is assessing the economic feasibility of different wastewater treatment sites at Kalobeyei settlement. The study will be based on one of the secondary schools served by Peace Winds Japan which has 847 students (626 male and 271 female students).

Figure 10-2: School Pit Latrines

For the analysis, four scenarios will be assessed as listed below.

1. Pit Latrines
2. Septic Tank
3. AD treatment system
4. EMR treatment system

Scenario 1 will be business, as usual, using pit latrines with a new block built once the previous one is full. Scenario 2 is using a septic tank on site that will be emptied once full using an exhauster truck.

Scenario 3 is using an AD-WWTP to treat the wastewater onsite and produce biogas for the kitchen using the Umande Trust system in Kenya as a comparative (Gebrezgabher et al., 2016). Scenario 4 is using an EMR-WWTP to treat the wastewater onsite and produce biogas for the kitchen.

10.3.1 Assumptions

The EMR technology is being designed for simple maintenance using a modular system, so parts can easily be replaced, reducing downtime to 2-3 days. Although as the system relies on biofilms the start-up time, maybe 7-14 days. We expect to mean time between failures (MTBF) to be over 6 months in a pilot stage, and during scale-up, we are expecting MTBF to be 12-24 months. For the case of this research, we are estimating that the MTBF will be 18 months, and the cost of maintenance will be 10% of the CAPEX costs per year.

Flow Rate

The predicted COD of faecal sludge waste is approximately 49,000mg/L (Heinss et al., 1999). The analysis has taken the approximation and reduced it for scenario 2-4 where a 1L pour-flush toilet will be required. For the study, we assumed all the students would use the toilet facilities for 7 hours of the day. A healthy person averages six or seven times every 24 hours, and it is considered normal to urinate between 4-10 times a day (Kjellström et al., 1978). It is assumed that during the school hours, the students will use the toilet three times and estimated to use a total of 1L of water for handwashing over the times they visit the toilet.

Adolescent children produce between 0.5-1ml/kg/hr (Hazinski, 1985), the average weight for males in Kenya is 64.9kg and females is 61.7kg (World Data, 2018). Females aged 13-16 ranged in weight of 45.8 – 53.5kg and males aged 13-16 weigh 45.3 – 60.8kg. Based on these numbers, it is assumed that the average weight of the students is 49.65 for females and 53.05 males, that will produce on average 0.75ml/kg/hr. The average adult produces between 250-350g of faeces a day (Feachem et al., 1983; Rose et al., 2015). Based on the average mass adolescents weigh between 18.07 - 18.3% less than adults, and it is assumed they will produce 18.2% fewer faeces (205-286g/day). An average of the two values gives a daily production of 246g/day. The school is open for 7hrs/day so the faecal waste produced is reduced by 3.5 due to the reduced time at the school. The total flow rate is shown in Table 10-1. For scenarios one it is assumed that there are no flushing facilities and will use a long drop, for scenario 2-4 the system will likely require a pour-flush system to ensure flow. The school is open five days a week, with three terms of 13 weeks per term making the system operational for 195 days.

The total faecal sludge the site will produce is an estimated 0.29 tonnes a day. From the theoretical biogas analysis in Chapter 4, 1 tonne will produce 9.97 m^3 of methane. The theoretical amount of biogas from the waste is 2.89 m^3 of methane a day. If all the sludge was converted into biomethane then the site could generate a net energy production of 29.64kWh that could save the school £520.18 per year based on the current cost of bottled LPG at £0.09 (Total, 2020).

Table 10-1. Calculation of predicted school wastewater flow rate

	Waste Production Volume Per Day (L)				
	Urine	Faeces	Hand washing	Low Flush (1L)	Total
*Student (*7hrs*)*					
Female	0.26	0.07	1.00		
Male	0.28				
Total					
271 Female	70.46				
626 Male	175.28				
Total (847 Students)	245.74	59.29	847		1152.03
Total (inc. pour flush)	245.74	59.29	847	2541	3693.03

The system is assumed to meet EU discharge standards. The current lab research was only able to reduce COD to 42.37± 2.05% for the spent grain batch tests and 51.7% after the fourth reactor in the series tests. The WFP pilot system had 46.9% decrease in COD without the system starting up effectively. The OLR of the lab test showed that the series system could reduce COD by 1150.25 mg/L/day. At the lab COD removal rates, the system would require 74 hours. It is assumed that the system will have increased efficiency with system modifications resulting in a higher mass transfer coefficient and increased COD removal. The EMR modules are built into a $1m^3$ IBC tanks containing nine electrode modules with eight electrode pairs within each module as shown below in Figure 10-3 and Figure 10-4. Each IBC will act as a baffle increasing the solid retention time. With the flow mixing improvements from the electrode module design and the baffling of the IBCs the system is assumed to have a 35% increase in COD removal, allowing a 48-hour retention time.

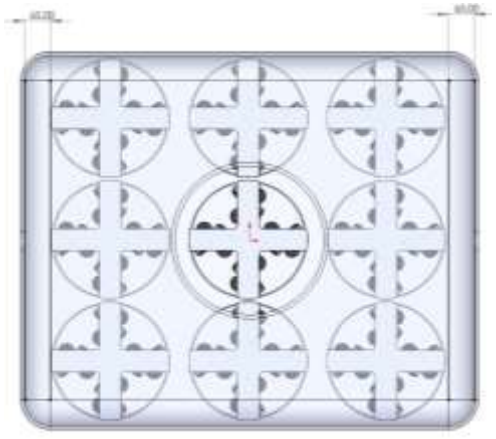

Figure 10-3: IBC EMR Top View Design

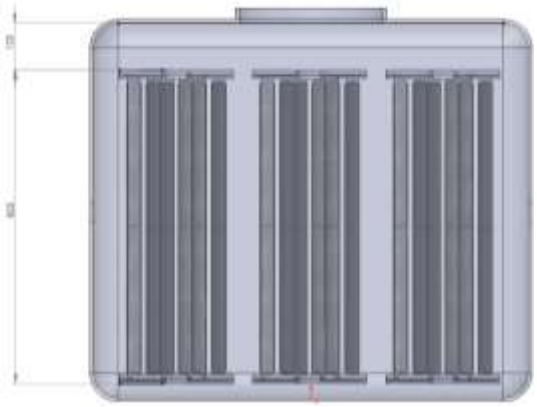

Figure 10-4: IBC EMR Side View Design

10.3.2 System Design

Below Figure 10-5 to Figure 10-8 show the different system flow diagrams for the four different scenarios.

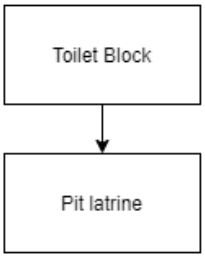

Figure 10-5: Scenario 1 - Pit Latrine

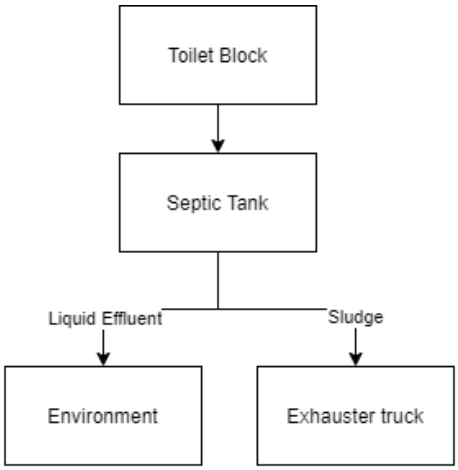

Figure 10-6: Scenario 2 - Septic Tank

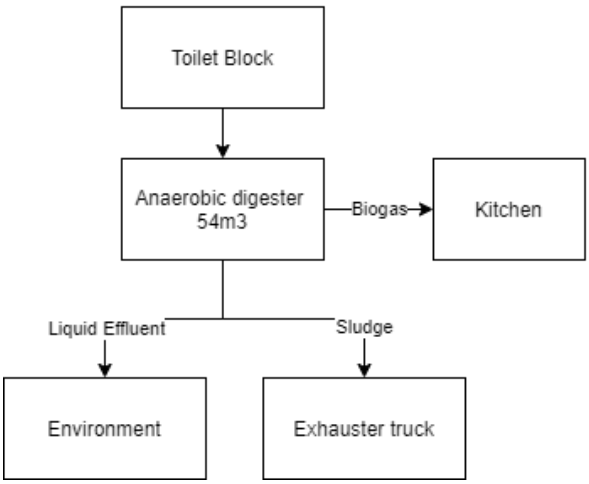

Figure 10-7: Scenario 3 – AD

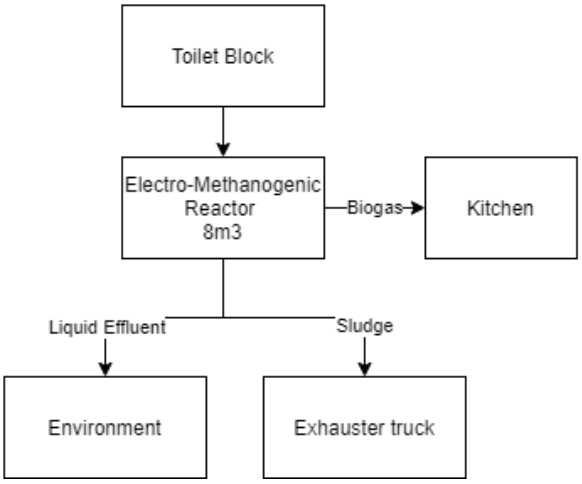

Figure 10-8:Scenario 4 - EMR

10.3.2.1.1 Reactor Size

Based on the predicted flow rate including a pour-flush system, the number of EMR units needed is:

Equation 10-13: $$EMR\ Reactor\ Volume\ (m^3) = Volume\ Flowrate\ (m^3/day) \times HRT(day)$$

$$\text{EMR Reactor Volume} = 3693 \times 2 = 7374 = 8\ x\ 1\text{m}^3\ \ units$$

The EMR reactor is unlikely to reduce the organic content and pathogens to be inline the discharge standards. It is assumed that a secondary low-cost sand filtration system will further reduce solids, helminth eggs and pathogens from the system.

System Outputs

The EMR system will generate biogas with methane being the energy carrier. The methane characteristics and assumptions used to calculate the energy production are shown in Table 10-2. The estimated amount of methane has been calculated using the COD reduction in Equation 10-14. It is assumed that the EMR will have a 100% substrate efficiency after the batch experimental analysis of the spent grains reached near 100% efficiency at 99.2± 15.3%. The COD has been estimated at 3971 mg/L after the sludge is diluted to an estimated 8.1% concentration from hand washing and flushing facilities. The estimate is in line with the WFP pilot which had an average COD of 2276 mg/L but instead of a pour-flush there was a cistern flush toilet.

Table 10-2. The assumptions used to calculate the methane production from the EMR

Assumptions and constants for methane production			Reference
AD methane production at 35deg [5]	0.35	$m^3_{Methane}/kg_{COD}$	(Filer et al., 2019)
Predicted EMR methane production at 35deg (EMR_{CH4})	0.35	m^3/kg_{COD}	
Methane density @ Standard Temperature & Pressure (STP)	0.717	kg/m^3	[2]
Methane Net Calorific Value (NCV)	13.9	kWh/kg	[3]
(COD_{OUT}) Aimed effluent COD	125	mg/l	
Gross Energy Density of Methane	55.7	MJ/kg	[4]
Gross Energy per volume	39.94	MJ/m^3	
Gross Power per volume	11.09	kWh/m^3	

Equation 10-14: $$Theoretical\ CH_4\ Production = (COD_{in} - COD_{out}) \left(\frac{kgCOD}{L}\right) \times\ Volume\ Flow \left(\frac{L}{d}\right) \times$$

$$EMR_{CH4}\left(\frac{m^3}{kgCOD}\right) \times CH_4\ Density\ at\ STP \left(\frac{kg}{m^3}\right) \times\ NVC\ of\ CH_4\left(\frac{kWh}{kg}\right)$$

$$CH_4\ Produced = \left((3971 - 125) \times 10^{-6}\right) \times 3687 \times 0.35 \times 0.717 \times 13.9$$

$$CH_4\ Produced\ = 44.6\ kWh/d$$

The estimated methane production from COD removal indicates that the system would generate a 55% increase in energy production compared to the theoretical maximum from the lab analysis. The compositional makeup of faecal sludge will vary depending on multiple factors, and the values can only be used as estimates. As a conservative estimate, the average of the two energy production values has been used at a 30% reduction to give an estimated 26 kWh/day.

Table 10-3. A table to summarise the calculated values

Number of students	Volumetric Flowrate, Q, (m3/d)	HRT (days)	Number of EMR units needed	Methane produced (kWh/d)
847	3.9	2	8	21.70

10.3.3 Cost Breakdown

CAPEX

Table 10-4 shows the CAPEX costs for the four scenarios in case study 1 and Table 10-5 to Table 10-8 show the CAPEX breakdown for the four scenarios.

Table 10-4: Case Study 1 CAPEX costs

	Scenario 1 – Pit Latrines	Scenario 2 – Septic Tank	Scenario 3 -AD	Scenario 4 - EMR
CAPEX	£8870	£10,886	£31,758	£15,534

Table 10-5: Case Study 1 - Scenario 1 Pit Latrine Costs

The cost of pit latrines per person for households is £35.64 per year which takes into account of building new latrines and desludging (International Rescue Committee, 2016). It is assumed that the costs for pit latrines will be used 50% less as the school is only open during the day and will reduce the costs accordingly. The attention rate at the school is also taken into account, as shown in Equation 10-15.

Equation 10-15:

$$Usage\ (\%) = \frac{Cost\ per\ person\ per\ year\ (\frac{£35.64}{yr})}{daily\ usage\ cost\ (£)\ (\frac{1}{2})} * \frac{days\ school\ is\ open\ (195)(d)}{Days\ in\ a\ year\ (365)(\frac{d}{yr})} = 26.71\%$$

Scenario 1 : Pit latrines				
Equipment	Size (PP)	Cost PP/day (£)	Inflation	Cost (£) - 2020
Primary Treatment				
Pit Latrine - 1year				
Source 1 (Household £/pp/year)	847	£35.64		
Adapted to school use @26.71%	847	£9.52	1.1%	£8870

Table 10-6: Case Study 1 - Scenario 2 Septic Tank Costs

The CAPEX for the septic tank system is calculated from the average of three sources as shown in the Appendix Table 13-6: Kenya Refugee Settlement Sanitation and Wastewater Treatment Costs from field research conducted in February 2020.

Scenario 2: Septic Tank - Exhausted

Equipment	Size (PP)	No. Required	Unit Cost	Total Cost (£) - 2020
Primary Treatment	-			
Source 1	1000	1	£3895	£3895
Source 2	1000	1	£1798	£1798
Source 3	125	3	£8988	£26965
Average Total	-			£10886

Table 10-7: Case Study 1 - Scenario 3 Anaerobic Digestion

The cost of the anaerobic digestion system is taken from TEA report about a sanitation block installed by the Umande Trust in Nairobi, Kenya (Gebrezgabher et al., 2016). The system was installed in 2004, and inflation was added to the system where £1 in 2004 equates to £1.55 today (UK Inflation Calculator, 2020). The Umande trust system is 54m^3 and designed for 1000 people, whilst the school has 847 students. To bring the costs in line with the reduced capacity, only 84.7% cost is used.

Scenario 3: Anaerobic Digestor			
Equipment	Cost (£) @84.7%	Cost (£) – 2020 @1.55 % inflation	Source
Primary Treatment			
None	-	-	
Secondary			
Anaerobic Digester	-	-	
Sub Total	£14,437	£23,927	(Gebrezgabher et al., 2016)
Installation	Included		
Total			

The costs for the EMR system is taken from the current manufacturing costs received from manufacturers. The costs have assumed a two day assembly time that will be in Kenya. The daily rate of a labourer including overheads is £40 and was provided by a local organisation (SNV).

Table 10-8: Case Study 1 - Scenario 4 EMR System

Scenario 4: Electro-Methanogenic Reactor		
Equipment	No. Units	Cost (£)
Secondary Treatment		
EMR Cost of Goods sold (COGs) per (1m^3)		
Electrodes		£630
Tank		£100
Fittings		£200
Assembly		£80
Mark-up @50%		£1,130
Shipping		£50
Import Duty @16%		£115
Total		£1,634
EMR (m^3)	8	£13,072
Remote monitoring & Controller	8	£3,008
Filtration System	1	£2000
Biogas Handling		
Biogas Bag	1	£500
Biogas H_2S and water filter	1	£50
Energy Supply		
4 kWh Solar System	*1*	*(£2,295)*
**cost shown for secondary analysis*		
Sub Total		£18,630 *(£20,925)*
Installation	10%	£1,863 *(£2,093)*
Total	-	£20,493 *(£23,018)*

OPEX

Depending on the scenario treatment technology presented all the case studies have possible routes to generate income or OPEX savings.

Water, Wastewater treatment and Desludging Costs

Desludging will be required in some scenarios and costs £393.24 for 30m^3 shown in the appendix, Table 13-6. As a precaution it is assumed that the EMR system will require desludging every 10 years which has been shown as a yearly cost. To also assess the implementation in schools within cities sewage costs will also be assessed. The sewage charges in Kenya vary across the state. The analysis is using Nairobi Water's sewage charges, which are 75% of the water costs, as shown in Table 10-9. For Scenarios 2,3 and 4 it is assumed that the system will require a flush and water charges have been included in the OPEX.

Table 10-9: Nairobi Water & Sewerage tariffs

	KSH			*GBP*			*Source*
Water	<6m^3	7-60m^3	>60	<6m^3	7-60m3	>60	(Water Services Regulatory Board, 2014)
Domestic/ Residential		53	64	0.00	0.39	0.47	
Commercial/ industrial		53	64	0.00	0.39	0.47	
	<600 m^3	601-1200m^3	>1200	<600 m^3	601-1200 m^3	>1200	
Public Schools	48	55	60	0.36	0.41	0.44	
Sewerage @75% of water	75%						

Bio solids / Fertiliser

All the scenarios can utilise the nutrients to grow crops, however the benefit from the use of the fertiliser does not present an economic value to the school. Using treated faecal waste adds complexity around social acceptability and would require behaviour change. It is assumed that the school will not benefit from the use of fertilisers at this current time.

Energy

Currently, the schools get given free firewood by a local NGO so no savings would be made. However, it is a temporary solution, and for this analysis, it is assumed that the school will be paying for firewood. Per person, firewood costs approximately £0.02 per day and charcoal is £0.05 per person per day shown in appendix 13.7, Table 13-8. The school cooks one meal per day, and it is estimated that per day students will require 50% of the daily amount costing £0.01 per student per day.

Below Table 10-10 shows the OPEX breakdown for the four scenarios.

Table 10-10: Case Study 1 - Scenario OPEX

	S1: Pit Latrine	*S2: Septic Tank*	*S3: AD*	*S4: EMR*
Maintenance Costs				
10%	£8,870	£0	£1,551	£2,049
Electricity Cost				
EMR @ 0.25 kWh/day/m³	£0	£0	£0	£56
Heating	£0	£0	£0	£0
Pumping	£0	£0	£0	£0
Thermal Costs				
Cooking	£2,017	£2,017	£2,017	£2,017
Heating	£0	£0	£0	£0
Water Costs	110	503	503	503
Sewage Costs	£0	£0	£0	£0
Desludging Costs		£1,573	£310	£39
Sub Total	£10,997	£4,093	£4,381	£4,665
Savings				
Biogas	£0	£0	£314	£460
Electricity	£0	£0	£0	£0
Fertilser	£0	£0	£0	£0
Water	£0	£0	£0	£252
Sub Total	£0	£0	£314	£712
OPEX per year	£10,997	£4,093	£4,067	£3,952
Administrative Costs				£1,063
Marketing				£501.62
OPEX (Service Based Model)				£5,517.7

Total System Costs

Below Table 10-11 shows the total lifetime cost for the four different scenarios and includes the additional lifetime cost, including the admin and marketing costs for a business to implement EMR as a service-based model. The service model costs also include the additional fuel the school requires for cooking.

Table 10-11: Lifetime cost analysis

	Scenario 1 Pit Latrine	*Scenario 2 Septic Tank*	*Scenario 3 AD*	*Scenario 4 EMR*
CAPEX	£ 8,870	£ 10,886	£ 23,927	£ 20,493
OPEX	£ 10,997	£ 4,093	£ 4,067	£ 3,952
Project Lifespan (yrs)	20	20	20	20
Total OPEX	£ 219,930	£ 81,859	£ 81,347	£ 79,050
Life time Cost	£ 228,800	£ 92,744	£ 105,274	£ 99,543
Cost Difference compared to EMR	£ 129,258	-£ 6,798	£ 5,732	£ -
Lifetime cost inc. Admin & Marketing				£ 110,355

10.4 Case Study 1 - Results and Discussion

Below Figure 10-9 compares the costs of the four scenarios. Scenario 1 with new pit latrines being built every year are the cheapest option for the first couple of years, but then the cost of septic tanks and periodic desludging become the cheapest option. Both the EMR and AD become cheaper than the pit latrines in year 4. The EMR provides a Return on Investment (ROI) of £5,557 in year 4 and a total saving of £118,261 over the 20 years lifespan. Over the 20 years, the septic tank is the most economical option followed by EMR, which is £6,798 more expensive than desludging a septic tank (Scenario 2). The septic tank provide a ROI in just 2 years with a lifetime saving of £125,059.

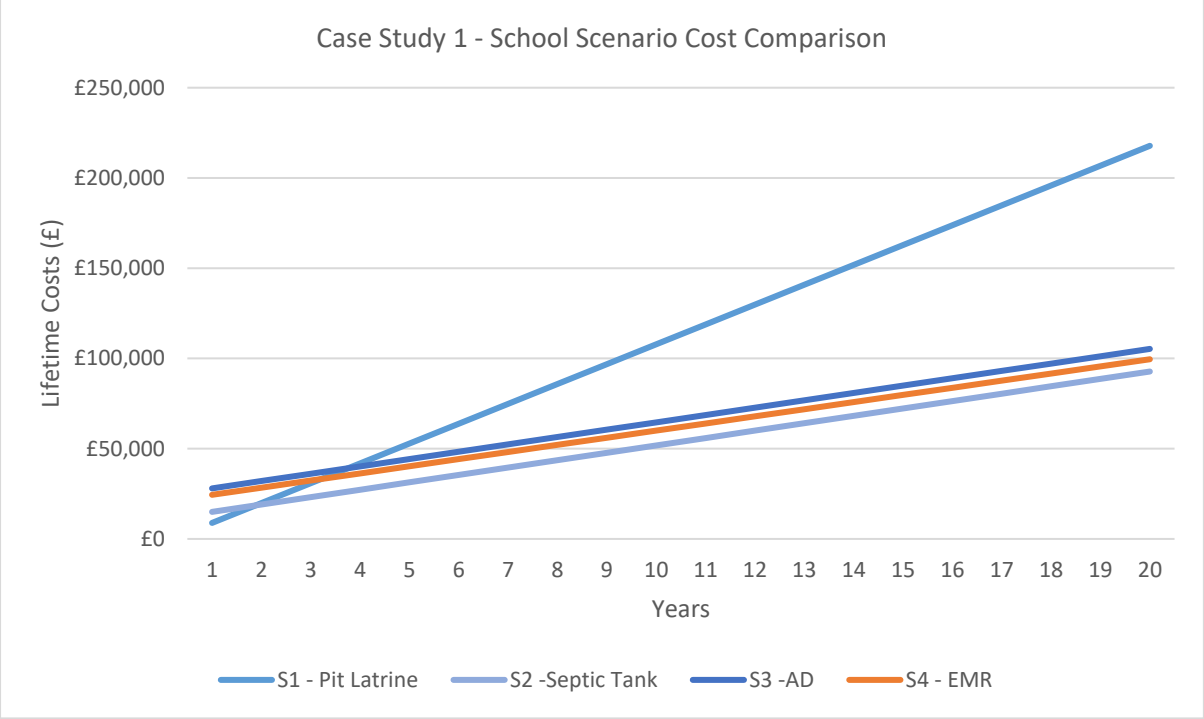

Figure 10-9: Case Study 1 School Cost Comparison

The high CAPEX of new infrastructure is often a barrier in Sub-Sharan Africa, with financers favouring solutions with low CAPEX and higher OPEX (United Nations Environment Program, 2012). One option to implement EMR could be through a service-based model where the business or operator covers the initial CAPEX of the systems. The lifetime cost of the system will increase due to the admin and marketing costs that the operating business will incur. The yearly cost of implementing the EMR system as a solution is £5,518/year, which is lower than the cost of installing pit latrines which have a yearly outlay of £8,870. The costs are still significantly higher than the OPEX of septic tanks which also have a low CAPEX of £10,886.

The higher costs of EMR currently do not provide financial savings compared to AD, which also produces energy. To assess the necessary improvements that are required of EMR to compete with other technologies, four alternative EMR scenarios are assessed in Table 10-12.

Alternative Scenarios:

1. Maintenance costs reduced to 5% instead of 10% to be in line with the maintenance costs of the AD system.
2. Removing fuel costs for the electricity and including a solar and battery storage system into the CAPEX.
3. Increasing methane production by 20%
4. All three of the performance increases into the system.

Table 10-12: EMR OPEX Improvement Analysis

	EMR Baseline	*S4 @5% Maintenance*	*S4 @Solar*	*S4 @+20% CH4*	*S4 @All*
CAPEX	£ 20,493	*£ 20,493*	*£ 23,018*	*£ 20,493*	*£ 23,018*
OPEX	£ 3,952	*£ 3,201*	*£ 3,896*	*£ 3,860*	*£ 3,053*
Project Lifespan	20	*20*	*20*	*20*	*20*
Total OPEX	£ 79,050	*£ 64,022*	*£ 77,930*	*£ 77,208*	*£ 61,060*
Life time Cost	£ 99,543	*£ 84,515*	*£ 100,947*	*£ 97,701*	*£ 84,078*

Below Figure 10-10 compares the four alternative scenarios that assess the improvements to the EMR system. Installing 4 kWh solar spanel unit to power the EMR increases initial CAPEX by £2525 and reduces the fuel costs by £56 per year. The lifetime cost is higher than the standard EMR system, however, the solar panels will generate excess energy that could create additional savings. When the school is shut, the solar could also be sold or distributed to nearby communities to provide free

lighting. These additional cost savings have not been calculated for this scenario. The solar system also gives security over future energy price fluctuations and will reduce the carbon impact. Standard EMR is the second most expensive system. A 50% reduction in the maintenance costs has a significant impact as the system becoming cheaper than using a septic tank after nine years. Increasing the biogas production by a further 20% means that the system is still more expensive than a septic tank. The analysis is assuming wood is the alternative fuel. Wood is the cheapest fuel source, and if other cooking fuels such as charcoal or LPG are used, the savings will increase further. The EMR with all the three updates is the cheapest option over 20 years; however, the ROI compared to a septic tank is longer.

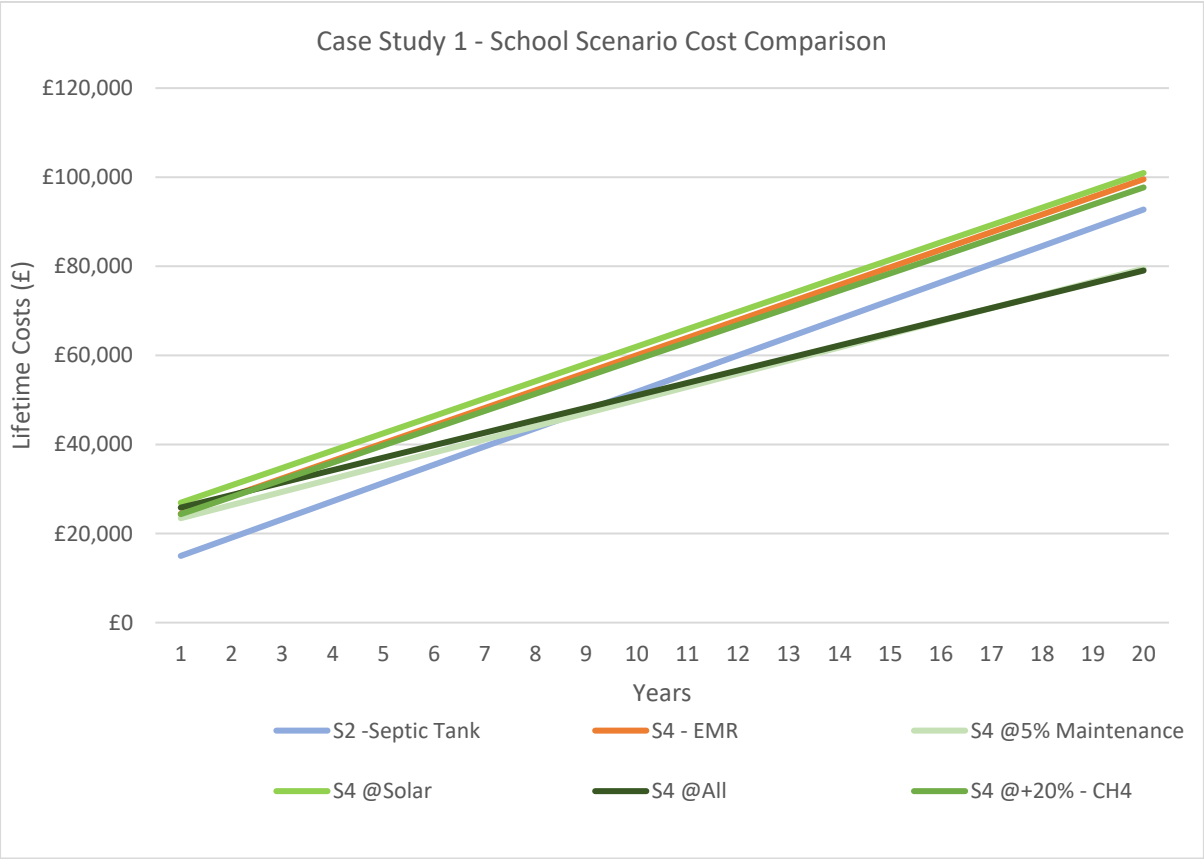

Figure 10-10: : Case Study 1 EMR Improvement Metric Analysis

10.4.1 Levelised Costs of Outputs

Below shows the Levelised Cost of Energy (LCOE) and Levelised Cost of Wastewater Treatment (LCOWT) of the EMR system. The levelised cost allows the cost of the wastewater treatment and energy to be compared to alternative technologies and solutions. The assessment compares to solutions available within the settlement as well as within cities to understand how the technology can add value during scaleup.

Table 10-13: Case Study 1 EMR Levelised Cost of Outputs

Assumptions – S4 EMR		*Standard Deviation*
Initial Investment Cost (£)	20,493	10%
Operations and Maintenance Costs (£/yr)	2,145	10%
O&M Growth Rate (%)	5.00%	5%
Annual Fuel Costs (£/yr)	56	10%
Annual Energy Output (kWh/yr)	5,070	15%
Annual water Output (m3/yr)	1,346	15%
Project Lifespan (years)	20	10%
Discount Rate (%)	7.00%	
Net Present Value (NPV) of Total Costs (£)	52,015	
NPV of Total Outputs – Biogas (kWh/yr)	53,708	
NPV of Total Outputs – Water treated (m^3/yr)	14,256	
Levelised Cost of Energy (LCOE)	£0.97/kWh	
Levelised Costs of Wastewater Treatment (LCOWT)	£3.65/m3	

The LCOE is high at £0.97/kWh, being an estimated 10.8 times more expensive than the cost of widely available LPG. LPG is one of the higher cost fuels with schools opting for cheaper but higher polluting fuels such as firewood and charcoal.

The LCOWT is significantly higher than the cost of sewage charges that are currently at £0.31 per m^3 of wastewater. The EMR system 12 times more expensive than if the costs if the school was connected to a sewer. However, in Nairobi 40% of the city has a sewage connection (World Bank Group, 2020b), making the low-cost wastewater treatment available to a small portion of the city. Most residents will need to pay for exhauster trucks which range from £6.24 to as high as £19.97 (Appendix 13.7, Table 13-7) which is between 1.7 to 5.5 times higher than installing a decentralised EMR wastewater treatment system which also has the added benefit of biogas production.

10.4.2 Monte Carlo Analysis

The LCOE and LCOWT are based on multiple assumptions. A Monte Carlo analysis can be used to provide a more realistic analysis of the costs as it incorporates risk and uncertainty (Heck et al., 2016). Table 10-14 shows the range of values for the simulation, which indicates that both the minimum LCOE and LCOWT are higher than LPG and sewer connection, respectively. Figure 10-11 and Figure 10-12 shows the spread of values across the Monte Carlo Analysis.

Table 10-14: Monte Carlo Analysis - Histogram Range

Histogram Calculations		
	LCOE	LCOWT
Average	£0.95/kWh	£3.13/m^3
Min	£0.60/kWh	£1.99/ m^3
Max	£1.97/kWh	£5.83/ m^3

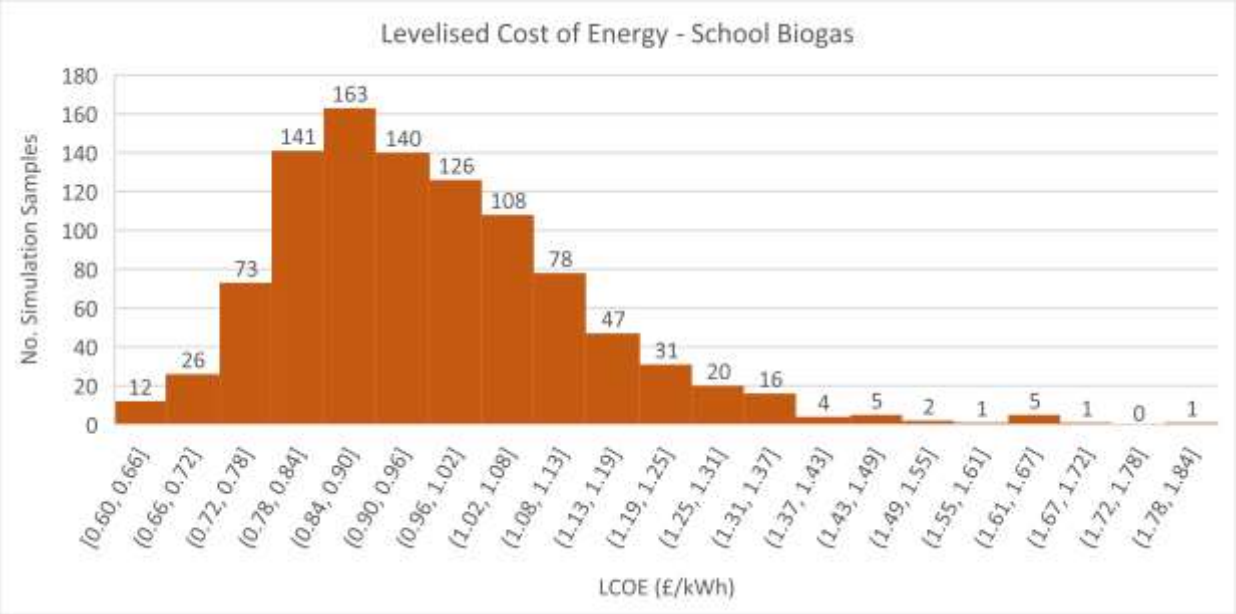

Figure 10-11: Levelised Cost of Energy - School Sanitation

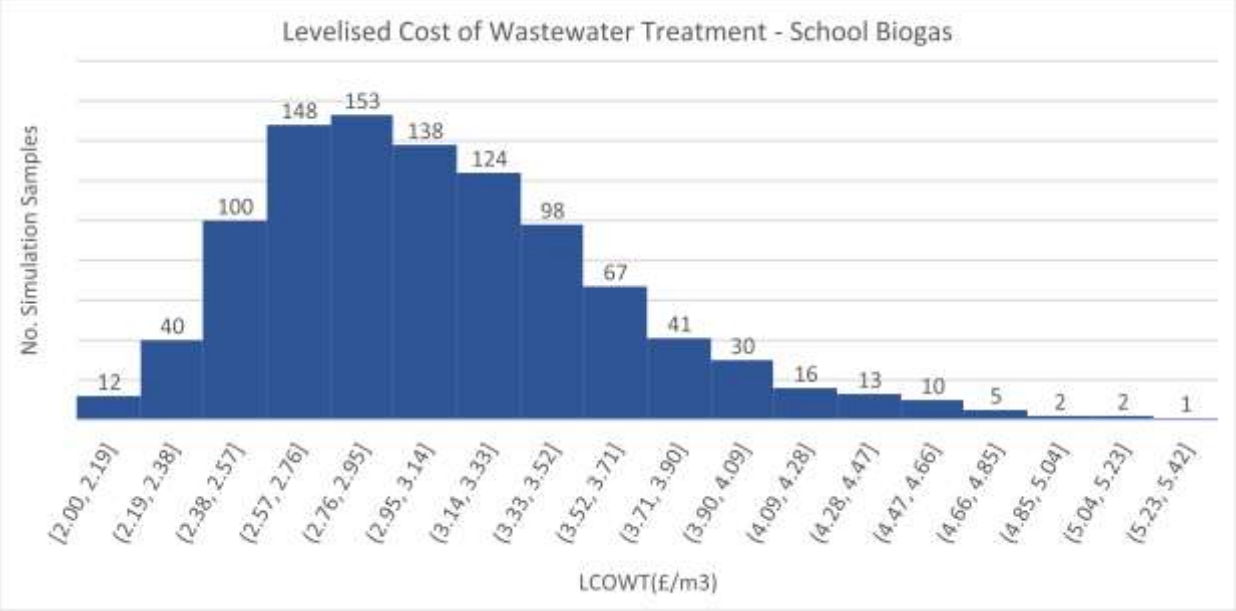

Figure 10-12: Levelised Cost of Wastewater Treatment - School Sanitation

The Monte Carlo analysis shows an average decrease in the LCOE by £0.02/kWh. The LCOE is still expensive compared to alternative sustainable energy solutions implemented in Kenya, as shown in Table 10-15: Levelised Cost of Energy for Sustainable energy production technologies in Kenya (Pueyo, 2016). The LCOWT decreased £0.52/m^3 but is still ten times higher than the cost of disposal to sewers.

Table 10-15: Levelised Cost of Energy for Sustainable energy production technologies in Kenya (Pueyo, 2016)

	Wind	*Solar*	*Hydro*	*Geothermal*	***EMR***
LCOE £/kWh	0.08	0.11	0.08	0.05	**(0.85)**

Currently, the Monte Carlo analysis is assessing the LCOE and LCOWT as separate entities, that does not represent a true cost. The untrue representation also gives an unfair comparison to alternative technologies where they are purely focused on energy production or wastewater treatment and not a blend of the two. If the focus is purely on energy production or wastewater treatment costs, then the calculations need to be adjusted. A second simulation was run for a combined LCOE and LCOWT. For the LCOE the O&M included the savings from the desludging of the septic tank compared to the desludging costs of the EMR and water the additional water savings, reducing the OPEX by £1808/year. For the LCOWT the OPEX included the biogas and water savings reducing the OPEX by £656/year.

Table 10-16 compares the two different methods to calculate the LCOE and LCOWT. The LCOE showed an average 55% reduction in costs, and the LCOWT had a 25% average cost reduction. The analysis indicated that it could reduce the risk of max costs users may face with the max LCOE reducing by 64% and the LCOWT by 55%. Surprisingly, the minimum cost of LCOWT increases by 3%. Figure 10-13 depicts the LCOE's and Figure 10-14 shows the LCOWT's histogram for the Monte Carlo analysis. With the adjusted method, the average LCOE is still £0.42/kWh nearly four times more than solar. The average LCOWT is £2.35/m^3 lower than the cost for desludging but is £2.04 higher than the sewage costs.

Table 10-16: Monte Carlo LCOE and LCOWT simulation comparison

	Histogram Calculations					
	LCOE *Standard*	LCOE *(- O&M Savings)*	LCOE % Difference	LCOWT *Standard*	LCOWT *(- O&M Savings)*	LCOWT % Difference
Average	£0.95/kWh	£0.42/kWh	56%	*£3.13/m^3*	£2.35/*m^3*	25%
Min	£0.60/kWh	£0.27/kWh	55%	*£1.99/m^3*	£2.09/*m^3*	-5%
Max	£1.97/kWh	£0.75/kWh	62%	*5.83/m^3*	£2.63/*m^3*	55%

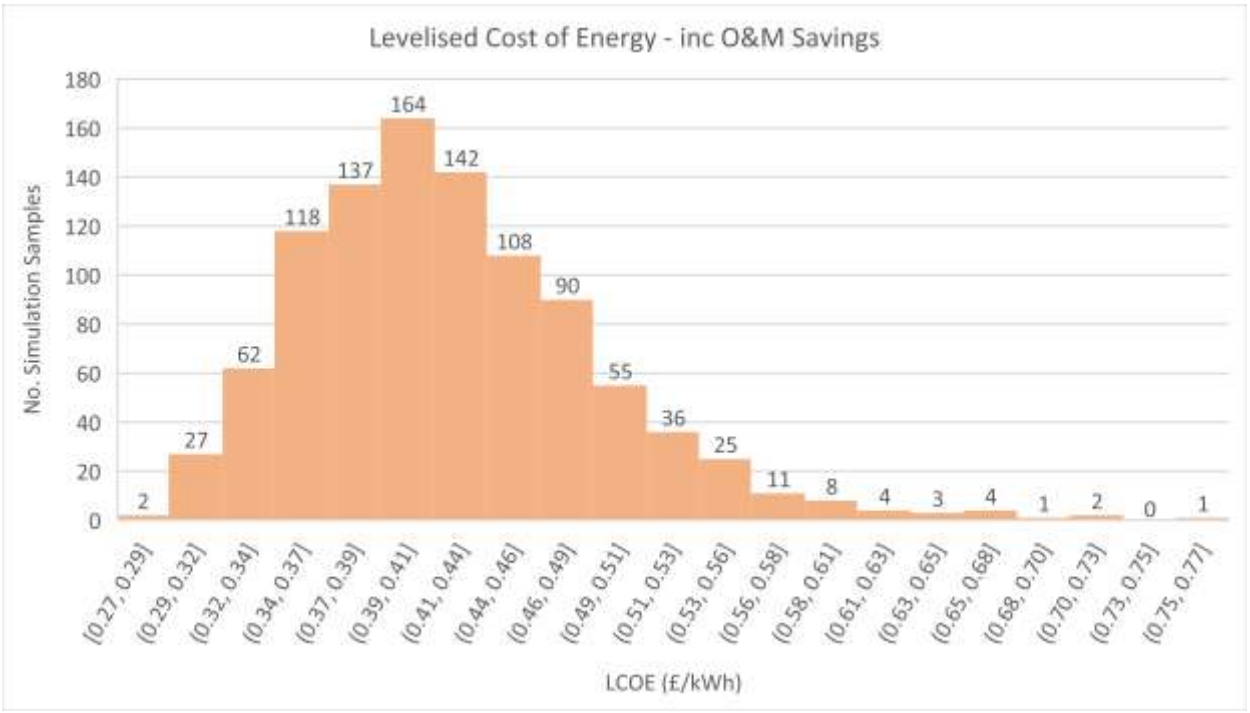

Figure 10-13: Levelised Cost of Energy with O&M minus desludging cost

Figure 10-14: Levelised Cost of Wastewater Treatment with O&M minus biogas value

10.4.3 Discount Factor Analysis

The discount factor or the loan interest to cover the CAPEX of the system can play a significant part in the economic viability of energy and waste management infrastructure. Typically developing communities are require a greater need for debt due to the growing demand in infrastructure as cities develop. Debt lenders see investments in developing communities as a higher risk compared to established markets. The combination of higher demand and risk means that developing communities are typically faced with higher-interest loans that can be up to 7.6% higher (Nelson and Shrimali, 2014). Another Monte Carlo Analysis was carried out to assess the impact of higher interest fees on economic viability. Typical interest rates for renewable energy projects are around 6% in established markets but can rise towards 14% in developing markets (Nelson and Shrimali, 2014). The 8% increase in interest rates in the simulation gave an average 44% increase in LCOE and a 42% increase in LCOWT, as shown in Table 10-17 and Table 10-18.

Table 10-17: Levelised Cost of Energy at variable discount factors

LCOE at Different Discount Factors

Discount Factor	6%	8%	10%	12%	14%	Increase
Average	£0.39/kWh	£0.46/kWh	£0.54/kWh	£0.61/kWh	£0.70/kWh	44%
Min	£0.25/kWh	£0.32/kWh	£0.36/kWh	£0.41/kWh	£0.47/kWh	46%
Max	£0.70/kWh	£0.87/kWh	£0.94/kWh	£1.22/kWh	£1.30/kWh	46%

Table 10-18: Levelised Cost of Wastewater Treatment at variable discount factors

LCOWT at Different Discount Factors

Discount Factor	6%	8%	10%	12%	14%	Increase
Average	£3.80/m^3	£4.14/m^3	£4.48/m^3	£4.91/m^3	£5.39/m^3	42%
Min	£2.56/m^3	£2.71/m^3	£2.72/m^3	£3.50/m^3	£3.52/m^3	37%
Max	£6.13/m^3	£6.54/m^3	£6.88/m^3	£7.56/m^3	£8.95/m^3	46%

10.5 Conclusion

The current analysis shows the technical and economic aspects of implementing EMR into schools in Kenya. The case study based the analysis on a situation within Kalyoubei refugee camp in Kenya, but also assessed costs relative to Nairobi. The analysis highlighted that the current costs of EMR systems are cheaper than building pit latrines but are significantly higher compared to septic tanks and desludging. However, from field research, often the desludging companies do not pay gate fees to dispose of the waste and often illegally dump the waste in the environment. The removal of gate fees significantly reduces the OPEX of the septic tank solution.

To make the EMR the most cost-efficient option, the system will need to reduce the cost of maintenance, increase energy production and also remove the electricity costs by integrating

renewables. Reducing the maintenance to 5% is unlikely for a new technology, but with maturity, a reduction is possible. Both wind and solar have seen significant reductions in operation and maintenance costs (O&M). Between 2005 and 2017 the O&M of wind has reduced 25% and solar has reduced 85%.

The analysis of the LCOE and LCOWT are good indicators to assess the cost of energy and wastewater treatment compared to alternative solutions. However, they only take into account their specific benefit of energy production or wastewater treatment and do not provide an analysis of the overall benefits. The revised LCOE and LCOWT give a comparative cost analysis of EMR to other renewables and treatment technologies. Although, the cost does not take into account multiple other benefits that EMR can provide from the wastewater treatment and environmental benefits such as the carbon savings and reduced deforestation.

If the focus of EMR is solely energy generation, the analysis shows that in its current state of technology is not economically viable when the feedstock is sewage sludge alone. The reason for this is the low energy value of sewage sludge where 1g of COD equates to just 0.35ml of CH_4 (Filer et al., 2019). To increase energy production, waste streams with higher energy values will be required or an increase in the EMR organic loading rate.

10.6 Further research

The study indicates that EMR in the school scenario can have lower LCOWT than exhausters but not sewage connections. To become competitive with sewage connections, higher flow rates will be required. If the school did connect to a sewer, then they would require higher flush volumes between 8-12L to ensure that the waste can easily flow to the sewers. The increase in water costs and sewage costs would increase the OPEX costs, and further research could compare sewage connections to EMR.

The TEA is the first step in understanding some of the future areas of research focus. The next stage of research required is to validate the improvement assumptions to understand if they are feasible. To validate the assumptions, a second pilot system with the optimised EMR design should be deployed where a guaranteed waste stream can be obtained.

11 Chapter 11 - Conclusions

The overall aim of the research was to explore the scaleup potential of EMRs for decentralised wastewater treatment, focusing on circular solutions to recover energy from waste. The research explored underserved communities alongside industrial applications for treating food and beverage manufacturing waste. Both sectors could benefit from EMRs, however there are still necessary technical improvements and cost reduction measures needed to make the systems economically viable.

The analysis of different feedstock highlighted that both brewery wastewater and organic waste, alongside faecal sludge, could be used to generate methane. The industrial wastewater streams contain more organics with a higher methane potential than faecal sludge. However, the scale at which faecal sludge is produced and the issues it causes, make it a valuable waste stream to explore. The social and environmental impact could provide significant strides within the sanitation sector. Treating the estimated 1.6 billion tonnes of faecal sludge could generate 161,283 GWh/year of sustainable biogas.

BES offers a new approach to treat wastewater. The research found that for underserved communities, EMR is likely to be the best route to market. However, it does not mean that research into either MECs or MFCs should stop, as they both have advantages over EMRs. With EMR technology being a likely stepping stone as the other systems improve. Assessing the combination of EMRs with MFCs as a tertiary treatment could help to lower the COD and meet EU discharge standards of 125mg/L; which was not achieved in the research.

1. Lab Research Conclusions

The lab research presented difficulties in designing and building low-cost bioreactors. These were required to carry out multiple tests which analysed how to optimise the system's electrode design, applied voltage and feedstock; ultimately calculating the system's overall efficiency and biomethane potential. During the research, various reactor designs where trialled and tested. The research has not been included within the main body of this thesis but is shown in appendix 13.8. One of the main challenges is addressing gas leaks, and mixing and operating continuous flow systems in low-cost reactor designs.

The first experiment of synthetic brewery wastewater showed low substrate efficiency, with the COD reduction not translating into methane production. As a result, the total energy efficiency was under 1%. The experiment highlighted low pH throughout the reactors, indicating that the VS loading rate was too high. The high VS indicates that a high concentration of VFA built up within the reactors inhibiting the methanogenic microorganisms. However, effluent analysis will provide a clearer picture. The EMR systems showed that they were able to increase the pH. Although, with the set HRT in the continuous system, the EMRs were unable to complete the breakdown of VFA to acetate and then into methane.

The reactors were unable to operate as a continuous system which would not have caused a VS overloading in the EMRs. A small continuous flow would provide a buffer period allowing the substrate to be converted into VFA and then broken down into acetate; increasing the pH. However, with the continuous batch system, the reactors were overloaded with VS, resulting in limited methane production.

During the off-gassing stage after the flow was stopped, the biogas production increased with methane concentrations reaching 70% in one of the reactors. There are a couple of reasons that may have affected the system performance; the inoculation period and the VS loading rate. The seven-day inoculation period may have been too short for a significant biofilm to establish itself on the anode. Particularly with the high flow rate which may have caused a bacterial washout. Developing an effective inoculation protocol can help start up systems and reduce bacterial washout.

The hydrolysis phase of AD lowers the pH as VFA are produced. However, the process is more efficient in a neutral pH range around 7 (Speece, 2007). Optimising the flow to manage the VS loading that is in line with the system's ability to breakdown the VFA can help neutralise the pH and improve system performance.

The batch test systems showed a stark difference in the performance when comparing the AD systems to EMR. The addition of the electrodes and applied voltage improved the performance of the system to increase the pH. The enhancement is likely due to the breakdown of the VFAs through exo-electrogenic bacteria that are more active at lower pH levels than methanogenic microorganisms. In contrast, the AD system with no electrodes was unable to regulate the pH effectively.

Both systems were inoculated with a mixture of effluent from EMRs and AD systems. The inoculum was not analysed to assess the microbial communities present. The AD and EMR inoculum were the same, and exoelectrogens would have likely been present as the EMR effluent from previous experiments was used. Therefore, with the AD system not regulating the pH, it indicates that the exoelectrogens have a lower impact when they are floating within the bulk liquid compared to when they form a fixed bed biofilm on the anode with an applied voltage.

The performance on the second system also showed that the substrate efficiency was high, reaching 99.2 ± 15.3%. The results indicate that the system is effectively converting the COD removed into methane. The system was only able to achieve a 44% reduction in COD; improvements are likely to be possible through improved reactor design when scaling up the system. The electrical efficiency was 100.4 ± 20.3%, indicating that the system can generate more energy than is consumed. The efficiency of the lab-scale system is less critical than full-scale systems as the setup was not designed for efficiency. When scaling up systems, assessing heat loss, heat recovery, and power supply efficiency, are essential parameters to reduce parasitic electrical losses.

The third experiment did not perform in the same way as the second system. The 55% increase in VS meant that the pH dropped below 4, inhibiting the microbes within the system. The EMR exhibited that they could recover from the low pH although the recovery time is longer than 30 days. One of the promising abilities of EMR is the ability to accelerate methane production and as a result, reduce the HRT (Park et al., 2018). The research shows that EMR does accelerate the process as well as

stabilise the reactions but is still affected by overloading the reactor with VS. Defining and optimising the OLR to work within the parameters of EMR can help determine the operational limits of EMR to support the scaleup. The system electrical efficiency reached 155.7% showing that the addition of the electrodes can have a significant improvement with minimal energy input. However, the disparity between the electrode energy consumption between the two batch experiments indicates that further research into this area is required.

All three lab experiments exhibited similar patterns found in AD systems with a drop in pH when organics are fed into the reactors and produce VFAs. Over time, the VFAs are broken down into simpler compounds, increasing the pH between 6-7. The series experiment failed to produce any substantial volume or quality of biogas whilst the system was continually being fed wastewater. During the lower pH levels, the system was generating biogas but the composition was not analysed due to the limitation of the Dynament Sensors.

The EMR systems may have been generating hydrogen at the cathode as hydrogen ions are formed within the substrate. At low pH, the methanogenic bacteria would be less able to convert the hydrogen to methane. If hydrogen production is occurring, it could increase the system's energy recovery. One of the issues that membrane MECs face is hydrogen scavenging from hydrogenotrophic methane production. When hydrogen is the desired route, another area of research could explore keeping the pH below 6 to reduce methane scavenging; if the results show that hydrogen is being produced.

One of the challenges that the series and batch experiments exhibited, was the inability to reduce the COD to levels that would not require post-treatment. Further research into reactor design and optimisation should be explored to further reduce COD. If EMR is to be used for faecal sludge management, tertiary treatment should be explored to ensure pathogens are removed from the wastewater. The tertiary treatment could range from pasteurisation/heating, electrolytic disinfection, chlorine dosing, microfiltration, and Ultra Violate light. The most suitable application is dependent on multiple factors including effluent, location, economic, environmental and social, to name a few.

The lab research presented information about electrical and system efficiency. Due to the small size and minimal reactor design and optimisation, the efficiency is not likely to be the same as a full-scale system. Further analysis into the full power demands of a large-scale system including, pumping, heating, mixing and powering the electrodes is required. The analysis could then be used to produce an estimated power requirement per litre of a substrate treated. The kWh/L can then be compared with the energy production of lab-scale systems to give a more realistic representation of system efficiency.

Lab research limitations

The project presented a few limitations with the scope of the research undertaken.

1. The limitations included the inability to calculate the cathode current density. The reason the current density could not be calculated was because it was too costly to access a potentiostat that could be used for multiple tests.

2. The biogas composition could only analyse the methane (0-100%), hydrocarbon (0-4%) and carbon dioxide (0-100%). Due to budget and laboratory limitations, the research was not able to get a full compositional analysis of the biogas, which showed a large percentage of the unknown gas. Understanding a full biogas composition will show what other gases are present and provide a better understanding of the reactions that are taking place within the EMR. It will also provide a better analysis of the bioenergy production if combustible gases such as hydrogen are present.
3. During the research, it was speculated that the VFAs built up within the AD and EMR system. Obtaining more knowledge of the VFAs within the reactors will help provide a better understanding of the different microbial species in AD and EMR, and their ability to breakdown VFAs. Understanding EMR's ability to effectively stop VFAs building up into high concentrations can help optimise scaling up systems to reduce pH drops that inhibit microbial activity.
4. The research was unable to identify the different microorganisms present within the reactors and on the biofilms. Future research should aim to incorporate 16S DNA sequencing, which other research has shown can provide a better understanding of electrode performance (San-Martín et al., 2019). For the series experiments, it would have provided insights into the different microorganisms within each phase of the reactor. Understanding the difference in composition could provide new knowledge into understanding which exo-electrogenic microorganisms are active at different pH ranges. A greater understanding of the microbial community can identify species that are more effective at the different phases of breaking down complex organic compounds to simple molecules. Batch tests would provide a better understanding of how the addition of bioanodes and biocathodes can change the composition of microorganisms that are present within an AD system. It will also provide insights into how the composition changes when different waste streams are added to understand which microorganisms prefer different waste streams. A greater understanding of the microbial composition could inform the ideal microbial species for inoculation. A specifically designed inoculum would help restart systems, which presented an issue during the pilot testing.
5. Biofilm coverage over the electrode is another vital area of research that was not explored. For smaller lab systems, the coverage is less important than large pilot systems, but it would still provide insights into electrode design and manufacture. Scanning Electron Micrographs (SEM) would have shown how the biofilm is adhering to both the bioanode and biocathode. The research planned to incorporate images after the batch and series tests; however, due to a nationwide Covid-19 lockdown, access to the facilities was not possible. Since then, the electrodes have been reused to continue the research into other waste streams.
6. Another aspect of the research failed to analyse the nutrient content of the wastewater. MECs and EMRs are not effective at removing nitrogen, phosphorous and potassium compared to other technologies and are likely to require post-treatment (Cotterill et al., 2017b). The research was unable to understand to what extent further post-treatment is required and this is an area that should be explored in future research.
7. Another limitation of the research, due to health and safety precautions, was the inability to do small lab scale tests on the effectiveness of faecal sludge. Due to the nature of the waste containing pathogens, the research laboratory at the time did not have the facilities to collect and safely treat the wastewater.

8. Further exploration into the effect of applied voltage would provide additional operational insights into the benefits of EMR over AD. The research did not explore the effect of having the electrodes within the system but with no applied voltage—another area to explore how system performance is affected by varying the applied differentials.
9. Adding positive and negative controls to the experiment can help compare experiments that may be affected by unknown variables. Creating a standardised test to calculate Biomethane Potential of feedstocks for AD has proved difficult with different labs obtaining different results due to different microbial communities used for tests (Raposo et al., 2012). Integrating a positive control into the experiments would likely best be achieved within each specific lab; using an EMR system that has been continually operating under the same conditions and a consistent feedstock.

Pilot Conclusions

The pilot aimed to demonstrate how EMR can be scaled up to provide a circular approach to decentralised wastewater treatment. The pilot system demonstrated a reduction in organics within the wastewater but was unsuccessful in producing biogas and would require post-treatment to meet EU environmental discharge standards. However, the pilot provided multiple insights into scaling up the EMRs and the design of future pilot studies, including duration and security of feedstock supply.

The duration of the project was limited to an initial three months and then extended to four after the operational issues that occurred onsite. The system was only operational for 58 days out of the 102 days it was installed and faced multiple issues surrounding the inoculation. For systems above 100L, the minimum start-up time recorded was 50 days (Baeza et al., 2017) but increased up to 90 days to produce hydrogen (Cotterill et al., 2017b). With the operational challenges faced, it would have been unlikely for the system to produce methane if it were to match these start-up times. Future pilots should explore effective start-up procedures and plan testing timelines accordingly.

Understanding why the system failed to produce gas would provide valuable information into the effectiveness of the system. The system analysed the current density, but it was unable to analyse the biofilm coverage and composition which would have provided more information on why the system did not produce biogas. Due to the nature of the pilot containing pathogens, the system had to be pasteurised and disinfected before the reactor could be shipped, removing the possibility of useful analysis back in the UK. SYBR gold staining can help to identify the coverage of biofilm on the electrodes as has been shown in (San-Martín et al., 2019), which can be used alongside SEM. Future pilots operating on substrates that are easier to handle can create new opportunities to understand more about the biofilm.

Unlike the lab results, the pH within the reactor was neutral, and the main impact for any changes are related to the heater malfunctions causing a temperature change, increasing H^+ concentrations. Although with the low OLR the pH would be unlikely to drop significantly like it did in the series and batch reactor systems. The effluent characterisation was limited, and there is no data on nutrient removal. Other research indicates that the MECs will require further chemical or biological treatment

for nutrient removal (Cotterill et al., 2017b). The system also requires pathogen removal for it to be safely reused for flushing or irrigation.

Pasteurisation is a method to destroy pathogens through heat and is often used in the food industry. To effectively inactivate pathogens, you need to heat the waste to 70°C for 10–15 minutes or 50 min at 65°C (Feachem et al., 1981). Researchers have found that faecal sludge treated in an AD system can generate enough biogas to heat the sludge between 65-75^{o}C to effectively destroy pathogens within the effluent (Forbis-Stokes et al., 2016). However, there were some operational issues with the pilot due to solids entering the heat exchanger and equipment failures which are likely corrected with continual development.

AD can operate at higher temperatures (55-65^{o}c) in thermophilic systems, providing both pathogen removal and energy recovery of faecal sludge. Thermophilic AD has successfully reduced *Salmonella* spp., and *Escherichia coli* below EU limits, however, *Clostridium perfringens* spores were still detectable above limits (4.63 $\log_{10}$ spores/mL) when operating at 55^{o}C with a hydraulic retention time between 16-28 days (Lloret et al., 2013). Pre-treatment of waste at 70^{o}C for 9 hours has also been shown to increase energy recovery in thermophilic AD operating at 55^{o}C in both batch and continuous systems (Ferrer et al., 2008). Thermophilic operation is another option of pathogen removal for faecal waste within MECs. There is research into MECs operating at thermophilic temperatures successfully (Cerrillo et al., 2017, 2016; Fu et al., 2015; Yin et al., 2019). However, none have explored pathogen removal and could provide an exciting opportunity for faecal sludge management.

A review of the pilot system indicated that the anode design was not optimised for electron recovery, requiring a well-established biofilm to aid in exo-electrogenic electron transfer. A review of biofilm coverage from other research shows that biofilm only forms on a small portion of the electrodes (San-Martín et al., 2019). Future anode designs should ensure that there is a short distance between carbon and the electron acceptor. Due to the short period for the reactor design and installation date, the pilot was unable to source a manufacturer for carbon brushes. The system used GAC as an alternative anode material. With the GAC plates also acting as baffles to increase turbulence within the flow. At high flow rates, it is possible that the plate design could provide benefits, but the pilot study was unable to validate the effectiveness of the reactor design.

Below, Table 11-1 compares the EMR test systems to alternative commercial wastewater treatment technologies. EMR needs to be competitive, which the technology will need to outperform. The EMR showed a range in the energy consumption per kg of COD removed. The table highlights that EMR can generate energy in some instances where the COD is high. The test EMR systems indicate that EMR can reduce the COD to a certain point. After which a secondary and tertiary treatment to reduce the COD below 125 mg/L as well as removing nutrients and pathogens. This approach can help to reduce energy-intensive technologies such as aeration within the wastewater treatment process.

Table 11-1: Technology system efficiency comparison

Technology	COD Reduction (%)		Energy Consumption (kWh/kg of COD)	References
	Min	Max		
EMR Series Exp.1	32	52	0.76	*Only continuous flow data days 0-30
EMR Batch Exp.2	40	46	-0.004	*COD reduction could be lower due to spoiled day 0 samples
EMR Batch Exp.3	30	40	-1.38	
EMR Pilot	20	80	0.52	*Not including heating
Biological reactors/ Clarifier	Not given	Not given	0.32	(Gurung et al., 2018; Tarallo, 2015)
Aeration / Activated Sludge	82	95	1.00	(Nadayil et al., 2015; van Lier et al., 2008)
Anaerobic Digestion	53	61	0.077	(Tarallo, 2015; Wendland et al., 2007)

TEA Conclusions

The research aimed to assess the economic viability of EMR, to provide decentralised wastewater treatment systems for underserved communities that are lacking infrastructure. The TEA focused on a school case study which is the main interest for the WFP.

The research was based on multiple assumptions, including consistent operational costs over the 20-year life span. Due to limited field data, a percentage of the CAPEX was used to calculate the maintenance costs. Whereas the costs would likely be lower in the first ten years than the second 10 years as components degrade. Going forward, long-duration field studies will inform the maintenance required that can then be used to develop more informed TEA. The fuel costs were also kept the same and inflation was not added.

Since 2015 the average inflation rate in Kenya has been 5.98% (Statista, 2020). Globally, fossil fuel costs fluctuate, and as solid fuel resources become scarcer due to deforestation, firewood and coal will also likely increase in price. The research was unable to obtain data for charcoal and firewood price fluctuations due to the informality of the markets and was therefore not included in the TEA assumptions. Future research should aim to analyse the historic increases in fuel costs and include them in the assumptions to understand the impact it could have on the costs. The cost of desludging and water are also the same, and as the cost of desludging is likely to be affected by inflation, it will increase the attractiveness of an onsite wastewater treatment system.

The WFP currently serves approximately 400 schools within Kenya, with their aim to reduce the amount of firewood and coal schools use to cook the food they provide for the students. Schools mainly use three-stone fires and in some cases, fuel-efficient stoves. Converting organic waste into

biogas could have a huge impact. The lower estimated CAPEX of EMR compared to a fixed dome AD system is promising, and shows the benefits the technology could have if the assumed performance could be replicated in field trials.

Overall, the research has undertaken 'proof of concept' (TRL 4) and developed a system to test under pilot-scale (TRL 6). Although the pilot system failed to generate biogas within the time frame of the pilot, it has laid the foundation for future pilot systems and is an important step to commercialise an EMR system. Going forward, it is essential to improve our understanding in different areas:

1. Developing a greater understanding of correct start-up procedures to accelerate the pilot systems.
2. Compare EMRs at scale to commercial AD systems.
3. Develop a greater understanding of EMR biofilms and the ability to regulate pH.
4. Test the effects of mixing for EMR systems and the increased performance.
5. Test the effects of multi-stage EMR systems to understand the variation in microorganisms.
6. Explore the effects of applied voltage depending on the different phases of complex molecules being broken down into simple molecules and into methane.
7. Develop a smart power control system that can optimise the flow rate and applied voltage to maximise the biogas and methane production.
8. Explore lower temperature ranges where the system can effectively produce methane to reduce the heating requirements.
9. Using pilot data to validate the TEA assumptions
10. Using pilot data develop a Life Cycle Assessment (LCA) to assess the environmental and social cost alongside the economic cost.

11.1 Next steps

To move EMRs towards commercialisation, a greater understanding of scaling up the technology is required. The electrode design needs to be created to make a modular system that can easily be placed into reactors of different sizes. The modular system will enable the electrodes and electrode housing to be mass-manufactured, reducing costs through economies of scale.

Future Research underway:

The research from this project is just the start. A research team has been created through WASE to build on the project and take the research towards commercialisation. Currently, multiple projects are underway to explore the next steps that have been highlighted through the research.

1. **Midsize 50L**

To develop an understanding of multi electrode systems, a mid-size system is being tested comparing EMR to AD. Four 50L reactors are treating co-digested waste. The main bulk of wastewater is from a toilet with a waste diversion to a holding tank that is mixed with 1.5 – 2.5kg of food waste. Each reactor is fed 5L a day to give a ten-day retention time. Two of the reactors are setup as EMR systems,

and two are AD. The research will provide essential data on multi-electrode systems and how EMR operates over a prolonged period.

Figure 11-1: 50L AD and EMR - Co-Digestion On-going Research

2. Pilot System 1.5m^3

A new 1.5 m3 pilot is being deployed to Kenya in November 2020. Two bag AD systems are being installed at SNV's head office in Nairobi. SNV is a humanitarian organisation that set up the Kenya Biogas Program. One bag will integrate new scaled up electrode modules that are 800 mm in length with a 350mm diameter. Nine electrode modules are going to insert into the bag so that it runs as an EMR system whilst the other is operating just as an AD system. The research will provide insights into comparing an AD and EMR system at a scale of 1.5m^3 which is commercially used for smallholder farmers in Kenya. The pilot system could provide small household waste and sanitation wastewater treatment.

3. Pilot system 4m^3

A second pilot project is underway in Kenya that is integrating four 1m^3 EMR systems connected in series to create a total reactor volume of 4m^3. The system is being deployed at the United Nations Office inNairobi, which is the UN's head office in Africa. At the site, the system will be treating waste from septic tanks, removing the need for desluding and to provide biogas for cooking. The system has

been designed following on from the series brewery wastewater treatment test. The system design allows it to operate as a scaled-up lab testing facility that can be tested at multiple sites with varying wastewater flows. The future research aims to understand the effects of a multi-stage EMR system to understand the different microorganisms present at the different phases, or organic breakdown within each chamber. The research will also provide valuable data about scaling up EMR systems to treat wastewater. After the pilot, the system will be moved to the Dadaab Refugee camp as part of the trial with the UN World Food Program, with an aim to start trials in a school at the end of 2021.

Figure 11-2: Pilot EMR in Development

12 References

ADBA, 2017. Chapter 3 Feedstocks. In: ADBA (Ed.), The Practical Guide to AD. pp. 23–47.

Ahn, Y., Im, S., Chung, J.W., 2017. Optimizing the operating temperature for microbial electrolysis cell treating sewage sludge. Int. J. Hydrogen Energy 42, 27784–27791.

Ahn, Y., Logan, B.E., 2010. Effectiveness of domestic wastewater treatment using microbial fuel cells at ambient and mesophilic temperatures. Bioresour. Technol. 101, 469–475.

Aiken, D.C., Curtis, T.P., Heidrich, E.S., 2019. Avenues to the financial viability of microbial electrolysis cells [MEC] for domestic wastewater treatment and hydrogen production. Int. J. Hydrogen Energy 44, 2426–2434.

Amoah, M., Cremer, T., Dadzie, P.K., Ohene, M., Marfo, O., 2019. Firewood collection and consumption practices and barriers to uptake of modern fuels among rural households in Ghana. Int. For. Rev. 21, 149–166.

Anand, C.K., Apul, D.S., 2014. Composting toilets as a sustainable alternative to urban sanitation - A review. Waste Manag. 34, 329–343.

Anderson, G.G., O'Toole, G.A., 2008. Innate and induced resistance mechanisms of bacterial biofilms. Curr. Top. Microbiol. Immunol. 322, 85–105.

Anirudh Bhanu, T.N. and C.D., 2019. Bioelectrochemical CO2 Reduction to Methane: MES Integration in Biogas Production Processes. MDPI.

Arroyo, G., Sanz, P.D., Préstamo, G., 1997. Effect of high pressure on the reduction of microbial populations in vegetables. J. Appl. Microbiol. 82, 735–742.

Aulenta, F., Canosa, A., Majone, M., Panero, S., Reale, P., Rossetti, S., 2008. Trichloroethene Dechlorination and H_2 Evolution Are Alternative Biological Pathways of Electric Charge Utilization by a Dechlorinating Culture in a Bioelectrochemical System. Environ. Sci. Technol. 42, 6185–6190.

Awe, O.W., Zhao, Y., Nzihou, A., Minh, D.P., Lyczko, N., 2017. A Review of Biogas Utilisation, Purification and Upgrading Technologies. Waste and Biomass Valorization.

Babanova, S., Carpenter, K., Phadke, S., Suzuki, S., Ishii, S., Phan, T., Grossi-Soyster, E., Flynn, M., Hogan, J., Bretschger, O., 2017. The Effect of Membrane Type on the Performance of Microbial Electrosynthesis Cells for Methane Production. J. Electrochem. Soc. 164, H3015–H3023.

Baeza, J.A., Martínez-Miró, À., Guerrero, J., Ruiz, Y., Guisasola, A., 2017. Bioelectrochemical hydrogen production from urban wastewater on a pilot scale. J. Power Sources 356, 500–509.

Bajpai, P., 2017. Basics of anaerobic digestion process. In: SpringerBriefs in Applied Sciences and Technology. Springer Verlag, pp. 7–12.

Bajracharya, S., ElMekawy, A., Srikanth, S., Pant, D., 2016. Cathodes for microbial fuel cells. In: Scott, K., Hao Yu, E. (Eds.), Microbial Electrochemical and Fuel Cells. Wood House Publishing,

Chippenham, pp. 179–206.

Baker, S., Thomson, N., Weill, F.-X., Holt, K.E., 2018. Genomic insights into the emergence and spread of antimicrobial-resistant bacterial pathogens. Science (80-.). 360, 733–738.

Bamwesigye, D., Antwi, D.S., Petra, H., Vaclav, K., 2018. Firewood and Charcoal Production in Uganda. For. Ecosyst. DI, 821–828.

Barber, W.P., Stuckey, D.C., 1999. The use of the anaerobic baffled reactor (ABR) for wastewater treatment: A review. Water Res.

Barbosa, S.G., Peixoto, L., Soares, O.S.G.P., Pereira, M.F.R., Heijne, A. Ter, Kuntke, P., Alves, M.M., Pereira, M.A., 2018. Influence of carbon anode properties on performance and microbiome of Microbial Electrolysis Cells operated on urine. Electrochim. Acta 267, 122–132.

Barth, R.., Simons, K.L., San, C., 2013. Polymers for Hydrogen Infrastructure and Vehicle Fuel Systems : Applications, Properties, and Gap Analysis 23–34.

Bastidas-Oyanedel, J.R., Schmidt, J.E., 2018. Increasing profits in food waste biorefinery-a techno-economic analysis. Energies 11.

Batlle-Vilanova, P., Puig, S., Gonzalez-Olmos, R., Vilajeliu-Pons, A., Bañ Eras, L., Dolors Balaguer, M., Colprim, J.S., 2014a. Assessment of biotic and abiotic graphite cathodes for hydrogen production in microbial electrolysis cells. Int. J. Hydrogen Energy 39, 1297–1305.

Batlle-Vilanova, P., Puig, S., Gonzalez-Olmos, R., Vilajeliu-Pons, A., Bañeras, L., Balaguer, M.D., Colprim, J., 2014b. Assessment of biotic and abiotic graphite cathodes for hydrogen production in microbial electrolysis cells. Int. J. Hydrogen Energy 39, 1297–1305.

Beck, M.B., Jiang, F., Shi, F., Walker, R.V., Osidele, O.O., Lin, Z., Demir, I., Hall, J.W., 2010. Re-engineering cities as forces for good in the environment. Proc. Inst. Civ. Eng. - Eng. Sustain. 163, 31–46.

Blasco-Gómez, R., Batlle-Vilanova, P., Villano, M., Balaguer, M.D., Colprim, J., Puig, S., 2017. On the edge of research and technological application: A critical review of electromethanogenesis. Int. J. Mol. Sci.

Bond, D.R., Lovley, D.R., 2003a. Electricity Production by Geobacter sulfurreducens Attached to Electrodes Electricity Production by Geobacter sulfurreducens Attached to Electrodes. Appl. Environ. Microbiol. 69, 1548–1555.

Bond, D.R., Lovley, D.R., 2003b. Electricity production by Geobacter sulfurreducens attached to electrodes. Appl. Environ. Microbiol. 69, 1548–1555.

Butti, S.K., Velvizhi, G., Sulonen, M.L.K., Haavisto, J.M., Oguz Koroglu, E., Yusuf Cetinkaya, A., Singh, S., Arya, D., Annie Modestra, J., Vamsi Krishna, K., Verma, A., Ozkaya, B., Lakaniemi, A.M., Puhakka, J.A., Venkata Mohan, S., 2016. Microbial electrochemical technologies with the perspective of harnessing bioenergy: Maneuvering towards upscaling. Renew. Sustain. Energy Rev.

Cai, W., Liu, W., Han, J., Wang, A., 2016. Enhanced hydrogen production in microbial electrolysis cell with 3D self-assembly nickel foam-graphene cathode. Biosens. Bioelectron. 80.

Call, D., Logan, B.E., 2008a. Hydrogen production in a single chamber microbial electrolysis cell lacking a membrane. Environ. Sci. Technol. 42, 3401–3406.

Call, D., Logan, B.E., 2008b. Hydrogen production in a single chamber microbial electrolysis cell lacking a membrane. Environ. Sci. Technol. 42, 3401–3406.

Call, D.F., Merrill, M.D., Logan, B.E., 2009a. High surface area stainless steel brushes as cathodes in microbial electrolysis cells. Environ. Sci. Technol. 43, 2179–2183.

Call, D.F., Merrill, M.D., Logan, B.E., 2009b. High surface area stainless steel brushes as cathodes in microbial electrolysis cells. Environ. Sci. Technol. 43, 2179–2183.

Carlotta-Jones, D.I., Purdy, K., Kirwan, K., Stratford, J., Coles, S.R., 2020. Improved hydrogen gas production in microbial electrolysis cells using inexpensive recycled carbon fibre fabrics. Bioresour. Technol. 304, 122983.

Castro, C.J., Goodwill, J.E., Rogers, B., Henderson, M., Butler, C.S., 2014. Deployment of the microbial fuel cell latrine in ghana for decentralized sanitation. J. Water Sanit. Hyg. Dev. 4, 663–671.

Cerrillo, M., Viñas, M., Bonmatí, A., 2016. Overcoming organic and nitrogen overload in thermophilic anaerobic digestion of pig slurry by coupling a microbial electrolysis cell. Bioresour. Technol. 216, 362–372.

Cerrillo, M., Viñas, M., Bonmatí, A., 2017. Unravelling the active microbial community in a thermophilic anaerobic digester-microbial electrolysis cell coupled system under different conditions. Water Res. 110.

Chae, K.J., Choi, M.J., Kim, K.Y., Ajayi, F.F., Chang, I.S., Kim, I.S., 2009. A solar-powered microbial electrolysis cell with a platinum catalyst-free cathode to produce hydrogen. Environ. Sci. Technol. 43, 9525–9530.

Chae, K.J., Choi, M.J., Kim, K.Y., Ajayi, F.F., Chang, I.S., Kim, I.S., 2010. Selective inhibition of methanogens for the improvement of biohydrogen production in microbial electrolysis cells. Int. J. Hydrogen Energy 35, 13379–13386.

Chakraborty, A., Ghosh, S., Mukhopadhyay, P., Dinara, S.M., Bag, A., Mahata, M.K., Kumar, R., Das, S., Sanjay, J., Majumdar, S., Biswas, D., 2014. Trapping effect analysis of AlGaN/InGaN/GaN Heterostructure by conductance frequency measurement. In: MRS Proceedings. pp. 81–87.

Chakraborty, I., Sathe, S.M., Khuman, C.N., Ghangrekar, M.M., 2020. Bioelectrochemically powered remediation of xenobiotic compounds and heavy metal toxicity using microbial fuel cell and microbial electrolysis cell. Mater. Sci. Energy Technol. 3, 104–115.

Chambers, R., 2009. Going to Scale with Community-Led Total Sanitation: Reflections on Experience, Issues and Ways Forward. IDS Pract. Pap. 2009, 01–50.

Champigneux, P., Delia, M.L., Bergel, A., 2018. Impact of electrode micro- and nano-scale topography on the formation and performance of microbial electrodes. Biosens. Bioelectron.

Cheng, S., Liu, H., Logan, B.E., 2006. Increased performance of single-chamber microbial fuel cells using an improved cathode structure. Electrochem. commun. 8, 489–494.

Cheng, S., Logan, B.E., 2007. Sustainable and efficient biohydrogen production via electrohydrogenesis. Proc. Natl. Acad. Sci. U. S. A. 104, 18871–3.

Cheng, S., Logan, B.E., 2011a. Increasing power generation for scaling up single-chamber air cathode microbial fuel cells.

Cheng, S., Logan, B.E., 2011b. High hydrogen production rate of microbial electrolysis cell (MEC) with reduced electrode spacing. Bioresour. Technol. 102, 3571–3574.

Cheng, S., Xing, D., Call, D.F., Logan, B.E., 2009. Direct biological conversion of electrical current into methane by electromethanogenesis. Environ. Sci. Technol. 43, 3953–3958.

Cho, K., Hoffmann, M.R., 2017. Molecular hydrogen production from wastewater electrolysis cell with multi-junction BiOx/TiO2 anode and stainless steel cathode: Current and energy efficiency. Appl. Catal. B Environ. 202, 671–682.

Choi, C., Hu, N., Lim, B., 2014. Cadmium recovery by coupling double microbial fuel cells. Bioresour. Technol. 170, 361–369.

Chookaew, T., Prasertsan, P., Ren, Z.J., 2014. Two-stage conversion of crude glycerol to energy using dark fermentation linked with microbial fuel cell or microbial electrolysis cell. N. Biotechnol. 31, 179–184.

Clean Energy Wire, 2018. German renewables meet 100% of power demand for second time ever [WWW Document]. URL https://www.climatechangenews.com/2018/05/03/german-renewables-meet-100-power-demand-second-time-ever/ (accessed 2.16.20).

Commault, A.S., Lear, G., Packer, M.A., Weld, R.J., 2013. Influence of anode potentials on selection of Geobacter strains in microbial electrolysis cells. Bioresour. Technol. 139, 226–234.

Cordell, D., Rosemarin, A., Schröder, J.J., Smit, A.L., 2011. Towards global phosphorus security: A systems framework for phosphorus recovery and reuse options. Chemosphere 84, 747–758.

Cotterill, S., Heidrich, E.S., Curtis, T.P., 2016. Microbial Electrolysis cells for hydrogen production. In: Scott, K., Hao Yu, E. (Eds.), Microbial Electrochemical and Fuel Cells. Wood House Publishing, Chippenham, pp. 287–316.

Cotterill, S.E., Dolfing, J., Curtis, T.P., Heidrich, E.S., 2018. Community Assembly in Wastewater-Fed Pilot-Scale Microbial Electrolysis Cells. Front. Energy Res. 6, 98.

Cotterill, S.E., Dolfing, J., Jones, C., Curtis, T.P., Heidrich, E.S., 2017a. Low Temperature Domestic Wastewater Treatment in a Microbial Electrolysis Cell with 1 m 2 Anodes: Towards System Scale-Up. Fuel Cells 17, 584–592.

Cotterill, S.E., Dolfing, J., Jones, C., Curtis, T.P., Heidrich, E.S., 2017b. Low Temperature Domestic Wastewater Treatment in a Microbial Electrolysis Cell with 1 m^2 Anodes: Towards System Scale-Up. Fuel Cells 17, 584–592.

Craine, S., Mills, E., Guay, J., 2014. Clean Energy Services for All: Financing Universal Electrification 1–14.

Croese, E., Jeremiasse, A.W., Marshall, I.P.G., Spormann, A.M., Euverink, G.J.W., Geelhoed, J.S., Stams, A.J.M., Plugge, C.M., 2014. Influence of setup and carbon source on the bacterial community of biocathodes in microbial electrolysis cells. Enzyme Microb. Technol. 61–62, 67–75.

Croese, E., Pereira, M.A., Euverink, G.J.W., Stams, A.J.M., Geelhoed, J.S., 2011. Analysis of the microbial community of the biocathode of a hydrogen-producing microbial electrolysis cell. Appl. Microbiol. Biotechnol. 92, 1083–1093.

Cui, M.H., Gao, L., Lee, H.S., Wang, A.J., 2020. Mixed dye wastewater treatment in a bioelectrochemical system-centered process. Bioresour. Technol. 297, 122420.

Cusick, R.D., Bryan, B., Parker, D.S., Merrill, M.D., Mehanna, M., Kiely, P.D., Liu, G., Logan, B.E., 2011a. Performance of a pilot-scale continuous flow microbial electrolysis cell fed winery wastewater. Appl. Microbiol. Biotechnol. 89, 2053–2063.

Cusick, R.D., Bryan, B., Parker, D.S., Merrill, M.D., Mehanna, M., Kiely, P.D., Liu, G., Logan, B.E., 2011b. Performance of a pilot-scale continuous flow microbial electrolysis cell fed winery wastewater. Appl. Microbiol. Biotechnol. 89, 2053–2063.

Cusick, R.D., Kiely, P.D., Logan, B.E., 2010. A monetary comparison of energy recovered from microbial fuel cells and microbial electrolysis cells fed winery or domestic wastewaters. Int. J. Hydrogen Energy 35, 8855–8861.

Danilenko, A., van den Berg, C., Macheve, B., Moffitt, L.J., 2014. The IBNET Water Supply and Sanitation Blue Book 2014: The International Benchmarking Network for Water and Sanitation Utilities Databook, The IBNET Water Supply and Sanitation Blue Book 2014: The International Benchmarking Network for Water and Sanitation Utilities Databook. The World Bank.

de la Sota, C., Lumbreras, J., Pérez, N., Ealo, M., Kane, M., Youm, I., Viana, M., 2018. Indoor air pollution from biomass cookstoves in rural Senegal. Energy Sustain. Dev. 43, 224–234.

Ding, A., Yang, Y., Sun, G., Wu, D., 2015. Impact of applied voltage on methane generation and microbial activities in an anaerobic microbial electrolysis cell (MEC). Chem. Eng. J. 283, 260–265.

Doorn, M.R.J.., Towprayoon, S.., Manso Vieira, S.M.., Irving, W.., Palmer, C.., Pipatti, R., Wang, 2006. Wastewater Treatment and Discharge. In: 2006 IPCC Guidelines for National Greenhouse Gas Inventories . IPCC, pp. 6.1-6.28.

Du, Z., Li, H., Gu, T., 2007. A state of the art review on microbial fuel cells: A promising technology for wastewater treatment and bioenergy. Biotechnol. Adv.

Dumas, C., Basseguy, R., Bergel, A., 2008. Electrochemical activity of Geobacter sulfurreducens biofilms on stainless steel anodes. Electrochim. Acta 53, 5235–5241.

Dumitru, A., Scott, K., 2016. Anode materials for microbial fuel cells. In: Scott, K., Hao Yu, E. (Eds.), Microbial Electrochemical and Fuel Cells. Wood House Publishing, Chippenham, pp. 117–152.

Embury-Dennis, T., 2017. Costa Rica's electricity generated by renewable energy for 300 days in 2017 | The Independent [WWW Document]. Independent. URL https://www.independent.co.uk/news/world/americas/costa-rica-electricity-renewable-energy-300-days-2017-record-wind-hydro-solar-water-a8069111.html (accessed 2.16.20).

Energy Agency, I., 2018. Global Energy & CO2 Status Report: The latest trends in energy and emissions in 2018.

Escapa, A., Gil-Carrera, L., García, V., Morán, A., Garc?a, V., Mor?n, A., 2012a. Performance of a continuous flow microbial electrolysis cell (MEC) fed with domestic wastewater. Bioresour. Technol. 117, 55–62.

Escapa, A., Gómez, X., Tartakovsky, B., Morán, A., 2012b. Estimating microbial electrolysis cell (MEC) investment costs in wastewater treatment plants: Case study. Int. J. Hydrogen Energy 37, 18641–18653.

Escapa, A., Manuel, M.F., Morán, A., Gómez, X., Guiot, S.R., Tartakovsky, B., 2009. Hydrogen production from glycerol in a membraneless microbial electrolysis cell. Energy and Fuels 23, 4612–4618.

Escapa, A., Mateos, R., Martínez, E.J., Blanes, J., 2016a. Microbial electrolysis cells: An emerging technology for wastewater treatment and energy recovery. from laboratory to pilot plant and beyond. Renew. Sustain. Energy Rev. 55, 942–956.

Escapa, A., Mateos, R., Martínez, E.J., Blanes, J., 2016b. Microbial electrolysis cells: An emerging technology for wastewater treatment and energy recovery. from laboratory to pilot plant and beyond. Renew. Sustain. Energy Rev.

Escapa, A., San-Martín, M.I.I., Mateos, R., Morán, A., 2015. Scaling-up of membraneless microbial electrolysis cells (MECs) for domestic wastewater treatment: Bottlenecks and limitations. Bioresour. Technol. 180, 72–78.

Fan, Y., Hu, H., Liu, H., 2007. Enhanced Coulombic efficiency and power density of air-cathode microbial fuel cells with an improved cell configuration. J. Power Sources 171, 348–354.

FAO, UNHCR, 2018. Guidance on the use of planted and natural forests to supply forest products and build resilience in displaced and host communities MANAGING FORESTS IN DISPLACEMENT SETTINGS. ROME.

Feachem, R.G., Bradley, D.J., Garelick, H., Mara, D.D., 1981. Appropriate Technology for Water Supply and Sanitation, World Bank.

Feachem, R.G., Bradley, D.J., Garelick, H., Mara, D.D., 1983. Sanitation and disease: health aspects of excreta and wastewater management. Sanit. Dis. Heal. Asp. excreta wastewater Manag.

Feng, Y., Yang, Q., Wang, X., Logan, B.E., 2010. Treatment of carbon fiber brush anodes for improving power generation in air-cathode microbial fuel cells. J. Power Sources 195, 1841–1844.

Ferrer, I., Ponsá, S., Vázquez, F., Font, X., 2008. Increasing biogas production by thermal (70 °C) sludge pre-treatment prior to thermophilic anaerobic digestion. Biochem. Eng. J. 42, 186–192.

Filer, J., Ding, H.H., Chang, S., 2019. Biochemical Methane Potential (BMP) Assay Method for Anaerobic Digestion Research. Water 11, 921.

Forbis-Stokes, A.A., O'Meara, P.F., Mugo, W., Simiyu, G.M., Deshusses, M.A., 2016. On-Site Fecal Sludge Treatment with the Anaerobic Digestion Pasteurization Latrine. Environ. Eng. Sci. 33,

898–906.

Franks, A.E., Nevin, K.P., Glaven, R.H., Lovley, D.R., 2010. Microtoming coupled to microarray analysis to evaluate the spatial metabolic status of Geobacter sulfurreducens biofilms. ISME J. 4, 509–519.

Fu, Q., Kuramochi, Y., Fukushima, N., Maeda, H., Sato, K., Kobayashi, H., 2015. Bioelectrochemical analyses of the development of a thermophilic biocathode catalyzing electromethanogenesis. Environ. Sci. Technol. 49, 1225–1232.

Garrido-Baserba, M., Vinardell, S., Molinos-Senante, M., Rosso, D., Poch, M., 2018. The Economics of Wastewater Treatment Decentralization: A Techno-economic Evaluation. Environ. Sci. Technol. 52, 8965–8976.

Gebrezgabher, S., Odero, J., Karanja, N., 2016. BIOGAS PRODUCTION FOR ENERGY SAVINGS Biogas from fecal sludge at Kibera communities at Nairobi (Umande Trust, Kenya).

Gil-Carrera, L., Escapa, A., Carracedo, B., Morán, A., Gómez, X., Mor??n, A., G??mez, X., 2013a. Performance of a semi-pilot tubular microbial electrolysis cell (MEC) under several hydraulic retention times and applied voltages. Bioresour. Technol. 146, 63–69.

Gil-Carrera, L., Escapa, A., Mehta, P., Santoyo, G., Guiot, S.R., Morán, A., Tartakovsky, B., 2013b. Microbial electrolysis cell scale-up for combined wastewater treatment and hydrogen production. Bioresour. Technol.

Grant, H., Poole, C., Lilley, A., Bailey, I., 2016. Farm Anaerobic Digestion: Growth and Performance.

Grudens-Schuck, N., Lundy Allen, B., Larson, K., Lundy, B., 2004. Methodology Brief: Focus Group Fundamentals Recommended Citation.

Gu, Y., Zhang, X., Are Myhren, J., Han, M., Chen, X., Yuan, Y., 2018. Techno-economic analysis of a solar photovoltaic/thermal (PV/T) concentrator for building application in Sweden using Monte Carlo method. Energy Convers. Manag. 165, 8–24.

Gude, V.G., 2016. Microbial fuel cells for wastewater treatment and energy generation. In: Scott, K., Hao Yu, E. (Eds.), Microbial Electrochemical and Fuel Cells. Wood House Publishing, Chippenham, pp. 247–276.

Guest, J.S., Skerlos, S.J., Barnard, J.L., Beck, M.B., Daigger, G.T., Hilger, H., Jackson, S.J., Karvazy, K., Kelly, L., Macpherson, L., Mihelcic, J.R., Pramanik, A., Raskin, L., Van Loosdrecht, M.C.M., Yeh, D., Love, N.G., 2009. A new planning and design paradigm to achieve sustainable resource recovery from wastewater. Environ. Sci. Technol.

Guo, H., Kim, Y., 2019. Stacked multi-electrode design of microbial electrolysis cells for rapid and low-sludge treatment of municipal wastewater. Biotechnol. Biofuels 12, 23.

Guo, K., Donose, B.C., Soeriyadi, A.H., Prévoteau, A., Patil, S.A., Freguia, S., Gooding, J.J., Rabaey, K., 2014. Flame oxidation of stainless steel felt enhances anodic biofilm formation and current output in bioelectrochemical systems. Environ. Sci. Technol. 48, 7151–7156.

Guo, K., Freguia, S., Dennis, P.G., Chen, X., Donose, B.C., Keller, J., Gooding, J.J., Rabaey, K., 2013.

Effects of surface charge and hydrophobicity on anodic biofilm formation, community composition, and current generation in bioelectrochemical systems. Environ. Sci. Technol. 47, 7563–7570.

Guo, K., Prévoteau, A., Patil, S.A., Rabaey, K., 2015. Engineering electrodes for microbial electrocatalysis. Curr. Opin. Biotechnol.

Guo, K., Prévoteau, A., Rabaey, K., 2017. A novel tubular microbial electrolysis cell for high rate hydrogen production. J. Power Sources 356, 484–490.

Gurung, K., Tang, W.Z., Sillanpää, M., 2018. Correction to: Unit Energy Consumption as Benchmark to Select Energy Positive Retrofitting Strategies for Finnish Wastewater Treatment Plants (WWTPs): a Case Study of Mikkeli WWTP (Environmental Processes, (2018), 5, 3, (667-681), 10.1007/s40710-018-0310-. Environ. Process. 5, 931.

Habermann, W., Pommer, E.H., 1991. Biological fuel cells with sulphide storage capacity. Appl. Microbiol. Biotechnol. 35, 128–133.

Hassanein, A., Witarsa, F., Guo, X., Yong, L., Lansing, S., Qiu, L., 2017. Next generation digestion: Complementing anaerobic digestion (AD) with a novel microbial electrolysis cell (MEC) design. Int. J. Hydrogen Energy 42, 28681–28689.

Hazinski, M.F., 1985. Nursing care of the critically ill child: a seven-point check. Pediatr. Nurs. 11, 453–461.

Heck, N., Smith, C., Hittinger, E., 2016. A Monte Carlo approach to integrating uncertainty into the levelized cost of electricity. Electr. J. 29, 21–30.

Heidrich, E.S., Curtis, T.P., Dolfing, J., 2011. Determination of the internal chemical energy of wastewater. Environ. Sci. Technol. 45, 827–832.

Heidrich, E.S., Dolfing, J., Scott, K., Edwards, S.R., Jones, C., Curtis, T.P., 2013a. Production of hydrogen from domestic wastewater in a pilot-scale microbial electrolysis cell. Appl. Microbiol. Biotechnol. 97, 6979–6989.

Heidrich, E.S., Dolfing, J., Scott, K., Edwards, S.R., Jones, C., Curtis, T.P., 2013b. Production of hydrogen from domestic wastewater in a pilot-scale microbial electrolysis cell. Appl. Microbiol. Biotechnol. 97, 6979–6989.

Heidrich, E.S., Dolfing, J., Wade, M.J., Sloan, W.T., Quince, C., Curtis, T.P., 2017. Temperature, inocula and substrate: Contrasting electroactive consortia, diversity and performance in microbial fuel cells. Bioelectrochemistry.

Heidrich, E.S., Edwards, S.R., Dolfing, J., Cotterill, S.E., Curtis, T.P., 2014. Performance of a pilot scale microbial electrolysis cell fed on domestic wastewater at ambient temperatures for a 12month period. Bioresour. Technol. 173, 87–95.

Heinss, U., Larmie, S.A., Strauss, M., Csir, W./, 1999. SOS-Management of Sludges EAWAG/SANDEC from On-Site Sanitation Characteristics of Faecal Sludges and their Solids-Liquid Separation Based on the Field Report Entitled “Sedimentation Tank Sludge Accumulation Study” SANDEC Dept. for Water and Sanitation in Developing Countries.

Hernández-Sancho, F., United Nations Environment Programme, B., Mateo-Sagasta, J., Qadir, M., 2015. Economic valuation of wastewater : the cost of action and the cost of no action. UNEP.

Hidalgo, D., Sacco, A., Hernández, S., Tommasi, T., 2015. Electrochemical and impedance characterization of Microbial Fuel Cells based on 2D and 3D anodic electrodes working with seawater microorganisms under continuous operation. Bioresour. Technol. 195, 139–146.

Holmes, D.E., Shrestha, P.M., Walker, D.J.F., Dang, Y., Nevin, K.P., Woodard, T.L., Lovley, D.R., 2017. Metatranscriptomic Evidence for Direct Interspecies Electron Transfer Between Geobacter and ... Appl. Environ. Microbiol. 83, e0022317.

Huang, L., Chen, J., Quan, X., Yang, F., 2010. Enhancement of hexavalent chromium reduction and electricity production from a biocathode microbial fuel cell. Bioprocess Biosyst. Eng. 33, 937–945.

Huang, L., Li, T., Liu, C., Quan, X., Chen, L., Wang, A., Chen, G., 2013a. Synergetic interactions improve cobalt leaching from lithium cobalt oxide in microbial fuel cells. Bioresour. Technol. 128, 539–546.

Huang, L., Sun, Y., Liu, Y., Wang, N., 2013b. Mineralization of 4-chlorophenol and analysis of bacterial community in microbial fuel cells. Procedia Environ. Sci. 18, 534–539.

Hussain, S.A., Perrier, M., Tartakovsky, B., 2018. Long-term performance of a microbial electrolysis cell operated with periodic disconnection of power supply. RSC Adv. 8, 16842–16849.

Ieropoulos, I., Greenman, J., Melhuish, C., 2010. Improved energy output levels from small-scale Microbial Fuel Cells. Bioelectrochemistry 78, 44–50.

Ieropoulos, I., Ledezma, P., Stinchcombe, A., Papaharalabos, G., Melhuish, C., Greenman, J., 2013. Waste to real energy: the first MFC powered mobile phone. Phys. Chem. Chem. Phys. 15, 15312–15316.

Ieropoulos, I.A., Greenman, J., Melhuish, C., Hart, J., 2005. Comparative study of three types of microbial fuel cell. Enzyme Microb. Technol. 37, 238–245.

Insulation Shop, 2020. 50mm Xtratherm Phenolic Insulation Board | Enhanced Fire Performance [WWW Document]. URL https://www.insulationshop.co/50mm_phenolic_insulation_board_safe-r.html (accessed 6.13.20).

Int ; Prabowo, A.K., Tiarasukma, A.P., Christwardana, M., Ariyanti, D., 2016. Microbial Fuel Cells for Simultaneous Electricity Generation and Organic Degradation from Slaughterhouse Wastewater. Int. J. Renew. Energy Dev. 5, 107–112.

International Rescue Committee, 2016. Cost Efficiency Analysis Latrine-Building Programs in Ethiopia.

Jeremiasse, A.W., Hamelers, H.V.M., Buisman, C.J.N., 2010. Microbial electrolysis cell with a microbial biocathode. Bioelectrochemistry 78, 39–43.

Jiang, D., Curtis, M., Troop, E., Scheible, K., McGrath, J., Hu, B., Suib, S., Raymond, D., Li, B., 2011. A pilot-scale study on utilizing multi-anode/cathode microbial fuel cells (MAC MFCs) to enhance

the power production in wastewater treatment. Int. J. Hydrogen Energy 36, 876–884.

Jiang, L., Huang, L., Sun, Y., 2014. Recovery of flakey cobalt from aqueous Co(II) with simultaneous hydrogen production in microbial electrolysis cells. Int. J. Hydrogen Energy 39, 654–663.

Jiang, Y., Su, M., Li, D., 2014. Removal of sulfide and production of methane from carbon dioxide in microbial fuel cells-microbial electrolysis cell (MFCs-MEC) coupled system. Appl. Biochem. Biotechnol. 172, 2720–2731.

Jugnia, L.B., Manno, D., Hendry, M., Tartakovsky, B., 2019. Removal of heavy metals in a flow-through vertical microbial electrolysis cell. Can. J. Chem. Eng. 97, 2608–2616.

Jung, S.P., Pandit, S., 2018. Important factors influencing microbial fuel cell performance. In: Biomass, Biofuels, Biochemicals: Microbial Electrochemical Technology: Sustainable Platform for Fuels, Chemicals and Remediation. pp. 377–406.

Kadier, A., Simayi, Y., Abdeshahian, P., Azman, N.F., Chandrasekhar, K., Kalil, M.S., 2016a. A comprehensive review of microbial electrolysis cells (MEC) reactor designs and configurations for sustainable hydrogen gas production. Alexandria Eng. J.

Kadier, A., Simayi, Y., Abdeshahian, P., Azman, N.F., Chandrasekhar, K., Kalil, M.S., 2016b. A comprehensive review of microbial electrolysis cells (MEC) reactor designs and configurations for sustainable hydrogen gas production. Alexandria Eng. J.

Kadier, A., Simayi, Y., Abdeshahian, P., Azman, N.F., Chandrasekhar, K., Kalil, M.S., Abudukeremu Kadier Peyman Abdeshahian, Nadia Farhana Azman, K. Chandrasekhar, Mohd Sahaid Kalil, Y.S., 2016c. A comprehensive review of microbial electrolysis cells (MEC) reactor designs and configurations for sustainable hydrogen gas production. Alexandria Eng. J. 55, 427–443.

Kaiser, D., 2007. Bacterial Swarming: A Re-examination of Cell-Movement Patterns. Curr. Biol. 17, 561–570.

Katuri, K.P., Ali, M., Saikaly, P.E., 2019. The role of microbial electrolysis cell in urban wastewater treatment: integration options, challenges, and prospects. Curr. Opin. Biotechnol.

Kaundinya, D.P., Balachandra, P., Ravindranath, N.H., 2009. Grid-connected versus stand-alone energy systems for decentralized power-A review of literature. Renew. Sustain. Energy Rev.

Kellenberger, A., Vaszilcsin, N., Brandl, W., Duteanu, N., 2007. Kinetics of hydrogen evolution reaction on skeleton nickel and nickel-titanium electrodes obtained by thermal arc spraying technique. Int. J. Hydrogen Energy 32, 3258–3265.

Keshavarz, T., Gomaa, O.M., Kyazze, G., 2019. In focus: microbial fuel cells, some considerations. J. Chem. Technol. Biotechnol. 94, 2069–2069.

Khan, M.Z., Nizami, A.S., Rehan, M., Ouda, O.K.M., Sultana, S., Ismail, I.M., Shahzad, K., 2017. Microbial electrolysis cells for hydrogen production and urban wastewater treatment: A case study of Saudi Arabia. Appl. Energy 185, 410–420.

Ki, D., Popat, S.C., Torres, C.I., 2016. Reduced overpotentials in microbial electrolysis cells through improved design, operation, and electrochemical characterization. Chem. Eng. J. 287, 181–188.

Kim, B.H., Chang, I.S., Gadd, G.M., 2007. Challenges in microbial fuel cell development and operation. Appl. Microbiol. Biotechnol.

Kim, K.N., Lee, S.H., Kim, H., Park, Y.H., In, S. Il, 2018. Improved microbial electrolysis cell hydrogen production by hybridization with a TiO2 nanotube array photoanode. Energies 11.

Kim, K.Y., Zikmund, E., Logan, B.E., 2017. Impact of catholyte recirculation on different 3-dimensional stainless steel cathodes in microbial electrolysis cells. Int. J. Hydrogen Energy 42, 29708–29715.

Kitching, M., Butler, R., Marsili, E., 2017. Microbial bioelectrosynthesis of hydrogen: Current challenges and scale-up. Enzyme Microb. Technol. 96, 1–13.

Kjellström, T., Borg, K., Lind, B., 1978. Cadmium in feces as an estimator of daily cadmium intake in Sweden. Environ. Res. 15, 242–251.

Kolev Slavov, A., 2017. Dairy Wastewaters – General Characteristics and Treatment Possibilities – A Review. Food Technol. Biotechnol. 55, 14.

Kuntke, P., Sleutels, T.H.J.A., Saakes, M., Buisman, C.J.N., 2014. Hydrogen production and ammonium recovery from urine by a Microbial Electrolysis Cell. Int. J. Hydrogen Energy 39, 4771–4778.

Kyazze, G., Popov, A., Dinsdale, R., Esteves, S., Hawkes, F., Premier, G., Guwy, A., 2010. Influence of catholyte pH and temperature on hydrogen production from acetate using a two chamber concentric tubular microbial electrolysis cell. Int. J. Hydrogen Energy 35, 7716–7722.

Lansing, S., Bowen, H., Gregoire, K., Klavon, K., Moss, A., Eaton, A., Lai, Y.J., Iwata, K., 2016. Methane production for sanitation improvement in Haiti. Biomass and Bioenergy 91, 288–295.

Lee, H.S., 2018. Electrokinetic analyses in biofilm anodes: Ohmic conduction of extracellular electron transfer. Bioresour. Technol. 256, 509–514.

Lee, H.S., Dhar, B.R., An, J., Rittmann, B.E., Ryu, H., Santo Domingo, J.W., Ren, H., Chae, J., 2016. The roles of biofilm conductivity and donor substrate kinetics in a mixed-culture biofilm anode. Environ. Sci. Technol. 50, 12799–12807.

Leflaive, X., Witmer, M., Martin-Hurtado, R., Bakker, M., Kram, T., Bouwman, L., Visser, H., Bouwman, A., Hilderlink, H., Kayoung, K., 2012. OECD Environmental Outlook to 2050 Chapter 5: Water 207–274.

Li, S., Cheng, C., Thomas, A., 2017. Carbon-Based Microbial-Fuel-Cell Electrodes: From Conductive Supports to Active Catalysts. Adv. Mater. 29, 1602547.

Li, Xiaomin, Ding, L., Yuan, H., Li, Xiaoming, Zhu, Y., 2020. Identification of potential electrotrophic microbial community in paddy soils by enrichment of microbial electrolysis cell biocathodes. J. Environ. Sci. (China) 87, 411–420.

Liang, S., Zhang, B., Shi, J., Wang, T., Zhang, L., Wang, Z., Chen, C., 2018. Improved decolorization of dye wastewater in an electrochemical system powered by microbial fuel cells and intensified by micro-electrolysis. Bioelectrochemistry 124, 112–118.

Lim, S.S., Fontmorin, J.M., Izadi, P., Wan Daud, W.R., Scott, K., Yu, E.H., 2020. Impact of applied cell

voltage on the performance of a microbial electrolysis cell fully catalysed by microorganisms. Int. J. Hydrogen Energy 45, 2557–2568.

Lim, S.S., Kim, B.H., Da Li, Feng, Y., Wan Daud, W.R., Scott, K., Yu, E.H., 2018. Effects of applied potential and reactants to hydrogen-producing biocathode in a microbial electrolysis cell. Front. Chem. 6, 1–19.

Lim, S.S., Yu, E.H., Daud, W.R.W., Kim, B.H., Scott, K., 2017. Bioanode as a limiting factor to biocathode performance in microbial electrolysis cells. Bioresour. Technol. 238, 313–324.

Liu, D., Roca-Puigros, M., Geppert, F., Caizán-Juanarena, L., Na Ayudthaya, S.P., Buisman, C., ter Heijne, A., 2018. Granular Carbon-Based Electrodes as Cathodes in Methane-Producing Bioelectrochemical Systems. Front. Bioeng. Biotechnol. 6.

Liu, D., Zhang, L., Chen, S., Buisman, C., Ter Heijne, A., 2016. Bioelectrochemical enhancement of methane production in low temperature anaerobic digestion at 10 °C. Water Res. 99, 281–287.

Liu, H., Grot, S., Logan, B.E., 2005a. Electrochemically assisted microbial production of hydrogen from acetate. Environ. Sci. Technol. 39, 4317–4320.

Liu, H., Grot, S., Logan, B.E., 2005b. Electrochemically assisted microbial production of hydrogen from acetate. Environ. Sci. Technol. 39, 4317–4320.

Liu, H., Logan, B.E., 2004. Electricity generation using an air-cathode single chamber microbial fuel cell in the presence and absence of a proton exchange membrane. Environ. Sci. Technol. 38, 4040–4046.

Liu, W., Cai, W., Guo, Z., Wang, L., Yang, C., Varrone, C., Wang, A., 2016. Microbial electrolysis contribution to anaerobic digestion of waste activated sludge, leading to accelerated methane production. Renew. Energy 91, 334–339.

Liu, W., Huang, S., Zhou, A., Zhou, G., Ren, N., Wang, A., Zhuang, G., 2012. Hydrogen generation in microbial electrolysis cell feeding with fermentation liquid of waste activated sludge. In: International Journal of Hydrogen Energy. pp. 13859–13864.

Liu, X., Zhuo, S., Rensing, C., Zhou, S., 2018. Syntrophic growth with direct interspecies electron transfer between pili-free Geobacter species. ISME J. 12, 2142–2151.

Lloret, E., Pastor, L., Pradas, P., Pascual, J.A., 2013. Semi full-scale thermophilic anaerobic digestion (TAnD) for advanced treatment of sewage sludge: Stabilization process and pathogen reduction. Chem. Eng. J. 232, 42–50.

Logan, B.E., 2007. Micorbial Fuel Cells, Wiley. Wiley.

Logan, B.E., Regan, J.M., 2006. Electricity-producing bacterial communities in microbial fuel cells. Trends Microbiol.

Lohner, S.T., Deutzmann, J.S., Logan, B.E., Leigh3, J., Spormann, A.M., 2014. Hydrogenase-independent uptake and metabolism of electrons by the archaeon Methanococcus maripaludis. ISME J. 8, 1673–1681.

Lovins, L.H., 2016. The Circular Economy of Soil. In: A New Dynamic 2 - Effective Systems in a Circular Economy. Ellen MacArthur Foundation Publishing, COWES, pp. 87–106.

Lu, L., Ren, Z.J., 2016. Microbial electrolysis cells for waste biorefinery: A state of the art review. Bioresour. Technol.

Lu, L., Xing, D., Liu, B., Ren, N., 2012a. Enhanced hydrogen production from waste activated sludge by cascade utilization of organic matter in microbial electrolysis cells. Water Res. 46, 1015–1026.

Lu, L., Xing, D., Ren, N., 2012b. Bioreactor performance and quantitative analysis of methanogenic and bacterial community dynamics in microbial electrolysis cells during large temperature fluctuations. Environ. Sci. Technol. 46, 6874–6881.

Luo, H., Fu, S., Liu, G., Zhang, R., Bai, Y., Luo, X., 2014. Autotrophic biocathode for high efficient sulfate reduction in microbial electrolysis cells. Bioresour. Technol. 167, 462–468.

Ma, S. jia, Ma, H. jun, Hu, H. dong, Ren, H. qiang, 2019. Effect of mixing intensity on hydrolysis and acidification of sewage sludge in two-stage anaerobic digestion: Characteristics of dissolved organic matter and the key microorganisms. Water Res. 148, 359–367.

Ma, X., Li, Z., Zhou, A., Yue, X., 2017. Energy recovery from tubular microbial electrolysis cell with stainless steel mesh as cathode. R. Soc. Open Sci. 4.

Marcus, A.K., Torres, C.I., Rittmann, B.E., 2007. Conduction-based modeling of the biofilm anode of a microbial fuel cell. Biotechnol. Bioeng. 98, 1171–1182.

Maria, K., Bsceng, F., 2009. Analysis of a Pilot-Scale Anaerobic Baffled Reactor Treating Domestic Wastewater.

Martínez-Blanco, J., Lehmann, A., Chang, Y.J., Finkbeiner, M., 2015. Social organizational LCA (SOLCA)—a new approach for implementing social LCA. Int. J. Life Cycle Assess. 20, 1586–1599.

Mo, W., Zhang, Q., 2013. Energy-nutrients-water nexus: Integrated resource recovery in municipal wastewater treatment plants. J. Environ. Manage.

Mohammed, A.J., Ismail, Z.Z., 2018. Slaughterhouse wastewater biotreatment associated with bioelectricity generation and nitrogen recovery in hybrid system of microbial fuel cell with aerobic and anoxic bioreactors. Ecol. Eng. 125, 119–130.

Montpart, N., Rago, L., Baeza, J.A., Guisasola, A., 2015. Hydrogen production in single chamber microbial electrolysis cells with different complex substrates. Water Res. 68, 601–615.

Moreno, R., Escapa, A., Cara, J., Carracedo, B., Gómez, X., 2015. A two-stage process for hydrogen production from cheese whey: Integration of dark fermentation and biocatalyzed electrolysis. Int. J. Hydrogen Energy 40, 168–175.

Moß, C., Patil, S.A., Schröder, U., 2019. Scratching the Surface—How Decisive Are Microscopic Surface Structures on Growth and Performance of Electrochemically Active Bacteria? Front. Energy Res. 7, 18.

Nadayil, J., Mohan, D., Dileep, K., Rose, M., Rose, R., Parambi, P., 2015. A Study on Effect of Aeration

on Domestic Wastewater. Int. J. Interdiscip. Res. Innov. 3, 10–15.

Nam, J.Y., Kim, H.W., Lim, K.H., Shin, H.S., 2010. Effects of organic loading rates on the continuous electricity generation from fermented wastewater using a single-chamber microbial fuel cell. In: Bioresource Technology. Elsevier Ltd, pp. S33–S37.

Nancharaiah, Y. V., Venkata Mohan, S., Lens, P.N.L., 2015. Metals removal and recovery in bioelectrochemical systems: A review. Bioresour. Technol. 195, 102–114.

Nandy, A., Sharma, M., Venkatesan, S.V., Taylor, N., Gieg, L., Thangadura, V., 2019. Comparative Evaluation of Coated and Non-CoatedCarbon Electrodes in a Microbial Fuel Cell forTreatment of Municipal Sludge. Energies 12, 1034.

Nelson, D., Shrimali, G., 2014. Finance Mechanisms for Lowering the Cost of Renewable Energy in Rapidly Developing Countries A CPI Series.

Nevin, K.P., Hensley, S.A., Franks, A.E., Summers, Z.M., Ou, J., Woodard, T.L., Snoeyenbos-West, O.L., Lovley, D.R., 2011. Electrosynthesis of organic compounds from carbon dioxide is catalyzed by a diversity of acetogenic microorganisms. Appl. Environ. Microbiol. 77, 2882–2886.

Noori, M.T., Ghangrekar, M.M., Mitra, A., Mukherjee, C.K., 2016. Enhanced Power Generation in Microbial Fuel Cell Using MnO2-Catalyzed Cathode Treating Fish Market Wastewater. Springer, New Delhi, pp. 285–294.

Noori, M.T., Vu, M.T., Ali, R.B., Min, B., 2020. Recent advances in cathode materials and configurations for upgrading methane in bioelectrochemical systems integrated with anaerobic digestion. Chem. Eng. J. 392, 123689.

Oh, S., Min, B., Logan, B.E., 2004. Cathode performance as a factor in electricity generation in microbial fuel cells. Environ. Sci. Technol. 38, 4900–4904.

Oh, S.E., Logan, B.E., 2007. Voltage reversal during microbial fuel cell stack operation. J. Power Sources 167, 11–17.

Onyango, L., 2019. Kenya regulator shuts down 4 firms for polluting Nairobi River - The East African [WWW Document]. URL https://www.theeastafrican.co.ke/scienceandhealth/firms-shut-down-for-polluting-Nairobi-River/3073694-5250300-xrqj6bz/index.html (accessed 5.2.20).

Palanisamy, G., Jung, H.Y., Sadhasivam, T., Kurkuri, M.D., Kim, S.C., Roh, S.H., 2019. A comprehensive review on microbial fuel cell technologies: Processes, utilization, and advanced developments in electrodes and membranes. J. Clean. Prod. 221, 598–621.

Pandev, M., Lucchese, P., Mansilla, C., Le Duigou, A., Abrashev, B., Vladikova, D., 2017. Hydrogen Economy: the future for a sustainable and green society, Bulgarian Chemical Communications.

Panjičko, M., Zupančič, G.D., Fanedl, L., Logar, R.M., Tišma, M., Zelić, B., 2017. Biogas production from brewery spent grain as a mono-substrate in a two-stage process composed of solid-state anaerobic digestion and granular biomass reactors. J. Clean. Prod. 166, 519–529.

Pant, D., Singh, A., Van Bogaert, G., Irving Olsen, S., Singh Nigam, P., Diels, L., Vanbroekhoven, K., 2012. Bioelectrochemical systems (BES) for sustainable energy production and product recovery

from organic wastes and industrial wastewaters. RSC Adv. 2, 1248–1263.

Park, D.H., Zeikus, J.G., 2000. Electricity generation in microbial fuel cells using neutral red as an electronophore. Appl. Environ. Microbiol. 66, 1292–1297.

Park, J., Lee, B., Tian, D., Jun, H., 2018. Bioelectrochemical enhancement of methane production from highly concentrated food waste in a combined anaerobic digester and microbial electrolysis cell. Bioresour. Technol. 247, 226–233.

Patten, M.L., 2018. Analyzing Data: Understanding Statistics. Underst. Res. Methods 201–257.

Pham, T.H., Boon, N., De Maeyer, K., Höfte, M., Rabaey, K., Verstraete, W., 2008. Use of Pseudomonas species producing phenazine-based metabolites in the anodes of microbial fuel cells to improve electricity generation. Appl. Microbiol. Biotechnol. 80, 985–993.

Pham, T.H., Rabaey, K., Aelterman, P., Clauwaert, P., De Schamphelaire, L., Boon, N., Verstraete, W., 2006. Microbial Fuel Cells in Relation to Conventional Anaerobic Digestion Technology. Eng. Life Sci. 6, 285–292.

Philips, J., Verbeeck, K., Rabaey, K., Arends, J.B.A., 2016. Electron Transfer Mechanisms in Biofilms. In: Scott, K., Hao Yu, E. (Eds.), Microbial Electrochemical and Fuel Cells. Wood House Publishing, Chippenham, pp. 67–113.

Ploux, L., Ponche, A., Anselme, K., 2010. Bacteria/material interfaces: Role of the material and cell wall properties. J. Adhes. Sci. Technol. 24, 2165–2201.

Pötschke, L., Huber, P., Schriever, S., Rizzotto, V., Gries, T., Blank, L.M., Rosenbaum, M.A., 2019. Rational Selection of Carbon Fiber Properties for High-Performance Textile Electrodes in Bioelectrochemical Systems. Front. Energy Res. 7.

Potter, M.C., 1911. Electrical Effects Accompanying the Decomposition of Organic Compounds. Proc. R. Soc. London 84, 260–276.

Powell, E.E., Hill, G.A., 2009. Economic assessment of an integrated bioethanol–biodiesel–microbial fuel cell facility utilizing yeast and photosynthetic algae. Chem. Eng. Res. Des. 87, 1340–1348.

Premier, G.., Michie, I.., Boghani, H.C., Fradler, K.., Kim, J.., 2016. Reactor Design and scale-up. In: Scott, K., Hao Yu, E. (Eds.), Microbial Electrochemical and Fuel Cells. Wood House Publishing, Chippenham, pp. 215–239.

Pueyo, A., 2016. Cost and Returns of Renewable Energy in Sub-Saharan Africa: A Comparison of Kenya and Ghana | Institute of Development Studies. IDS Evid. Rep.

Qin, B., Luo, H., Liu, G., Zhang, R., Chen, S., Hou, Y., Luo, Y., 2012. Nickel ion removal from wastewater using the microbial electrolysis cell. Bioresour. Technol. 121, 458–461.

Rabaey, K., 2009. Bioelectrochemical Systems: From Extracellular Electron Transfer to Biotechnological Application. Water Intell. Online 8.

Rabaey, K., Clauwaert, P., Aelterman, P., Verstraete, W., 2005. Tubular microbial fuel cells for efficient electricity generation. Environ. Sci. Technol. 39, 8077–8082.

Rabaey, K., Verstraete, W., 2005. Microbial fuel cells: Novel biotechnology for energy generation. Trends Biotechnol.

Rader, G.K., Logan, B.E., 2010. Multi-electrode continuous flow microbial electrolysis cell for biogas production from acetate. Int. J. Hydrogen Energy 35.

Rago, L., Baeza, J.A., Guisasola, A., 2017a. Bioelectrochemical hydrogen production with cheese whey as sole substrate. J. Chem. Technol. Biotechnol. 92, 173–179.

Rago, L., Baeza, J.A., Guisasola, A., 2017b. Bioelectrochemical hydrogen production with cheese whey as sole substrate. J. Chem. Technol. Biotechnol. 92, 173–179.

Rajendran, K., Murthy, G.S., 2019. Techno-economic and life cycle assessments of anaerobic digestion – A review. Biocatal. Agric. Biotechnol. 20, 101207.

Ramírez-Vargas, C.A., Prado, A., Arias, C.A., Carvalho, P.N., Esteve-Núñez, A., Brix, H., 2018. Microbial electrochemical technologies for wastewater treatment: Principles and evolution from microbial fuel cells to bioelectrochemical-based constructed wetlands. Water (Switzerland) 10, 1–29.

Ran, Z., Gefu, Z., Kumar, J.A., Chaoxiang, L., Xu, H., Lin, L., 2014. Hydrogen and methane production in a bio-electrochemical system assisted anaerobic baffled reactor. Int. J. Hydrogen Energy 39, 13498–13504.

Raposo, F., De La Rubia, M.A., Fernández-Cegrí, V., Borja, R., 2012. Anaerobic digestion of solid organic substrates in batch mode: An overview relating to methane yields and experimental procedures. Renew. Sustain. Energy Rev. 16, 861–877.

Read, S.T., Dutta, P., Bond, P.L., Keller, J., Rabaey, K., 2010. Initial development and structure of biofilms on microbial fuel cell anodes. BMC Microbiol. 10, 98 (1–10).

Rivera, I., Bakonyi, P., Buitrón, G., 2017. H2 production in membraneless bioelectrochemical cells with optimized architecture: The effect of cathode surface area and electrode distance. Chemosphere 171, 379–385.

Roller, S.D., Bennetto, H.P., Delaney, G.M., Mason, J.R., Stirling, J.L., Thurston, C.F., 1984. Electron-transfer coupling in microbial fuel cells: 1. comparison of redox-mediator reduction rates and respiratory rates of bacteria. J. Chem. Technol. Biotechnol. Biotechnol. 34, 3–12.

Rose, C., Parker, A., Jefferson, B., Cartmell, E., 2015. The characterization of feces and urine: A review of the literature to inform advanced treatment technology. Crit. Rev. Environ. Sci. Technol. 45, 1827–1879.

Rousseau, R., Etcheverry, L., Roubaud, E., Basséguy, R., Délia, M.L., Bergel, A., 2020. Microbial electrolysis cell (MEC): Strengths, weaknesses and research needs from electrochemical engineering standpoint. Appl. Energy.

Rozendal, R.A., Hamelers, H.V.M., Buisman, C.J.N., 2006a. Effects of membrane cation transport on pH and microbial fuel cell performance. Environ. Sci. Technol. 40, 5206–5211.

Rozendal, R.A., Hamelers, H.V.M., Euverink, G.J.W., Metz, S.J., Buisman, C.J.N., 2006b. Principle and perspectives of hydrogen production through biocatalyzed electrolysis. Int. J. Hydrogen Energy

31, 1632–1640.

Rozendal, R.A., Hamelers, H.V.M., Molenkamp, R.J., Buisman, C.J.N., 2007. Performance of single chamber biocatalyzed electrolysis with different types of ion exchange membranes. Water Res. 41, 1984–1994.

Rozendal, René A, Hamelers, H.V.M., Rabaey, K., Keller, J., Buisman, C.J.N., 2008. Towards practical implementation of bioelectrochemical wastewater treatment. Trends Biotechnol.

Rozendal, R. A., Sleutels, T.H.J.A., Hamelers, H.V.M., Buisman, C.J.N., 2008. Effect of the type of ion exchange membrane on performance, ion transport, and pH in biocatalyzed electrolysis of wastewater. Water Sci. Technol. 57, 1757–1762.

Saheb-Alam, S., Singh, A., Hermansson, M., Persson, F., Schnürer, A., Wilén, B.M., Modin, O., 2018. Effect of start-up strategies and electrode materials on carbon dioxide reduction on biocathodes. Appl. Environ. Microbiol. 84.

San-Martín, M.I., Sotres, A., Alonso, R.M., Díaz-Marcos, J., Morán, A., Escapa, A., 2019. Assessing anodic microbial populations and membrane ageing in a pilot microbial electrolysis cell. Int. J. Hydrogen Energy 44, 17304–17315.

Sangeetha, T., Guo, Z., Liu, W., Cui, M., Yang, C., Wang, L., Wang, A., 2016. Cathode material as an influencing factor on beer wastewater treatment and methane production in a novel integrated upflow microbial electrolysis cell (Upflow-MEC). Int. J. Hydrogen Energy 41, 2189–2196.

Santoro, C., Babanova, S., Artyushkova, K., Cornejo, J.A., Ista, L., Bretschger, O., Marsili, E., Atanassov, P., Schuler, A.J., 2015. Influence of anode surface chemistry on microbial fuel cell operation. Bioelectrochemistry 106, 141–149.

Saratale, R.G., Saratale, G.D., Pugazhendhi, A., Zhen, G., Kumar, G., Kadier, A., Sivagurunathan, P., 2017. Microbiome involved in microbial electrochemical systems (MESs): A review. Chemosphere 177, 176–188.

Schellenberg, T., Subramanian, V., Ganeshan, G., Tompkins, D., Pradeep, R., 2020. Wastewater Discharge Standards in the Evolving Context of Urban Sustainability–The Case of India. Front. Environ. Sci. 8, 30.

Schouten, M.A.C., Mathenge, R.W., 2010. Communal sanitation alternatives for slums: A case study of Kibera, Kenya. Phys. Chem. Earth 35, 815–822.

Scott, K, 2016. 1 - An introduction to microbial fuel cells. In: Scott, Keith, Hao Yu, E. (Eds.), Microbial Electrochemical and Fuel Cells. Wood House Publishing, pp. 3–27.

Scott, K., 2016. Membranes and Seperators for Microbial Fuel Cells. In: Scott, Keith, Hao Yu, E. (Eds.), Microbial Electrochemical and Fuel Cells. Chippenham, pp. 153–178.

SE4ALL, 2011. Achieving Universal Energy Access.

Selembo, P.A., Merrill, M.D., Logan, B.E., 2009a. The use of stainless steel and nickel alloys as low-cost cathodes in microbial electrolysis cells. J. Power Sources 190, 271–278.

Selembo, P.A., Perez, J.M., Lloyd, W.A., Logan, B.E., 2009b. High hydrogen production from glycerol or glucose by electrohydrogenesis using microbial electrolysis cells. Int. J. Hydrogen Energy 34, 5373–5381.

Shaoan Cheng, †, Hong Liu, † and, Bruce E. Logan*, †,‡, 2006. Increased Power Generation in a Continuous Flow MFC with Advective Flow through the Porous Anode and Reduced Electrode Spacing.

SIBA, 2020. THE UK'S SMALL INDEPENDENT BREWING SECTOR IN FOCUS.

Siegert, M., Li, X.F., Yates, M.D., Logan, B.E., 2014a. The presence of hydrogenotrophic methanogens in the inoculum improves methane gas production in microbial electrolysis cells. Front. Microbiol. 5, 1–12.

Siegert, M., Yates, M.D., Call, D.F., Zhu, X., Spormann, A., Logan, B.E., 2014b. Comparison of Nonprecious Metal Cathode Materials for Methane Production by Electromethanogenesis. ACS Sustain. Chem. Eng. 2, 910–917.

Song, H.-L., Zhu, Y., Li, J., 2015. Electron transfer mechanisms, characteristics and applications of biological cathode microbial fuel cells â€" A mini review.

Speece, R., 2007. Anaerobic biotechnology and odor/corrosion control for municipalities and industries. Archae press, Nashville Tennessee.

Starkl, M., Brunner, N., Feil, M., Hauser, A., 2015. Ensuring Sustainability of Non-Networked Sanitation Technologies: An Approach to Standardization. Environ. Sci. Technol. 49, 6411–6418.

Statista, 2020. • Kenya - Inflation rate 2021 | Statista [WWW Document]. URL https://www.statista.com/statistics/451115/inflation-rate-in-kenya/ (accessed 9.19.20).

Streitwieser, D.A., 2017. Comparison of the anaerobic digestion at the mesophilic and thermophilic temperature regime of organic wastes from the agribusiness. Bioresour. Technol. 241, 985–992.

Subramani, V., Angelo, B., Veziroğlu, T.N., 2016. Compendium of hydrogen energy. Elsevier.

Sun, D., Chen, J., Huang, H., Liu, W., Ye, Y., Cheng, S., 2016. The effect of biofilm thickness on electrochemical activity of Geobacter sulfurreducens. Int. J. Hydrogen Energy 41, 16523–16528.

Sun, D., Wang, A., Cheng, S., Yates, M., Logan, B.E., 2014. Geobacter anodireducens sp. nov., an exoelectrogenic microbe in bioelectrochemical systems. Int. J. Syst. Evol. Microbiol. 64, 3485–3491.

Sun, H., Li, J., Yang, M., Shao, Q., 2019. Influence of initial pH on anodic biofilm formation in single-chambered microbial electrolysis cells. Polish J. Environ. Stud. 28, 1377–1384.

Sun, R., Zhou, A., Jia, J., Liang, Q., Liu, Q., Xing, D., Ren, N., 2015. Characterization of methane production and microbial community shifts during waste activated sludge degradation in microbial electrolysis cells. Bioresour. Technol. 175, 68–74.

Sun, Y., Garrido-Baserba, M., Molinos-Senante, M., Donikian, N.A., Poch, M., Rosso, D., 2020. A composite indicator approach to assess the sustainability and resilience of wastewater

management alternatives. Sci. Total Environ. 725, 138286.

Taiganides, P.E., 1992. Pig Waste Management & Recycling - The Singapore Experience. International Development Research Centre 1992, Ottawa.

Tang, X., Guo, K., Li, H., Du, Z., Tian, J., 2011. Electrochemical treatment of graphite to enhance electron transfer from bacteria to electrodes. Bioresour. Technol. 102, 3558–3560.

Tao, H.C., Zhang, L.J., Gao, Z.Y., Wu, W.M., 2011. Copper reduction in a pilot-scale membrane-free bioelectrochemical reactor. Bioresour. Technol. 102, 10334–10339.

Tarallo, S., 2015. A Guide to Net-Zero Energy Solutions for Water Resource Recovery Facilities, Water Intelligence Online.

Tayhas, R., Palmore, G., Whitesides, G.M., 1994. Microbial and Enzymatic Biofuel Cells. Power 566, 271–290.

The World Bank, 2020. People using safely managed sanitation services (% of population) | Data [WWW Document]. URL https://data.worldbank.org/indicator/SH.STA.SMSS.ZS (accessed 6.6.20).

Topriska, E., Kolokotroni, M., Dehouche, Z., Novieto, D.T., Wilson, E.A., 2016. The potential to generate solar hydrogen for cooking applications: Case studies of Ghana, Jamaica and Indonesia. Renew. Energy 95, 495–509.

Topriska, E., Kolokotroni, M., Dehouche, Z., Wilson, E., 2015. Solar hydrogen system for cooking applications: Experimental andnumerical study. Renew. Energy 83, 717–728.

Total, 2020. No Title [WWW Document]. URL https://www.total.co.ke/products/total-gas/total-gas-prices-cylinders-accessories

Trapero, J.R., Horcajada, L., Linares, J.J., Lobato, J., 2017. Is microbial fuel cell technology ready? An economic answer towards industrial commercialization. Appl. Energy 185, 698–707.

Trendewicz, A.A., Braun, R.J., 2013. Techno-economic analysis of solid oxide fuel cell-based combined heat and power systems for biogas utilization at wastewater treatment facilities. J. Power Sources 233, 380–393.

UK Inflation Calculator, 2020. £1 in 1853 → 2020 | UK Inflation Calculator [WWW Document]. URL https://www.in2013dollars.com/uk/inflation/2004?amount=1 (accessed 7.4.20).

UN-Water, 2014. Water and Energy Information brief.

UNESCO, 2016. Fact 38: Investments & economic health | United Nations Educational, Scientific and Cultural Organization [WWW Document]. UNESCO. URL http://www.unesco.org/new/en/natural-sciences/environment/water/wwap/facts-and-figures/all-facts-wwdr3/fact-38-investments-economic-health/ (accessed 5.31.20).

UNHCR, 2020. Kalobeyei Settlement - UNHCR Kenya [WWW Document]. URL https://www.unhcr.org/ke/kalobeyei-settlement (accessed 2.16.20).

United Nations Environment Program, 2012. Drivers and barriers for private finance in sub-Saharan Africa Financing renewable energy in developing countries.

US-EPA, n.d. Anaerobic Digester Project Screening Tool | Municipal Solid Waste Knowledge Platform [WWW Document]. URL https://www.waste.ccacoalition.org/document/anaerobic-digester-project-screening-tool (accessed 8.1.20).

Van Eerten-Jansen, M.C.A.A., Heijne, A. Ter, Buisman, C.J.N., Hamelers, H.V.M., 2012a. Microbial electrolysis cells for production of methane from CO 2: Long-term performance and perspectives. Int. J. Energy Res. 36, 809–819.

Van Eerten-Jansen, M.C.A.A., Heijne, A. Ter, Buisman, C.J.N., Hamelers, H.V.M., 2012b. Microbial electrolysis cells for production of methane from CO2: long-term performance and perspectives. Int. J. Energy Res. 36.

van Lier, J.B., Mahmoud, N., Zeeman, Z., 2008. Anaerobic Wastewa. In: Henze, M., van Loosdrecht, M.C.M., Ekama, G.A., Brdjanovic, D. (Eds.), Biological Wastewater Treatment: Principles, Modeling and Design. IWA Publishing, London, UK, pp. 401–442.

Van Loosdrecht, M.C.M., Brdjanovic, D., 2014. Anticipating the next century of wastewater treatment. Science (80-.).

Viana, M.B., Freitas, A. V., Leitão, R.C., Pinto, G.A.S., Santaella, S.T., 2012. Anaerobic digestion of crude glycerol: a review. Environ. Technol. Rev. 1, 81–92.

Villano, M., Aulenta, F., Ciucci, C., Ferri, T., Giuliano, A., Majone, M., 2010. Bioelectrochemical reduction of CO2 to CH4 via direct and indirect extracellular electron transfer by a hydrogenophilic methanogenic culture. Bioresour. Technol. 101, 3085–3090.

Wagner, R.C., Regan, J.M., Oh, S.E., Zuo, Y., Logan, B.E., 2009. Hydrogen and methane production from swine wastewater using microbial electrolysis cells. Water Res. 43, 1480–1488.

Wan, L.L., Li, X.J., Zang, G.L., Wang, X., Zhang, Y.Y., Zhou, Q.X., 2015. A solar assisted microbial electrolysis cell for hydrogen production driven by a microbial fuel cell. RSC Adv. 5, 82276–82281.

Wang, A., Liu, W., Ren, N., Zhou, J., Cheng, S., 2010. Key factors affecting microbial anode potential in a microbial electrolysis cell for H2 production. Int. J. Hydrogen Energy 35, 13481–13487.

Wang, G., Huang, L., Zhang, Y., 2008. Cathodic reduction of hexavalent chromium [Cr(VI)] coupled with electricity generation in microbial fuel cells. Biotechnol. Lett. 30, 1959–1966.

Wang, H., Ren, Z.J., 2013. A comprehensive review of microbial electrochemical systems as a platform technology. Biotechnol. Adv. 31, 1796–1807.

Wang, L., He, Z., Guo, Z., Sangeetha, T., Yang, C., Gao, L., Wang, A., Liu, W., 2019. Microbial community development on different cathode metals in a bioelectrolysis enhanced methane production system. J. Power Sources 444.

Wang, L., Liu, W., Kang, L., Yang, C., Zhou, A., Wang, A., 2014. Enhanced biohydrogen production from waste activated sludge in combined strategy of chemical pretreatment and microbial

electrolysis. Int. J. Hydrogen Energy 39, 11913–11919.

Wang, X., Cheng, S., Feng, Y., Merrill, M.D., Saito, T., Logan, B.E., 2009. Use of carbon mesh anodes and the effect of different pretreatment methods on power production in microbial fuel cells. Environ. Sci. Technol. 43, 6870–6874.

Wang, Y., Weng, G.J., 2018. Electrical Conductivity of Carbon Nanotube- and Graphene-Based Nanocomposites. In: Micromechanics and Nanomechanics of Composite Solids. Springer International Publishing, pp. 123–156.

Wang, Z., Lim, B., Choi, C., 2011. Removal of Hg2+ as an electron acceptor coupled with power generation using a microbial fuel cell. Bioresour. Technol. 102, 6304–6307.

Water Services Regulatory Board, 2014. Water Tariffs [WWW Document]. Wasreb. URL http://wasreb.go.ke/tariffs/index.php?wsp=5 (accessed 6.27.20).

Wendland, C., Deegener, S., Behrendt, J., Toshev, P., Otterpohl, R., 2007. Anaerobic digestion of blackwater from vacuum toilets and kitchen refuse in a continuous stirred tank reactor (CSTR). In: Water Science and Technology. IWA Publishing, pp. 187–194.

Werner, C., Panesar, A., Rüd, S.B., Olt, C.U., 2009. Ecological sanitation: Principles, technologies and project examples for sustainable wastewater and excreta management. Desalination 248, 392–401.

WHO, 2016. WHO | UN-water global analysis and assessment of sanitation and drinking-water (GLAAS) 2014 - report. WHO.

WHO, 2019. Sanitation [WWW Document]. URL https://www.who.int/news-room/fact-sheets/detail/sanitation (accessed 8.15.20).

WHO, n.d. Household air pollution and health [WWW Document]. 2018. URL https://www.who.int/news-room/fact-sheets/detail/household-air-pollution-and-health (accessed 3.28.20).

Wojciechowska-Shibuya, M., 2015. The UNSGAB Journey.

World Bank, G., 2014. Electric power consumption (kWh per capita) | Data [WWW Document]. World Bank. URL https://data.worldbank.org/indicator/EG.USE.ELEC.KH.PC (accessed 8.15.20).

World Bank Group, 2020a. Access to Energy - Our World in Data [WWW Document]. URL https://ourworldindata.org/energy-access#access-to-clean-fuels-for-cooking (accessed 5.31.20).

World Bank Group, 2020b. Providing Sustainable Sanitation and Water services to Low-income Communities in Nairobi [WWW Document]. URL https://www.worldbank.org/en/news/feature/2020/02/19/providing-sustainable-sanitation-and-water-services-to-low-income-communities-in-nairobi (accessed 7.4.20).

World Data, 2018. Average height of men and women worldwide [WWW Document]. World Data Info. URL https://www.worlddata.info/average-bodyheight.php#by-population (accessed 6.20.20).

World Economic Forum, 2020. The Global Risks Report 2020 Insight Report 15th Edition, 15th Edition.

World Health Organization, 2014. UN-Water global analysis and assessment of sanitation and drinking-water (GLAAS) 2014 report: Investing in Water and Sanitation - Increasing access, reducing inequalities, World Health Organization. WHO Document Production Services.

Wu, D., Sun, F., Zhou, Y., 2017. Degradation of Chloramphenicol with Novel Metal Foam Electrodes in Bioelectrochemical Systems. Electrochim. Acta 240, 136–145.

WWAP, 2017. The United Nations World Water Development Report 2017.

Xu, S., Zhang, Y., Luo, L., Liu, H., 2019. Startup performance of microbial electrolysis cell assisted anaerobic digester (MEC-AD) with pre-acclimated activated carbon. Bioresour. Technol. Reports 5, 91–98.

Yamashita, T., Yokoyama, H., 2018. Molybdenum anode: A novel electrode for enhanced power generation in microbial fuel cells, identified via extensive screening of metal electrodes. Biotechnol. Biofuels 11.

Yan, Weifu, Xiao, Y., Yan, Weida, Ding, R., Wang, S., Zhao, F., 2019. The effect of bioelectrochemical systems on antibiotics removal and antibiotic resistance genes: A review. Chem. Eng. J. 358, 1421–1437.

Yang, W., Zhang, F., He, W., Liu, J., Hickner, M.A., Logan, B.E., 2014. Poly(vinylidene fluoride-co-hexafluoropropylene) phase inversion coating as a diffusion layer to enhance the cathode performance in microbial fuel cells. J. Power Sources 269, 379–384.

Yang, Z., Wang, W., He, Y., Zhang, R., Liu, G., 2018. Effect of ammonia on methane production, methanogenesis pathway, microbial community and reactor performance under mesophilic and thermophilic conditions. Renew. Energy 125, 915–925.

Yasri, N., Roberts, E.P.L., Gunasekaran, S., 2019. The electrochemical perspective of bioelectrocatalytic activities in microbial electrolysis and microbial fuel cells. Energy Reports 5, 1116–1136.

Yasri, N.G., Nakhla, G., 2017. The performance of 3-D graphite doped anodes in microbial electrolysis cells. J. Power Sources 342, 579–588.

Yin, C., Shen, Y., Yuan, R., Zhu, N., Yuan, H., Lou, Z., 2019. Sludge-based biochar-assisted thermophilic anaerobic digestion of waste-activated sludge in microbial electrolysis cell for methane production. Bioresour. Technol. 284, 315–324.

Yongtae Ahn, S.I. and J.-W., 2017. Optimizing the operating temperature for microbial electrolysis cell treating sewage sludge. Hydrog. Energy.

Yu, Z., Leng, X., Zhao, S., Ji, J., Zhou, T., Khan, A., Kakde, A., Liu, P., Li, X., 2018. A review on the applications of microbial electrolysis cells in anaerobic digestion. Bioresour. Technol. 255, 340–348.

Yun-Hai, W., Bai-Shi, W., Bin, P., Qing-Yun, C., Wei, Y., 2013. Electricity production from a bio-electrochemical cell for silver recovery in alkaline media. Appl. Energy 112, 1337–1341.

Zhang, F., Pant, D., Logan, B.E., 2011. Long-term performance of activated carbon air cathodes with different diffusion layer porosities in microbial fuel cells. Biosens. Bioelectron. 30, 49–55.

Zhang, Q., Zhang, Y., Li, D., 2017. Cometabolic degradation of chloramphenicol via a meta-cleavage pathway in a microbial fuel cell and its microbial community. Bioresour. Technol. 229, 104–110.

Zhang, S., Bing, H., Yuxin, H., 2015. Effects of Three Types of Separator Membranes on the Microbial Fuel Cells Performance. In: International Conference on Mechatronics, Electronic, Industrial and Control Engineering. pp. 1592–1596.

Zhang, T., Nie, H., Bain, T.S., Lu, H., Cui, M., Snoeyenbos-West, O.L., Franks, A.E., Nevin, K.P., Russell, T.P., Lovley, D.R., 2013. Improved cathode materials for microbial electrosynthesis. Energy Environ. Sci. 6, 217–224.

Zhang, X., He, W., Ren, L., Stager, J., Evans, P.J., Logan, B.E., 2015. COD removal characteristics in air-cathode microbial fuel cells. Bioresour. Technol. 176, 23–31.

Zhang, Y., Merrill, M.D., Logan, B.E., 2010. The use and optimization of stainless steel mesh cathodes in microbial electrolysis cells. Int. J. Hydrogen Energy 35, 12020–12028.

Zhao, F., Slade, R.C.T., Varcoe, J.R., 2009. Techniques for the study and development of microbial fuel cells: an electrochemical perspective. Chem. Soc. Rev. 38, 1926–1939.

Zhu, H., Dong, Z., Huang, Q., Song, T.S., Xie, J., 2019. Fe3O4/granular activated carbon as an efficient three-dimensional electrode to enhance the microbial electrosynthesis of acetate from CO2. RSC Adv. 9, 34095–34101.

Zhu, N., Chen, X., Zhang, T., Wu, P., Li, P., Wu, J., 2011. Improved performance of membrane free single-chamber air-cathode microbial fuel cells with nitric acid and ethylenediamine surface modified activated carbon fiber felt anodes. Bioresour. Technol. 102, 422–426.

13 Appendix

13.1 MEC Research Papers

Table 13-1: MEC Research Papers

No.	Substrate / Feedstock	Inoculation Source	COD Input Range (mg/L)	Batch / Flow	Architecture type	Scale (L)	No. of electrodes	Specific Anode Surface Area SSCA (m2/m3)	Specific Cathode Surface Area SSCA (m2/m3)	Anode Material & Design (+) means treated
1	Acetate				Dual Chamber	0.003				Graphite Felt
2	Synthetic WW +	Effluent from previous MFC	1 g/L sodium acetate, 50 mM phosphate buffer	Batch	Single Chamber	0.028	2		810 m2/m3	Graphite fibre brush
4	Cheese whey	MFC and M	1000 mg/L	Continuous	Single	0.032		0.18 m2		Graphite brush
5					Dual Chamber	0.044				Graphite Granules
6	Synthetic WW	10 mL anaerobic mixed culture		Continuous	Dual Chamber	0.066	2	22 cm2	764 m2/g	Platinum-iridium-coated titanium plate
7	Synthetic WW	10 mL anaerobic mixed culture		Continuous	Dual Chamber	0.066	2	23 cm2	0.438 m2/g	Platinum-iridium-coated titanium plate
8	Synthetic WW	-	-	-	Dual Chamber	0.1	-	10.56	10.55497345	Graphite and titanium wire
9	Acetate				Dual Chamber	0.22				Carbon Cloth
10	Synthetic WW			Flow	Single Chamber	0.25	2			Graphite felt
11	Urban WW				Single Chamber	0.3				BiOx/TiO2
12	Synthetic WW +	Sln from existing MEC	1000 mg/L		Single Chamber	0.4		18200 m2/m3	14 cm2 each	Graphite Brush
13	Synthetic WW	UASB sludge	5 000 mg/L	Flow	Single Chamber	0.56	2	1.7 m2/m3	0.025 m2	Pt- coated (50 g/m2) titanium mesh

14	Artificial Beer wastewater +	Urban wastewater +	1500-2000	Continuous	Single Chamber	0.6	2	N/A	N/A	Granular Graphite
15	Artificial Beer wastewater	Urban wastewater +	1500-2000	Continuous	Single Chamber	0.6	2	N/A	N/A	Granular Graphite
16	Artificial Beer wastewater	Urban wastewater +	1500-2000	Continuous	Single Chamber	0.6	2	N/A	N/A	Granular Graphite
17	Acetate				Dual Chamber	0.62				Carbon Cloth
19	Acetate				Dual Chamber	0.7				Carbon Fibres and titanium plate
20	Synthetic WW +	Sludge fermation liquid	1500 mg/L	Continuous		1.2	2			Carbon brush in the external tube.
21	Acetate				Dual Chamber	1.22				Carbon Cloth
22	Acetate				Tri Chamber	1.7				Carbon Brush
23	Domestic WW	Domestic WW	121 mg/L	Continuous	Single Chamber	2	2			Carbon Felt
24	Brewery WW		1125 +/- 66 mg/L	Semi - continuous	Single	2.1	2			Graphite fibre brushes
25	Synthetic WW +	Acetic acid fed MFC 1:1 ratio	1000 mg/L	Continuous	Single Chamber	2.5	16	5300 m2/m3	64 m2/m3	Graphite Brush +
26	Urban WW +	AD effluent		Batch	Single Chamber	2.5	2			Graphite rod
27	Synthetic WW +	MFC inoculum	3500 mg/Le4000 mg/	Continuous	£ compartments	3.46	6	60 cm2		Anode Film
28	Urban WW	Urban WW		Continuous	Dual Chamber	8	10			Carbon Fibres & Titanium plate +
29	Urban WW	Urban WW		Continuous	Dual Chamber	8	10			Carbon Fibres & Titanium plate +
30	Urban WW	Urban WW		Continuous	Dual Chamber	8	10			Carbon Fibres & Titanium plate +
31	Urban WW	Urban WW		Continuous	Dual Chamber	8	10			Graphite Felt
32	Urban WW	Urban WW + Acetate	365 - 476	Batch	Dual Chamber	8	2	2.226	2.226	Graphite Felt
33	Urban WW	Urban WW + Acetate	164.4	Continuous	Dual Chamber	8	2	2.226	2.226	Graphite Felt

34	Pig Slurry	Urban WW Digestate	2610	Batch	Dual Chamber	16	2	11.25	11.25	Graphite Felt
35	Urban WW	Urban WW	260 ± 85	Continuous	Dual Chamber	30	8	32	13	Graphite Felt
36	Urban WW	Urban WW + Acetate	147 - 1976	Continuous	Dual Chamber	120	18	16.4	3.4	Carbon Felt
37	Urban WW	Urban WW + Acetate	140	Continuous	Dual Chamber	120	-	16.4	3.4	Carbon Felt
38	Glycerole	AD Sludge +	400	Continuous	Dual Chamber	130	10	1.63	2.72	Graphite Fibre Plate +
39	Synthetic WW +	AD Sludge +	400	Continuous	Dual Chamber	130	10	1.63	2.72	Graphite Fibre Plate +
40	Urban WW	AD Sludge +	500	Continuous	Dual Chamber	130	10	1.63	2.72	Graphite Fibre Plate +
41	Urban WW	Urban WW	261 ± 85	Continuous	Dual Chamber	175	3	34	13	Graphite Felt
42	Winery WW	Raw WW + Sludge	700 - 2000	Continuous	Single Chamber	1000	144		18.1	Graphite Fibre Brush +
43	Synthetic Brewery WW	AD Digestate	65.3 g/L	Batch/Flow	Single Chamber	5.6	2	6.05875	6.05875	graphite rod
44	Urine	Suspended bacteria	-	Batch	Dual Chamber			18200		Graphite Brush +
45	Acetate				Single Chamber					Graphite Felt
46	Urban WW		8-16kg/m3/day	Continuous	Single		20			

No.	Operation (days)	pH Range	HRT (hrs)	Duration (days)	Start-up (days)	Voltage Applied (V)	Temp (C)	Volumetric gas Production (m3 gas/m3 reactor volume/day)	H2 %	CH4%	CO2%	Author
1						0.5	30	0.020				(Liu et al., 2005b)
2		7		6		0.6	30	1.7 +/- 0.1		N/A	N/A	(Call et al., 2009b)
4		6.3	120		5 days	0.8	37	0.8		0.00%		(Rago et al., 2017b)
5								1.1				(Ki et al., 2016)
6		7.1	0.16	90				65	0.00%			(D. Liu et al., 2018)
7		7.1	0.14	90				65	0.00%			(D. Liu et al., 2018)
8		-	-	-	-	-	30	-	-	-	-	(Siegert et al., 2014b)
9			168				-					(Heidrich et al., 2014)
10		7	1600			1	30			N/A	N/A	(Jeremiasse et al., 2010)
11							-					(Babanova et al., 2017)
12		7		30		0.7	30	0.9 mmol-CH4 d−1 m−2	656 mmol CH4/d/ m^2	99.00%		(Cheng et al., 2009)
13		7	0.10	188		0.7	30	0.05 +/- 0.03				(Van Eerten-Jansen et al., 2012b)

14		5.9-6.5	24	15		0.8	30	0.281				(Sangeetha et al., 2016)
15		7.1 - 7.4	25	16		0.8	30	0. 367				(Sangeetha et al., 2016)
16		5.9 - 6.5	26	17		0.8	30	0.130				(Sangeetha et al., 2016)
17						0.25						(Cheng et al., 2009)
19			22.25				30					(Rivera et al., 2017)
20		7	24	30		0.8	25	0.163				(W. Liu et al., 2016)
21			336			-	-					(Rivera et al., 2017)
22			22.25				31	-				(Babanova et al., 2017)
23		6.9	10	90			20	0.391	96.20%	3.80%		(Gil-Carrera et al., 2013a)
25		7		18	3	0.9			neglible	92.00%	~ 8%	(Rader and Logan, 2010)
26		7.8	24	60		0.8	35	9.05 mmol/L/day		90.00%	7.00%	(Anirudh Bhanu, 2019)
27		7	24	56	14	0.9	35 +/- 1 oC			87.00%		(Ran et al., 2014)
28			8	95	18	1		0.0198				(Carlotta-Jones et al., 2020)
29			8	95		1		0				(Carlotta-Jones et al., 2020)
30			8	95	13	1		0.0668				(Carlotta-Jones et al., 2020)
31			8	95	42	1		0.0037				(Carlotta-Jones et al., 2020)
32		7.215	168	-		0.7	19.2	0.026	-	-	-	(Escapa et al., 2015)
33		7.215	24	-		0.7	19.2	0.026	-	-	-	(Escapa et al., 2015)
34		7.9	86	103	25	1	19.2	0.2	98	0	0	(San-Martín et al., 2019)
35		6 - 8.5	5	217	-	0.9	9 - 16	0.041	-	-	-	(Cotterill et al., 2017a)
36			24	365	64	1.1	1 - 22	0.007	98.50%	0.00%	-	(Heidrich et al., 2014)
37		7	24	149	64	1.1	13.5 - 21	0.015	100.00%	0.00%	0.00%	(Heidrich et al., 2013b)
38			48	210	50	1.5	18 - 22	0.013	80.00%	20.00%	-	(Baeza et al., 2017)
39			48	210	50	1.5	18 - 22	0.028	76.30%	23.70%	-	(Baeza et al., 2017)
40		7.32 - 7.6	48	210	50	1.5	18 - 22	0.031	94.10%	5.90%	-	(Baeza et al., 2017)
41		7 - 8.5	5	217	90	0.9	9 - 16	0.005	95.00%	0.00%	-	(Cotterill et al., 2017a)
42		>6	24	100	60	0.9	31	0.190	0.00%	86.00%	-	(Cusick et al., 2011a)
43	140 days	7.7-6	5.6 days	120 days	20	0.5 V changing to 1.0 V	35 +/- 2 oC	0.88-1.6		63.10%		(Xu et al., 2019)
44			1	308		1	30±1	**48.600**	-	-	-	(Call and Logan, 2008b)
45			36			0.8	32	0.220				(Cho and Hoffmann, 2017)
46			0.63			0.13						(Guo and Kim, 2019)

13.2 Feedstock Analysis

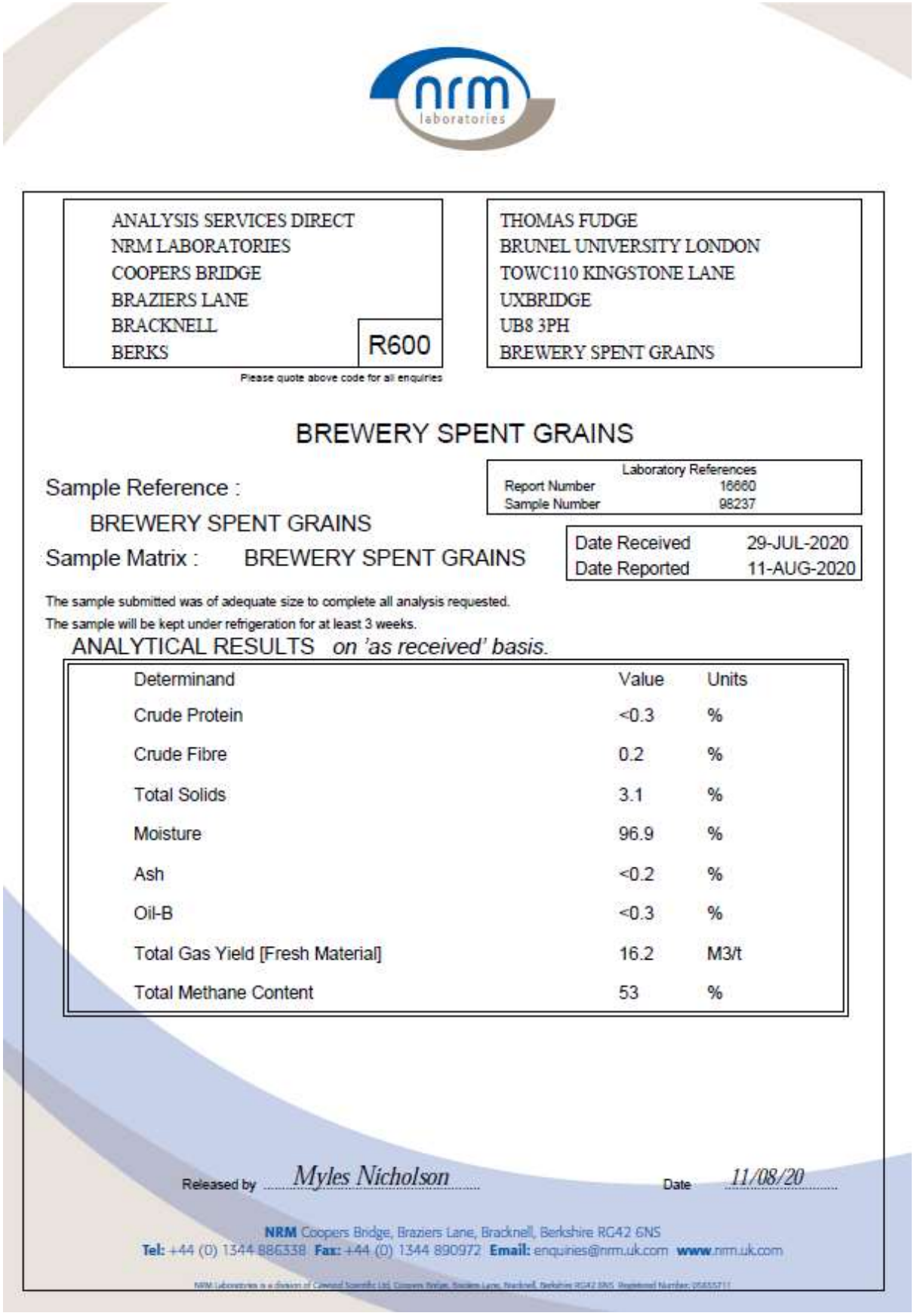

ANALYSIS SERVICES DIRECT
NRM LABORATORIES
COOPERS BRIDGE
BRAZIERS LANE
BRACKNELL
BERKS
R600

Please quote above code for all enquiries

THOMAS FUDGE
BRUNEL UNIVERSITY LONDON
TOWC110 KINGSTONE LANE
UXBRIDGE
UB8 3PH
BREWERY SPENT GRAINS

BREWERY SPENT GRAINS

Sample Reference :
BREWERY SPENT GRAINS
Sample Matrix : BREWERY SPENT GRAINS

Laboratory References	
Report Number	16660
Sample Number	98237

Date Received	29-JUL-2020
Date Reported	11-AUG-2020

The sample submitted was of adequate size to complete all analysis requested.
The sample will be kept under refrigeration for at least 3 weeks.

ANALYTICAL RESULTS *on 'as received' basis.*

Determinand	Value	Units
Crude Protein	<0.3	%
Crude Fibre	0.2	%
Total Solids	3.1	%
Moisture	96.9	%
Ash	<0.2	%
Oil-B	<0.3	%
Total Gas Yield [Fresh Material]	16.2	M3/t
Total Methane Content	53	%

Released by *Myles Nicholson* Date *11/08/20*

NRM Coopers Bridge, Braziers Lane, Bracknell, Berkshire RG42 6NS
Tel: +44 (0) 1344 886338 **Fax:** +44 (0) 1344 890972 **Email:** enquiries@nrm.uk.com **www**.nrm.uk.com

ANALYSIS SERVICES DIRECT
NRM LABORATORIES
COOPERS BRIDGE
BRAZIERS LANE
BRACKNELL
BERKS

R600

Please quote above code for all enquiries

THOMAS FUDGE
BRUNEL UNIVERSITY LONDON
TOWC110 KINGSTONE LANE
UXBRIDGE
UB8 3PH
FECAL SLUDGE

FECAL SLUDGE

Sample Reference :
FECAL SLUDGE
Sample Matrix : FECAL SLUDGE

Laboratory References	
Report Number	16661
Sample Number	96238

Date Received	29-JUL-2020
Date Reported	11-AUG-2020

The sample submitted was of adequate size to complete all analysis requested.
The sample will be kept under refrigeration for at least 3 weeks.

ANALYTICAL RESULTS *on 'as received' basis.*

Determinand	Value	Units
Crude Protein	2.3	%
Crude Fibre	0.1	%
Total Solids	3.8	%
Moisture	96.2	%
Ash	0.8	%
Oil-B	<0.3	%
Total Gas Yield [Fresh Material]	15.1	M3/t
Total Methane Content	66	%

Released by *Myles Nicholson* Date *11/08/20*

NRM Coopers Bridge, Braziers Lane, Bracknell, Berkshire RG42 6NS
Tel: +44 (0) 1344 886338 **Fax:** +44 (0) 1344 890972 **Email:** enquiries@nrm.uk.com **www**.nrm.uk.com

ANALYSIS SERVICES DIRECT
NRM LABORATORIES
COOPERS BRIDGE
BRAZIERS LANE
BRACKNELL
BERKS
R600

Please quote above code for all enquiries

THOMAS FUDGE
BRUNEL UNIVERSITY LONDON
TOWC110 KINGSTONE LANE
UXBRIDGE
UB8 3PH
BREWERY TANK BOTTOM

BREWERY TANK BOTTOM

Sample Reference :
BREWERY TANK BOTTOM
Sample Matrix : BREWERY TANK BOTTOM

Laboratory References	
Report Number	16659
Sample Number	98236

Date Received	29-JUL-2020
Date Reported	11-AUG-2020

The sample submitted was of adequate size to complete all analysis requested.
The sample will be kept under refrigeration for at least 3 weeks.

ANALYTICAL RESULTS *on 'as received' basis.*

Determinand	Value	Units
Crude Protein	2.4	%
Crude Fibre	<0.1	%
Total Solids	8.8	%
Moisture	91.2	%
Ash	0.4	%
Oil-B	<0.3	%
Total Gas Yield [Fresh Material]	43.7	M3/t
Total Methane Content	55	%

Released by *Myles Nicholson* Date *11/08/20*

NRM Coopers Bridge, Braziers Lane, Bracknell, Berkshire RG42 6NS
Tel: +44 (0) 1344 886338 **Fax:** +44 (0) 1344 890972 **Email:** enquiries@nrm.uk.com **www**.nrm.uk.com

ANALYSIS SERVICES DIRECT
NRM LABORATORIES
COOPERS BRIDGE
BRAZIERS LANE
BRACKNELL
BERKS

R600

Please quote above code for all enquiries

THOMAS FUDGE
BRUNEL UNIVERSITY LONDON
TOWC110 KINGSTONE LANE
UXBRIDGE
UB8 3PH
BREWERY BOIL WATER

BREWERY BOIL WATER

Sample Reference :

BREWERY BOIL WATER

Sample Matrix : BREWERY BOIL WATER

Laboratory References	
Report Number	16658
Sample Number	98235

Date Received	29-JUL-2020
Date Reported	11-AUG-2020

The sample submitted was of adequate size to complete all analysis requested.
The sample will be kept under refrigeration for at least 3 weeks.

ANALYTICAL RESULTS *on 'as received' basis.*

Determinand	Value	Units
Crude Protein	1.2	%
Crude Fibre	<0.1	%
Total Solids	13.8	%
Moisture	86.2	%
Ash	0.5	%
Oil-B	<0.3	%
Total Gas Yield [Fresh Material]	71.4	M3/t
Total Methane Content	51	%

Released by *Myles Nicholson* Date *11/08/20*

NRM Coopers Bridge, Braziers Lane, Bracknell, Berkshire RG42 6NS
Tel: +44 (0) 1344 886338 **Fax:** +44 (0) 1344 890972 **Email:** enquiries@nrm.uk.com **www.**nrm.uk.com

13.3 MR Series Brewery Wastewater Analysis

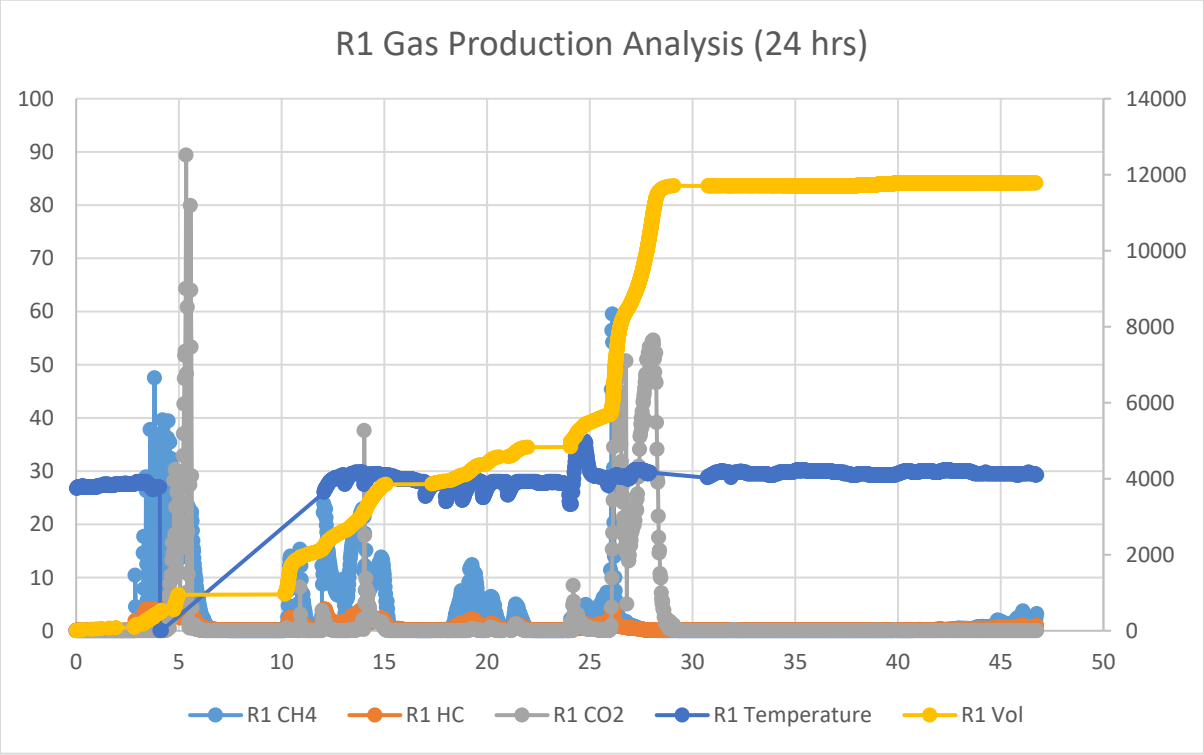

Figure 13-1: EMR Series Test Reactor 1 - (1st series)

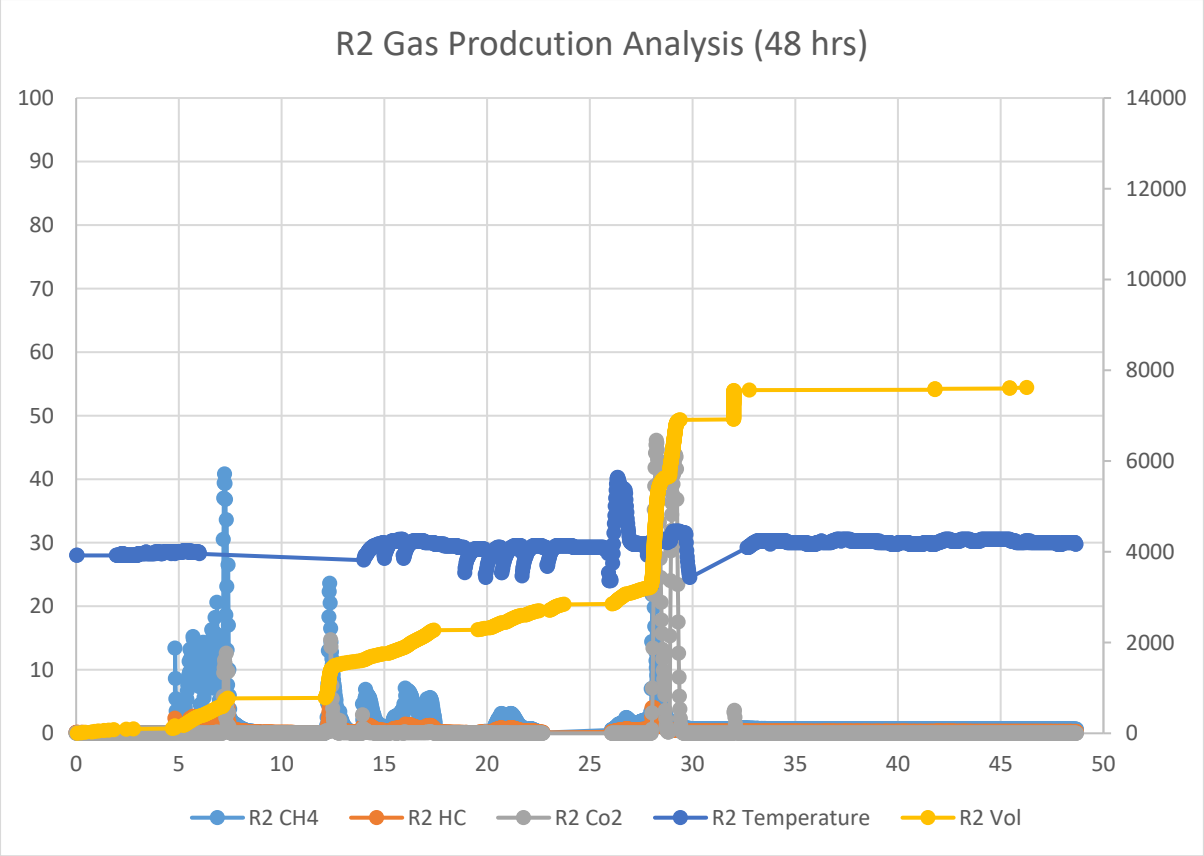

Figure 13-2: EMR Series Test Reactor 2 - (2nd series)

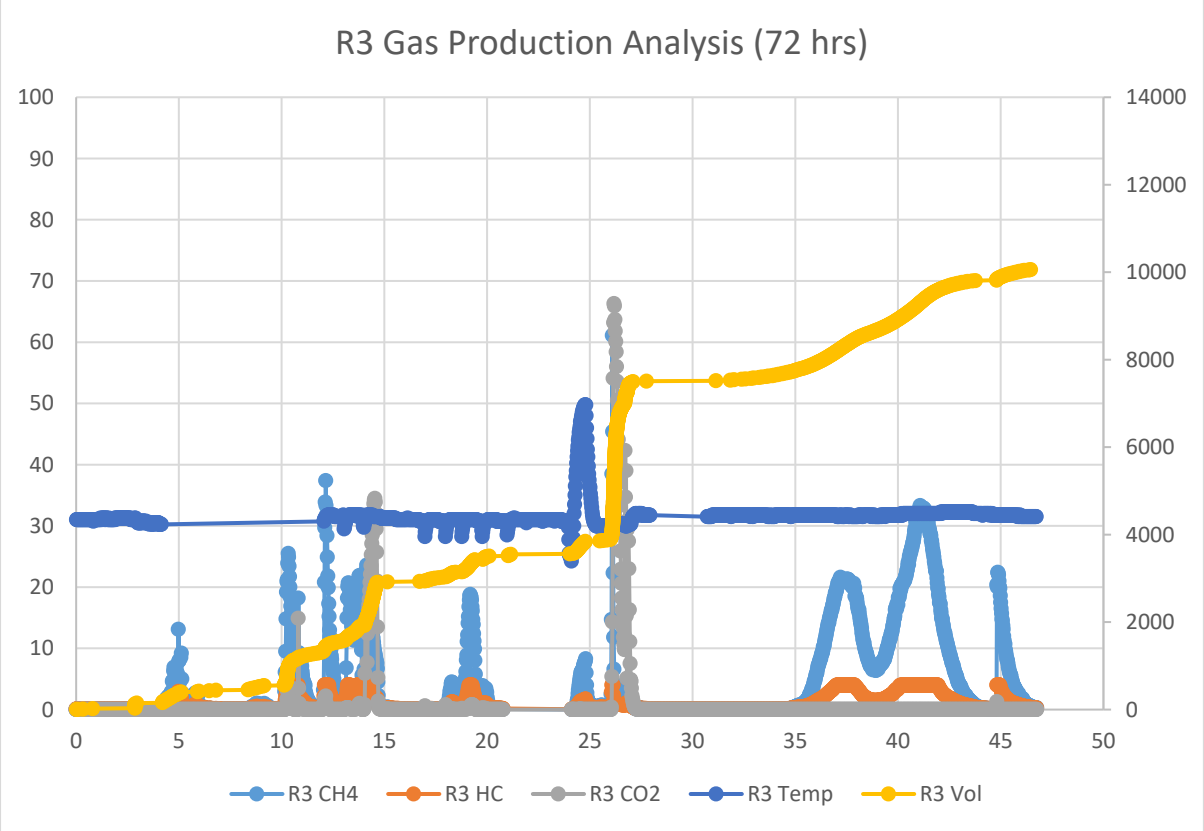

Figure 13-3: EMR Series Test Reactor 3 - (3rd series)

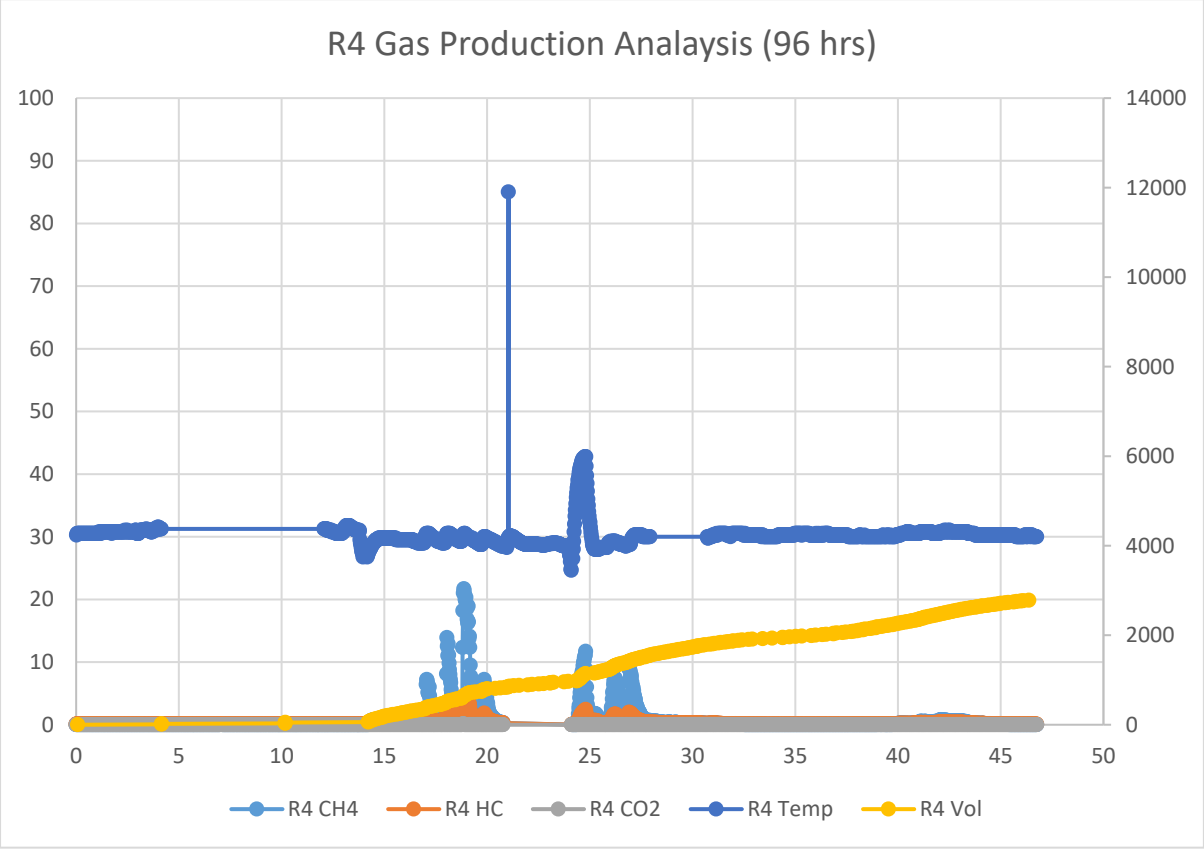

Figure 13-4: EMR Series Test Reactor 4 - (4th series)

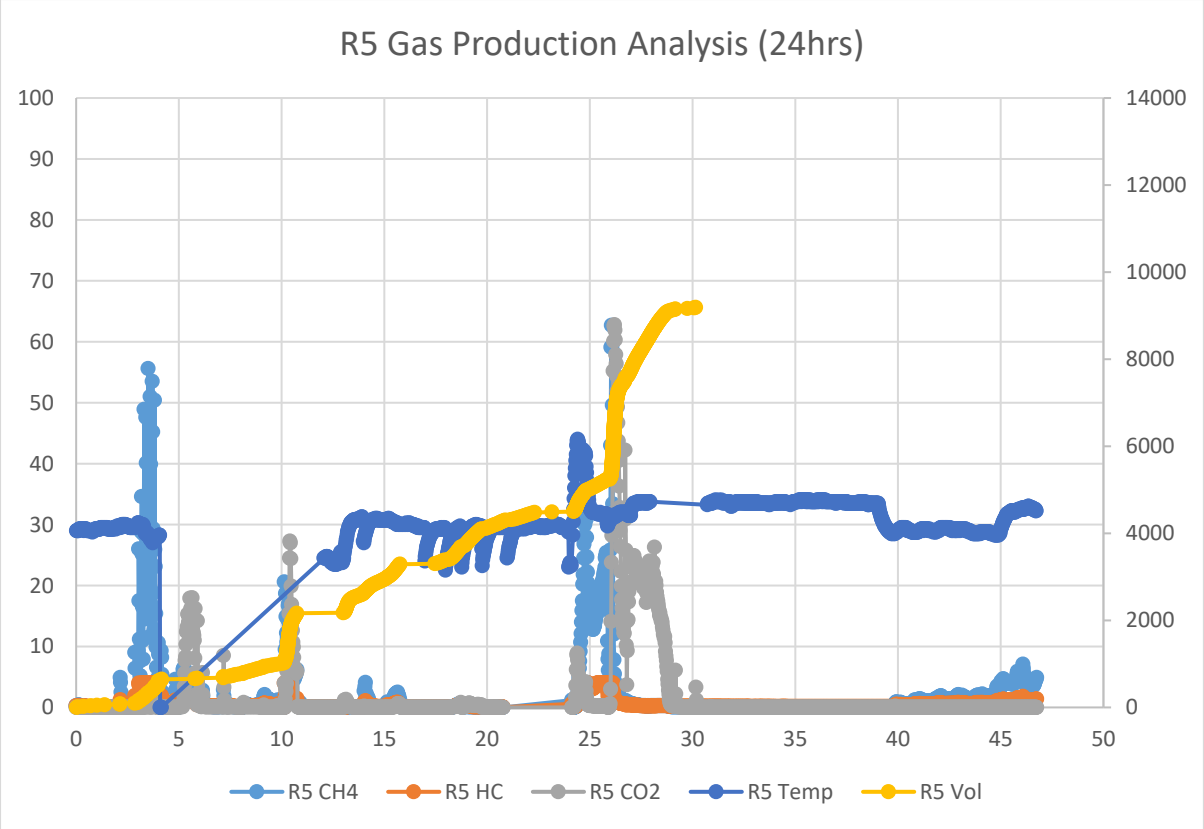

Figure 13-5: EMR Series Test Reactor 5 - (1st series)

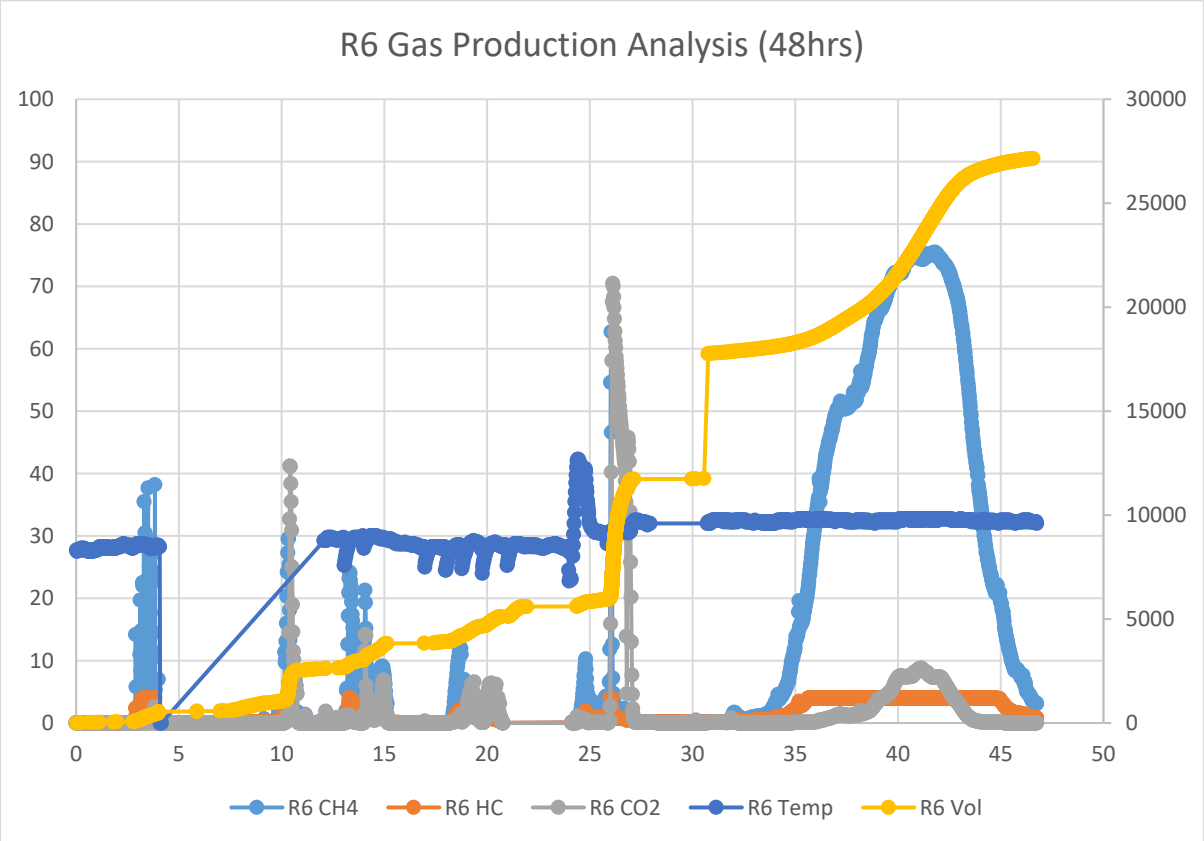

Figure 13-6: EMR Series Test Reactor 6 - (2nd series)

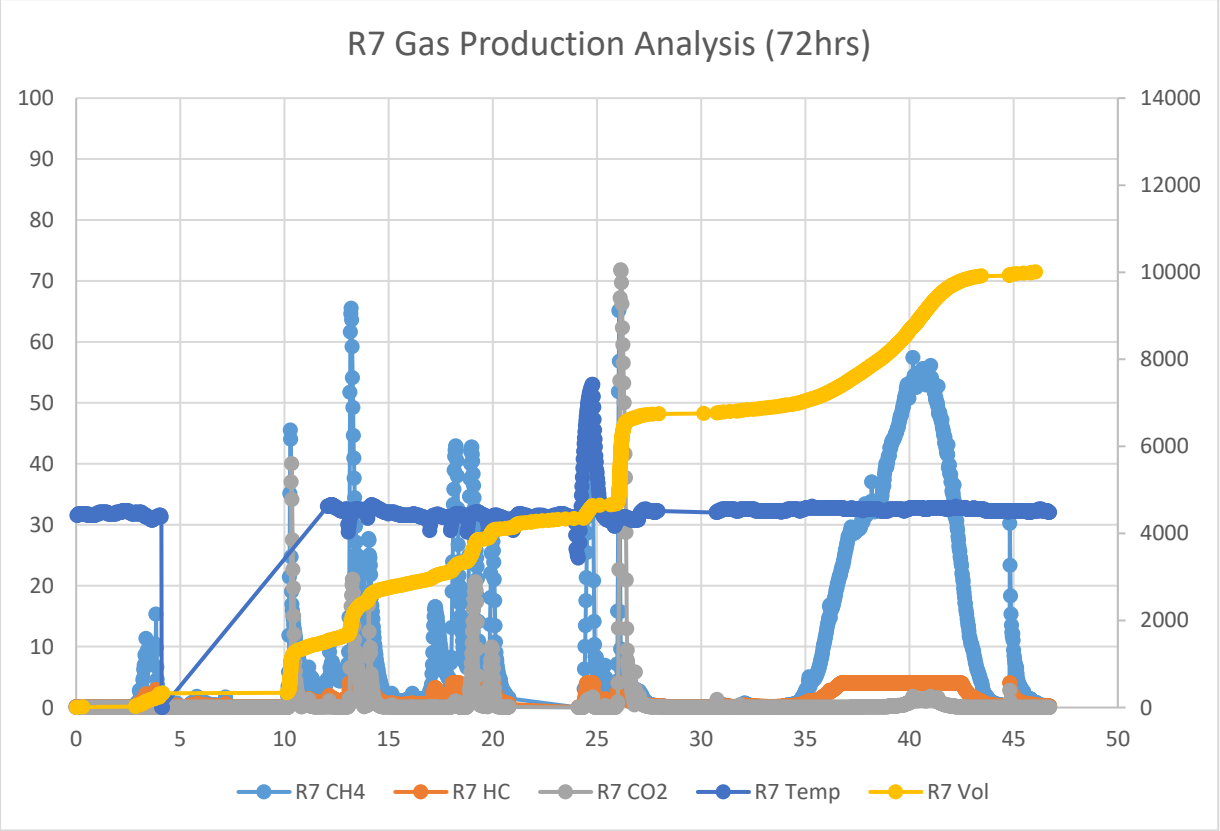

Figure 13-7: EMR Series Test Reactor 7 - (3rd series)

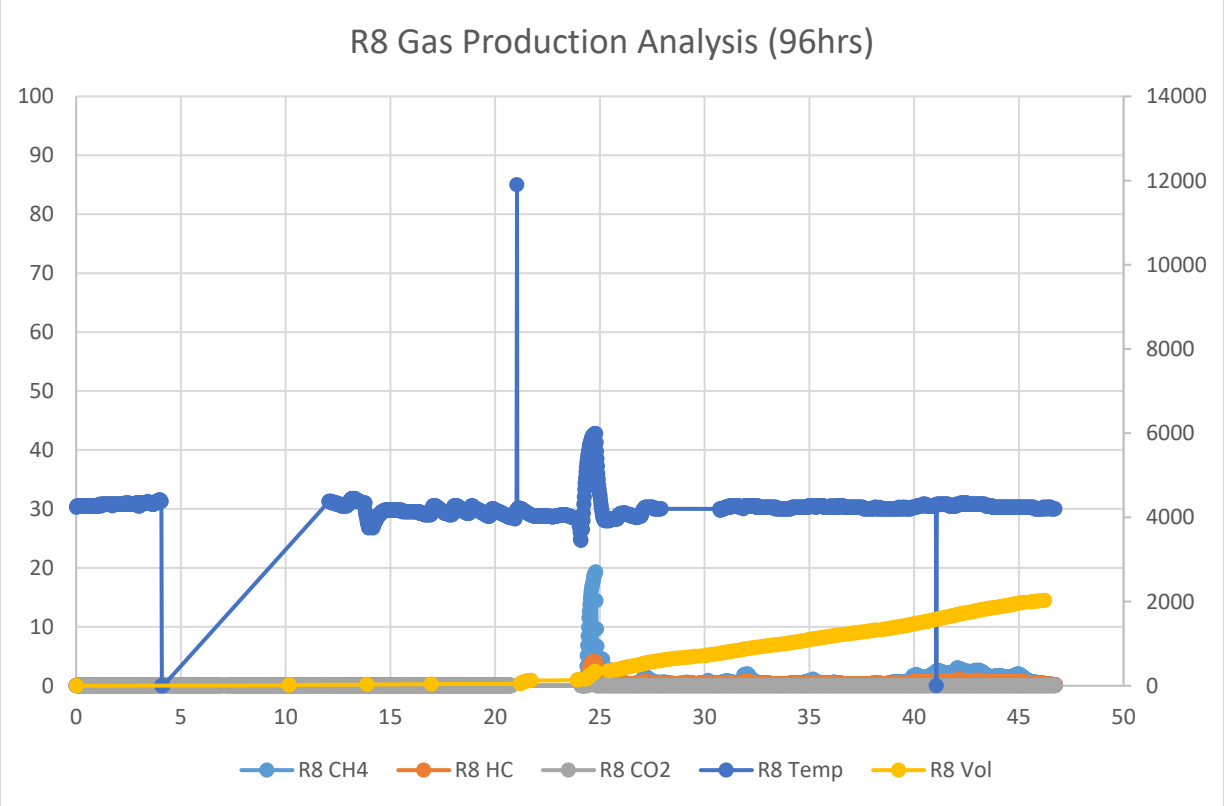

Figure 13-8: EMR Series Test Reactor 8 - (4th series)

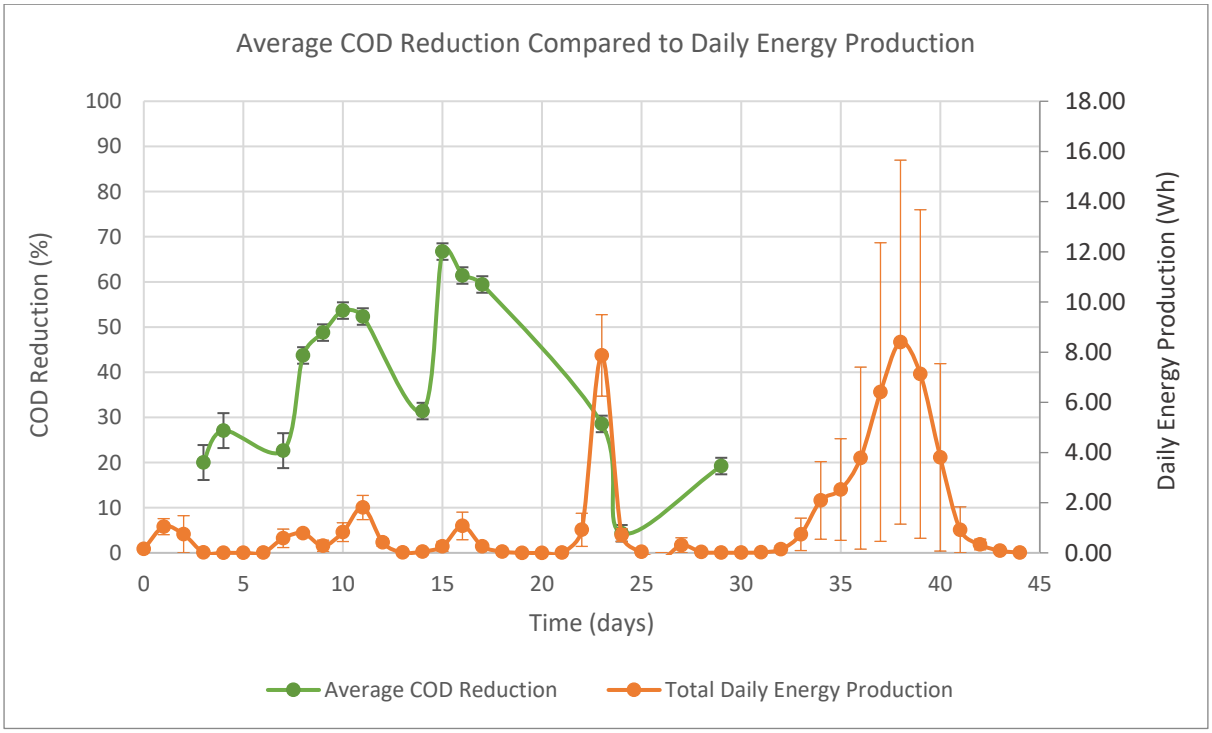

Figure 13-9: Series EMR - Brewery Wastewater COD Percentage Reduction

Table 13-2: Series EMR - Litres and Moles Produced

	Litres of methane			*Moles Recovered*		
Days	0-23	0-30	31-44	0-23	0-30	31-44
R1	0.176	0.240	0.415	0.0061	0.0083	0.0143
R2	0.044	0.071	0.165	0.0015	0.0025	0.0057
R3	0.072	0.096	0.484	0.0025	0.0033	0.0167
R4	0.005	0.009	0.023	0.0002	0.0003	0.0008
R5	0.105	0.135	0.256	0.0036	0.0047	0.0089
R6	0.092	0.144	3.437	0.0032	0.0050	0.1187
R7	0.161	0.195	0.922	0.0056	0.0067	0.0318
R8	0.000	0.001	0.014	0.0000	0.0000	0.0005
First	0.139	0.185	0.120	0.0048	0.0064	0.0042
Second	0.069	0.110	3.134	0.0024	0.0038	0.1082
Third	0.115	0.145	1.353	0.0040	0.0050	0.0467
Fourth	0.002	0.004	0.016	0.0001	0.0002	0.0006

Table 13-3: Series EMR – COD Removed

	COD Removed (g)	
Days	0-23	0-30
R1	110.96	140.13
R2	108.06	136.47
R3	110.31	139.31
R4	154.41	195.00
R5	110.41	139.44
R6	124.62	157.39
R7	143.20	180.85
R8	163.30	206.23
First	112.63	142.24
Second	117.32	148.17
Third	127.43	160.93
Fourth	159.27	201.15
Total	516.66	652.49

13.4 EMR & AD Batch Spent Grain Analysis

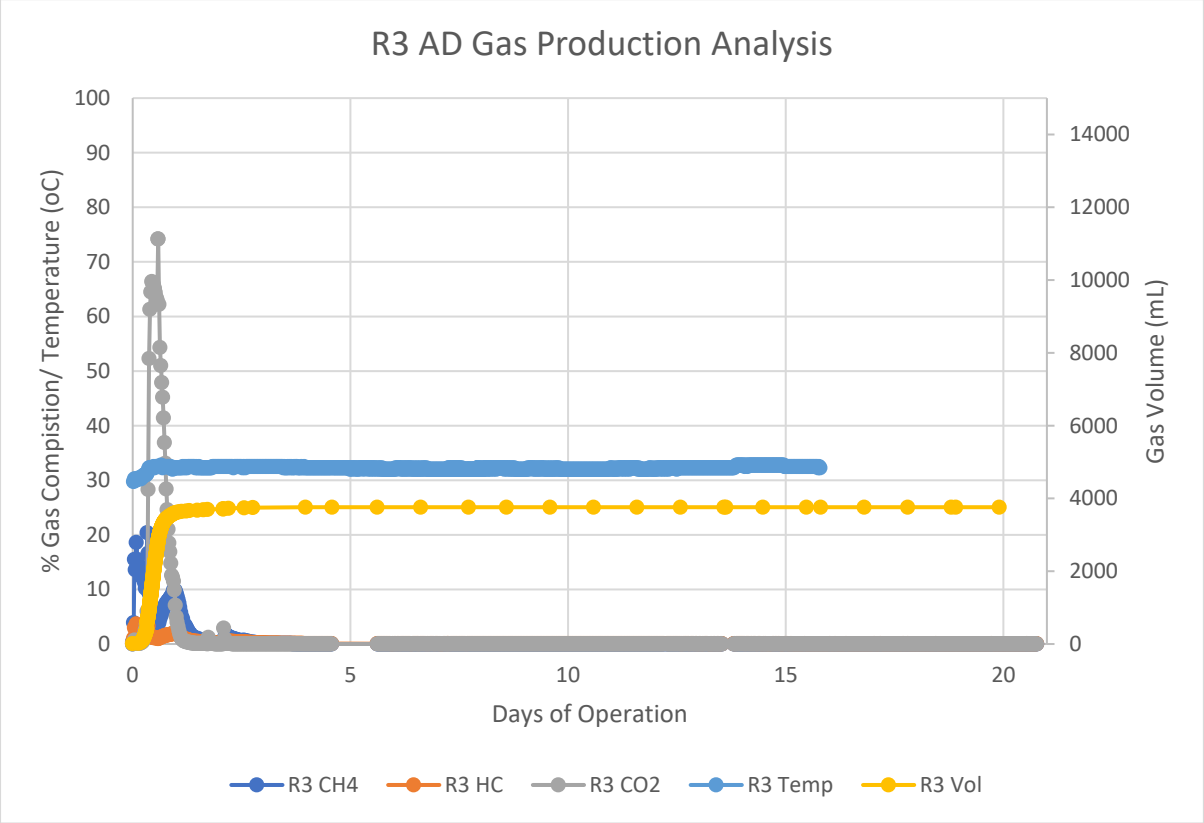

Figure 13-10: Batch – Brewery Spent Grain – AD Reactor 3

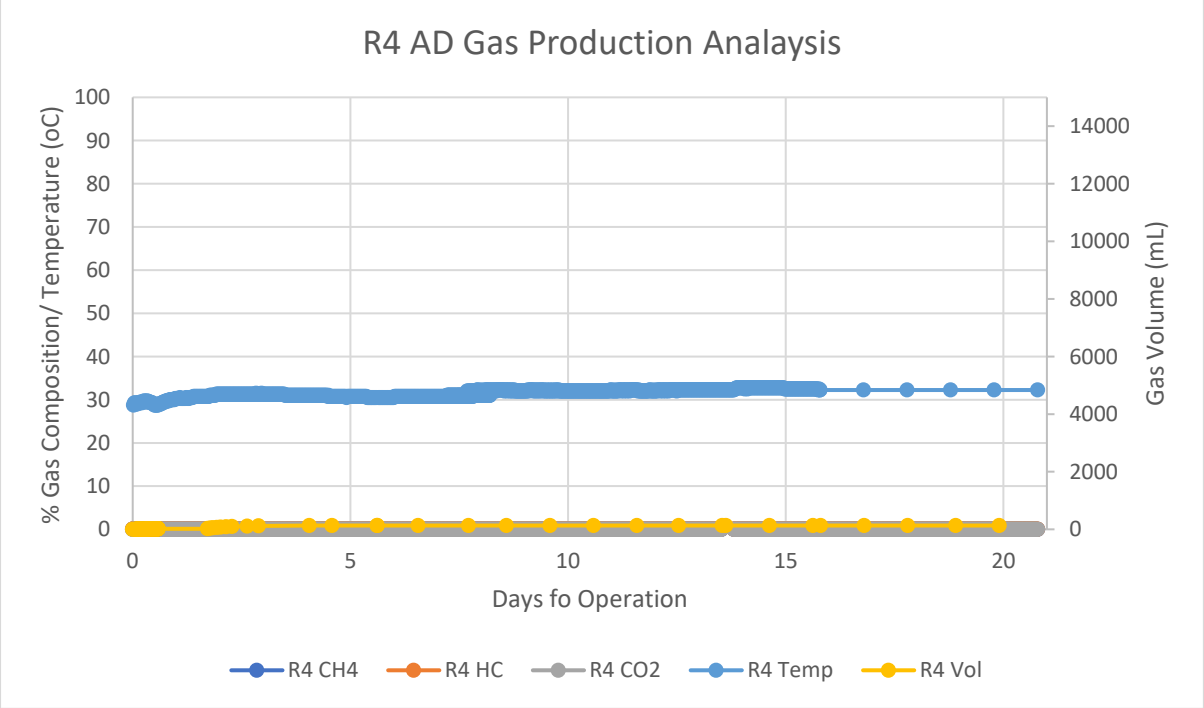

Figure 13-11: Batch – Brewery Spent Grain – AD Reactor 4

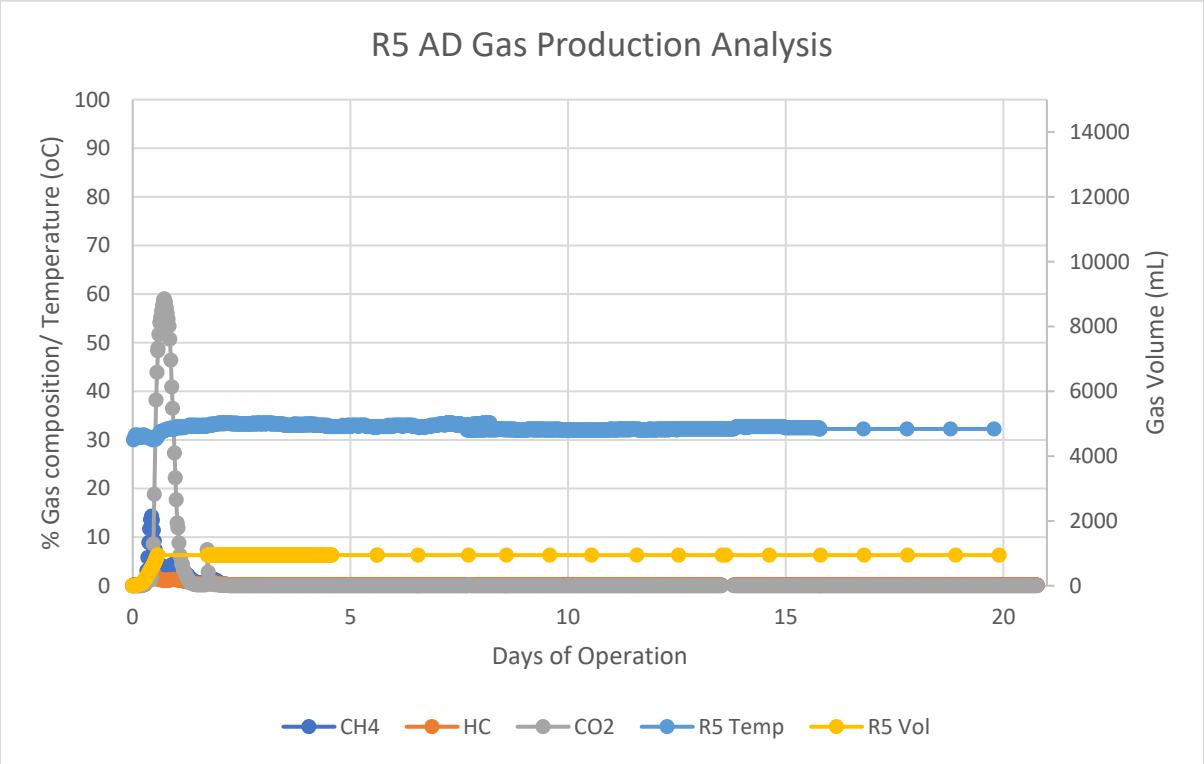

Figure 13-12: Batch – Brewery Spent Grain – AD Reactor 5

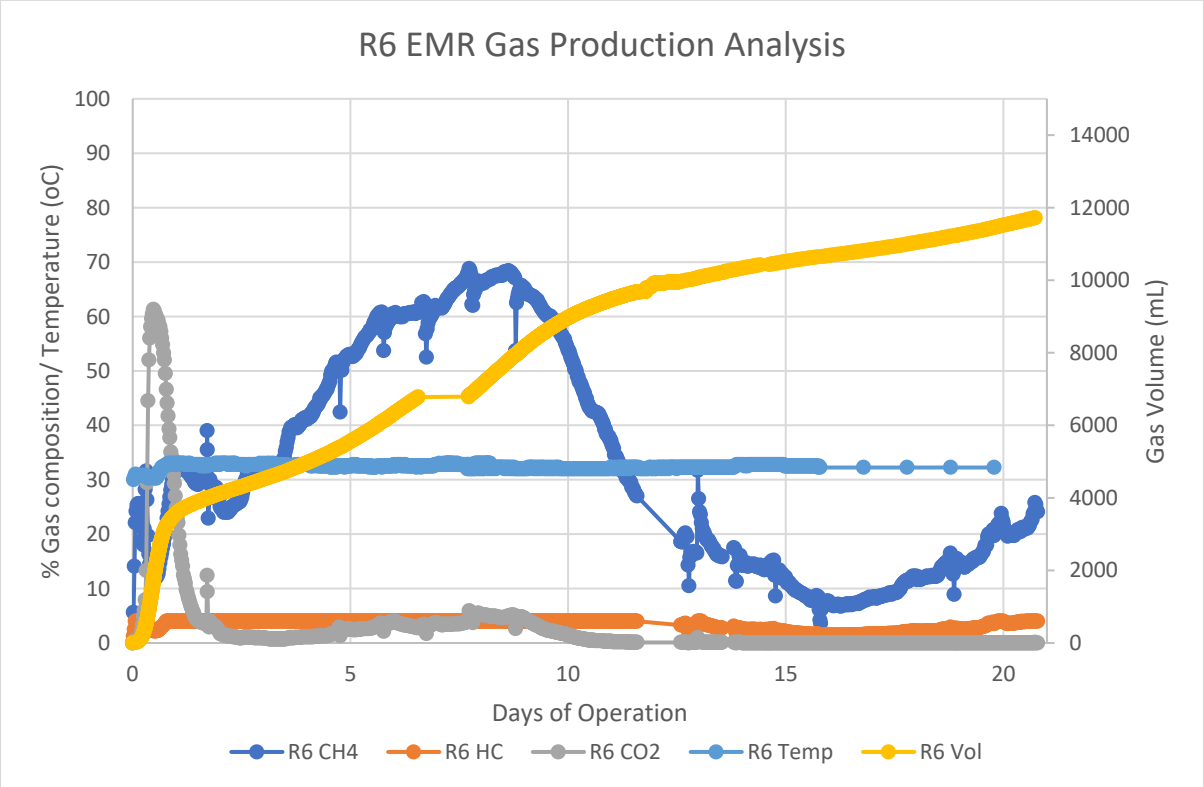

Figure 13-13: Batch – Brewery Spent Grain – EMR Reactor 6

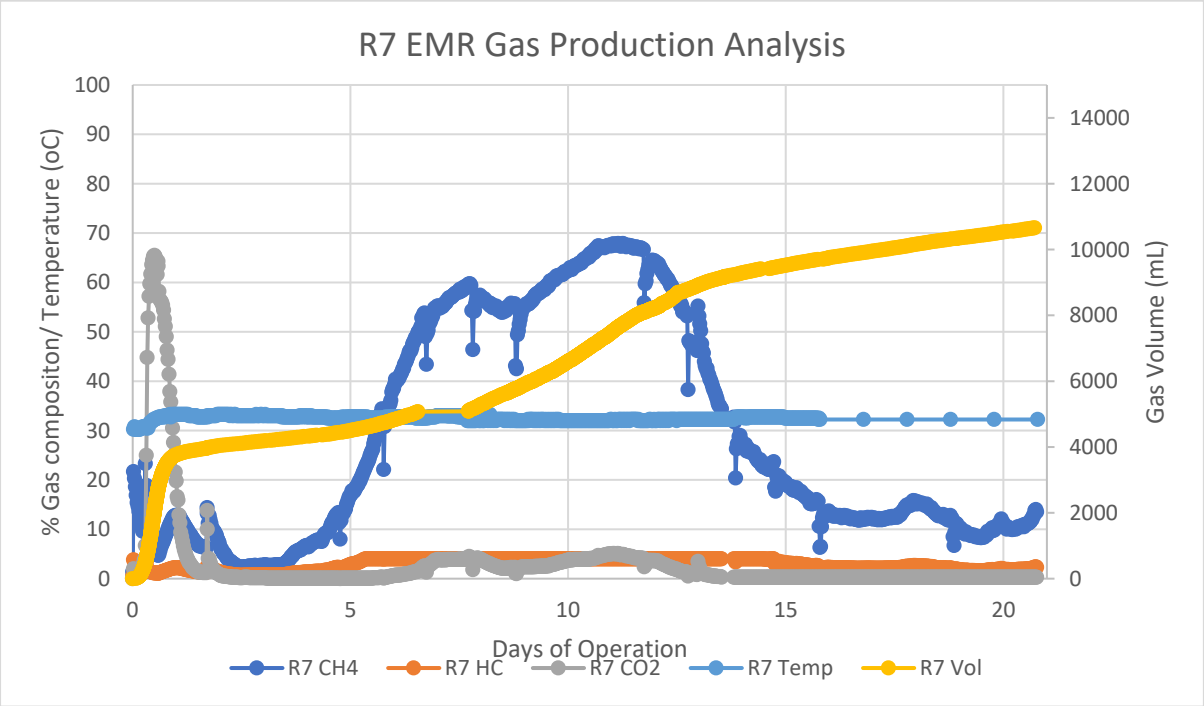

Figure 13-14: Batch – Brewery Spent Grain – EMR Reactor 7

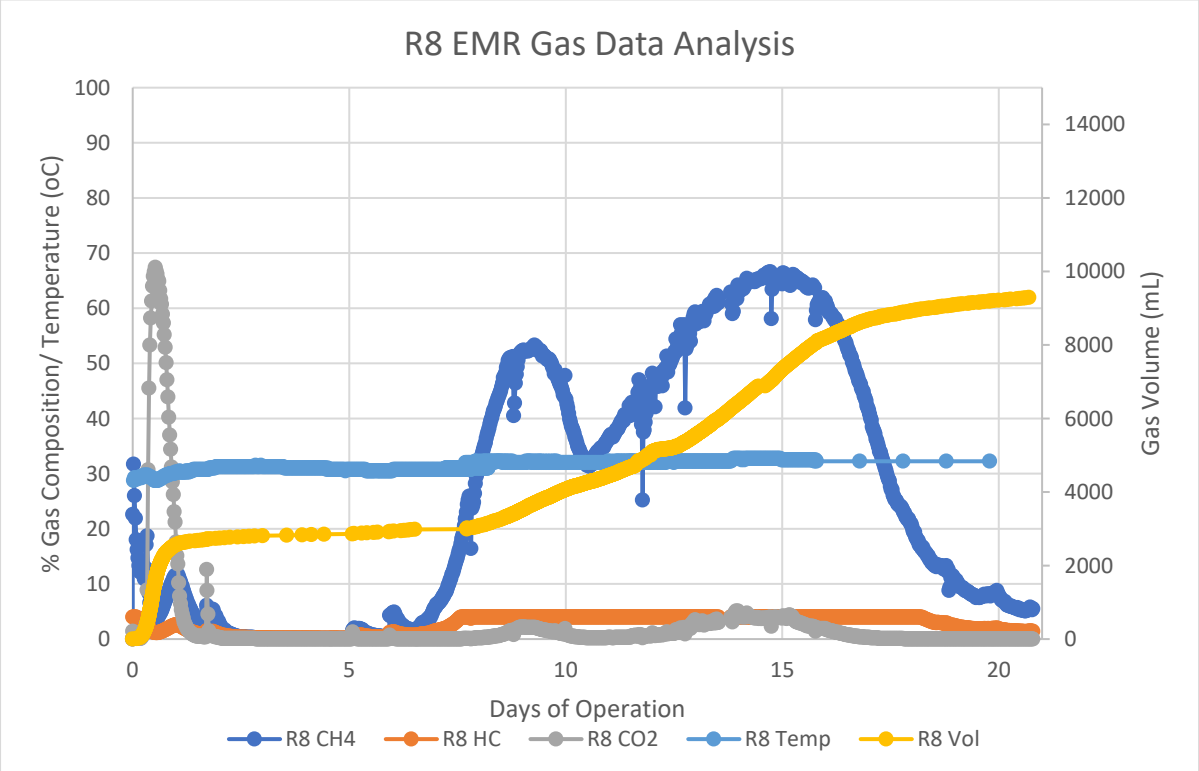

Figure 13-15: Batch – Brewery Spent Grain – EMR Reactor 8

Table 13-4: EMR & AD Batch Wastewater Reactor Effluent Analsyis

	Turbidity	*TDS (g/2ml)*	*TSS (g/2ml)*	*TS (g/10ml)*	*VS (g/10 ml)*
R3 Effluent	3490	0.012	0.0069	0.113	0.029
R4 Effluent	3590	0.015	0.0109	0.125	0.038
R5 Effluent	3460	0.014	0.008	0.173	0.059
R6 Effluent	1830	0.011	0.006	0.071	0.023
R7 Effluent	2050	0.012	0.0092	0.08	0.028
R8 Effluent	2290	0.008	0.0096	0.085	0.025

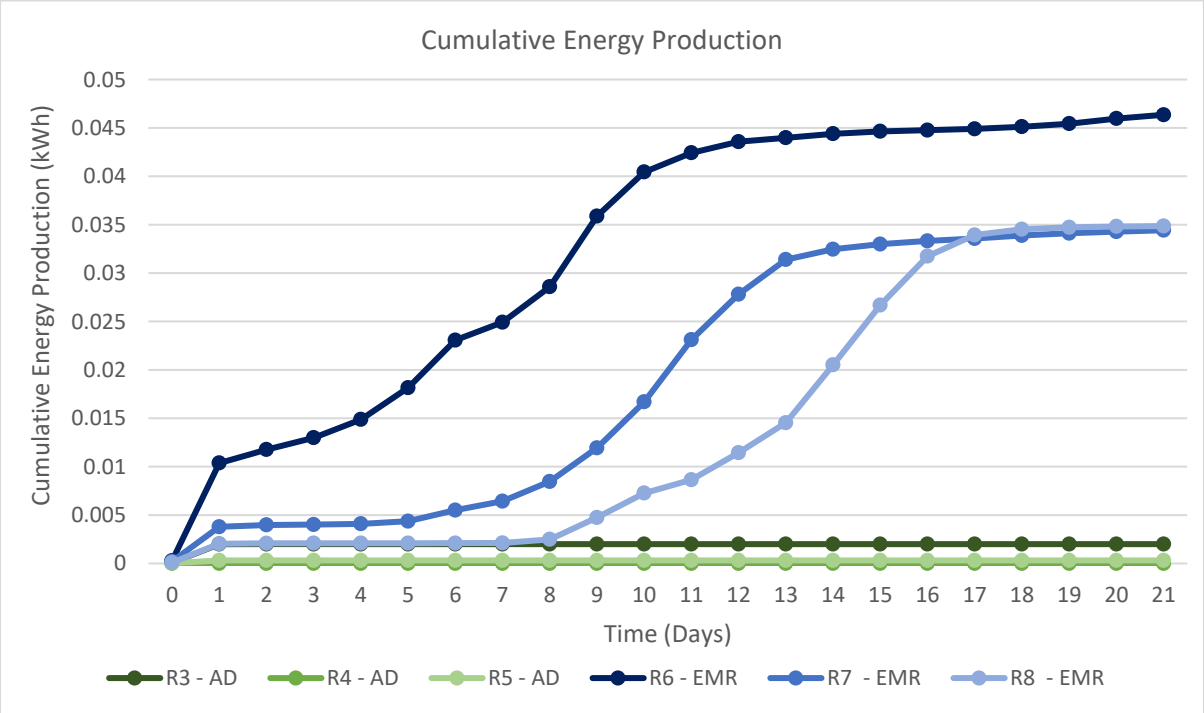

Figure 13-16: Batch EMR & AD –Spent Grain Cumulative Energy Production

EMR & AD Batch Brewery Boil Analysis

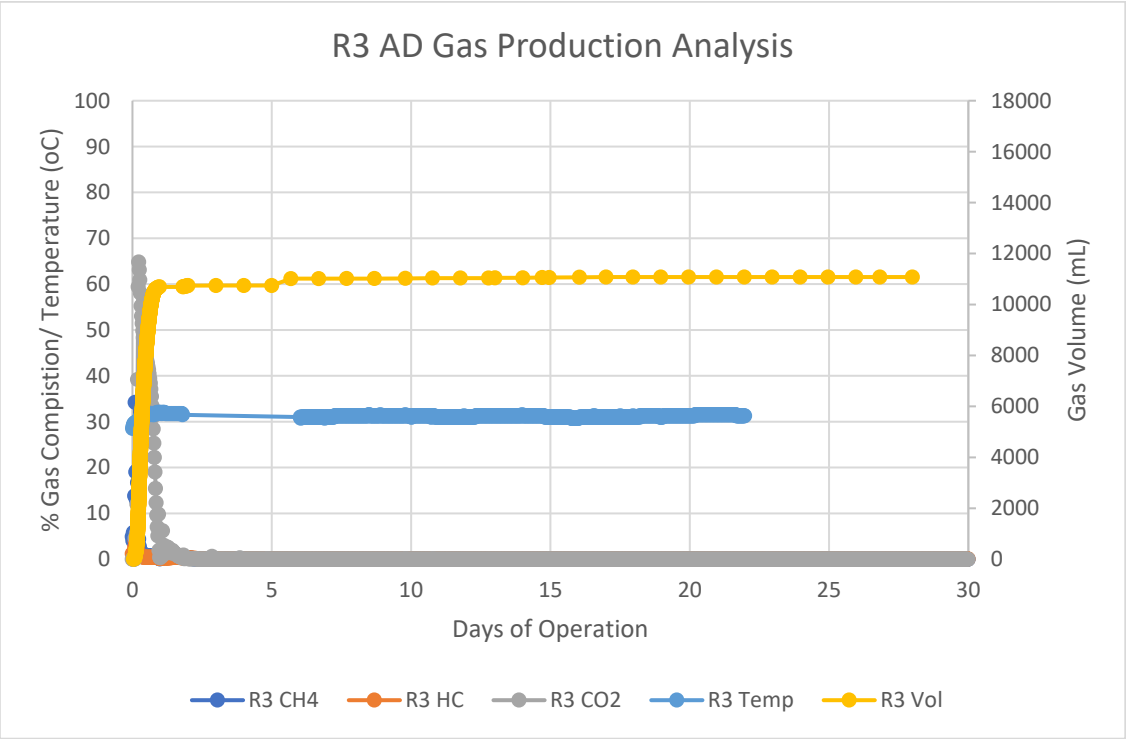

Figure 13-17: Batch – Brewery Boil – AD Reactor 3

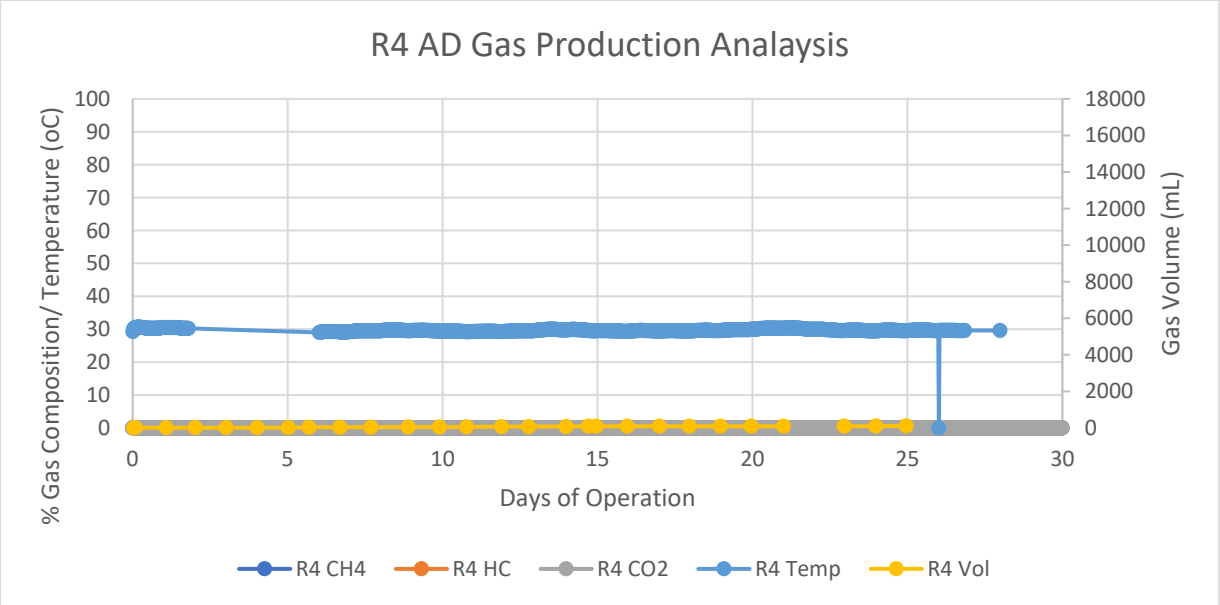

Figure 13-18: Batch – Brewery Boil – AD Reactor 4

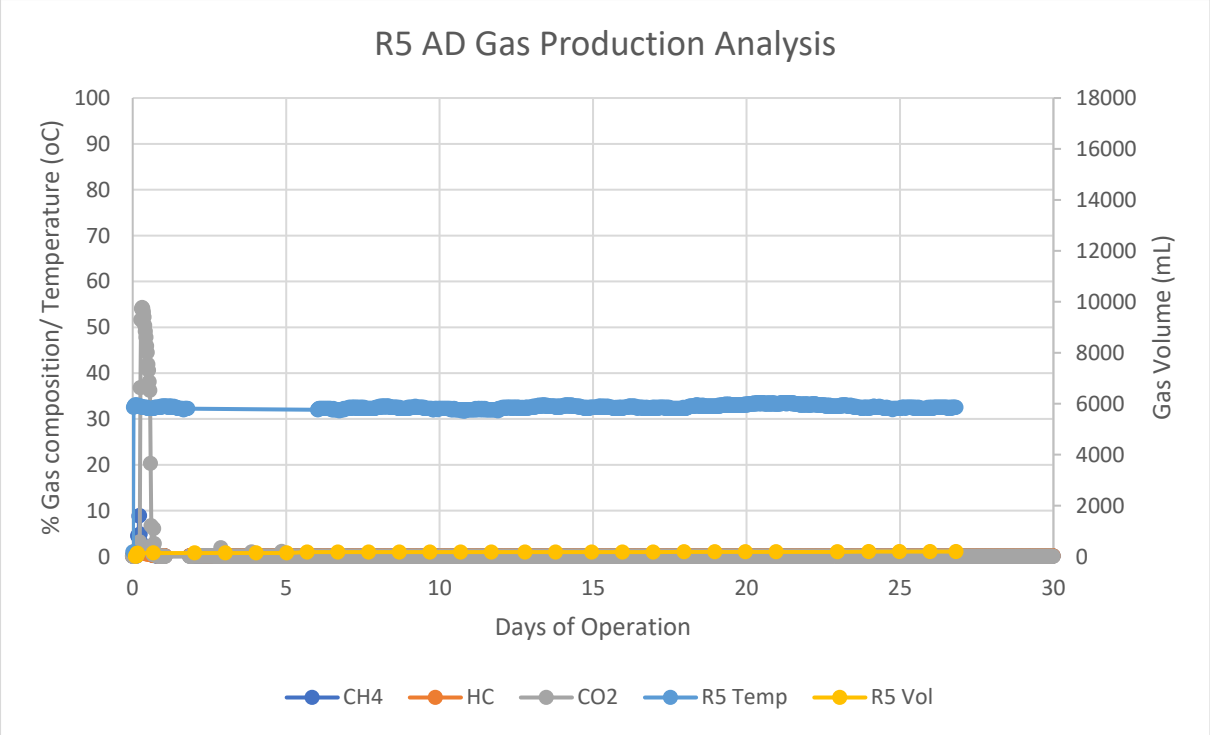

Figure 13-19: Batch – Brewery Boil – AD Reactor 5

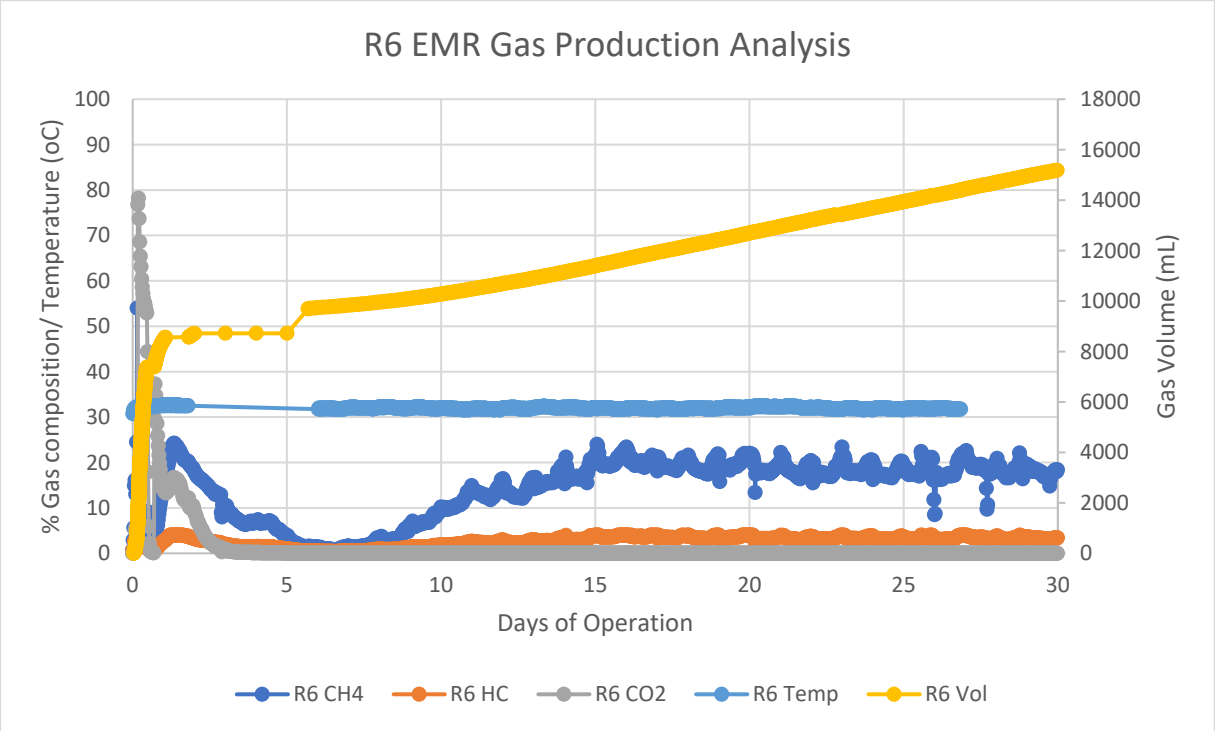

Figure 13-20: Batch – Brewery Boil – EMR Reactor 6

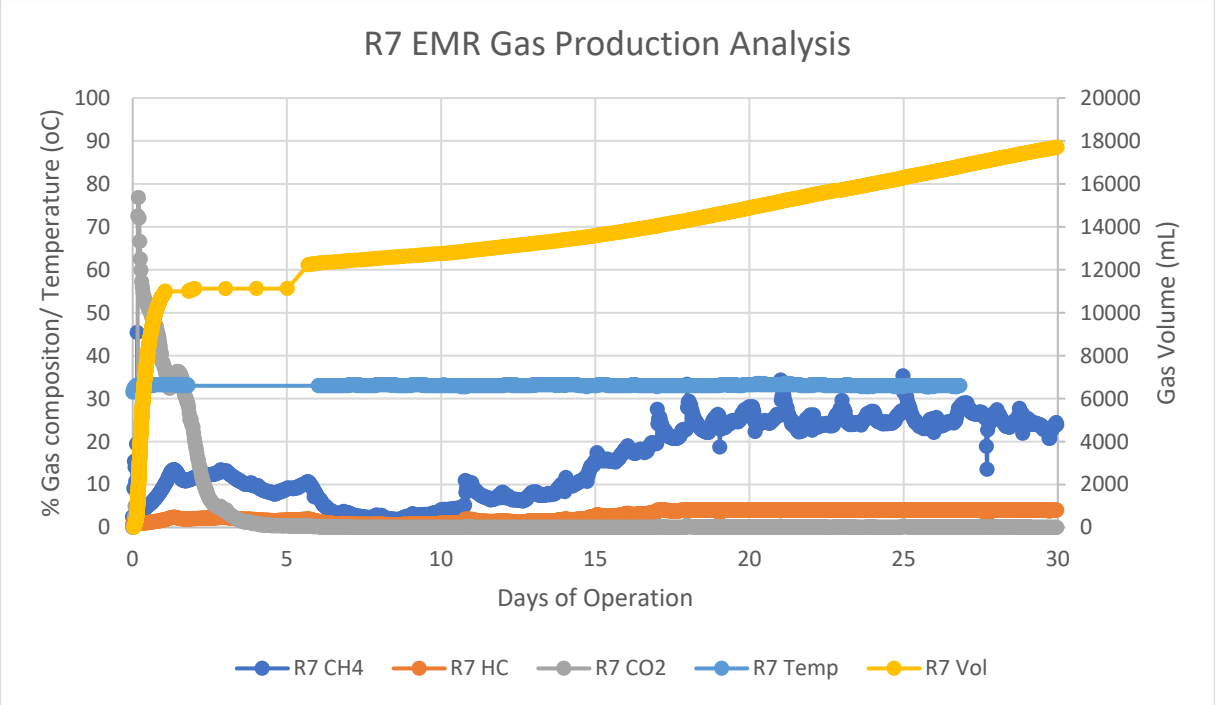

Figure 13-21: Batch – Brewery Boil – EMR Reactor 7

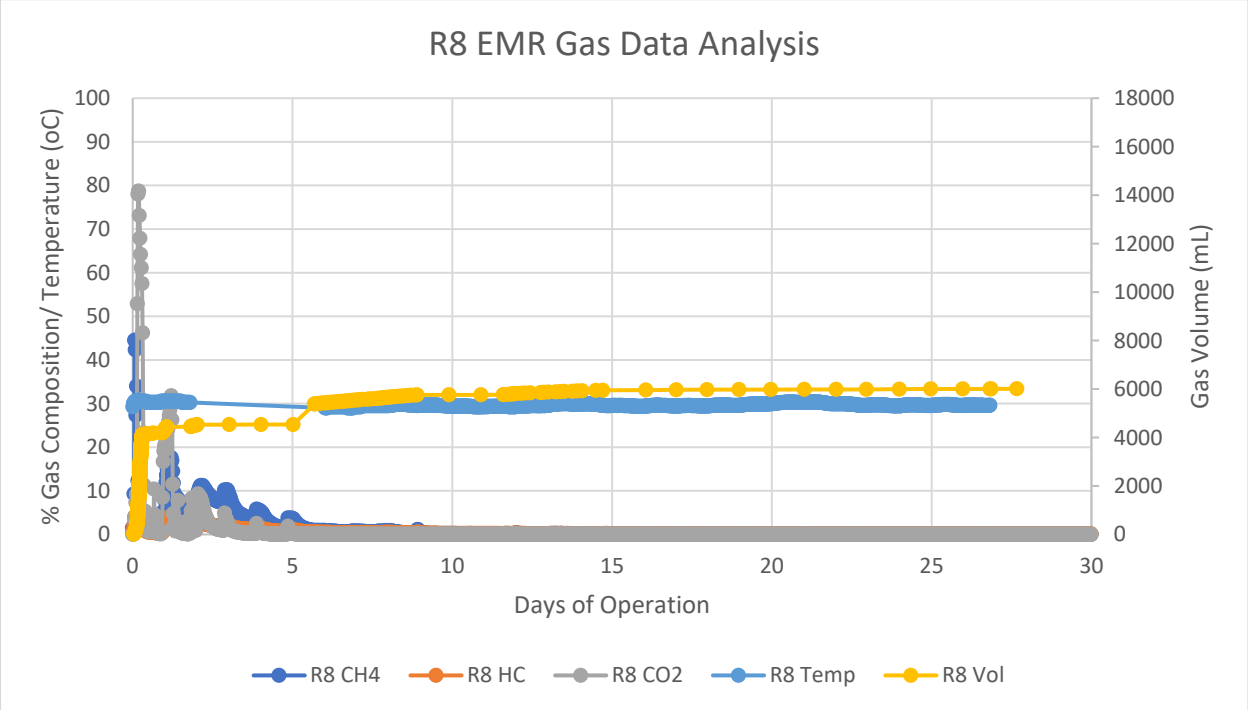

Figure 13-22: Batch – Brewery Boil – EMR Reactor 8

13.5 EMR Pilot Interview Guide Questions

1. How did users react to using the ablution unit?
2. How did users react to the concept of using biogas for cooking that has been produced from faecal sludge?
3. How did users perceive the pilot EMR system?
4. Where would you foresee issues around the installation of EMR technology in the humanitarian context?
5. What concerns do you have around the operational aspects of the technology if it is to be successfully deployed in the field?

13.6 EMR Manufacturing Cost

Table 13-5: EMR Electrode Manufacturing Costs

			Cost per 10,000 unit order		
Part No.	**Item**	**Quantity. (m3)**	**Unit Cost**	**Electrode Blade**	**Cost per 1m^3 Vol.**
	Blade - B - Long electrodes				
A-001	Stainless Steel Pocket	72	£ 2.50	£ 10.00	£ 180.00
A-002	GAC	72	£ 0.40	£ 1.60	£ 28.80
A-003	Carbon Fibre Brush	72	£ 3.00	£ 0.40	£ 216.00
A-004	Rails	72	£ 1.50	£ 6.00	£ 108.00
A-005	Titanium wire	36	£ 0.66	£ 1.32	£ 23.76
A-006	Bolts	72	£ 0.05	£ 0.20	£ 3.60
A-008	Cable Stress Relief	36	£ 0.05	£ 0.10	£ 1.80
	Sub Total				£ 561.96
	Support Frame				
G-001	Cages	0	£ 2.00	£ -	£ -
G-002	Fibreglass rods	43.2	£ 0.40	£ 1.92	£ 17.28
G-003	3 Core Wire	9	£ 1.40	£ 1.40	£ 12.60
G-004	WAGO/Splices	27	£ 0.20	£ 0.60	£ 5.40
	Sub Total				£ 35.28
	Total				£ 630.52

13.7 Kenya – primary data collection field research

Table 13-6: Kenya Refugee Settlement Sanitation and Wastewater Treatment Costs from field research conducted in February 2020

Source	Settlement	Type	Cost (KSH)	Cost (GBP)
UNHCR	Dadaab	Pit Latrine	$270 *(3m)*	
NRC	Dadaab	Pit Latrine	6000 *(1000 per m)* Slab 5000	44.94 - Pit 37.45 - Slab
NRC	Kakuma	Pit Latrine	12,000 total Slab 2900 – *can be reused 2x*	89.88 total 21.72 – Slab
Beneficiary	Kalyobeyei	Pit latrine	10,000 *(3m deep)*	74. 90
		Excavate per metre	500	3.75
Beneficiary	Kalyobeyei	Pit latrine	9600 *(3m deep)*	71.91
		Excavate per meter	3500	26.22
		Poles	700	5.24
		Zinc panels	600 *(need 8 - 4800)*	4.49 *(35.95)*
		SATO Pan	600	4.49
World Vision	Kakuma	Septic Tank 40m^3	1.2 Million KSH	8988.36
Edensfield Sanitation	Kisumu	Septic Tank 100 People (PP) – 30m3	280,000	2097.28
		500 PP – 70 m^3	360,000	2696.51
		1000 PP – 110 m^3	520,000	3894.96
Herri-Tech Ventures	Nairobi	120 PP	150,000	1123.55
		500 PP	190,000	1423.16
		1000 PP	240,000	1797.67
Sistema Bio	Kenya	1000PP School biogas treatment system	$20,000	15943.24

Table 13-7: Kenya Refugee Settlement Sludge Exhauster Costs from field research conducted in February 2020

Source	Settlement	Volume Excavated	Cost (KSH)	Cost (GBP)	LCOWT (£/m3)
World Vision	Kakuma	30,000L	80,000	599.22	19.97
Peace Winds Japan	Kakuma	30,000L	25,000	187.26	6.24

For the potential scaleup of EMR systems within refugee settlements, the offset in fuel costs is crucial. Below is a list of the different fuels for purchase and their costs. The costs vary depending on the location and also the purchaser. Beneficiaries within the settlement mentioned different costs within the same area and at different times of the year.

Table 13-8: Kenya Refugee Settlement cooking fuel costs from field research conducted in February 2020

Source	Settlement	Wood/Charcoal	Quantity	Cost (KSH)	Cost (GBP)
RRDO	Dadaab	Wood	Household (4PP)	20 per day	0.15/day
			Donkey Kart (400-500kg)	2000	14.98
UNHCR	Dadaab – Daligali	Wood	Donkey Kart	2500	18.73
Restaurant Owner	Kakuma	Charcoal	Large Bag – 50kg	700 per bag - *use 6 per week*	5.24
Market Seller	Kakuma	Charcoal	Large Bag – 50kg	800	5.99
			Bucket	250	1.87
			Small bundle – *1/2 days worth*	20	0.15
Lokada	Kakuma	Charcoal	Large bag – 35kg *(supposedly all large bags are 35kg, not 50kg)*	800-1000 *(lasts 1 month)*	5.99 - 7.49
		Prosopis Charcoal	Large bag – 35Kg	650-800 *(depending on wet/dry season)*	4.87 – 5.99
Beneficiary *(Family of 5)*	Kalobeyei	Charcoal	Bucket *(use 4 per month)*	200	1.50
Beneficiary *(Family of 6)*	Kalobeyei	Charcoal	Bucket *(use 4 per month)*	250	1.87
WFP	Dadaab	TBC	TBC	TBC	

Table 13-9: Kenya Refugee Settlement electricity costs from field research conducted in February 2020

Source	Settlement		Cost (KSH)	Cost (GBP)
Beneficiaries	Dadaab – IFO	HH lighting/phone Charging	1000 - 1500/month	7.49 – 11.24/month
Fiada	Dadaab – Hagadera	HH lighting/phone Charging	500/month	3.75/month
Beneficiaries	Dadaab – IFO	Light – Battery torch	100	0.75
	Dadaab – IFO	Phone charge	10	0.08
	Dadaab – IFO	Smart phone	20	0.15
Beneficiaries	Dadaab – Daligali	Freezer - Shop	200/day	1.50/day
	Dadaab – Daligali	Fan – Shop	50/day	0.37/day
	Dadaab – Daligali	Phone charging - Shop	100/day	0.75/day
Generator Seller – *6 business but more want connection*	Kakuma	Fridge	200/day	1.50/day
		Light Households	500/month	3.75/day

13.8 Other Research

Reactor Test systems

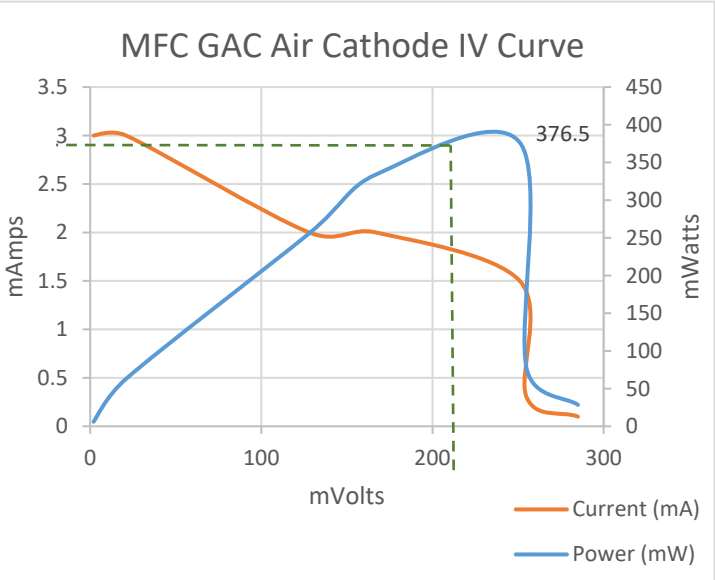

Figure 13-23: MFC Air-Cathode Test System and IV curves

Test of low cost air cathode MFC operating on brewery wastewater to test acidity, graphs showing the IV curves from the initial tests.

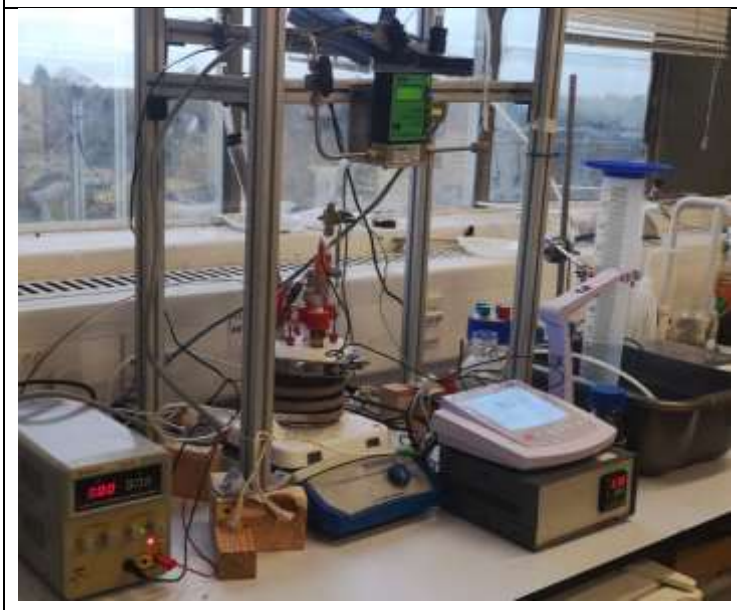

Figure 13-24: EMR - 1L experimental setup

EMR – 1L test reactor operating on dried cassava waste.

Figure 13-25: EMR Electrode Plate Design - 50L Test System

Trial test system of the EMR GAC plate design was installed and tested at the Calthorpe community project in parallel to the AD system operated on food waste.

Figure 13-26: 7L AD and EMR test system

The 7L tubular system was used to test the full size electrodes from the pilot system.